Short-lived trace gases (DMS, isoprene, acetaldehyde and acetone) in the surface waters of the western Pacific and eastern Atlantic Oceans

Dissertation

ZUR ERLANGUNG DES DOKTORGRADES
DER MATHEMATISCH - NATURWISSENSCHAFTLICHEN FAKULTÄT
DER CHRISTIAN-ALBRECHTS-UNIVERSITÄT ZU KIEL

VORGELEGT VON
CATHLEEN ZINDLER
KIEL, 2013

GEOMAR
Helmholtz-Zentrum für Ozeanforschung Kiel

Referent: PD Dr. Hermann W. Bange
Koreferent: Prof. Dr. Christa A. Marandino

Tag der mündlichen Prüfung: 15.04.2013
Zum Druck genehmigt:

gez. Prof. Dr. Wolfgang J. Duschl, Dekan

This thesis is based on the following manuscripts

C. Zindler, A. Bracher, C. A. Marandino, B. Taylor, E. Torrecilla, A. Kock, and H. W. Bange, Sulphur compounds, methane, and phytoplankton: interactions along a north-south transit in the western Pacific Ocean, Biogeosciences Discuss., 9, 15011-15049, 2012, doi:10.5194/bgd-9-15011-2012.

Author Contribution: Cathleen Zindler measured most of the sulphur samples, analysed the sulphur data and wrote the paper. Astrid Bracher, Bettina Taylor and Elena Torrecilla analysed the pigment data and wrote the parts of the material and method and results sections concerning the pigment data. Annette Kock measured and analysed the methane samples. Hermann Bange und Christa Marandino reviewed the paper.

C. A. Marandino, S. Tegtmeier, K. Krüger, C. Zindler, E. L. Atlas, F. Moore, and H. W. Bange, Dimethylsulphide (DMS) emissions from the West Pacific Ocean: a potential marine source for the stratospheric sulphur layer, Atmos. Chem. Phys. Discuss., 12, 30543-30570, 2012, doi:10.5194/acpd-12-30543-2012.

Author Contribution: Cathleen Zindler measured most of the sulphur seawater samples, analysed these samples, calculated the air-sea flux of DMS and created the Figure 2 and 3 in the paper as well as contributed to the material and method part. Christa Marandino wrote the paper. Susann Tegtmeier analysed the data with the FLEXPART model and wrote parts of the material and method and the discussion section. Elliot Atlas and F. Moore provided the atmosphere DMS data. Kirstin Kruger and Hermann Bange reviewed the paper.

C. Zindler, C. A. Marandino, H. W. Bange, E. S. Saltzman, D. W. R. Wallace, Dissolved dimethylsulfide (DMS) and isoprene in the ocean surface layer along a north-south transit in the eastern Atlantic Ocean (ms in preparation for ocean science).

Author Contribution: Cathleen Zindler measured and analysed the DMSP data and wrote

the manuscript. Christa Marandino measured and analysed the DMS and isoprene data and wrote parts of the material and method section and reviewed the paper. Eric Saltzman, Douglas Wallace and Hermann Bange reviewed the manuscript.

C. Zindler, C. A. Marandino and H. W. Bange, Marine Sources and Sinks of the OVOCs acetaldehyde and acetone (ms in preparation).

Author contribution: Cathleen Zindler and Christa Marandino conducted the experiments and measured the OVOCs and CDOM. Cathleen Zindler analysed most of the OVOC data, measured and anlysed the pigment data and measured the flow cytometry data and wrote the OVOC chapter. Christa Marandino and Hermann Bange reviewed the chapter.

Zusammenfassung

Der Austausch von Spurengasen zwischen der Ozeanoberfläche und der unteren Atmosphäre hat in den letzten Jahren speziell im Zusammenhang mit globalen Umweltveränderungen wie Eutrophierung, Ozeanerwärmung, Ozeanversauerung usw. eine erhöhte Aufmerksamkeit erlangt. Der Ozean ist bekannt als Reservoir vieler klimarelevanter Spurengase. Trotzdem sind Verteilung und Reaktionswege von Spurengasen wie Isopren, Aceton und Acetaldehyd in der Oberfläche der Ozeane wenig verstanden. Selbst die Reaktionswege des viel untersuchten Gases Dimethylsufid (DMS) sind nicht vollkommen verstanden. Diese Doktorarbeit führt verschiedene Studien zusammen, welche neue Einblicke über das Schicksal von kurzlebigen, klimarelevanten Spurengasen wie DMS, Isopren, Aceton und Acetaldehyde in der Obenflächenschicht des pazifischen und atlantischen Ozeans geben.

- Die Verteilung von und die Reaktionen zwischen DMS, Dimethylsulfoniumpropionat (DMSP) und Dimethylsulfoxid (DMSO) in der Oberflächenschicht wurden in Verbindung mit der Phytoplanktonzusammensetzung und Methan entlang eines Nord-Süd-Schnittes in westlichen Pazifik von Tomakomai (Japan) nach Townsville (Australien) an Bord von FS Sonne zwischen den 9.9.2009 und 24.9.2009 untersucht (Projekt: TransBrom). Ein enger Zusammenhang zwischen DMSP und DMSO wurde basierend auf Korrelationen beider Verbindungen gefunden. Zusätzlich korrelierten die gleichen Phytoplanktonpigmente mit DMSP und DMSO, was auf eine gleiche Quelle beider Verbindungen hindeutet. Das gemessene Verhältnis von $\mathrm{DMSP_p}$ zu $\mathrm{DMSO_p}$ schien typisch für den oligotrophen, tropischen Atlantik zu sein. Dieses Verhältnis könnte als möglicher Indikator für Stressbedingungen für das Phytoplankton durch intensive solare Einstrahlung und Nährstofflimitierung dienen. Die Limitierung von Nährstoffen könnte die Urasche für die Akkumulation von DMSO im oberflächennahen Westpazifik sein. Es schien, dass die Reaktionswege von DMSP und DMSO enger aneinander gekoppelt sind als an die von DMS. Es konnten keine Phytoplanktongruppen als Quelle für DMS identifiziert werden, welches auf andere Quellen von DMS, wie z. B. Bakterien, hinweist. Desweiteren wurden DMSP und DMSO als mögliche Substrate für die Methanproduktion entlang des ganzen Nord-Süd-Schnittes identifiziert, was die mögliche bedeutende Rolle von beiden Substanzen als Vorstufe eines klimarelevanten Spurengases heraushebt.

- Die atmosphärische Verteilung von DMS wurde ebenso entlang der gleichen Nord-Süd-Route im Westpazifik untersucht. Aus dem Westpazifik ausgegastes DMS schien von Sturmereignissen beeinflusst worden zu sein, welche sich zeitgleich entlang der Route ereigneten. Die gemessenen atmosphärischen DMS-Konzentrationen unterschieden sich vom berechneten DMS-Fluss, woraus geschlossen werden konnte, dass die atmophärische DMS-Konzentration von atmosphärischen Transportprozessen dominiert wurde. Einflüsse dieser Transportprozesse auf die troposphärische DMS-Verteilung wurden mit dem Lagrangeschen FLEXPART Modell untersucht. Obwohl keine erhöhten Werte von DMS im Wasser gemessen wurden, gab es sichere Vorzeichen, dass Starkwindereignisse für signifikante Flusserhöhungen sorgten. In Gebieten starker Konvektion, entlang der Fahrtroute, war der vom Modell berechnete Gehalt an DMS (und seiner Oxidationsprodukte), welcher in die tropische Tropopausenschicht transportiert wurde, regional signifikant. Im Vergleich mit Flugzeugmessungen waren die DMS-Konzentrationen in der oberen Troposphäre in gutem Einklang. Da DMS bisher nicht als Quelle für Schwefel in der oberen Troposphäre/unteren Stratosphäre gesehen wurde, gibt es kaum Messungen, welche über 12 km hinausgehen. Der Eintrag von DMS durch die Tropopause in die Stratosphäre konnte nicht bestimmt werden, aber es ist möglich, dass DMS eine regional und saisonal wichtige Schwefelquelle für die permanente stratosphärische Schwefelschicht ist.
- Da sowohl DMS als auch Isopren als mögliche Vorstufen für Kondensationskerne für Wolken bekannt sind, wurde die Verteilung und Beziehung der beiden Gase entlang eines Nord-Süd Transits im östlichen Atlantik von Bremerhaven nach Kapstadt (Südafrika) an Bord von FS Polarstern (ANTXXV-1) im November 2008 untersucht. Positive und negative Korrelationen zwischen DMS und Isopren wurden in verschiedenen Regionen identifiziert, welche zusammen zwei Drittel des Transits ausmachten. Zusätzlich zeigten DMS und Isopren ähnliche Verteilungen im Zusammenhang mit Phytoplanktongruppen, wie Dinoflagellaten, Haptophyten und Chrysophyten, wenn diese nach N:P-Verhältnis gruppiert werden. Das deutet auf eine gemeinsame biologische Quelle von DMS und Isopren hin. DMS ist allerdings eher dadurch bekannt, von Bakterien statt von Phytoplankton produziert zu werden. Daher war es wahrscheinlicher, dass Isoprene und DMSP gleiche Quellen hatten und DMS über DMSP produziert wurde. DMSP und Isopren korrelierten ebenfalls miteinander, wenn sie nach N:P-Verhältnis gruppiert wurden. Die Verbindung zwischen DMS und Isopren könnte daher eher durch die Aktivität von Bakterien erklärt werden, die beide Verbindungen konsumieren oder produzieren könnten. Allerdings ist dies nicht bewiesen und sollte in Zukunft untersucht werden. Das Verhältnis von DMS zu Isopren veränderte sich mit den hydrographischen Regionen in Ostatlantik. Erhöhte DMS Konzentrationen wurden in Auftriebsgebieten gemessen, während höhere Isoprenkonzentrationen in oligotrophen Regionen detektiert wur-

den. Allerdings wiesen beide Verbindungen die höchsten Konzentrationen in einer Frühjahrsblüte in der Nähe von Südafrika auf. Dies unterstützt die Vermutung, dass DMS und Isopren hauptsächlich biologische Quellen haben. Zusätzlich konnte gezeigt werden, dass Transportprozesse möglicherweise ebenfalls die Verteilung von Isopren beeinflussen.

- Um marine Quellen und Senken von Acetaldehyd und Aceton zu identifizieren, wurden Inkubationsexperimente durchgeführt. Dazu wurden Wasserproben von der Ostsee am Institutspier von GEOMAR aus der Kieler Förde genommen. Die gleichen Experimente wurden im östlichen äquatorialen Atlantik während der MSM 18/3 Forschungsreise auf Maria S. Merian (von Mindelo, Kap Verden nach Libreville, Gabun) zwischen dem 21.6.2011 und 19.7.2011 durchgeführt. Der Einfluss von biologischen und chemischen Prozessen auf die Produktions- und Konsumraten beider Verbindungen wurde unter Lichteinfluss und in Dunkelexperimenten untersucht. Acetaldehyd und Aceton wurden eher konsumiert als produziert. Dies wurden in beiden Beprobungsgebieten festgestellt. Der Lichteinfluss spielte eine geringe Rolle für die Produktion beider Verbindungen, obwohl der photochemische Zerfall von CDOM als Hauptquelle beider Verbindungen gilt. Es konnte im Durchschnitt eine leicht erhöhte Konsumrate von Aceton unter biologischen Einfluss festgestellt werden, wenn chemische und biologische Experimente miteinander verglichen wurden. Allerdings konnte kein deutlicher Unterschied zwischen beiden Experimentarten allgemein festgestellt werden. Genauere Analysen sind erforderlich, um feine Unterschiede zwischen den Experimenten zu bestimmen. Vor allem biologische Prozesse scheinen einen Einfluss auf die Produktions- und Konsumraten beider Verbindungen zu haben. Dies muss in jedem Experiment individuell untersucht werden, da die Variabilität zwischen den Experimenten groß war, was auf eine komplexe Interaktion zwischen verschiedenen Quellen und Senken für Acetaldehyd und Aceton hinweist.

Abstract

The exchange of trace gases between the surface ocean and the lower atmosphere has received increasing attention during the last years especially in view of ongoing global environmental changes such as eutrophication, warming of the ocean, ocean acidification etc.. The ocean has been identified as a huge reservoir of various climate-relevant trace gases. However, the distributions and the pathways of the trace gases such as isoprene, acetone and acetaldehyde, in the surface seawater is poorly understood. Even consensus regarding the intensively studied dimethylsulphide (DMS) pathways continues to elude researchers to date. This thesis compiles different studies which contribute new insight into the fates of a group of short-lived, climate-relevant traces gases including DMS, isoprene, acetaldehyde and acetone in the surface layers of the Pacific and Atlantic Oceans:

- The distribution of and the interactions between DMS, dimethylsulphoniopropionate (DMSP) and dimethylsulphoxide (DMSO) in surface seawater were examined in conjunction with the phytoplankton composition and methane along a north-south transit in the western Pacific Ocean on board the R/V Sonne (TransBrom) from Tomakomai (Japan) to Townsville (Australia) from 9^{th} to 24^{th} 2009. A close link between DMSP and DMSO was found based on correlations between the two compounds and similar phytoplankton pigments, which were identified as presumably sources of both DMSP and DMSO. The detected $\mathrm{DMSP_p}$:$\mathrm{DMSO_p}$ seemed to be typical for an oligotrophic tropical ocean and might indicate stress conditions for phytoplankton due to intensive solar radiation and nutrient limitation which in turn may have led to an accumulation of DMSO in the surface water of the western Pacific Ocean. It seems that DMSP and DMSO were more closely related to each other than to DMS. It was evident that different factors influence the DMS distribution, as underlined by the failure to identify phytoplankton groups as sources for DMS. Moreover, DMSP and DMSO were identified as possible substrates for methane production along the entire north-south transit, emphasizing the potential role of both compounds as precursors of a climate relevant trace gas.
- The atmospheric distribution of DMS was also examined along the same north-south transit in the western Pacific Ocean. DMS emitted from the western Pacific Ocean appeared to be influenced by storms events which were encountered along the same north-south transit. The distribution of the computed DMS flux differed from the distribution of measured atmospheric DMS concentrations, indicating that

atmospheric transport processes governed the pattern of atmospheric DMS concentrations. The Langrangian FLEXPART model was used to examine the influence of transport processes on the distribution of DMS in the troposphere. Although the concentration of DMS in the surface ocean was not elevated above background levels, there were certain instances of elevated flux relating to the high winds from storm events. In regions of the cruise track influenced by convective processes, the amount of DMS (and likely its oxidation products) transported to the tropical tropopause layer, as computed by the model, was regionally significant. The modeled DMS concentrations with altitude were in general agreement with aircraft measurements. However, because DMS has never been considered as a source of sulphur to the upper troposphere/lower stratosphere, there are hardly measurements above 12 km. The actual amount of DMS crossing the tropopause could not be determined, but it is possible that one regionally and seasonally important source of sulphur to the persistent stratospheric sulphur layer is marine derived DMS.

- Because DMS and isoprene have both been identified as potential cloud condensation nuclei precursors over the remote oceans, the distribution and the relationship between the two gases were studied in surface seawater along a north-south transit in the eastern Atlantic Ocean on board of R/V Polarstern (ANTXXV-1) from Bremerhaven (Germany) to Cape Town (South Africa) in November 2008. Positive and negative correlations between DMS and isoprene were found in different regions which extended over two-thirds of the transit. Additionally, DMS and isoprene showed a similar distribution pattern together with phytoplankton groups like dinoflagellates, haptophytes and chrysophytes when clustered by N:P, indicating a biological source of both compounds. However, DMS is known to be produced by bacteria rather than by phytoplankton. Thus, isoprene and DMSP were most likely produced by phytoplankton, which was reflected in the correlation between the two compounds dependent on the N:P ratio. The relationship between DMS and isoprene observed in oligotrophic to eutrophic regions might be based instead on microbial activities. It might be possible that bacteria exist which can produce both DMS and isoprene concurrently. However, this is highly speculative and needs to be further investigated. In addition, DMS:isoprene corresponded to the hydrographic regimes in the eastern Atlantic Ocean. Enhanced DMS concentrations occurred in upwelling regions, while isoprene showed elevated concentrations in oligotrophic regions. However, both compounds showed the highest concentrations in a spring bloom near South Africa, likely pointing to biological activities as the main source. The possibility that transport could be an important control on the isoprene distribution in the surface ocean was also determined.

- In order to identify marine sources and sinks of acetaldehyde and acetone, incubation experiments were conducted with water samples from the Baltic Sea taken at

the GEOMAR institute pier (Kiel Fjord) and samples from the eastern equatorial Atlantic Ocean taken during the research cruise MSM 18/3 on board of the R/V Maria S. Merian from Mindelo (Cape Verde Islands) to Libreville (Gabon) from 21^{st} of June to 19^{th} of July 2011. The effect of biological and chemical processes on the production and consumption of the two compounds was investigated under light and dark conditions. Acetaldehyde and acetone were consumed rather than produced in both oceanic regions. The effect of solar radiation was of minor importance for the production and degradation of acetone and acetaldehyde. Although, the consumption of acetone in biology treatments was slightly higher compared to the chemical treatments, no overarching differences could be determined between biology and chemistry samples, in general. However, there were hints that the biota was important for the production and consumption of both acetaldehyde and acetone, which needs to be further examined in detail. The measured production and degradation rates were variable among the individual experiments, pointing to a complex interaction between different sources and sink processes under varying environmental controls. That will be elucidated in future work with a detailed examination of the individual experiments.

Contents

1 Introduction **1**

1.1 Trace gases – linking the ocean and the atmosphere 1
1.2 The sulphur cycle 2
1.3 Organic sulphur compounds in the surface ocean 4
1.4 Isoprene 6
1.5 Oxygenated volatile organic compounds (OVOC) 8

Thesis outline **15**

2 Sulphur compounds, methane, and phytoplankton: Interactions along a north-south transit in the western Pacific Ocean **17**

2.1 Introduction 18
2.2 Methods 19
2.3 Results and Discussion 22
2.4 Summary 40

3 Dimethylsulphide (DMS) emissions from the West Pacific Ocean: a potential marine source for the stratospheric sulphur layer **55**

3.1 Introduction 56
3.2 Data and Model 57
3.3 Results and Discussion 61
3.4 Conclusions 69

4 Dimethylsulfide (DMS) and isoprene in the ocean surface layer along a north-south transit in the eastern Atlantic Ocean **75**

4.1 Introduction 76
4.2 Methods 77
4.3 Setting of the eastern Atlantic Ocean in November 2008 78
4.4 Results and Discussion 81
4.5 Summary 98

5 Marine sources and sinks of acetaldehyde and acetone **105**

5.1 Material and Method 105

5.2 Results and Discussion 125

6 Conclusion and Outlook **147**

Acknowledgments **151**

Erklärung **153**

1 Introduction

1.1 Trace gases – linking the ocean and the atmosphere

The atmosphere contains a wide variety of different low molecular weight chemical species which have important impacts on the climate, biosphere and elemental cycles. The so-called trace gases have low abundances in the atmosphere compared to nitrogen and oxygen, but are essential for protection against harmful solar radiation, the oxidation capacity of the atmosphere and temperature stability on the earth (Graedel and Crutzen, 1994; Warneck, 1988). Certain trace gases, such as the greenhouse gases CO_2, N_2O, and CH_4, have a relatively long lifetime and are responsible for 10 to 20% of the greenhouse effect (IPCC, 2007), the phenomenon by which these gases reduce the loss rate of infrared radiation from the earth surface and keep the lower atmosphere warm enough to sustain life. The trace gases discussed in this dissertation are short lived, biogenic and low molecular weight chemical compounds, for example the sulphur species dimethylsulphide (DMS) and the hydrocarbons isoprene, acetone and acetaldehyde.

Although the gases have low concentrations, in the parts per trillion range (ppt), their impact on atmospheric chemistry is noteworthy and their potential to counteract the heating due to greenhouse gases is under debate. The oceans, because of their large extent and the complex biological, chemical and physical processes occurring at the air-sea interface, have important influence on the distribution of these gases (Liss *et al.*, 2013).

DMS and related sulphur compounds, isoprene and the oxygenated volatile organic compounds (OVOC), namely acetone and acetaldehyde, will be described in detail in the following sections. These trace gases are potential precursors of aerosols, thereby contributing to the increase of the earth albedo. It is known that the oceans are the biggest source for atmospheric DMS. However, it is not fully clarified if the oceans are also a significant source and/or sink for isoprene and OVOCs. Nonetheless, several studies refer to the oceans (especially in remote marine regions) as potential contributors to the global atmospheric isoprene and OVOC budgets which will be also discussed in detail in the following sections.

1.2 The sulphur cycle

The chemical transformation of sulphur is complex due to its fast chemical and biological cycling in the environment and due to its different oxidation levels. Three sulphur species occur mainly in nature: sulphide (HS^-), sulphur (S^0) and sulphate (SO_4^{2-}). Most sulphur spieces can be found in sediments and rocks, mainly as pyrite (FeS_2) and gypsum ($CaSO_4$). However, the ocean is the most important reservoir of sulphur for the biosphere (Madigan *et al.*, 2001). Figure 1.1 shows the global sulphur cycle and the amount of transported sulphur. Figure 1.2 presents the redox-cycle of sulphur.

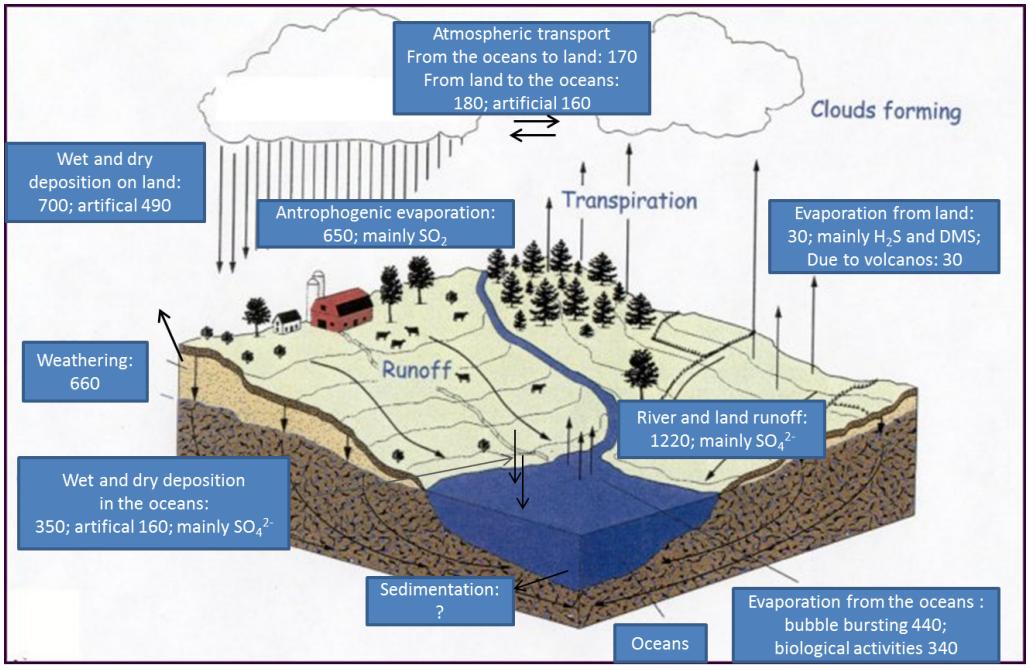

Fig. 1.1: *Schematic of the global sulphur cycle. Numbers are given in 1011 g per year (Madigan et al., 2001). Cartoon modified according to http://mff.dsisd.net/Environment/PICS/WaterCycle.jpg.*

Sulphate is the second most abundant anion in the oceans and its formation to sea salt sulphate aerosols in the marine boundary layer is an important transport mechanism between the sulphur reservoirs. In addition to these inorganic sulphur compounds, biological activities produce a broad spectrum of organic sulphur species. The most common organic sulphur compound in nature is dimethylsulphide (DMS), which is produced mainly in the ocean as degradation product of dimethylsulphoniumpropionate (DMSP). The production of DMS in the ocean is large and its flux into the atmosphere ranges between 15 and 33 Tg S per year (Kettle and Andreae, 2000). Thus, DMS is the most important biogenic sulphur compound in the ocean and atmosphere (Vogt and Liss, 2009).

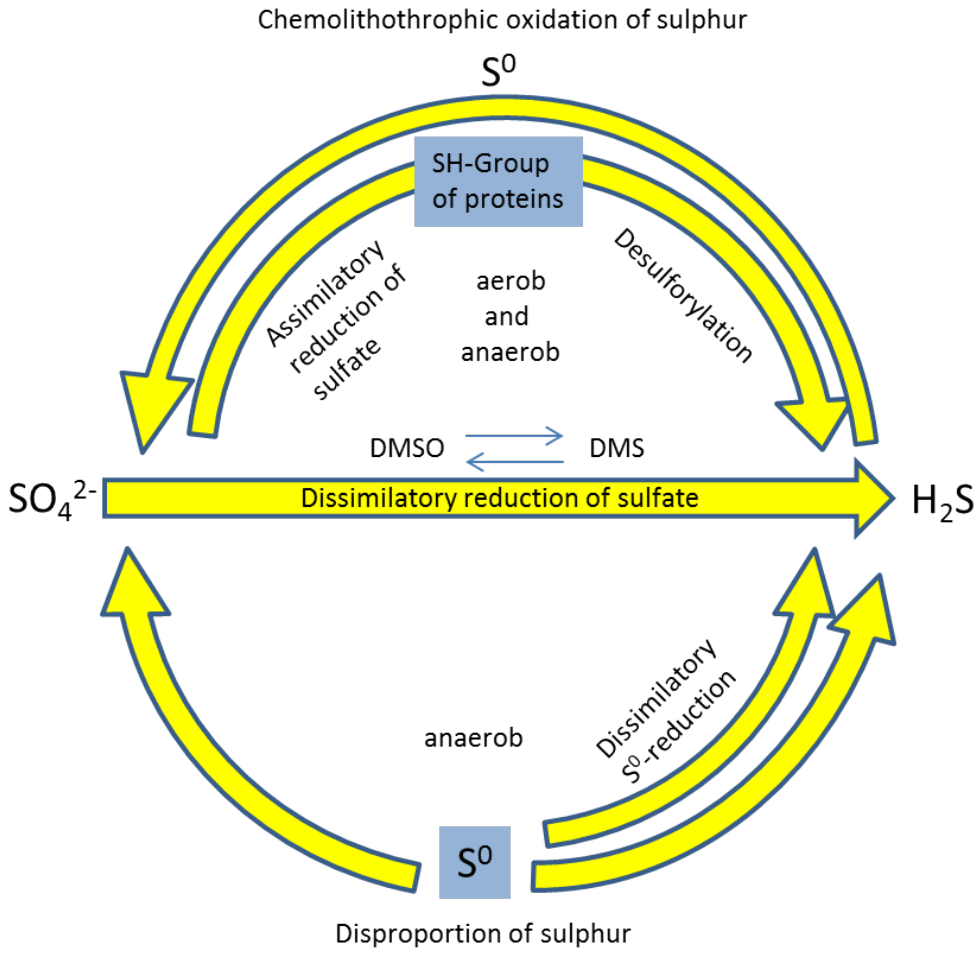

Fig. 1.2: *Redox-cycle of sulphur modified according to Madigan et al. (2001). DMS, dimethylsulphide; DMSO, dimethylsulphoxide*

DMS received much scientific attention with the postulation of the CLAW hypothesis (Charlson *et al.*, 1987). It was suggested that DMS produced by phytoplankton and emitted to the atmosphere can be converted into aerosols that can act as cloud condensation nuclei (CCN). These CCN can scatter solar radiation and are responsible for cloud formation and subsequent precipitation, increasing the earth albedo and having a cooling effect on the climate. The debate about whether or not DMS might have a climate regulating effect is still ongoing. Quinn and Bates (2011) argued against the biota-climate feedback hypothesis via DMS. They showed that the source of CCN comes from a complex combination of bubble bursting, wind speed and biological activities in surface seawater. These processes release organic (other than DMS) and inorganic molecules as well as complex organic macromolecules from surface seawater to the atmosphere and, thus, determine the concentration of CCN in the remote marine boundary layer (MBL). Although, the DMS

contribution to marine boundary layer cloud formation in the CLAW hypothesis scheme might be rejected, the effect of DMS on marine atmospheric chemistry and climate is still potentially significant.

1.3 Organic sulphur compounds in the surface ocean

DMS (average global concentration: 1-5 $\mathrm{nmol\,L^{-1}}$) and its precursor DMSP (average global concentration: 10-15 $\mathrm{nmol\,L^{-1}}$) as well as its oxidation product dimethylsulphoxide (DMSO, average global concentration: 5-10 $\mathrm{nmol\,L^{-1}}$) are involved in a complex biogeochemical cycle in surface seawater in the world oceans (Figure 1.3). Specialized algae taxa like dinoflagellates, coccolithophores and chrysophytes are important DMSP producers and can be responsible for a substantial increase of DMSP concentration (in the $\mathrm{nmol\,L^{-1}}$ range) in seawater during strong bloom events in the boreal and subarctic regions.

The biosynthesis of DMSP in algae cells (referred to particulate DMSP, $\mathrm{DMSP_p}$) starts with the uptake of SO_4^{2-} from seawater, which gets chemically transformed into the amino acids methionine or cysteine, the precursors of DMSP, via a complex reaction mechanism. The function of DMSP in algae cells is still debated. It was shown that DMSP can act e. g. as an osmoregulator, cryoprotector or methyl donor (Simó, 2001). During enhanced solar radiation DMSP is also involved in anti-oxidation mechanisms that scavenge harmful reactive oxygen species (ROS) within the cells (Sunda *et al.*, 2002).

$\mathrm{DMSP_p}$ is subject to different degradation pathways in algae cells, like the enzymatic cleavage into DMS and acrylate. Additionally, it can be directly released from the cells into the water column, referred to as dissolved DMSP ($\mathrm{DMSP_d}$). The $\mathrm{DMSP_d}$ in the water column can be taken up rapidly by specialized bacteria, mainly *Roseobater*, or specialized algae species. Dependent on the sulphur demand of the bacterioplankton, DMSP is either incorporated into their biomass through the demethylation/demethiolation pathway (Figure 1.3) or enzymatically cleaved to DMS and acrylate via DMSP-lyases and released into the water column (Kiene *et al.*, 2000). The amount of released DMS is usually very small; however, it can be considerably during spring bloom events of DMSP producing phytoplankton. DMS in the water column can be taken up by bacteria (80%) (Archer *et al.*, 2001; Simó, 2004), removed due to photolysis in the upper 20 m (Brimblecombe and Shooter, 1986; Toole *et al.*, 2004) or biologically/chemically oxidized to DMSO.

During stormy weather conditions, air-sea gas exchange can be the most important sink

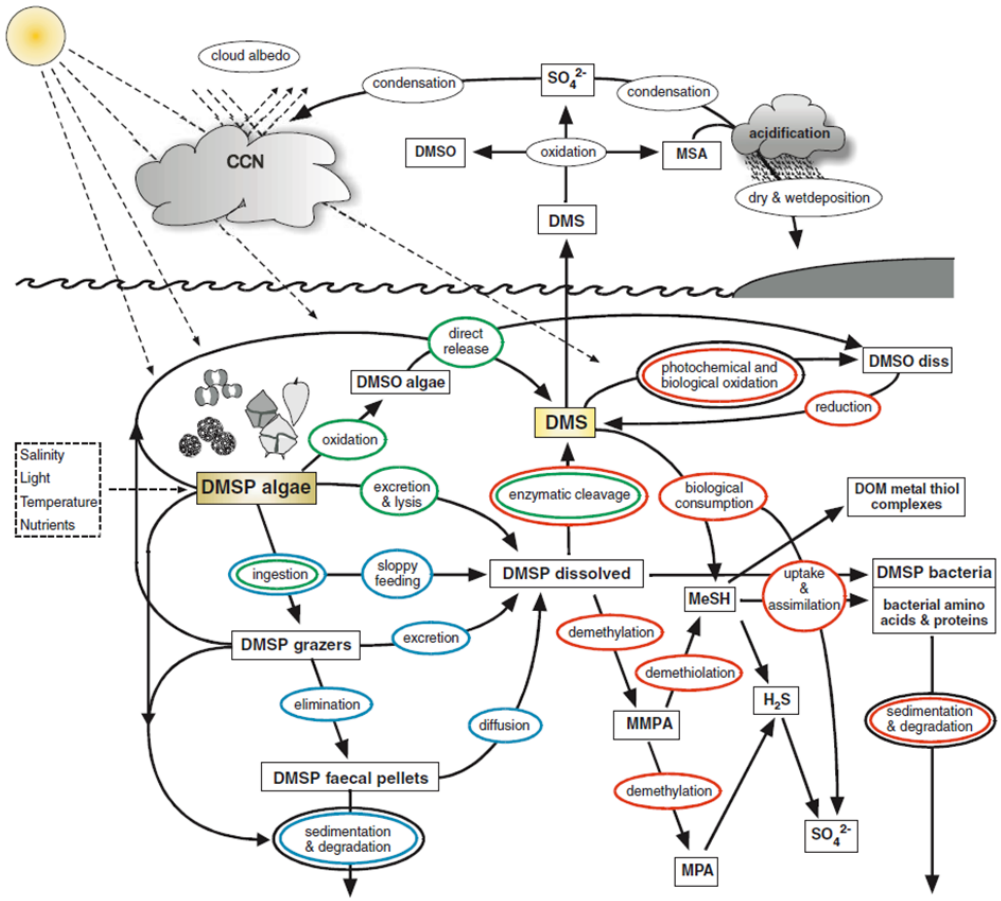

Fig. 1.3: *The biogenic sulphur cycle in surface seawater (Stefels et al., 2007). MeSH, methanethiol; MPA, mercaptopropionate; MMPA, methylmercaptopropionate; MSA, methanesulphonic acid; DOM, dissolved organic matter.*

for DMS in the upper few meters. However, the flux is only responsible for about 10% of the DMS loss in surface seawater, in general, when all marine sinks for DMS are considered (Archer *et al.*, 2001).

For the last two decades DMSO has received increased scientific attention because it can serve both as a sink and a source for DMS in the oceans. Additionally, DMSO is ubiquitously distributed in the ocean water column (detected also in 4000 m depth, Hatton *et al.* (1999)), in fresh water, in the polar regions and in the atmosphere (Hatton *et al.*, 2005). The DMSO concentration in seawater is usually between the concentrations of DMS and DMSP. However, elevated DMSO, up to approximately 140 $\mathrm{nmol\,L^{-1}}$, has been measured (Hatton *et al.*, 1998). DMSO can be produced in specialized algae species and is part of the anti-oxidation cascade in phytoplankton cells during solar radiation stress. Furthermore, DMSO might serve as a nutrient for the bacterioplankton in the water column (Lee *et al.*, 1999).

The small fraction of DMSP which is converted to DMS (< 1%) is responsible for a large flux of biogenic sulphur into the atmosphere. Additionally, DMSP serves as one of the most important single substrates in seawater (Kiene *et al.*, 2000). Due to the annually high amount of DMS transported into the atmosphere, DMS is an important compound for atmospheric chemistry and maybe for climate control. DMSO seems to be the biggest organic sulphur pool in the oceans because of its occurrence throughout the entire water body. These facts illustrate the importance of the marine organic sulphur species for biogeochemical processes in the oceans and atmosphere and, thus, it is essential to understand their global cycle.

1.4 Isoprene

Isoprene and its degradation products represent almost 50% of all biogenic atmospheric non-methane hydrocarbons (NMHC) and is therefore the most abundant NMHC. Isoprene is an important source for secondary organic aerosols (SOA) and has a strong effect on the oxidative balance of the atmosphere due to its potential to form formaldehyde and thus peroxy radicals (RO_2) (Claeys *et al.*, 2004; Ayers *et al.*, 1997; Baker *et al.*, 2000). Additionally, isoprene can influence the production of ozone in the marine boundary layer when nitrogen oxide chemical species (NO_x = NO + NO_2) are present (Williams *et al.*, 2010). The main source of isoprene is terrestrial vegetation, such as the tropical rain forests. It is still not completely clarified why isoprene is produced in plants. It seems to increase temperature tolerance and might protect against ROS in leaves (Sharkey *et al.*, 2008). The annual terrestrial emissions of isoprene range between 400 and 750 Tg C $\mathrm{yr^{-1}}$

(Arnold *et al.*, 2009).

The global oceans seem to be only a minor source of isoprene to the atmosphere, with an annual mean emission of 0.1 – 1.9 Tg C yr^{-1} (Luo and Yu, 2010). However, the quantification and the local importance of the ocean as an isoprene source are still debated. Meskhidze and Nenes (2006) suggested isoprene as the most likely link between a phytoplankton bloom and marine clouds in the Southern Ocean. They proposed that the oxidation of emitted isoprene from algae form SOA in the atmosphere and, thus, influence the chemical composition of CCN and the number of cloud droplets. In contrast, Arnold *et al.* (2009) proposed that marine isoprene is of minor importance for the formation of marine aerosol in remote regions. However, Gantt *et al.* (2009) showed, using model calculations, that isoprene contributes significantly to the sub-micron organic carbon fraction of marine aerosols in tropical regions. They conclude that isoprene has the potential to modulate marine cloud properties and influence the climate.

Baker *et al.* (2000) and Broadgate *et al.* (1997) measured maximum isoprene concentrations at the depth of maximum chlorophyll concentrations and hypothesized that the isoprene production might be a general feature of phytoplankton. Diatoms, dinoflagellates, coccolithoprhids and cyanobacteria were identified as isoprene producers while cyanobacteria seems to be the strongest emitter (Moore and Wang, 2006; Bonsang *et al.*, 2010; Shaw *et al.*, 2003; Milne *et al.*, 1995). Thus, biologically productive regions, such as upwelling areas, coastal regions or the boreal open ocean during bloom events, might be seasonally important isoprene sources to the atmosphere.

Culture experiments of different algae groups, e.g. *Synechococcus*, *Prochlorococcus* or *Emiliania huxleyi*, showed highest isoprene production during the exponential growth phase. High light intensity and temperature supported the isoprene production (Shaw *et al.*, 2003; Bonsang *et al.*, 2010; Gantt *et al.*, 2009). Thus, tropical and subtropical oceanic regions dominated by *Prochlorococcus* can be important regions for isoprene production. The role of isoprene in phytoplankton cells is still unclear. It might be a byproduct of photosynthesis or may be directly related to the metabolism in the cells (Bonsang *et al.*, 2010; Shaw *et al.*, 2003). It was shown that isoprene production was maximum in algae cultures during high light intensities which triggered photoinhibition (Shaw *et al.*, 2003). Whether isoprene has a protective function for the photosynthesis mechanism in the manner of terrestrial plants or another role in algae cells needs to be resolved.

Only few studies investigated the role of bacteria on the marine isoprene distribution. Bacterial communities were observed which consumed isoprene and used it as a carbon or energy source (Alvarez *et al.*, 2009). Additionally, Kuzma *et al.* (1995) identified sev-

eral bacteria species which produced isoprene. Thus, bacteria seem to be important for controlling for marine isoprene. Even less is known about the abiotic sources of marine isoprene. The production of isoprene via photochemical degradation of dissolved organic matter (DOM) exposed to UV light could not be proven (Ratte *et al.*, 1998).

Only a few studies report isoprene concentrations and temporal/spatial distribution patterns in the ocean (Baker *et al.*, 2000; Bonsang *et al.*, 1992; Matsunaga *et al.*, 2002; Shaw *et al.*, 2010). Thus, more studies are needed to understand the global cycle of isoprene in the oceans and its influence on the atmosphere. In addition, environmental controls on the concentrations and distribution patterns are mainly unknown and should be the subject for future investigations.

1.5 Oxygenated volatile organic compounds (OVOC)

OVOCs belong to the NMHC group and consist of aldehydes, ketones, alcohols and carboxylic acids, for example acetaldehyde, acetone, ethanol and formic acid, respectively. OVOCs are ubiquitous and can account for a high amount of NMHC in certain regions dependent on the season (Lewis *et al.*, 2005; Singh *et al.*, 1995).

1.5.1 Importance of OVOCs in the atmosphere

The atmospheric cycling of OVOCs is complex because they are involved in a broad range of chemical reactions in the atmosphere (Figure 1.4). The distribution and amount of trace gases in the atmosphere are controlled generally by their reaction with the hydroxyl radical, OH. The OH concentration depends mainly on the presence of water vapor and ozone (O_3), as well as on light levels and temperature (Spivakovsky *et al.*, 1990). OVOCs have been suggested as OH precursors, especially in the upper troposphere, where water vapor is too low for the production of the high amount of OH observed (Lary and Shallcross, 2000; Singh *et al.*, 1995; Wennberg *et al.*, 1998). Additionally, OVOCs are suggested as an important source for RO_2 (Monks, 2005; Muller and Brasseur, 1999; Singh *et al.*, 1994), which are involved in the formation of harmful O_3 in the troposphere. In polluted regions, ozone can be produced via chemical reactions including hydrocarbons and NO_x. Furthermore, chemical reactions of OVOCs (especially acetone) are responsible for a considerable concentration of peroxyacetylnitrate (PAN) in the free troposphere (Singh *et al.*, 1995). PAN is a harmful compound for the biota and an important reservoir for nitrogen containing radicals. PAN is relatively stable and temperature sensitive compound which can be transported over long distances especially in colder regions. In remote regions it

can break down into NO_x and RO_x radicals and can therefore indirectly influence the atmospheric chemistry in clean air. OVOCs are also recognized as precursors of secondary aerosols. Some of these aerosol species have the potential to form CCN. Thus, OVOCs might be climate active compounds similar to isoprene and DMS (Blando and Turpin, 2000).

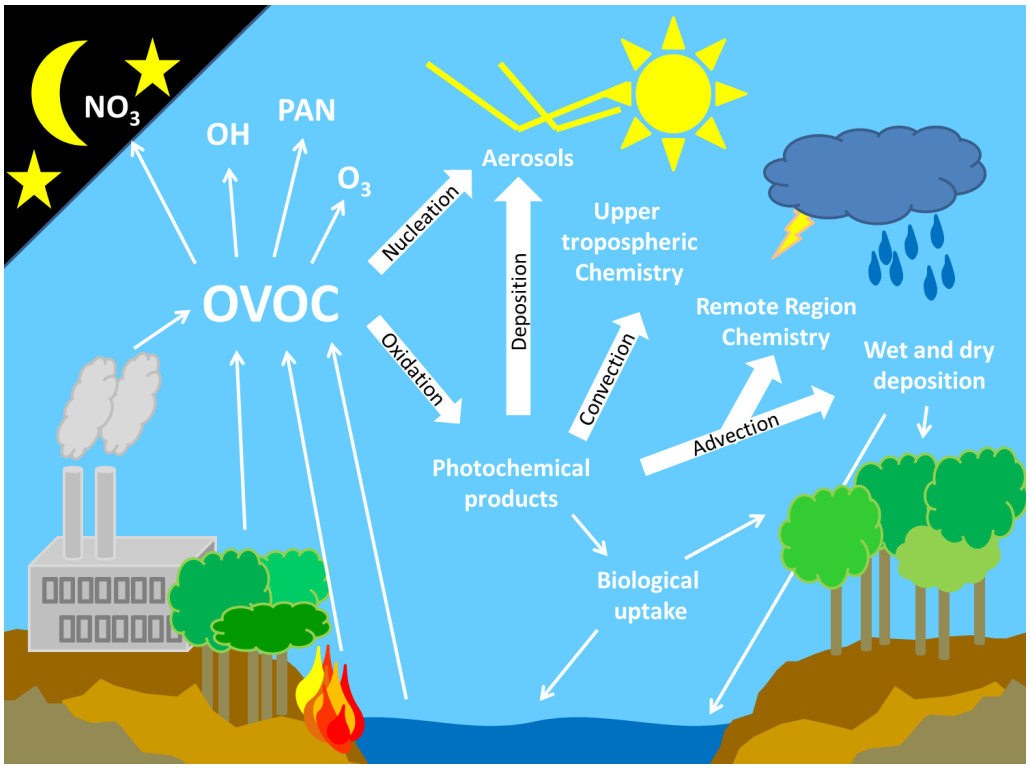

Fig. 1.4: *A cartoon depicting the global cycle of OVOCs in the atmosphere and their sources and sinks.*

1.5.2 The atmospheric budget of OVOCs

Determination of global sources and sinks for OVOCs only started since the last decade and is still under controversial discussion. Models, atmospheric measurements and satellite data are used to calculate the atmospheric budget of these compounds (Heikes *et al.*, 2002; Jacob *et al.*, 2002; Rinsland *et al.*, 2007). The main sources of OVOCs are anthropogenic and biogenic emissions, biomass burning, atmospheric oxidation of precursors and plant decay (Heikes *et al.*, 2002; Jacob *et al.*, 2002; Jacob *et al.*, 2005). Additionally OVOCs can be produced due to the transformation of other OVOCs (Nádasdi *et al.*, 2010; Heikes *et al.*, 2002). The main sinks are wet and dry deposition, reaction with OH, and photochemical oxidation (Heikes *et al.*, 2002; Jacob *et al.*, 2002; Jacob *et al.*, 2005). However, the strength and the balance of the listed sources and sinks are still controver-

sially discussed in current literature (Figure 1.5 and 1.6). Due to the imbalance between the sources and sinks of the OVOCs, unknown sources and sinks must exist. The global oceans are considered as a potential candidate due to their large extent and biogeochemical productivity. Especially in highly convective regions, it is possible that marine OVOCs are transported in the upper troposphere and influence the chemical reactivity there. Indeed, several studies have shown that the ocean is a source and/or sink for a broad range of OVOCs, such as methanol, acetone and acetaldehyde, dependent on regional biological productivity and light intensity (Marandino *et al.*, 2005; Sinha *et al.*, 2007; Millet *et al.*, 2010; Williams *et al.*, 2004). However, the global ocean source or sink term is still not quantified.

1.5.3 OVOCs in the oceans

Only a few studies present concentrations as well as sources and sinks and diurnal cycles of OVOCs in different regions of the oceans, e.g. the Caribbean and Sargasso Sea, Atlantic and Pacific Ocean (Beale *et al.*, 2010; Dixon *et al.*, 2011b; Marandino *et al.*, 2005; Zhou and Mopper, 1997). The most investigated and likely marine source of OVOCs is production from photochemical and/or photosensitized oxidation of dissolved organic matter (DOM) (Mopper and Stahovec, 1986; Ehrhardt and Weber, 1991; Obernosterer *et al.*, 1999). Other possible sources are air/sea gas exchange, biological production and the oxidation of DOM due to radicals (Dixon *et al.*, 2011a, b; Nemecek-Marshall *et al.*, 1995; Mopper and Stahovec, 1986). Oceanic sinks for OVOCs are even less investigated compared to the sources. Possible sinks are biological uptake, air/sea gas exchange, oxidation due to radicals and photochemistry. For example, Dixon *et al.* (2011, a, b) showed that methanol is consumed by bacteria and is used as an energy and carbon source.

The work of this thesis is focused on acetaldehyde and acetone. Therefore, the current knowledge about global sources and sinks of acetaldehyde and acetone will be described in detail in the following sections.

1.5.4 Acetaldehyde

In marine air acetaldehyde together with methanol and acetone can contribute up to 85% of the total mass of organic compounds, with the exception of methane. Additionally, these three OVOC species can be an important sink for OH (80%) (Lewis *et al.*, 2005). Only a few studies describe the global distribution and sources/sinks of acetaldehyde (Fig. 1.5, Millet *et al.* (2010)). It appears that the most important source of acetaldehyde to the atmosphere is atmospheric oxidation of hydrocarbons (alkanes, alkenes and ethanol).

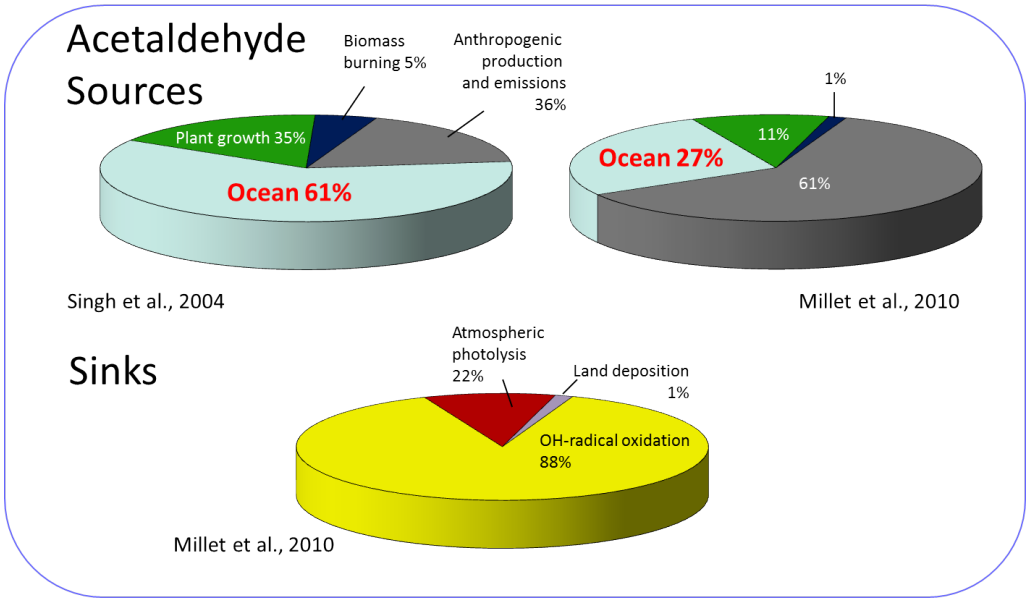

Fig. 1.5: *Possible sources and sinks of atmospheric acetaldehyde. The global proportions are suggested by different studies.*

The oceans are most likely the second largest source of acetaldehyde (Millet *et al.*, 2010). An important source of acetaldehyde in surface seawater is its direct production due to the photolysis of chromophoric dissolved organic matter (CDOM) (deBruyn *et al.*, 2011; Mopper and Stahovec, 1986). The rapid uptake by biota seems to be an important sink (Mopper and Stahovec, 1986). The light dependent production and the fast consumption should be responsible for a diurnal cycle of acetaldehyde in surface seawater, which has been supported by field observations (Mopper and Stahovec, 1986). In contrast, acetaldehyde can also be emitted from the ocean to the atmosphere, depending on phytoplankton abundance, as observed in mesocosm experiments (Sinha *et al.*, 2007). Acetaldehyde enrichment of the sea surface microlayer has also been detected and seems to be an oceanic source for atmospheric acetaldehyde (Zhou and Mopper, 1997). However, the cycling and turnover rates of acetaldehyde in the ocean mixed layer as well as controlling environmental parameters are widely unknown.

1.5.5 Acetone

Different sources and sinks for atmospheric acetone have been widely reported in the literature (Fig. 1.6). However, their proportions and the role of the oceans in the atmospheric budget are also still considerably debated.

An important source for acetone in the surface oceans is its formation via photolysis of

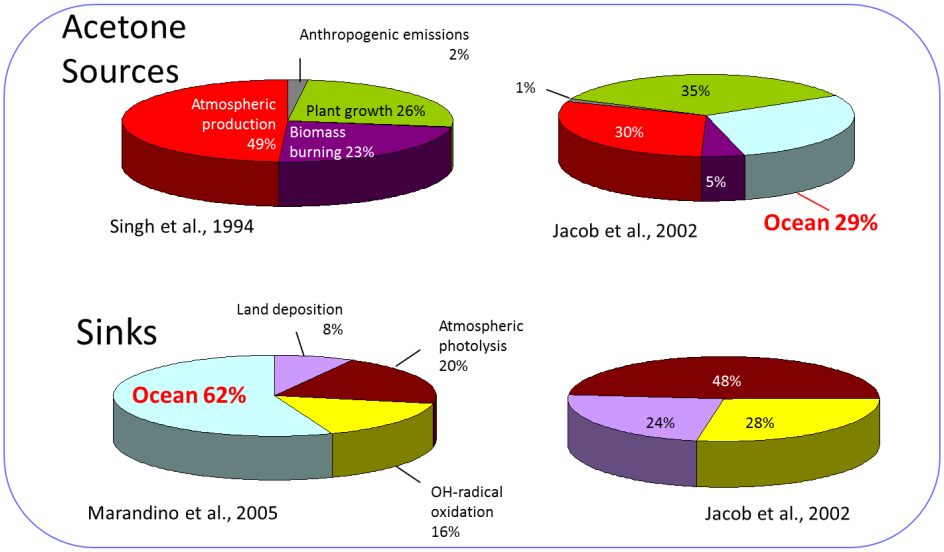

Fig. 1.6: *Suggested global sources and sinks for acetone. The proportions of the different sources and sinks and especially the role of the oceans are still considerably discussed in current literature.*

CDOM in combination with oxygen and OH (deBruyn *et al.*, 2011). The South Pacific seems to be a large photochemical marine source (Jacob *et al.*, 2002), as well as coastal regions or upwelling areas with high CDOM concentrations. Additionally, acetone can also be produced by marine *Vibrio* bacteria which might be associated with phytoplankton (Nemecek-Marshall *et al.*, 1995; Nemecek-Marshall *et al.*, 1999). Marandino *et al.* (2005) showed that the ocean is an important sink for atmospheric acetone (Figure 1.6). It is most likely that dissolved acetone might be consumed due to microbes as suggested by Jacob *et al.* (2002) who simulated the seasonal variation of atmospheric acetone during spring blooms in European sites and Artic summers by including an oceanic sink. However, the degradation/consumption pathways of acetone in the ocean are less studied.

An important sink for acetone in the atmosphere is its degradation via two possible reaction pathways which can occur in the upper troposphere with the initial formation of different radical species (Arnold *et al.*, 2004).

$$CH_3COCH_3 + h\nu + 2O_2 \rightarrow CH_2O_2 + CH_3C(O)O_2 \tag{1.1}$$

$$CH_3COCH_3 + OH + O_2 \rightarrow CH_3COCH_2O_2 + H_2O \tag{1.2}$$

These pathways are most likely the main source of HO_x radicals ($OH + HO_2$) in the upper troposphere, and thus, an important source for O_3 (Singh *et al.*, 1995). The formation of

HO_x is dependent on altitude, water vapor and temperature and thus, variable in different regions and seasons. The upper troposphere is relatively dry and therefore water vapor as a precursor cannot explain the concentrations of HO_x found there.

Although, acetone is important for the atmospheric chemistry and the ocean was identified as a major source of acetone in the atmosphere, the biogeochemical cycle of marine acetone is widely unknown and needs to be investigated.

Thesis outline

The current literature shows the importance of short-lived trace gases such as DMS, isoprene, acetaldehyde and acetone for the chemical reactivity of the atmosphere as well as their potential effects on climate regulation. However, many questions still exist about their global pathways. These questions have to be answered to understand future impacts of short-lived trace gases on atmospheric processes and the earth's climate. Although, the understanding of the biogeochemical pathways of DMS and related sulphur compounds such as DMSP and DMSO strongly increased over last decades, it is still not possible to quantitatively predict the global distribution of DMS in the ocean and atmosphere. Furthermore, the global biogeochemical pathways of isoprene and OVOCs in the oceans are poorly understood. Main questions remain about their sources and sinks, interactions, turnover rates, distribution patterns and fluxes between the oceans and the atmosphere.
Therefore, the major motivation of this PhD thesis was to investigate (i) the distribution patterns of DMS and isoprene in the surface ocean, (ii) the transport mechanisms and distribution pattern of DMS in the atmosphere and (iii) to identify marine sources and sinks of acetaldehyde and acetone.

The results are presented in four chapters:
Chapter 2: The interactions between DMS and related sulphur compounds as well as the influence of the phytoplankton community on the sulphur species were investigated in the surface seawater along a north south transit in the western Pacific Ocean. This region is sparsely sampled for organic sulphur compounds. Furthermore, the influence of sulphur species on the methane concentration in the surface ocean was explored.
Chapter 3: The distribution and fate of marine DMS emitted into the atmosphere was examined in the highly convective region above the western tropical Pacific Ocean using the Langrangian dispersion model FLEXPART. The amount of DMS which gets transported into the upper troposphere/lower stratosphere and the implications of this transport are assessed.
Chapter 4: The distribution pattern of DMS and isoprene in surface seawater as well as their interactions were examined along a north south transit in the eastern Atlantic Ocean.
Chapter 5: Incubation experiments with natural seawater were conducted to investigate consumption and production rates of acetaldehyde and acetone. These experiments provided information about possible sources and sinks of these compounds and the environ-

mental factors controlling their surface ocean cycling in the western Baltic Sea and the equatorial eastern Atlantic Ocean.

2 Sulphur compounds, methane, and phytoplankton: Interactions along a north-south transit in the western Pacific Ocean

Abstract

Here we present results of the first comprehensive study of sulphur compounds and methane in the oligotrophic tropical West Pacific Ocean. The concentrations of dimethylsulphide (DMS), dimethylsulphoniopropionate (DMSP), dimethylsulphoxide (DMSO), and methane (CH_4), as well as various phytoplankton marker pigments in the surface ocean were measured along a north-south transit from Japan to Australia in October 2009. DMS (0.9 $\mathrm{nmol\,L^{-1}}$), dissolved DMSP ($\mathrm{DMSP_d}$, 1.6 $\mathrm{nmol\,L^{-1}}$) and particulate DMSP ($\mathrm{DMSP_p}$, 2 $\mathrm{nmol\,L^{-1}}$) concentrations were generally low, while dissolved DMSO ($\mathrm{DMSO_d}$, 4.4 $\mathrm{nmol\,L^{-1}}$) and particulate DMSO ($\mathrm{DMSO_p}$, 11.5 $\mathrm{nmol\,L^{-1}}$) concentrations were comparably enhanced. Positive correlations were found between DMSO and DMSP as well as DMSP and DMSO with chlorophyll a, which suggests a similar source for both compounds. Similar phytoplankton groups were identified as being important for the DMSO and DMSP pool, thus, the same algae taxa might produce both DMSP and DMSO. In contrast, phytoplankton seemed to play only a minor role for the DMS distribution in the western Pacific Ocean. The observed $\mathrm{DMSP_p} : \mathrm{DMSO_p}$ ratios were very low and seem to be characteristic of oligotrophic tropical waters representing the extreme endpoint of the global $\mathrm{DMSP_p} : \mathrm{DMSO_p}$ ratio vs. SST relationship. It is most likely that nutrient limitation and oxidative stress in the tropical West Pacific Ocean triggered enhanced DMSO production leading to an accumulation of DMSO in the sea surface. Positive correlations between $\mathrm{DMSP_d}$ and CH_4, as well as between DMSO (particulate and total) and CH_4, were found along the transit. We conclude that DMSP and DMSO and/or their degradation products might serve as potential substrates for CH_4 production in the oxic surface layer western Pacific Ocean.

2.1 Introduction

Oceanic dimethylsulphide (DMS) is the most important source of biogenic sulphur to the atmosphere and, thus, the oceanic DMS flux constitutes a significant component of the global sulphur cycle, see e.g. Vogt and Liss (2009). The oceanic distributions of DMS and its major precursor dimethylsulphoniopropionate (DMSP) result from a complex interplay of biological and non-biological pathways, such as formation by phytoplankton and microbial cleavage of DMSP to DMS on the one hand, and microbial consumption as well as photochemical oxidation of DMS and its loss to the atmosphere on the other hand (Simó, 2004; Stefels *et al.*, 2007; Vogt and Liss, 2009; Schäfer *et al.*, 2010). Although dimethylsulphoxide (DMSO) is recognized as an important reservoir of sulphur in the ocean, its production and consumption pathways are poorly understood. The principal production mechanisms for DMSO are the photochemical and bacterial oxidation of DMS, as well as direct synthesis in marine algae cells (Lee and De Mora, 1999; Lee *et al.*, 1999a). Bacterial consumption, reduction to DMS, further oxidation to dimethylsulphone ($DMSO_2$), and export to deep waters via sinking particles are possible sinks for DMSO in the euphotic zone (Hatton *et al.*, 2005). It is well-known, that DMS, DMSP and DMSO play important roles in the oceanic nutrient cycle. They are ubiquitous in the ocean and are responsible for the transfer and cycling of sulphur and carbon between different trophic levels in plankton (Kiene *et al.*, 2000; Simó, 2004; Simó *et al.*, 2002; Yoch, 2002). DMSP, for example, can completely satisfy the sulphur demand for bacterioplankton and can deliver 48% of the sulphur requirement for microzooplankton (Kiene and Linn, 2000; Simó, 2004). Additionally, DMSP can supply between 8 and 15% of carbon for bacteria and can serve as an energy source, which makes it the most important single substrate for marine bacterioplankton (Kiene *et al.*, 2000; Simó *et al.*, 2002). DMSO seems to be an important substrate for specialized bacteria which use DMSO as carbon or electron source (Lee *et al.*, 1999a; Simó *et al.*, 2000).

Methane (CH_4) is an atmospheric trace gas which contributes significantly to the greenhouse effect and chemistry of the Earth's atmosphere (IPCC, 2007). CH_4 is mainly produced by methanogenesis as part of the microbial decomposition of organic matter (Cicerone and Oremland, 1988; Ferry, 2010). Despite the fact that methanogenesis requires strictly anaerobic conditions (see e.g. Ferry (2010)), CH_4 concentrations above the equilibrium concentration with the atmosphere are usually found in the ventilated (i.e. oxic) open ocean surface layer (see e.g. Reeburgh (2007)). This indicates that the open ocean is indeed a source of CH_4 to the atmosphere. Several explanations for this obvious 'oceanic CH_4 paradox' have been suggested. For example, methanogens might live in anoxic micro-niches such as found in sinking organic particles and inside of zooplankton guts (de Angelis and Lee, 1994; Karl and Tilbrook, 1994). Only recently Karl *et al.* (2008) suggested an aerobic CH_4 production pathway by Trichodesmium which can use methylphosphonate as an alternative phosphate source. The degradation products of

DMSP (i.e. methanethiol, methylmercaptopropionate and DMS) have been suggested as important methylated precursors for marine microbial CH_4 production under anoxic conditions (Finster *et al.*, 1992; Tallant and Krzycki, 1997) as well as oxic conditions (Damm *et al.*, 2010; Damm *et al.*, 2008). Several bacteria groups have been identified that have the ability to metabolize DMSP and its degradation products by producing CH_4 (Kiene *et al.*, 1986; Oremland *et al.*, 1989; van der Maarel and Hansen, 1997). Accumulation of CH_4, dependent on DMSP consumption in the surface ocean, has been observed under oligotrophic conditions as well as in a phytoplankton bloom (Damm *et al.*, 2010).

This study presents measurements of the surface ocean distributions of DMS, DMSP, DMSO, CH_4 and phytoplankton pigments in the western Pacific Ocean, an area that is considerably undersampled for all the listed compounds. By using statistical methods we investigated (i) the interactions and links between the different sulphur compounds and how these might control their distributions, (ii) the role of phytoplankton community composition in determining the surface distributions of the sulphur compounds and (iii) the role of sulphur compounds as potential precursors for CH_4 in the surface ocean. All data were retrieved during a north-south transit cruise in October 2009 (Krüger and Quack, 2012) as part of the "TransBrom" project.

2.2 Methods

Water samples were collected aboard the R/V Sonne from 9^{th} to 24^{th} October 2009 during a transit cruise from Tomakomai (Japan) to Townsville (Australia) in order to analyse the sea surface concentrations of DMS, DMSP, DMSO, CH_4 and phytoplankton composition (Fig. 2.1). Samples were collected every three or twelve hours from approximately 5 m depth using the underway pump system installed in the hydrographic shaft.

2.2.1 Analysis of sulphur compounds and CH_4

Three replicate sub-samples (10 ml) were analysed for DMS, dissolved DMSP ($\mathrm{DMSP_d}$) and DMSO ($\mathrm{DMSO_d}$). The total and, thus, the particulate fraction of DMSP ($\mathrm{DMSP_t}$, $\mathrm{DMSP_p}$) and DMSO ($\mathrm{DMSO_t}$, $\mathrm{DMSO_p}$) were analysed in additional three replicate sub-samples (10 ml). All sub-samples of one sampling station were taken out of one 250 ml sample bottle which was sampled from the pump system. Samples were measured immediately after collection, with the exception of DMSO. DMSO samples were stored in the dark and analysed later in the GEOMAR laboratory directly after the cruise. It has been shown that storage of DMSO in hydrolysed samples with gas tight closure does not alter the DMSO concentration (Simó *et al.,* 1998). Samples for the analysis of DMS and the dissolved fraction of DMSP and DMSO were gently filtered by using a syringe as

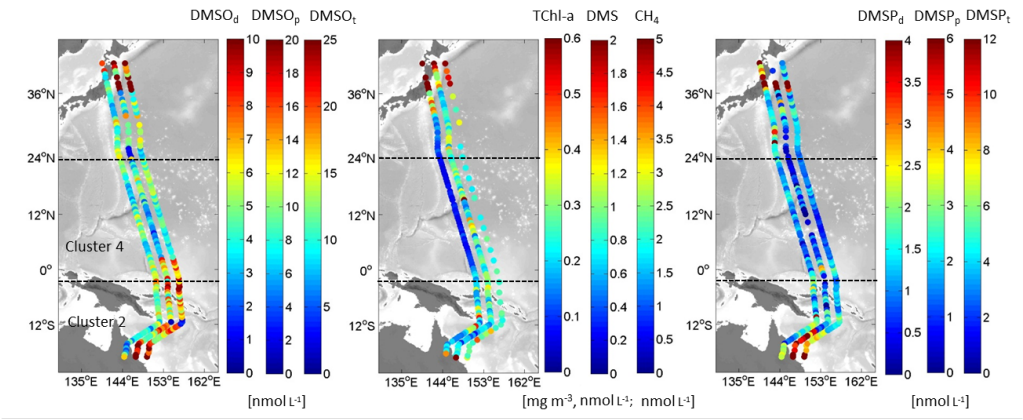

Fig. 2.1: *Distribution of a) DMSO [*$\mathrm{nmol\,L^{-1}}$*], b) total chl-a [*$\mathrm{mg\,m^{-3}}$*] (HPLC in-situ measurements), DMS, and methane [*$\mathrm{nmol\,L^{-1}}$*], and c) DMSP [*$\mathrm{nmol\,L^{-1}}$*] along the cruise track. The middle line in each panel shows the exact position of the cruise track. The dashed lines show the approximate location of cluster 2 and 4. The order of the colorbars corresponds to the order of the individual coloured cruise tracks in the figure panels.*

described in Zindler *et al.* (2012). DMS, $\mathrm{DMSP_d}$ and $\mathrm{DMSP_t}$ samples were analysed by purge and trap coupled to a gas chromatograph-flame photometric detector (GC-FPD) directly on-board after sampling, as described in Zindler *et al.* (2012). Two minor modifications were made: i) replacement of the previously used Tenax with trapping in liquid nitrogen, ii) injection onto the GC by immersion in hot water. DMS were analysed first in the samples. Afterwards $\mathrm{DMSP_d}$ were measured out of the same samples by converting DMSP into DMS by using sodium hydroxide (NaOH). $\mathrm{DMSP_t}$ was analysed from unfiltered alkaline sub-samples. $\mathrm{DMSP_p}$ were calculated by subtracting DMS and $\mathrm{DMSP_d}$ from the $\mathrm{DMSP_t}$ value. After the DMSP analysis, the alkaline samples were stored for DMSO measurements back in the lab at GEOMAR. $\mathrm{DMSO_d}$ and $\mathrm{DMSO_t}$ were analysed from the same samples used for analysing $\mathrm{DMSP_d}$ and $\mathrm{DMSP_t}$, respectively. DMSO was converted into DMS by adding cobalt dosed sodium borohydride ($NaBH_4$) and analysed immediately with the same technique as mentioned above. The final $\mathrm{DMSO_p}$ values were calculated by subtracting $\mathrm{DMSO_d}$ from the total DMSO concentration. The mean errors given as standard deviations of the triplicate measurements, calculated according to David (1951) were ± 0.2 $\mathrm{nmol\,L^{-1}}$ (±20%) for DMS, ±0.4 $\mathrm{nmol\,L^{-1}}$ (±23%) for $\mathrm{DMSP_d}$, and ±0.5 $\mathrm{nmol\,L^{-1}}$ (±20%) for particulate $\mathrm{DMSP_p}$. For $\mathrm{DMSO_p}$ and $\mathrm{DMSO_d}$ a mean analytical error of ±2.3 $\mathrm{nmol\,L^{-1}}$ (±15%) and ± 0.5 $\mathrm{nmol\,L^{-1}}$ (±12%) was determined, respectively. Calibrations by using liquid standards were conducted every second day during the cruise and during the analysis in the lab. The precision and accuracy of the system was tested in the lab prior the cruise as described in Zindler *et al.* (2012). The entire analytical system was tested for blanks with carrier gas only and together with pure 18 MΩ MilliQ water (used for cleaning and standard preparation) as well as MilliQ water

enriched with sodium hydroxide in order to exclude contamination with environmental DMSO.

Concentrations of dissolved CH_4 were measured with a static equilibration method as described in detail in Bange *et al.* (2010). Distinct triplicate water samples for the determination of CH_4 were taken from the same underway seawater supply in parallel to the sampling of the sulphur compounds and phytoplankton pigments every twelve hours. The samples were poisoned with $HgCl_2$ (aq.) and analysed immediately after the cruise in the GEOMAR laboratory. The mean analytical error of dissolved CH_4 was ±17%. CH_4 saturations (Sat in %) were roughly estimated as Sat = 100 $[CH_4]/[CH_4]$eq, where $[CH_4]$eq is the equilibrium concentration (see Wiesenburg and Guinasso Jr., 1979) calculated with the *in-situ* temperature and salinity and a mean atmospheric CH_4 dry mole fraction of 1.80 ppm, which was considered to be a representative mean for the western Pacific Ocean during the time of the transit (Terao *et al.*, 2011).

2.2.2 Phytoplankton analysis

2.2.2.1 Phytoplankton pigments and group composition

Water samples for pigment and absorption analysis were filtered on GF/F filters, shock-frozen in liquid nitrogen, stored at -80°C and analysed in the AWI laboratory right after the cruise. The analysis of phytoplankton pigments was performed with High Performance Liquid Chromatography (HPLC) according to Taylor *et al.* (2011). Particulate and phytoplankton absorption was determined with a dual-beam UV/VIS spectrophotometer (Cary 4000, Varian Inc.) equipped with a 150 mm integrating sphere (external DRA-900, Varian, Inc. and Labsphere Inc., made from Spectralon™ using a quantitative filter pad technique as described in a modified version in Taylor *et al.* (2011) (for more details see also Rottgers and Gehnke (2012)). Table 2 in Taylor *et al.* (2011) summarizes the pigments analysed in this study and provides the information about which pigments have been allocated as marker pigments for the different phytoplankton groups. According to a procedure proposed by Vidussi *et al.* (2001) which was modified by Uitz *et al.* (2006) and most recently by Hirata *et al.* (2011), we estimated the contributions of three phytoplankton size classes (i.e. micro-, nano- and picophytoplankton representing the size classes of 20-200 µm, 2-20 µm and <2 µm, respectively) and seven phytoplankton groups based on the measured concentrations of seven diagnostic pigments (DP) to the biomass. The DP, the calculation procedure of the weighted relationships of these marker pigments and the determination of their biomasses are described in the supplemental material.

2.2.2.2 Identifying phytoplankton assemblages with hierarchical cluster analysis

In order to identify clusters of phytoplankton community composition, an unsupervised hierarchical cluster analysis (HCA) according to Torrecilla *et al.* (2011) was applied. The HCA groups the pigment measurements from the individual stations into different clusters according to their phytoplankton pigment compositions. The results were evaluated with an additional clustering of hyperspectral phytoplankton absorption coefficients (described in detail in the supplemental material).

2.2.3 Statistical Analysis

Linear regression analysis performed with the statistical computing software by RStudio™ (R Development Core Team, 2010; http://www.rstudio.org/) was used to identify significant correlations between sulphur compounds as well as between sulphur compounds and CH_4. Prior to the regression analysis, data were tested for Gaussian distribution and log-transformed if necessary. The F-statistic, the p-value and the R^2 were calculated.

Multiple linear regression models (MLRM) computed with RStudio™ were used to identify how the sulphur compounds might influence each other and which phytoplankton pigments might influence the sulphur compounds (for more details about the analytical procedure see the supplemental material). The MLRM were performed for the entire north-south-transit and again for the two main sub-regions referred as cluster 2 and cluster 4, which were demarcated according to the phytoplankton composition (Fig. 2.1, section 2.3.1). No statistical analysis could be performed for cluster 1 and cluster 3 due to the lack of a sufficient amount of data in these clusters.

2.3 Results and Discussion

2.3.1 Phytoplankton community structure in the western Pacific Ocean

In total, 106 surface stations along the north-south transit were measured. Phytoplankton biomass given as total chlorophyll a (TChl-a concentration in $\mathrm{mg\,m^{-3}}$) was very low (0.05-0.25 $\mathrm{mg\,m^{-3}}$), except for north of 36°N (TChl-a > 1 $\mathrm{mg\,m^{-3}}$) where colder waters (16°-20°C) of the Oyashio Current were observed, in the vicinity of islands (which were passed at 4°S, 8°S, 10°S and 12°S) and in the region of the Great Barrier Reef (Fig. 2.1b). Measured concentrations of marker pigments (e.g. fucoxanthin, see supplemental material for full description) and chlorophyll a (Chl-a) along the transit were used to

calculate the biomass of the major phytoplankton groups (Fig. 2.2). The phytoplankton biomass was generally dominated by picoplankton (sum of biomass of prochlorophytes and other cyanobacteria), with at least 50% contribution by the group of prochlorophytes, except in the Oyashio Current. At the stations with elevated TChl-a values, haptophytes contributed significantly to the phytoplankton biomass. Diatoms and chlorophytes only made a significant contribution (between 20 and 30%) to the biomass in the Oyashio Current.

Four phytoplankton clusters were identified in both the normalized pigment concentrations and the hyperspectral phytoplankton absorption coefficients data (Fig. 2.3). The resulting cluster trees are presented in Fig. 2.10 and 2.11 of the supplemental material. The high cophenetic index of 0.712 (see supplemental material) between the two cluster trees indicates a very good agreement between the two data sets used to identify the phytoplankton clusters.

The stations located in the Oyashio Current (north of 36°N) belong to cluster 1 which is characterized by high phytoplankton biomass (TChl-a $\sim$1 $\mathrm{mg\,m^{-3}}$) and a dominance of eukaryotic algae (mainly chlorophytes and haptophytes, and a smaller contribution from diatoms) and an absence of prochlorophytes. The majority of the stations belong to cluster 2 with low TChl-a (0.05-0.3 $\mathrm{mg\,m^{-3}}$). Cyanobacteria are dominating cluster 2, with prochlorophytes contributing more than other cyanobacteria. Cluster 2 stations are mainly found between 36° and 25°N (associated with the Kuroshio Current waters) as well as south of the equator (Fig. 2.3). Cluster 3 stations were found between 36°N and 25°N (the Kuroshio Current) and south of 10°S. They are mingled with cluster 2 stations. At cluster 3 stations waters are elevated in TChl-a (0.4-0.6 $\mathrm{mg\,m^{-3}}$) and cyanobacteria, mainly prochlorophytes, are dominating. Haptophytes were identified as the second largest group. Cluster 4 stations are mainly found in waters between 25°N and the equator and are characterized by a very low biomass (TChl-a <0.15 $\mathrm{mg\,m^{-3}}$). Cyanobacteria are dominating cluster 4 almost exclusively with prochlorophytes and other cyanobacteria contributing equally. The spatial distributions of the cluster 1 reflect the biogeographic province Kuroshio Current (KURO) as defined by Longhurst (1998) while cluster 2 to 4 are distributed throughout the three main provinces North Pacific Tropical Gyre (West) (NPTW), West Pacific Warm Pool (WARM) and Archipelagic Deep Basins (ARCH) (Fig. 2.3).

2.3.2 DMS, DMSP and DMSO concentrations in the western Pacific Ocean

Over the entire transit the average surface seawater (i.e. 5 m) concentrations for DMS as well as for dissolved DMSP ($\mathrm{DMSP_d}$) and DMSO ($\mathrm{DMSO_d}$) were 0.9, 1.6 and 4.4 $\mathrm{nmol\,L^{-1}}$, respectively. The average values for particulate DMSP ($\mathrm{DMSP_p}$) and DMSO

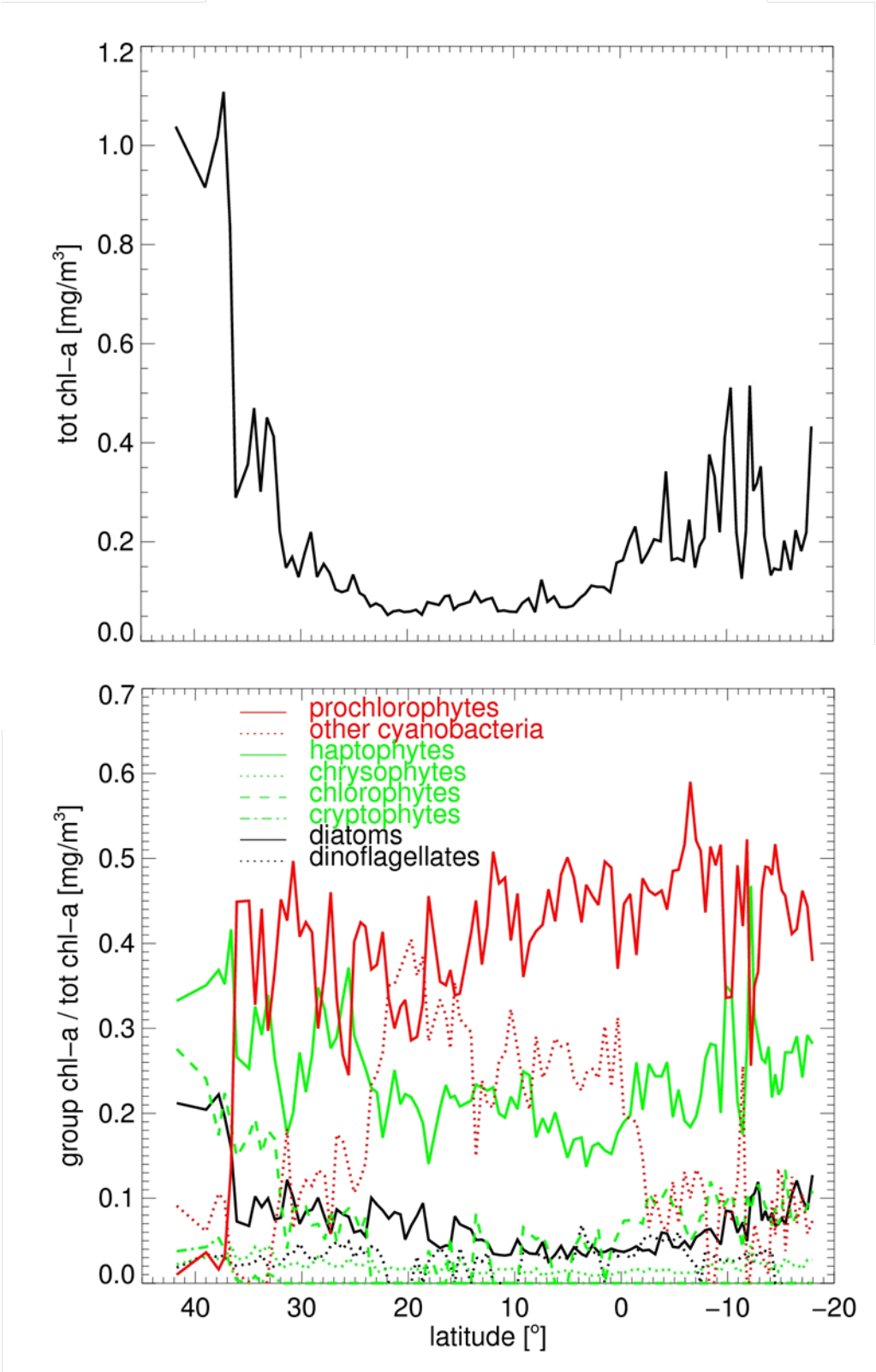

Fig. 2.2: *TChl-a concentration of main phytoplankton groups [$\mathrm{mg\,m^{-3}}$] as derived from major pigment composition (upper panel); ratio of phytoplankton group divided by the TChl-a concentration in correspondence to the latitude sampled (lower panel).*

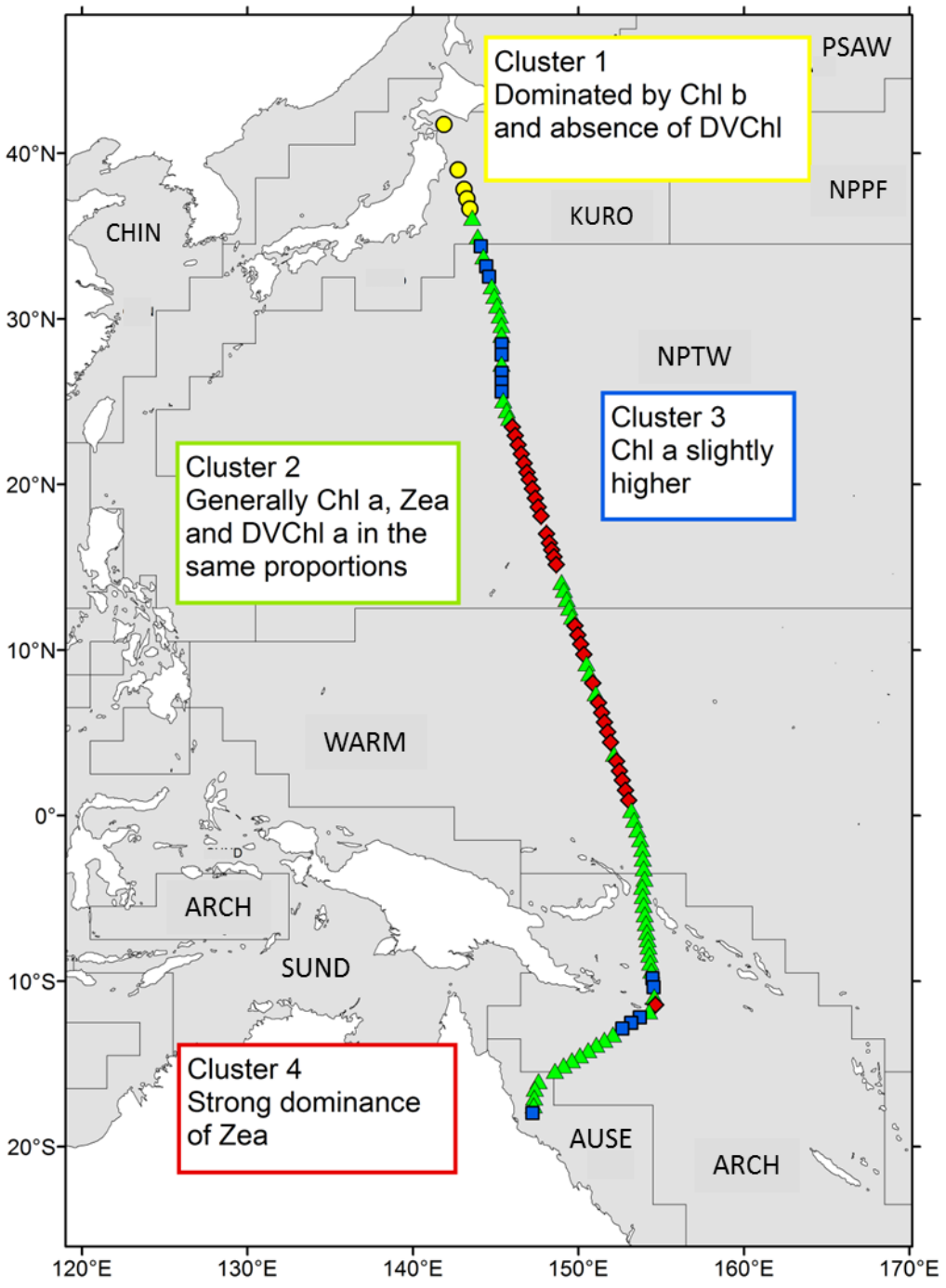

Fig. 2.3: *Distribution of clusters among pigment stations with the Longhurst provinces shown underneath. Yellow indicates cluster 1 (circles), green is cluster 2 (triangles), blue is cluster 3 (squares), and red is cluster 4 (diamonds).*

($DMSO_p$) were 2 and 11.5 $nmol\,L^{-1}$, respectively (Table 2.1). Highest concentrations for all sulphur compounds were measured when approaching the coasts of Japan and Australia (Fig. 2.1). The concentrations measured during this cruise were lower than the average surface measurements of DMS (1.8 $nmol\,L^{-1}$), $DMSP_d$ (5.9 $nmol\,L^{-1}$), and $DMSP_p$ (16.2 $nmol\,L^{-1}$) based on data collected between 1987 and 2004 in the upper 6 m of the western Pacific Ocean (data retrieved from the Global Surface Seawater DMS Database: http://saga.pmel.noaa.gov/dms). The climatology of DMS concentrations published by Lana *et al.* (2011) shows a lack of October data from the tropical West Pacific (i.e. Longhurst provinces NPTW and WARM, see Fig. 2.3). For the Longhurst provinces KURO, ARCH and AUSE (see Fig. 2.3) the mean October concentrations of DMS of the climatological predictions are given as $\sim$1 $nmol\,L^{-1}$, $\sim$5 $nmol\,L^{-1}$ and $\sim$4 $nmol\,L^{-1}$, respectively (Lana *et al.*, 2011). The differences between the climatological data and the data from our cruise might be caused by interannual variability and a general mismatch between climatological means and *in-situ* data. The increased DMS concentrations found off the Australian Coast are in agreement with previous finding that the Great Barrier Reef is a site of enhanced production of DMS (Fischer and Jones, 2012). The DMSO concentrations presented here are in agreement with the few published measurements of DMSO from the open Pacific Ocean, which range from 4 to 20 $nmol\,L^{-1}$, and DMSO measurements from the coastal areas of the Pacific Ocean which can reach values up to 181 $nmol\,L^{-1}$ (see overview in Hatton *et al.* (2005)).

2.3.3 Linear regressions between sulphur compounds

In this section and those that follow, correlations (linear regressions and multiple linear regressions) between sulphur compounds, phytoplankton pigments and methane are described. We are aware that correlations do not necessarily indicate causal relationships. However, they do illustrate interactions between the tested parameters, which hint at where further investigation may be fruitful. Therefore, we describe the significant correlations found and propose explanations for the possible relationships. These explanations are based on the current knowledge of the marine sulphur cycle and proof for these hypotheses requires further investigation.

We found a positive correlation between $DMSP_t$ and $DMSO_t$ (R^2 = 0.47, n = 104, p = <0.001, Fig. 2.4) as well as $DMSP_p$ and $DMSO_p$ (R^2 = 0.41, n = 85, p = <0.001, Fig. 2.4). This is in agreement with the finding of Simó and Vila-Costa (2006) who also reported a correlation between $DMSP_p$ and $DMSO_p$ and concluded that both compounds have the same source, namely phytoplankton. A strong link between the DMSP and DMSO pool were also found in several studies elsewhere (Lee and De Mora (1999) and references therein). They referred to a possible direct biosynthesis of DMSO in algae cells and doubt the DMS oxidation as the sole source of DMSO in the ocean.

Tab. 2.1: *DMS, DMSP and DMSO [$\mathrm{nmol\,L^{-1}}$] and total chl-a [$\mathrm{mg\,m^{-3}}$] concentrations as well as DMS, DMSP and DMSO versus total chl-a [$\mathrm{nmol\,mg^{-1}}$] for the entire transit and for cluster 2 and 4. The errors given in ± present standard deviation calculated according to David (1951). TChl-a errors were 2%.*

	DMS average range	$\mathrm{DMSP_d}$ average range	$\mathrm{DMSP_p}$ average range	$\mathrm{DMSP_t}$ average range
transit	0.88 ±0.2	1.57 ±0.4	2.04 ±0.5	4.01 ±0.7
	0.26 - 2.85	0.22 - 6.54	0.03 - 7.53	1.22 - 15.07
cluster 2	0.78 ±0.1	1.38 ±0.4	2.32 ±0.5	4.12 ±0.6
	0.26 - 1.25	0.54 - 2.57	0.03 - 7.53	1.22 - 8.73
cluster 4	0.99 ±0.3	1.10 ±0.3	1.08 ±0.4	2.81 ±0.5
	0.5 - 2.85	0.22 - 1.83	0.05 - 2.67	1.48 - 5.04
	$\mathrm{DMSO_d}$ average range	$\mathrm{DMSO_p}$ average range	$\mathrm{DMSO_t}$ average range	TChl-a average range
transit	4.42 ±0.5	11.46 ±2.3	15.50 ±2.3	0.21
	1.81 - 8.06	1.12 - 72.05	3.07 - 76.49	0.05 - 1.11
cluster 2	4.54 ±0.5	10.74 ±1.2	14.74 ±1.9	0.18
	1.81 - 7.82	2.01 - 22.5	3.07 - 25	0.08 - 0.38
cluster 4	4.26 ±0.5	8.11 ±1.0	12.11 ±1.5	0.08
	2.5 - 6.13	1.12 - 16.88	4.18 - 20.71	0.05 - 1.11
	DMS:TChl-a	$\mathrm{DMSP_d}$:TChl-a	$\mathrm{DMSP_p}$:TChl-a	$\mathrm{DMSP_t}$:TChl-a
transit	7.54	10.72	12.39	27.65
	1.01 - 39.48	2.12 - 44.83	0.12 - 52.44	2.88 - 60.85
cluster 2	5.08	8.57	13.62	24.97
	1.47 - 16.08	2.45 - 19.31	0.12 - 52.44	6.68 - 60.85
cluster 4	14.00	15.20	13.65	38.14
	5.96 - 39.48	3.27 - 24.26	0.61 - 24.78	20.22 - 58.24
	$\mathrm{DMSO_d}$:TChl-a	$\mathrm{DMSO_p}$:TChl-a	$\mathrm{DMSO_t}$:TChl-a	
transit	35.84	74.92	108.53	
	3.59 - 104.79	8.92 - 215.98	13.99 - 237.26	
cluster 2	29.42	62.99	89.46	
	8.1 - 69.59	14.7 - 128.34	13.99 - 154.67	
cluster 4	60.18	112.70	169.70	
	24.35 - 104.79	8.92 - 215.98	33.27 - 237.26	

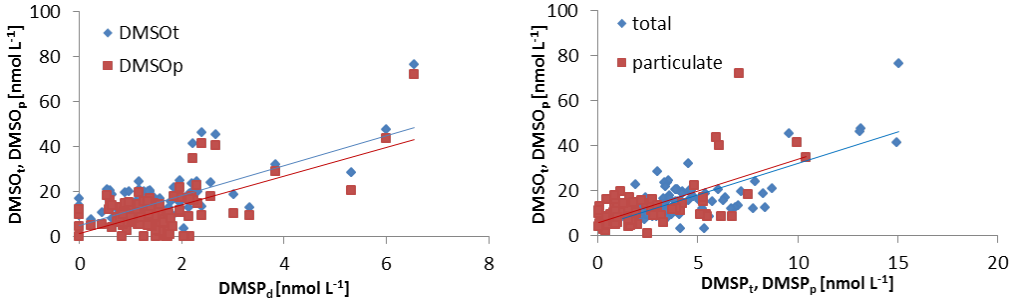

Fig. 2.4: *Left panel: Linear regression between DMSPd and DMSOt: y=6.66x+5.06,* R^2 *= 0.33, p-value: 1.414e-10, F-statistic: 50.86, n=105, and between DMSPd and DMSOp:* R^2 *= 0.35, y=6.41x+1.42, p-value: 6.493e-11, F-statistic: 53.53, n=102, both regressions for the entire data set. Right panel: Linear regression between DMSPt and DMSOt: y=2.84x+4.28,* R^2 *= 0.47, p-value: 9.613 e-16, F-statistic: 90.87, n=104 and between DMSPp and DMSOp, y=2.84x+5.68,* R^2 *= 0.41, p-value: 5.849e-11, F-statistic: 56.54, n=85, both regressions for the entire data set.*

No correlation was found between DMS and DMSO which is in contrast to the finding by Hatton *et al.* (1999, 2005) who attributed the correlation to photochemical and/or bacterial oxidation of DMS to DMSO in the water column (Hatton, 2002). However, the oxidation of DMS as a source for DMSO in the western Pacific Ocean cannot be excluded in general: A significant positive correlation was found between $DMSP_d$ and $DMSO_p$ (R^2 = 0.35, n = 102, p = <0.001, Fig. 2.4) as well as between $DMSP_d$ and $DMSO_t$ (R^2 = 0.33, n = 105, p = <0.001, Fig. 2.4) which may suggest that DMS, as an intermediate of the transformation of $DMSP_d$ to DMSO, is rapidly oxidised.

2.3.4 Relationship between sea surface temperature and $DMSP_p$: $DMSO_p$ ratio

A negative correlation between sea surface temperature (SST) and $DMSP_p$: $DMSO_p$ ratio was found by Simó and Vila-Costa (2006) based on a compilation of data from various oceanic regions (mainly from the North Atlantic Ocean and its adjacent marginal seas). On the basis of the data listed in Simó and Vila-Costa (2006), we recalculated mean $DMSP_p$: $DMSO_p$ ratios as well as mean SST for the various campaigns. In addition, we added other data: from the East China Sea (ratio: 0.27, 17.2°C) (Yang and Yang 2011), the northern Baffin Bay (ratio: 0.20, estimated 0°C) (Bouillon *et al.*, 2002) and the average $DMSP_p$: $DMSO_p$ ratio (0.22 ±0.27) and the average SST (28.3 ± 2.7 °C) computed from the measurements during the transit presented here (see Fig. 2.5). In agreement with Simó and Vila-Costa (2006) we found a significant negative linear correlation between $DMSP_p$: $DMSO_p$ ratios and SST for the temperature range 5° to 28°C (R^2 = 0. 61). Moreover, a positive correlation (R^2 = 0.67) was also visible in the SST range <10°C indicating that there seems to be a maximum of $DMSP_p$: $DMSO_p$ ratios at approximately

5°-10°C. This is in line with the observations that blooms of coccolithophorids (major DMSP producers (Simó, 2001)) usually occur in high (subpolar) latitudes at SST around 9°C (3°-15°C) (Iglesias-Rodriguez *et al.*, 2002). Our findings are in line with the argumentation of Simó and Vila-Costa (2006) who proposed that (i) in warm waters DMSO enriched nano- and picoplankton is dominating the phytoplankton community (indeed we found that nano- and picoplankton was dominant during the transit, see section 3.1), and (ii) high SST could be associated with surface waters receiving a high solar radiation dose which triggers a cascade reaction system, including enhanced DMSO production, as a reply to nutrient limitation and oxidative stress (Sunda *et al.*, 2002).

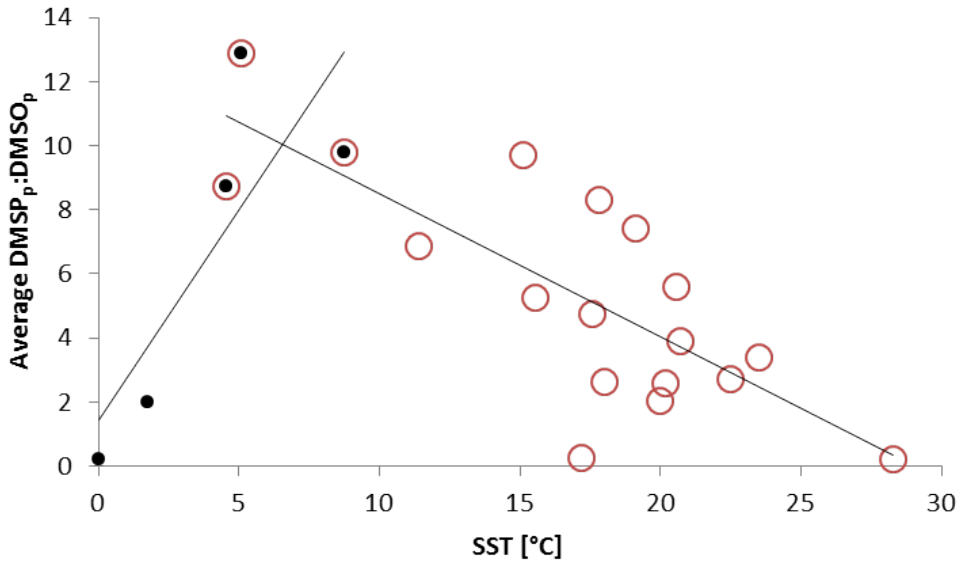

Fig. 2.5: *Average DMSPp:DMSOp ratios vs. SST. Mean ratios for individual campaigns are recalculated from the data listed in Simó and Vila-Costa (2006). We added data points consisting of the mean DMSPp:DMSOp and SST (given in parenthesis) from the East China Sea (0.27, 17.2°C) (Yang and Yang 2011), the northern Baffin Bay (0.20, estimated 0°C) (Bouillon et al., 2002) and the western Pacific Ocean (0.22, 28°C) (this study). The linear correlations are y = -0.445x + 12.96 (R^2 = 0.61, open circles) and y = 1.312x + 1.44 (R^2 = 0.67, solid circles).*

2.3.5 Interactions between sulphur compounds explained by multiple linear regression models (MLRM)

In order to find further statistically significant interactions between the different sulphur compounds, MLRM were used. The MLRM calculations were performed either with the entire data set or with a subset of cluster 2 and cluster 4 data, respectively. Both cluster 2 and 4 were characterized by low biomass and were mainly dominated by cyanobacteria

like prochlorophytes which are not known to be DMSP producers (Keller *et al.*, 1989). This resulted in low DMS and DMSP concentrations (see section 2.3.2, Fig. 2.1). In the following sections we discuss the main results of the MLRM (see Table 2.2). The complete MLRM results are listed in the supplemental material (Figure 2.8).

2.3.5.1 DMS

Over the entire transit, the DMS concentration is influenced by the $\mathrm{DMSP_p}$ and $\mathrm{DMSO_p}$ distribution ($\mathrm{R^2}$ = 0.32, Table 2.2, a). It is possible that the DMS concentration was coupled to particulate DMSP and DMSO through the antioxidation system in algae cells (Sunda *et al.*, 2002). It is most likely that in the tropical waters of the western Pacific Ocean the radiative stress on phytoplankton was enhanced. Furthermore, Spiese *et al.* (2009) suggested that the ability of marine phytoplankton to reduce DMSO to DMS is ubiquitous. This mechanism might be an additional explanation for the link between DMS and DMSO in the western Pacific Ocean. Within the clusters 2 and 4 all sulphur compounds have an influence on the DMS pool (Figure 2.8, supplemental material).

2.3.5.2 DMSP

A link between $\mathrm{DMSP_d}$ and the DMSO pool for the entire transit could be found ($\mathrm{R^2}$ = 0.32, Table 2.2, d). A same source for both compounds in certain algae species might explain the link between these compounds. The MLRM showed, especially in the clusters 2 and 4, that all sulphur compounds correlated with the $\mathrm{DMSP_{d/p}}$ pool (Figure 2.8, supplemental material). This is in line with several studies which referred to the fast cycling, within a few hours, between the different sulphur compounds (Simó, 2004; Stefels *et al.*, 2007).

2.3.5.3 DMSO

The MLRM showed that $\mathrm{DMSP_d}$ and DMS influenced the $\mathrm{DMSO_d}$ pool for the entire transit ($\mathrm{R^2}$ = 0.19, Table 2.2, i). It is most likely that $\mathrm{DMSO_d}$ is directly produced due to the oxidation of DMS in the water column (Hatton *et al.*, 2005). $\mathrm{DMSP_d}$ might be used by free living bacteria in the water column as a substrate to produce DMSO. Additionally, $\mathrm{DMSP_d}$ could be converted to DMS by bacteria which can contribute to the DMS pool. However, these processes might be of minor importance because it only explains 19% of the $\mathrm{DMSO_d}$ distribution. Thus, other factors are probably more important for the $\mathrm{DMSO_d}$ concentration, such as direct synthesis in algae cells and release into the water column (Simó *et al.*, 1998), and photo-oxidation of DMS to DMSO (Hatton *et al.*, 1996).

Tab. 2.2: *Significant multiple linear regressions between DMS, DMSP and DMSO (d=dissolved, p=particulate, t=total) for the entire data set and within the cluster 2 and 4. Single coefficients and p-values of each multiple linear regression model as well as* R^2*, F-statistic and p-value of each entire model are given. The response variable is given under the model number. The independent variable squared shows a quadratic relationship to the response variable. The complete output of all models is given in the supplemental material (the data presented here is extracted from Figure 2.8 in the supplement). Abbr.: st.: statistic; e. m.: entire model; e. d. s.: entire data set; a – m: number of models*

model no.	single coefficients	p-value	R^2, F-st., p-value (e. m.)
a	$DMSP_p$	2.36E-09	0.32
DMS	$DMSO_p$	1.49E-07	24.57
e. d. s.			1.83E-09
d	$DMSO_p^2$	1.14E-07	0.32
$DMSP_d$	$DMSO_d^2$	0.02	16.22
e. d. s.	$DMSP_p$:$DMSO_p$	3.27E-04	1.084e-08
i	$DMSP_d$	0.04	0.19
$DMSO_d$	DMS^2	5.13E-05	8.05
e.d.s.	$DMSP_d^2$	0.03	7.26E-05
j	$DMSP_p$	0.03	0.28
$DMSO_d$	$DMSP_d$	0.01	4.82
cluster 2	$DMSP_p^2$	0.05	0.002
	$DMSP_p$:$DMSP_d$	0.005	
k	$DMSP_p$	0.001	0.35
$DMSO_d$	$DMSO_p$	0.004	4.59
cluster 4	$DMSP_p$:$DMSO_p$	0.002	0.01
l	$DMSP_d$	5.61E-07	0.43
$DMSO_p$	$DMSP_p$	6.72E-08	36.53
e. d. s.			1.49E-12
n	DMS	0.06	0.46
$DMSO_p$	$DMSP_d$	0.05	7.23
cluster 4	$DMSP_p$	1.26E-04	0.001

In cluster 2, $DMSO_d$ seemed to be dependent only on the DMSP pool (R^2 = 0.28, Table 2.2, j), while in cluster 4, $DMSP_p$ and $DMSO_p$ were significant contributors (R^2 = 0.35, Table 2.2, k). Furthermore, $DMSO_p$ was directly dependent on $DMSP_{d/p}$ (R^2 = 0.43, Table 2.2, l) over the entire transit and in the region of cluster 4 (R^2 = 0.46, Table 2.2, n) comparable to $DMSO_d$.

These findings are in line with the direct correlations (see section 2.3.3) and confirm the assumption of direct biosynthesis of DMSO in the phytoplankton and the possible same source of $DMSO_p$ and $DMSP_p$ in certain algae taxa. Due to the ability of DMSO to permeate easily through membranes, a coupling of $DMSO_d$ and $DMSO_p$ seems reasonable. The production of $DMSO_p$ from $DMSP_d$ may be explained by bacteria that are attached to particles and use $DMSP_d$ as a substrate. The statistical analysis underlines the importance of DMSO for the sulphur cycle and the tight coupling especially between DMSO and DMSP.

2.3.6 Influence of phytoplankton on the DMS, DMSP and DMSO distributions in surface seawater

Linear positive correlations between TChl-a and $DMSO_p$, $DMSO_t$, $DMSP_d$ as well as $DMSP_p$ were found for the entire dataset (R^2 = 0.25, n=94; R^2 = 0.22, n=96; R^2 = 0.29, n=99; and R^2 = 0.23, n=87, for all p=<0.001, respectively). These correlations were somewhat weak, which may result from a dependency on certain algae taxon and not on phytoplankton in general for both DMSP and DMSO. In contrast, Lee *et al.* (1999b) found a negative correlation between $DMSO_p$ and Chl-a in a Canadian Fjord. They explained this observation with an increase in photosynthetic activity and, therefore, an increase in free radicals which reacted with DMSO. However, the correlations found in the Fjord were dependent on temporal variability and on the nano- to picoplankton fraction, in contrast to the general correlations presented in this section. Thus, more detailed correlations between phytoplankton and DMSO in western Pacific Ocean might shed more light on the possible relationships (see section 2.3.6.3).

2.3.6.1 DMS and phytoplankton groups

The influence of a variety of phytoplankton groups on the different sulphur compounds for the entire transit and within the clusters 2 and 4 were also tested by using the MLRM. The following phytoplankton groups were tested (characteristic marker pigments are given in parenthesis): diatoms (fucoxanthin (main indicator for diatoms), diatoxanthin, diadinoxanthin (both unspecific, mainly diatoms)), dinoflagellates (peridinin), cryptophytes (alloxanthin), haptophytes (19'- hexanoyloxyfucoxanthin), chrysophytes (19'- butanoyloxyfucoxanthin), prasinophytes (prasinoxanthin), chlorophytes (violaxanthin), cromophytes

Tab. 2.3: *Significant multiple linear regressions between DMS, DMSP and DMSO (d=dissolved, p=particulate, t=total) and phytoplankton marker pigments for the entire data set and within the cluster 2 and 4. Single coefficients and p values of each multiple linear regression model as well as* R^2*, F-statistic and p-value of each entire model are given. The response variable is given under the model number. The independent variable squared shows a quadratic relationship to the response variable. The complete output of all models is given in the supplemental material (the data presented here is extracted from Table II in the supplement). Abbr.: st.: statistic; e. m.: entire model; e. d. s.: entire data set; fuco: fucoxanthin; hex: 19'-hexanoyloxyfucoxanthin, peri: peridinin, diato: diatoxanthin,dia: diadinoxanthin, diato: diatoxanthin, but: 19'-butanoyloxyfucoxanthin;zea: zeaxanthin*

model no.	single coefficients	p-value	R^2, F-st., p-value (e. m.)	model no.	single coefficients	p-value	R^2, F-st., p-value (e. m.)
a	fuco	0.004	0.32	**i**	diato	0.03	0.42
DMS	hex	0.01	3.66	$DMSO_d$	hex^2	1.11E-04	7.55
cluster 2	$peri^2$	0.003	0.005	e. d. s.	but^2	9.68E-05	1.65E-07
b	but	1.01E-05	0.44	**j**	peri	1.24E-05	0.45
$DMSP_d$	peri	2.96E-04	11.34	$DMSO_d$	dia	4.38E-02	10.1
e. d. s.	zea	2.01E-06	2.36E-09	cluster 2	but	8.61E-03	4.81E-06
c	fuco	0.01	0.61	**k**	fuco	6.83E-06	0.54
$DMSP_d$	diato	0.01	5.93	$DMSO_p$	diato	1.09E-03	9.18
cluster 2	but^2	1.91E-03	1.15E-05	e. d. s.	zea	1.76E-06	8.46E-10
					$peri^2$	1.50E-05	
d	peri	9.88E-03	0.37				
$DMSP_p$	but	9.23E-05	9.3	**l**	peri	7.63E-03	0.84
e. d. s.	fuco	0.05	5.01E-08	$DMSO_p$	diato	3.56E-03	12.98
				cluster 2	but	0.04	1.93E-09
e	fuco	2.32E-04	0.73				
$DMSP_p$	diato	2.46E-03	11.94				
cluster 2	zea	5.32E-04	4.02E-08				
	hex	3.51E-02					

(anthreaxanthin) and cyanobacteria (zeaxanthin). Chlorophyll pigments were not used for the calculations due to their occurrence in all phytoplankton groups.

The model showed that algae groups played a minor role for the DMS distribution over the entire transit. Only in cluster 2, diatoms, haptophytes and dinoflagellates were tested significantly for DMS (R^2 = 0.32, Table 2.3, a). Bürgermeister *et al.* (1990) and Merzouk *et al.* (2008) found increased DMS concentrations caused by diatoms in the Atlantic Ocean. Elevated abundance of haptophytes and dinoflagellates were measured together with enhanced DMS concentrations in different oceanic regions in general. Additionally, all these algae groups were identified as important contributors to the $DMSP_d$/p pool with the MLRM in this study (see below), which indicated that DMS was probably only indirectly dependent on these algae via bacteria. This finding is in line with Yoch (2002), Kiene *et al.* (2000) and Schäfer *et al.* (2010), reporting that DMS is mainly controlled by the activity of bacterioplankton. It might be possible that DMS was rapidly converted into DMSO by bacteria which used DMS as an energy source (Boden *et al.*, 2011; Green *et al.*, 2011). This fast conversion could explain the low DMS concentrations and the lack of correlations between algae and DMS along the western Pacific Ocean transit.

2.3.6.2 DMSP and phytoplankton groups

Over the entire transit, the main phytoplankton groups which influenced the $DMSP_d$ distribution were dinoflagellates, chrysophytes, and cyanobacteria, although cyanobacteria are not considered to be important DMSP producers (Keller *et al.*, 1989). In contrast, diatoms appear to be the most important algae group in cluster 2 both for $DMSP_d$ and $DMSP_p$ (R^2 = 0.61, Table 2.3, c; R^2 = 0.73, Table 2.3, e; respectively). Dinoflagellates, chrysophytes, and diatoms appeared to be the most important contributors to the $DMSP_p$ pool (R^2 = 0.37, Table 2.3, d) for the entire transit. In cluster 4 no pigment was found that contributed significantly to $DMSP_{d/p}$.

Belviso *et al.* (2001) showed a clear relationship between $DMSP_p$ and haptophytes as well as chrysophytes with over 200 samples from different regions (Atlantic Ocean, Mediterranean Sea and Southern Ocean) by using linear regression. Although haptophytes were only important for $DMSP_p$ in cluster 2 chrysophytes were identified as important algae group for all DMSP pools in this study. Dinoflagellates were identified as producers for all DMSP pools in the Pacific Ocean, which is in agreement with findings in other marine regions (Keller *et al.*, 1989; Stefels, 2000; Steinke *et al.*, 2002). Surprisingly, diatoms and cyanobacteria influenced DMSP, although these algae groups are thought to be minor DMSP producers in general (Keller *et al.*, 1989). The cyanobacteria and diatoms were distributed in similar patterns to the DMSP producing taxa, possibly causing the model to identify them as contributors to the DMSP pool. It should also be considered that cyanobacteria were dominating the main part of the West Pacific Ocean transit

and were mainly responsible for the TChl-a concentration, which correlated slightly with DMSP. In addition, some specialized diatom species in the Pacific Ocean may also be able to produce a sizable amount of DMSP. Keller *et al.* (1989) showed that certain species of diatoms can be significant for the DMSP pool. Thus, this alga taxon cannot be dismissed as DMSP contributor in general.

2.3.6.3 DMSO and phytoplankton groups

Diatoms, haptophytes and chrysophytes correlated significantly with $\mathrm{DMSO_d}$ ($\mathrm{R^2}$ = 0.42, Table 2.3, i). In cluster 2, dinoflagellates, diatoms and chrysophytes were the most important pigments for the $\mathrm{DMSO_d}$ as well as for the $\mathrm{DMSO_p}$ distribution ($\mathrm{R^2}$ = 0.45, Table 2.3, j; $\mathrm{R^2}$ = 0.84, Table 2.3, l, respectively). Furthermore, diatoms, cyanobacteria and dinoflagellates seemed to influence the $\mathrm{DMSO_p}$ distribution for the entire data set ($\mathrm{R^2}$ = 0.54, Table 2.3, k). In cluster 4 no significant correlations could be found.

For DMSP and DMSO the same algae groups were identified as important sulphur producers but in different compositions dependent on the sulphur compound and the region. Field measurements conducted by Lee *et al.* (1999b) and culture experiments with dinoflagellates and haptophytes which showed high $\mathrm{DMSO_p}$ production (Simó *et al.*, 1998) suggested that $\mathrm{DMSO_p}$ might be produced by a broad range of phytoplankton comparable to that of DMSP producing algae groups. The authors did not exclude that other species, which are not known as DMSP producers, might also be responsible for a significant amount of DMSO. In this study, we also found that $\mathrm{DMSO_p}$ correlated with phytoplankton pigments of known DMSP producers. However, the pigment analysis did not show direct correlations between DMSO and pigments from non-DMSP producing phytoplankton. Cryptophytes, prasinophytes, chlorophytes and cromophytes showed no or a negligible influence on the distribution of all tested sulphur species in the western Pacific.

Only few correlations were found in cluster 4 compared to cluster 2 and the entire transit. Cluster 4 included mainly the oligotrophic warm waters of the West Pacific Ocean dominated by cyanobacteria. The distribution pattern of phytoplankton is similar to cluster 2. However, cluster 4 was different from other clusters by its particularly low biomass, as well as the lowest sulphur concentrations of the entire transit (Fig. 2.1). It seems that the very low biomass was the main factor governing the concentrations of sulphur in this region, with a minor influence of the algae composition. Thus, large regions in the subtropical and tropical western North Pacific Ocean did not have a highly dynamic sulphur cycle in the surface ocean during the transit in October 2009.

2.3.7 Sulphur compounds as precursors for methane

The CH_4 concentrations (corresponding saturations are given in parenthesis) during the cruise were in the range from 1.8 to 4.8 $\mathrm{nmol\,L^{-1}}$ (91 – 218 %) with an average (± standard deviation) of 2.5 ±0.8 $\mathrm{nmol\,L^{-1}}$ (127 ±32 %). The highest CH_4 concentrations (3.8 – 4.8 $\mathrm{nmol\,L^{-1}}$; 159 – 218 %) were measured at the beginning of the cruise in the cold waters of the Oyashio Current (north of 36°N), followed by a drop in CH_4 concentrations to 2.8 – 1.8 $\mathrm{nmol\,L^{-1}}$ (142 – 96 %) when the warm Kuroshio Current was crossed (between 36° and 25°N). The lowest CH_4 concentrations (2.0 ±0.2 $\mathrm{nmol\,L^{-1}}$; 104 ±11 %) were measured between the equator and 28°N and, thus, they were roughly associated with cluster 4 (see section 3.1). The average CH_4 concentrations between the equator and 19°S was 2.4 ±0.5 $\mathrm{nmol\,L^{-1}}$ (127 ±26 %). Thus we conclude that the ocean during the transit was an overall weak net source of CH_4 to the atmosphere. Comparable mean surface CH_4 concentrations of 2.5 ±0.3 $\mathrm{nmol\,L^{-1}}$ and 2.2 ±0.02 $\mathrm{nmol\,L^{-1}}$ were measured along 165°E between 40°N and 5°S and in the Kuroshio Current waters (27-30°N, 133-142°E), respectively, by Watanabe *et al.* (1995). Rehder and Suess (2001) measured CH_4 surface concentrations in the range from 2.5 to 5 $\mathrm{nmol\,L^{-1}}$ between 38.6° and 42°N in the Tsugaro Current outflow/Oyashio Current mixing region and a drop in CH_4 concentrations to 2.3 $\mathrm{nmol\,L^{-1}}$ when Kuroshio Current waters were measured in the coastal waters off Honshu further south. Moreover, Bates *et al.* (1996) reported CH_4 concentrations between 1.6 and 3.6 $\mathrm{nmol\,L^{-1}}$ for a series of five latitudinal transects in the Pacific Ocean.

We found a significant positive correlation between TChl-a and CH_4 surface concentrations (R^2 = 0.69, p=<0.001, n=36, Fig. 2.6). There are only a few other studies which report a correlation between Chl-a and CH_4 (Owens *et al.*, 1991; Damm *et al.*, 2008). Watanabe *et al.* (1995) found a general trend but no significant correlation along 165°E. Since the majority of the studies did not find a correlation between Chl-a and CH_4 and direct evidence from lab experiments with (axenic) algae cultures has not been published yet, it is widely accepted that the accumulation of CH_4 in the upper open ocean is not related to a direct production by algae.

In our study, significant positive linear correlations were found between $\mathrm{DMSO_p}$ and CH_4 (R^2 = 0.37, p=<0.001, n=31) and $\mathrm{DMSO_t}$ and CH_4 (R^2 = 0.42, p=<0.001, n=33), as well as between $\mathrm{DMSP_d}$ and CH_4 (R^2 = 0.57, p=<0.001, n=35) for the entire north-south transit (Fig. 2.7). Additionally, we found a good correlation between CH_4 and the marker pigment for chrysophyceae (R^2 = 0.76, p=<0.001, n=36, Fig. 2.6), which are known as DMSP producers (Belviso *et al.*, 2001) and which were well correlated with $\mathrm{DMSP_d}$ and $\mathrm{DMSO_t}$ in our study (see sections 2.3.6.2 , 2.3.6.3). Therefore, we conclude that algae derived DMSP and DMSO might be considered as possible precursors for CH_4 production in the western Pacific Ocean. However, further direct evidence is necessary to support this suggestion.

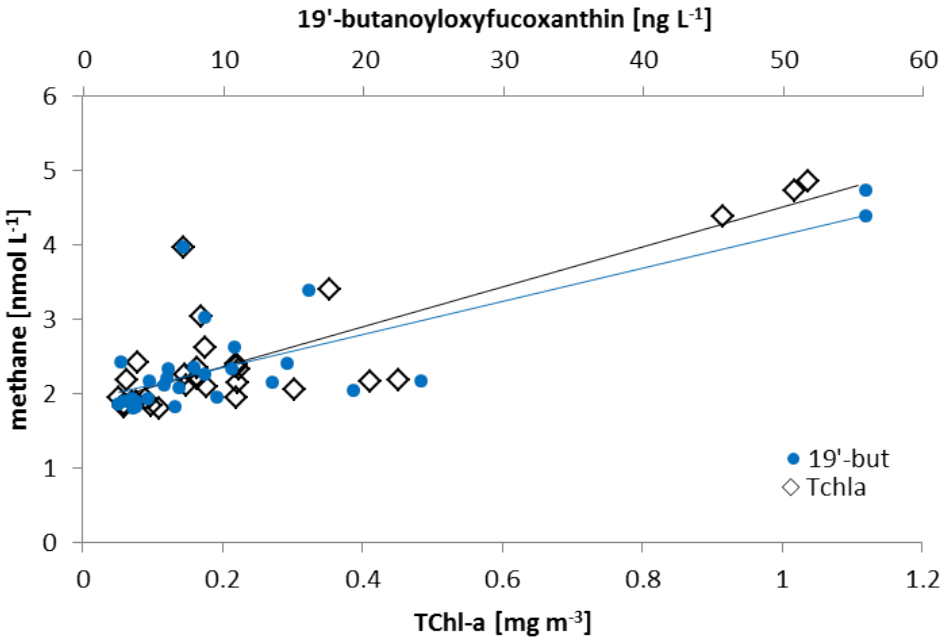

Fig. 2.6: *Linear regression between TChl-a and methane (y=0.0027x+1.82,* R^2 *= 0.69, F-statistic: 63, p-value <0.001, n = 36, open diamonds) and between chrysophytes (indicated by marker pigments 19'- butanoyloxyfucoxanthin, upper x-axis) and methane (y=0.044x+1.92,* R^2 *= 0.76, F-statistic: 80, p-value: <0.001, n = 36, solid circles).*

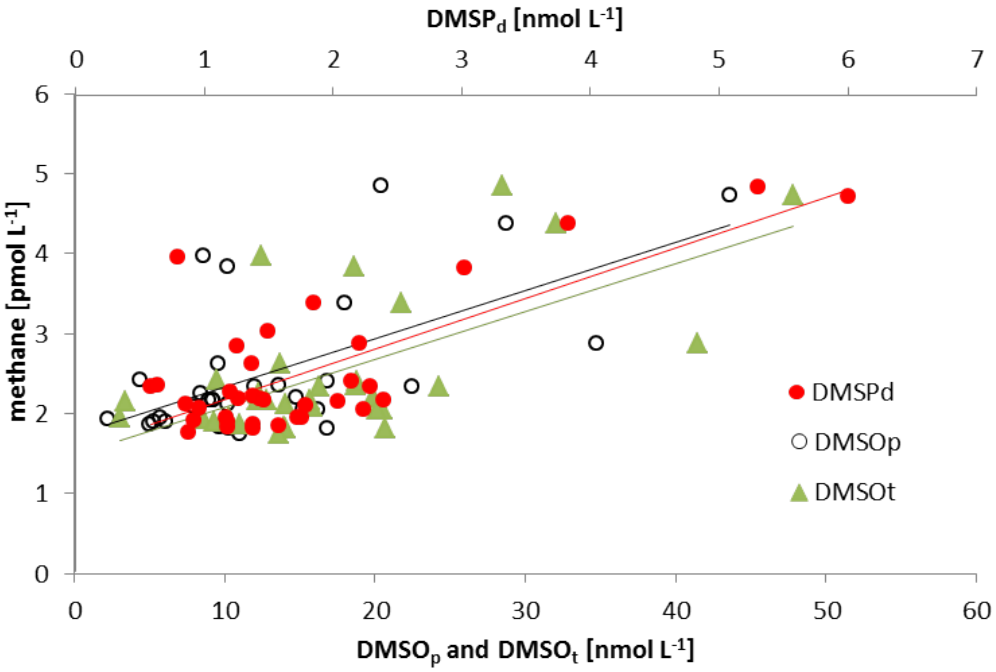

Fig. 2.7: *Relationship between the sulphur compounds (*$\mathrm{DMSP_d}$, $\mathrm{DMSO_p}$, $\mathrm{DMSO_t}$ *[*$\mathrm{nmol\,L^{-1}}$*]) and methane [*$\mathrm{nmol\,L^{-1}}$*] in the surface water of the north-south transit in the Western Pacific Ocean.* $\mathrm{DMSP_d}$ *vs. methane: y=0.55x+1.54,* R^2 *= 0.57, F statistic: 43.08, p-value: 1.85e-7, n=36;* $\mathrm{DMSO_p}$ *vs. methane: y=0.06x+1.72,* R^2 *= 0.37, F statistic: 17.25, p-value: 2.64e-4, n=31;* $\mathrm{DMSO_t}$ *vs. methane: y=0.06x+1.48,* R^2 *= 0.42, F statistic: 22.49, p-value: 4.5e-05, n=33.*

Damm *et al.* (2008) showed a significant negative correlation between $\mathrm{DMSP_t}$ and CH_4 (R^2 = 0.55) in the surface waters of an Arctic shelf region (Storfjorden, Svalbard Archipelago), which is in contrast to the positive correlation with $\mathrm{DMSP_d}$ found in our study. Moreover, we could not find any correlation between $\mathrm{DMSP_t}$ and CH_4 in our data from the western Pacific Ocean. Thus, there are obvious differences between the results from the Storfjorden and the West Pacific Ocean (despite the fact that the conclusions are identical): The algal community in the West Pacific Ocean during our cruise was very likely suffering from continuous oxidative stress and nutrient limitation which could have led to a continuous production of $\mathrm{DMSP_p}$ (Sunda *et al.* 2002), and thus, $\mathrm{DMSP_d}$. This, in turn, implies a continuous formation of CH_4 from $\mathrm{DMSP_d}$ via the demethylation pathway (Moran *et al.*, 2012) and may explain the positive correlation between the $\mathrm{DMSP_d}$ and CH_4. In contrast, a bloom situation was encountered in the Storfjorden which implies that the algae did not suffer from oxidative stress and/or nutrient limitation and therefore a continuous production of DMSP was not necessary. The negative correlation found in Storfjorden might have been caused by the fact that CH_4 has been produced from intermediates resulting from a DMSP pool which was not replenished at the time of the bloom. Additionally, it should be noted that Damm *et al.* (2008) observed increasing CH_4 concentrations when $\mathrm{DMSP_t}$ concentrations were >5 $\mathrm{nmol\,L^{-1}}$ but could see no effect on the CH_4 concentrations when $\mathrm{DMSP_t}$ levels were <5 $\mathrm{nmol\,L^{-1}}$. In our study, however, a correlation between $\mathrm{DMSP_d}$ and CH_4 was found although the concentrations for both compounds were much lower. This reflects less intensive biological activity, perhaps due to different assemblages of bacterioplankton, physiological stages of the bacteria and/or nutrient limitation and oxidative stress compared to the Storfjorden.

A negative correlation between CH_4 and $\mathrm{DMSP_t}$ was also found in phosphate enriched, but nitrogen depleted, oligotrophic Arctic Sea waters originating from the Pacific Ocean. This indicates that CH_4 production from $\mathrm{DMSP_t}$ degradation products in oligotrophic Arctic waters seems to be mainly depending on the availability of phosphate (Damm *et al.*, 2010). Despite the fact that nutrient data are not available for the TransBrom cruise, it is reasonable to assume that the surface waters in the western tropical Pacific Ocean during TransBrom were depleted in both phosphate and nitrate (see e.g. World Ocean Atlas of the National Oceanographic Data Center[1]). Thus, the CH_4 production from DMSP degradation products in the west Pacific Ocean seems to be triggered by a different mechanism than the one found in Arctic waters. In a microcosm experiment conducted in the central Arctic, three main proteobacteria groups were identified as possible CH_4 producers which seemed to have produced CH_4 (indirectly) by degradation of DMSP (Damm *et al.*, 2010): *Rhodobacter*, *Sulfitobacter* (both in the family: *Rhodobacteraceae*) and *Mesorhizobium* types. It is noteworthy that bacteria of *Rhodobacteraceae* are widespread in the oligotrophic oceans and have genes that metabolize DMSP (Moran *et al.*, 2007;

[1] http://www.nodc.noaa.gov/OC5/SELECT/woaselect/woaselect.html

Moran *et al.*, 2003; Moran *et al.*, 2012) and therefore we may conclude that they could have been responsible for the CH_4 production along the north-south transit in the Pacific Ocean. However, this needs to be proven directly by conducting experiments with these bacteria groups in lab culture experiments.

For the first time a correlation between DMSO and CH_4 could be observed in surface ocean waters. There are two possible pathways: 1) DMSO was reduced to DMS (Hatton *et al.*, 2005; Spiese *et al.*, 2009), which, in turn, may act as a precursor for CH_4 and 2) a direct (biological or non-biological) production of CH_4 from DMSO. However, microbial production of CH_4 from DMS as well as a chemical production of CH_4 via reaction of OH with $\mathrm{DMSO_d}$ (Eberhardt and Colina, 1988) are known to occur only under anoxic conditions. Thus, the exact pathway and mechanism of CH_4 production from DMSO in the oxic surface layer remains to proven. If DMSO is a potential precursor or substrate for the marine CH_4 production, the influence of DMSO on the CH_4 pool in the deep oceans is underestimated because of the widespread distribution of DMSO throughout the entire water column (Bouillon *et al.*, 2002; Hatton *et al.*, 1999).

2.4 Summary

Along the north-south transit of the TransBrom cruise, the western Pacific Ocean contained low biomass except in the cold Oyashio Current waters, in coastal regions in the vicinity of islands and the Great Barrier Reef. The low biomass regions were dominated by picoplankton with prochlorophytes dominating. In high TChl-a regions, haptophytes contributed significantly to the biomass.

For the first time a DMSO distribution pattern was presented in surface seawater along a north-south transit in the western Pacific Ocean. Correlations between DMSO and DMSP, as well as DMSO and DMSP with TChl-a, were observed for the entire transit, suggesting a similar source for both sulphur species, namely biosynthesis in specialized algae. Several algae groups were identified as contributors to the DMSP and DMSO pool, mostly haptophytes, chrysophytes and dinoflagellates. Diatoms were also identified although they are not known to be significant sulphur producers. DMSP and DMSO seemed to be influenced by largely the same algae species, indicating that DMSP producing algae might have the potential to synthesis DMSO as well.

The observed $\mathrm{DMSP_p} : \mathrm{DMSO_p}$ ratios were extremely low and generally <1. They seem to be characteristic for oligotrophic tropical waters representing the extreme endpoint of the global $\mathrm{DMSP_p} : \mathrm{DMSO_p}$ ratio vs. SST relationship. It is most likely that nutrient limitation and oxidative stress in the tropical West Pacific Ocean triggered enhanced DMSO production. $\mathrm{DMSP_d}$ and $\mathrm{DMSO_{p/t}}$ were positively correlated with CH_4 for the entire north-south transit, although the concentrations of both sulphur compounds and

CH_4 were low. We conclude that DMSP could be considered as a potential precursor for CH_4 production in the surface waters of the western Pacific Ocean. For the first time we could show that DMSO might act as a precursor or substrate for CH_4 production as well. However, further studies are necessary to understand how sulphur compounds are converted into CH_4 in oxic environments.

Acknowledgements

We acknowledge the support of the captain and crew of R/V Sonne as well as Birgit Quack, chief scientist of the "TransBrom-Sonne" project. We thank Franziska Wittke for assistance with the measurements of the sulphur compounds. Funding for the Phytooptics group was provided by the HGF Innovative Network Funds (Phytooptics) and via the EU project SHIVA-226224-FP7-ENV-2008-1. Part of this study was performed during a visit of ET at the Phytooptics group supported by the Spanish National Research Council CSIC (project ANERIS PIF08-015) and the Spanish Ministry of Education (PhD European Mentoring Program). We thank Janina Seemann, Erika Allhusen, and Sonja Wiegmann for lab analysis and Anja Bernhardt, Tilman Dinter, Dörte Stange and Kim Quack for their work on board for Phytooptics and all other scientists for their support on board. Financial support for this study was provided by the BMBF SOPRAN grants FKZ 03F0462A and FKZ 03F0611A and by the WGL project TransBrom. The R/V Sonne transit cruise was financed by the BMBF through grant 03G0731A. This work is a contribution to the EU project SHIVA.

References

Bange, H., Bergmann, K., Hansen, H. P., Kock, A., Koppe, R., Malien, F., and Ostrau, C.: Dissolved methane during hypoxic events at the boknis eck time series station (eckernförde bay, sw baltic sea), Biogeosciences (BG), 7, 1279-1284, 2010.

Bates, T. S., Kelly, K. C., Johnson, J. E., and Gammon, R. H.: A reevaluation of the open ocean source of methane to the atmosphere, J. Geophys. Res., 101, 6953-6961, 10.1029/95jd03348, 1996.

Belviso, S., Claustre, H., and Marty, J. C.: Evaluation of the utility of chemotaxonomic pigments as a surrogate for particulate dmsp, Limnol. Oceanogr., 46, 989-995, 2001.

Boden, R., Murrell, J. C., and Schäfer, H.: Dimethylsulfide is an energy source for the heterotrophic marine bacterium sagittula stellata, FEMS Microbiol. Lett., 322, 188-193, 10.1111/j.1574-6968.2011.02349.x, 2011.

Bouillon, R.-C., Lee, P. A., de Mora, S. J., Levasseur, M., and Lovejoy, C.: Vernal distribution of dimethylsulphide, dimethylsulphoniopropionate, and dimethylsulphoxide in

the north water in 1998, Deep Sea Research Part II: Topical Studies in Oceanography, 49, 5171-5189, 10.1016/s0967-0645(02)00184-4, 2002.
Bürgermeister, S., Zlmmermann, R. L., Georgii, H. W., Bingemer, H. G., Kirst, G. O., Janssen, M., and Ernst, W.: On the biogenic origin of dimethylsulfide: Relation between chlorophyll, atp, organismic dmsp, phytoplankton species, and dms distribution in atlantic surface water and atmosphere, J. Geophys. Res., 95, 20607-20615, 10.1029/JD095iD12p20607, 1990.
Cicerone, R. J., and Oremland, R. S.: Biogeochemical aspects of atmospheric methane, Global Biogeochem. Cycles, 2, 299-327, 10.1029/GB002i004p00299, 1988.
Damm, E., Kiene, R. P., Schwarz, J., Falck, E., and Dieckmann, G.: Methane cycling in arctic shelf water and its relationship with phytoplankton biomass and dmsp, Marine Chemistry, 109, 45-59, 10.1016/j.marchem.2007.12.003, 2008.
Damm, E., Helmke, E., Thoms, S., Schauer, U., Nothig, E., Bakker, K., and Kiene, R. P.: Methane production in aerobic oligotrophic surface water in the central arctic ocean, Biogeosciences, 7, 1099-1108, 2010.
David, H. A.: Further applications of range to analysis of variance, Biometrika, 38, 393–409, 1951.
de Angelis, M. A., and Lee, C.: Methane production during zooplankton grazing on marine-phytoplankton, Limnology and Oceanography, 39, 1298-1308, 1994.
Eberhardt, M. K., and Colina, R.: The reaction of oh radicals with dimethyl sulfoxide. A comparative study of fenton's reagent and the radiolysis of aqueous dimethyl sulfoxide solutions, The Journal of Organic Chemistry, 53, 1071-1074, 1988.
Ferry, J. G.: How to make a living by exhaling methane, in: Annual review of microbiology, vol 64, 2010, edited by: Gottesman, S., and Harwood, C. S., Annual review of microbiology, 453-473, 2010.
Finster, K., Tanimoto, Y., and Bak, F.: Fermentation of methanethiol and dimethylsulfide by a newly isolated methanogenic bacterium, Archives of Microbiology, 157, 425-430, 10.1007/bf00249099, 1992.
Fischer, E., and Jones, G.: Atmospheric dimethysulphide production from corals in the great barrier reef and links to solar radiation, climate and coral bleaching, Biogeochemistry, 110, 31-46, 10.1007/s10533-012-9719-y, 2012.
Green, D. H., Shenoy, D. M., Hart, M. C., and Hatton, A. D.: Coupling of dimethylsulfide oxidation to biomass production by a marine flavobacterium, Applied and Environmental Microbiology, 77, 3137-3140, 10.1128/aem.02675-10, 2011.
Hatton, A. D., Malin, G., Turner, S. M., and Liss, P. S.: Dmso: A significant compound in the biogeochemical cycle of dms, Plenum Press, New York and London, 430 pp., 1996.
Hatton, A. D., Malin, G., and Liss, P. S.: Distribution of biogenic sulphur compounds during and just after the southwest monsoon in the arabian sea, Deep Sea Research Part II: Topical Studies in Oceanography, 46, 617-632, 10.1016/s0967-0645(98)00120-9, 1999.
Hatton, A. D.: Influence of photochemistry on the marine biogeochemical cycle of di-

methylsulphide in the northern north sea, Deep Sea Research Part II: Topical Studies in Oceanography, 49, 3039-3052, 10.1016/s0967-0645(02)00070-x, 2002.
Hatton, A. D., Darroch, L., and Malin, G.: The role of dimethylsulphoxide in the marine biogeochemical cycle of dimethylsulphide, in: Oceanography and marine biology: An annual review, vol 42, edited by: Gibson, R. N., Atkinson, R. J. A., and Gordon, J. D. M., Oceanography and marine biology, Crc Press-Taylor & Francis Group, Boca Raton, 29-55, 2005.
Hirata, T., Hardman-Mountford, N. J., Brewin, R. J. W., Aiken, J., Barlow, R., Suzuki, K., Isada, T., Howell, E., Hashioka, T., Noguchi-Aita, M., and Yamanaka, Y.: Synoptic relationships between surface chlorophyll-a and diagnostic pigments specific to phytoplankton functional types, Biogeosciences, 8, 311-327, 10.5194/bg-8-311-2011, 2011.
Iglesias-Rodriguez, M. D., Brown, C. W., Doney, S. C., Kleypas, J., Kolber, D., Kolber, Z., Hayes, P. K., and Falkowski, P. G.: Representing key phytoplankton functional groups in ocean carbon cycle models: Coccolithophorids, Glob. Biogeochem. Cycle, 16, 10.1029/2001gb001454, 2002.
IPCC: Climate change 2007: The physical science basis. Contribution of working group i to the fourth assessment report of the intergovernmental panel on climate change, edited by: S. Solomon, D. Q., M. Manning, Z. Chen, M. Marquis, K. B. Averyt, M. Tignor and H. L. Miller, Cambridge University Press, Cambridge, UK and New York, NY, USA., 996 pp., 2007.
Karl, D. M., and Tilbrook, B. D.: Production and transport of methane in oceanic particulate organic matter, Nature, 368, 732-734, 1994.
Karl, D. M., Beversdorf, L., Bjorkman, K. M., Church, M. J., Martinez, A., and DeLong, E. F.: Aerobic production of methane in the sea, Nature Geoscience, 1, 473-478, 10.1038/ngeo234, 2008.
Keller, M. D., Bellows, W. K., and Guillard, R. R. L.: Dimethyl sulfide production in marine-phytoplankton, Acs Symposium Series, 393, 167-182, 1989.
Kiene, R. P., Oremland, R. S., Catena, A., Miller, L. G., and Capone, D. G.: Metabolism of reduced methylated sulfur-compounds in anaerobic sediments and by a pure culture of an estuarine methanogen, APPLIED AND ENVIRONMENTAL MICROBIOLOGY, 52, 1037-1045, 1986.
Kiene, R. P., and Linn, L. J.: Distribution and turnover of dissolved dmsp and its relationship with bacterial production and dimethylsulfide in the gulf of mexico, Limnol. Oceanogr., 45, 849-861, 2000.
Kiene, R. P., Linn, L. J., and Bruton, J. A.: New and important roles for dmsp in marine microbial communities, Journal of Sea Research, 43, 209-224, 10.1016/ s1385-1101(00)00023-x, 2000.
Krüger, K., and Quack, B.: Introduction to special issue: The transbrom sonne expedition in the tropical west pacific, Atmos. Chem. Phys. Discuss., 12, 1401-1418, 10.5194/acpd-12-1401-2012, 2012.

Lana, A., Bell, T. G., Simó, R., Vallina, S. M., Ballabrera-Poy, J., Kettle, A. J., Dachs, J., Bopp, L., Saltzman, E. S., Stefels, J., Johnson, J. E., and Liss, P. S.: An updated climatology of surface dimethlysulfide concentrations and emission fluxes in the global ocean, Global Biogeochem. Cycles, 25, GB1004, 10.1029/2010gb003850, 2011.
Lee, P. A., and De Mora, S. J.: Intracellular dimethylsulfoxide (dmso) in unicellular marine algae: Speculations on its origin and possible biological role, Journal of Phycology, 35, 8-18, 10.1046/j.1529-8817.1999. 3510008.x, 1999.
Lee, P. A., de Mora, S. J., and Levasseur, M.: A review of dimethylsulfoxide in aquatic environments, Atmosphere-Ocean, 37, 439-456, 10.1080/07055900.1999.9649635, 1999a.
Lee, P. A., Haase, R., de Mora, S. J., Chanut, J. P., and Gosselin, M.: Dimethylsulfoxide (dmso) and related sulfur compounds in the saguenay fjord, quebec, Canadian Journal of Fisheries and Aquatic Sciences, 56, 1631-1638, 10.1139/f99-094, 1999b.
Longhurst, A.: Ecological geography of the sea, Academic Press, San Diego, 1998.
Merzouk, A., Levasseur, M., Scarratt, M., Michaud, S., Lizotte, M., Rivkin, R. B., and Kiene, R. P.: Bacterial dmsp metabolism during the senescence of the spring diatom bloom in the northwest atlantic, Marine Ecology-Progress Series, 369, 1-11, 10.3354/meps 07664, 2008.
Moran, M. A., Gonzalez, J. M., and Kiene, R. P.: Linking a bacterial taxon to sulfur cycling in the sea: Studies of the marine roseobacter group, Geomicrobiology Journal, 20, 375-388, 10.1080/01490450303901, 2003.
Moran, M. A., Belas, R., Schell, M. A., Gonzalez, J. M., Sun, F., Sun, S., Binder, B. J., Edmonds, J., Ye, W., Orcutt, B., Howard, E. C., Meile, C., Palefsky, W., Goesmann, A., Ren, Q., Paulsen, I., Ulrich, L. E., Thompson, L. S., Saunders, E., and Buchan, A.: Ecological genomics of marine roseobacters, Applied and Environmental Microbiology, 73, 4559-4569, 10.1128/aem.02580-06, 2007.
Moran, M. A., Reisch, C. R., Kiene, R. P., and Whitman, W. B.: Genomic insights into bacterial dmsp transformations, in: Annual review of marine science, vol 4, edited by: Carlson, C. A., and Giovannoni, S. J., Annual review of marine science, 523-542, 2012.
Oremland, R. S., Kiene, R. P., Mathrani, I., Whiticar, M. J., and Boone, D. R.: Description of an estuarine methylotrophic methanogen which grows on dimethyl sulfide, Applied and Environmental Microbiology, 55, 994-1002, 1989.
Owens, N. J. P., Law, C. S., Mantoura, R. F. C., Burkill, P. H., and Llewellyn, C. A.: Methane flux to the atmosphere from the arabian sea, Nature, 354, 293-296, 1991.
Reeburgh, W. S.: Oceanic methane biogeochemistry, Chemical Reviews, 107, 486-513, 10.1021/cr050362v, 2007.
Rehder, G., and Suess, E.: Methane and pco2 in the kuroshio and the south china sea during maximum summer surface temperatures, Marine Chemistry, 75, 89-108, 10.1016/ s0304-4203(01)00026-3, 2001.
Rottgers, R., and Gehnke, S.: Measurement of light absorption by aquatic particles: Improvement of the quantitative filter technique by use of an integrating sphere approach,

Applied Optics, 51, 1336-1351, 2012.
Schäfer, H., Myronova, N., and Boden, R.: Microbial degradation of dimethylsulphide and related c1-sulphur compounds: Organisms and pathways controlling fluxes of sulphur in the biosphere, Journal of Experimental Botany, 61, 315-334, 10.1093/jxb/erp355, 2010.
Simó, R., Hatton, A. D., Malin, G., and Liss, P. S.: Particulate dimethyl sulphoxide in seawater: Production by microplankton, Marine Ecology Progress Series, 167, 291-296, 10.3354/meps167291, 1998.
Simó, R., Pedrós-Alió, C., Malin, G., and Grimalt, J. O.: Biological turnover of dms, dmsp and dmso in contrasting open-sea waters, Marine Ecology Progress Series, 203, 1-11, 10.3354/meps203001, 2000.
Simó, R.: Production of atmospheric sulfur by oceanic plankton: Biogeochemical, ecological and evolutionary links, Trends in Ecology & Evolution, 16, 287-294, 10.1016/s0169-5347(01)02152-8, 2001.
Simó, R., Archer, S. D., Pedros-Alio, C., Gilpin, L., and Stelfox-Widdicombe, C. E.: Coupled dynamics of dimethylsulfoniopropionate and dimethylsulfide cycling and the microbial food web in surface waters of the north atlantic, Limnol. Oceanogr., 47, 53-61, 2002.
Simó, R.: From cells to globe: Approaching the dynamics of dms(p) in the ocean at multiple scales, Canadian Journal of Fisheries and Aquatic Sciences, 61, 673-684, 10.1139/f04-030, 2004.
Simó, R., and Vila-Costa, M.: Ubiquity of algal dimethylsulfoxide in the surface ocean: Geographic and temporal distribution patterns, Marine Chemistry, 100, 136-146, 10.1016/j.marchem.2005.11.006, 2006.
Spiese, C. E., Kieber, D. J., Nomura, C. T., and Kiene, R. P.: Reduction of dimethylsulfoxide to dimethylsulfide by marine phytoplankton, Limnology and Oceanography, 54, 560, 2009.
Stefels, J.: Physiological aspects of the production and conversion of dmsp in marine algae and higher plants, Journal of Sea Research, 43, 183-197, 10.1016/s1385-1101(00)00030-7, 2000.
Stefels, J., Steinke, M., Turner, S., Malin, G., and Belviso, S.: Environmental constraints on the production and removal of the climatically active gas dimethylsulphide (dms) and implications for ecosystem modelling, Biogeochemistry, 83, 245-275, 10.1007/s10533-007-9091-5, 2007.
Steinke, M., Malin, G., Archer, S. D., Burkill, P. H., and Liss, P. S.: Dms production in a coccolithophorid bloom: Evidence for the importance of dinoflagellate dmsp lyases, Aquatic Microbial Ecology, 26, 259-270, 10.3354/ame026259, 2002.
Sunda, W., Kieber, D. J., Kiene, R. P., and Huntsman, S.: An antioxidant function for dmsp and dms in marine algae, Nature, 418, 317-320, 10.1038/nature00851, 2002.
Tallant, T. C., and Krzycki, J. A.: Methylthiol:Coenzyme m methyltransferase from

methanosarcina barkeri, an enzyme of methanogenesis from dimethylsulfide and methylmercaptopropionate, Journal of Bacteriology, 179, 6902-6911, 1997.
Taylor, B. B., Torrecilla, E., Bernhardt, A., Taylor, M. H., Peeken, I., Rottgers, R., Piera, J., and Bracher, A.: Bio-optical provinces in the eastern atlantic ocean and their biogeographical relevance, Biogeosciences, 8, 3609-3629, 10.5194/bg-8-3609-2011, 2011.
Terao, Y., Mukai, H., Nojiri, Y., Machida, T., Tohjima, Y., Saeki, T., and Maksyutov, S.: Interannual variability and trends in atmospheric methane over the western pacific from 1994 to 2010, Journal of Geophysical Research-Atmospheres, 116, 10.1029/2010jd015467, 2011.
Torrecilla, E., Stramski, D., Reynolds, R. A., Millan-Nunez, E., and Piera, J.: Cluster analysis of hyperspectral optical data for discriminating phytoplankton pigment assemblages in the open ocean, Remote Sensing of Environment, 115, 2578-2593, 10.1016/j.rse.2011.05.014, 2011.
Uitz, J., Claustre, H., Morel, A., and Hooker, S. B.: Vertical distribution of phytoplankton communities in open ocean: An assessment based on surface chlorophyll, J. Geophys. Res.-Oceans, 111, 10.1029/2005jc003207, 2006.
van der Maarel, M. J. E. C., and Hansen, T. A.: Dimethylsulfoniopropionate in anoxic intertidal sediments: A precursor of methanogenesis via dimethyl sulfide, methanethiol, and methiolpropionate, Marine Geology, 137, 5-12, 10.1016/s0025-3227(96)00074-6, 1997.
Vidussi, F., Claustre, H., Manca, B. B., Luchetta, A., and Marty, J. C.: Phytoplankton pigment distribution in relation to upper thermocline circulation in the eastern mediterranean sea during winter, J. Geophys. Res.-Oceans, 106, 19939-19956, 10.1029/1999jc000308, 2001.
Vogt, M., and Liss, P. S.: Dimethylsulfide and climate, Surface ocean - lower atmosphere processes, 187, Geophysical Monograph Series, edited by C. Le Quéré and E. S. Saltzman, AGU, Washingtion, DC, 197–232, doi: 10.1029/2008GM000790, 2009.
Watanabe, S., Higashitani, N., Tsurushima, N., and Tsunogai, S.: Methane in the western north pacific, Journal of Oceanography, 51, 39-60, 1995.
Wiesenburg, D. A., and Guinasso Jr., N. L.: Equilibrium solubilities of methane, carbon monoxide, hydrogen in water and seawater, J. Chem. Eng. Data, 24, 356–360, 1979.
Yoch, D. C.: Dimethylsulfoniopropionate: Its sources, role in the marine food web, and biological degradation to dimethylsulfide, APPLIED AND ENVIRONMENTAL MICROBIOLOGY, 68, 5804-5815, 10.1128/aem.68.12.5804-5815.2002, 2002.
Zindler, C., Peeken, I., Marandino, C. A., and Bange, H. W.: Environmental control on the variability of dms and dmsp in the mauritanian upwelling region, Biogeosciences, 9, 1041-1051, 10.5194/bg-9-1041-2012, 2012.

Supplement

2.4.1 Phytoplankton pigments, group composition and absorption coefficients

The following diagnostic pigments were used to identify seven phytoplankton groups: fucoxanthin (Fuco), peridinin (Peri), alloxanthin (Allo), 19´-hexanoyloxyfucoxanthin (19HF), 19´-butanoyloxyfucoxanthin (19BF), zeaxanthin (Zea), and total chlorophyll-b (TChlb, i.e. the sum of monovinylchl-b, chl-b, and divinylchl-b (div-b)). According to Hirata *et al.* (2011) the weighted relationships of these diagnostic pigments (DPw) were calculated by multiple regression analysis as follows:

% pico (<2 μm) = 100*(0.86 Zea)/DPw
% nano (2 -20 μm) = 100*(1.27 19HF +1.01 TChlb +0.35 19BF +0.6 Allo)/DPw
% micro (>20 μm) = 100*(1.41 Fuco +1.41Peri)/DPw
% diatoms = 100*(1.41 Fuco)/DPw
% dinoflagellates = 100*(1.41 Peri)/DPw
% haptophytes = 100*(1.2719HF)/DPw
% chrysophytes = 100*(0.3519BF)/DPw
% cryptophytes = 100*(0.6Allo)/DPw
% chlorophytes = 100*(1.01TChlb)/DPw
% all cyanobacteria = 100*(0.86Zea)/DPw

where,
DPw = 0.86 Zea +1.01 TChlb +1.27 19HF +0.35 19BF +0.6 Allo +1.41 Fuco +1.41 Peri.

By multiplying the total chl-a concentration (TChl-a) (i.e. the sum of monovinylchl-a, chl-a, and divinylchl-a, div-a) with %-values for each group, the chl-a concentration for each group was derived. In addition, TChl-a concentration of prochlorophytes, a subgroup of cyanobacteria which is characterized by very low size ($\sim$0.5 μm), and the pigments of div-a and div-b, was calculated from div-a/(div-a+chl-a). The chl-a concentration of all other cyanobacteria was calculated by subtracting prochlorophytes chl-a from all cyanobacteria chl-a concentration.

Identifying phytoplankton assemblages with hierarchical cluster analysis

The clustering of the hyperspectral phytoplankton absorption coefficients generates a cluster tree to partition an input data set into subsets or clusters with no previous information regarding membership of input data objects to predefined classes. Each cluster tree is

obtained based on a selected linkage algorithm that considers a previously calculated similarity distance between all samples included in the input data set. To minimize variability in pigment composition associated with changes in phytoplankton biomass, the input to the cluster analysis was represented by the ratio of individual pigment concentrations to the surface TChl-a. In that sense, the information regarding the dominance of pigments for each stations can be better assessed. Otherwise, the analysis would be mainly driven by the amount of total pigments concentration. In addition, a Euclidean distance was utilized to generate the pigment-based cluster partition in order to indicate differences in magnitude of ratios of concentrations of individual pigments to TChl-a rather than differences in shape. The cluster partition obtained from the pigment data served as a reference for partitioning the entire data set into distinct groups - clusters, each characterized by a different phytoplankton pigment composition (shown in Fig. 2.10 of supplement). The feasibility of using pigment data for identifying phytoplankton assemblages was tested by comparisons of the clustering of the hyperspectral phytoplankton absorption (see Fig. 2.11 of supplement) data with using the cophenetic index (see details in Torrecilla *et al.*, 2011), an objective criterion of cluster similarity ranging from 0 (for no similarity) to 1 (for maximum similarity). Because we focus in this study on spectral signatures related to the specific pigment composition, when computing the similarity between pairs of phytoplankton absorption spectra, an angular distance was utilized. This distance reflects better the differences in the spectral shape of optical data.

Statistical analysis

Multiple linear regression models (MLRM) computed with RStudio™ were used. The terms were added and removed from a MLRM based on their statistical significance. At each step an F-test was performed to test the regressions with and without certain terms. A term was added to the model if it contributed significantly at the 95%-confidence level or removed from the model if it did not contribute at the 95%-confidence level. To identify the simplest MLRM with the best explanatory power, each model was compared with the previous one using Analysis of Variances (ANOVA) to test if the latest and simpler model showed no significant differences to the former model. The influence of the interaction of two or more parameters on the sulphur compound concentrations was additionally tested with the same procedure as described above.

Different diagnostic tests were performed to determine if the assumptions made to perform the regression model calculations were valid. All response variables were tested for normal distribution with the Shapiro-Wilk normality test or the Anderson-Darling test (for more than 100 data points) and got transformed if necessary. A tree model was used to obtain an overview of the interactions between the predictor variables prior the calculation of the MLRM. After each calculation, the model was tested for multicollinearity by

computing the variance inflation factor (VIF). The heteroscedascity of the models as well as the normal distribution of the residuals were examined graphically. A Durbin-Watson Test was used to find auto-correlations in the residuals. Data points that had a strong influence on the models were identified graphically with the Cook's distance. The model was compared with the next to last simplest model using the Akaike's Information Criterion to check if the simplest model with the best prediction was selected. The entire outputs for all MLRM are given in Figure 2.8 between the different sulphur compounds and in Figure 2.9 between sulphur compounds and phytoplankton marker pigments.

model no.	single coefficients	Esti-mate	Std. Error	t value	p-value	R^2, F-st., p-value (e. m.)	model no.	single coefficients	Esti-mate	Std. Error	t value	p-value	R^2, F-st., p-value (e. m.)
a	Intercept	-0.20	0.04	-4.71	7.65E-06	0.32	g	Intercept	1.49	0.21	7.11	3.92E-10	0.4
DMS	DMSPp	-0.11	0.02	-6.54	2.36E-09	24.57	DMSPp	DMS	-1.19	0.50	-2.35	0.02	7.92
e. d. s.	DMSOp	0.02	0.00	5.64	1.49E-07	1.83E-09	e. d. s.	DMSOp	0.02	0.01	4.57	1.73E-05	2.57E-07
								DMS^2	0.53	0.30	1.79	0.08	
b	Intercept	-0.54	0.40	-1.34	0.19	0.48		DMSPd^2	0.06	0.02	2.67	9.09E-03	
DMS	DMSPp	0.10	0.05	2.00	0.05	6.01		DMSOp^2	0.0005	0.0002	1.96	0.05	
cluster 2	DMSOd	0.31	0.13	2.42	0.02	5.27E-05		DMSOp:DMSPd	-0.01	0.004	-2.78	6.78E-03	
	DMSOp	0.02	0.005	3.34	0.002			DMSPd:DMSOd	-0.02	0.01	-1.83	0.07	
	DMSPd	0.54	0.29	1.85	0.07								
	DMSOd^2	-0.02	0.01	-1.82	0.08		h	Intercept	1.82	0.31	5.94	2.7E-09	0.38
	DMSPd^2	-0.18	0.10	-1.78	0.08		DMSPp	DMSOp	0.09	0.03	3.47	0.001	10.09
	DMSPp:DMSOd	-0.04	0.01	-3.08	0.004		cluster 2	DMS	-1.43	0.36	-3.94	2.5E-04	2.62E-05
								DMSOp:DMSPd	-0.03	0.01	-2.49	0.016	
c	Intercept	-0.60	0.78	-0.78	0.45	0.58							
DMS	DMSPd	-0.56	0.16	-3.53	0.002	5.62	i	Intercept	2.93	0.42	6.91	4.28E-10	0.19
cluster 4	DMSOd	0.73	0.37	1.99	0.06	0.002	DMSOd	DMSPd	0.72	0.36	2.04	0.04	8.05
	DMSPp	-1.04	0.24	-4.34	0.0003		e.d.s.	DMS^2	1.04	0.25	4.23	5.13E-05	7.26E-05
	DMSOd^2	-0.09	0.04	-2.13	0.05			DMSPd^2	-0.13	0.06	-2.23	0.03	
	DMSPd:DMSPp	0.68	0.19	3.63	0.002								
							j	Intercept	2.66	0.82	3.24	0.002	0.28
d	Intercept	0.027	0.08	0.32	0.75	0.32	DMSOd	DMSPp	0.96	0.42	2.26	0.03	4.82
DMSPd	DMSOp^2	0.002	0.0003	5.71	1.14E-07	16.22	cluster 2	DMSPd	1.40	0.49	2.84	0.01	0.002
e. d. s.	DMSOd^2	0.01	0.003	2.32	0.02	1.084e-08		DMSPp^2	-0.09	0.04	-2.01	0.05	
	DMSPp:DMSOp	-0.01	0.002	-3.72	3.27E-04			DMSPp:DMSPd	-0.49	0.17	-2.94	0.005	
e	Intercept	0.65	0.18	3.53	9.81E-04	0.47	k	Intercept	6.31	0.63	10.05	1.91E-10	0.35
DMSPd	DMSPp	0.23	0.08	2.99	0.005	5.01	DMSOd	DMSPp	-1.56	0.43	-3.65	0.001	4.59
Cluster 2	DMSOd	0.06	0.02	2.55	0.014	1.77E-04	cluster 4	DMSOp	-0.26	0.08	-3.14	0.004	0.01
	DMSOp	-0.04	0.01	-3.12	0.003			DMSPp:DMSOp	0.18	0.05	3.43	0.002	
	DMS	0.38	0.15	2.63	0.01								
	DMSPp^2	-0.015	0.008	-1.99	0.05		l	Intercept	1.57	0.10	16.24	2.00E-16	0.43
	DMSOp^2	0.003	0.0006	4.094	1.7E-04		DMSOp	DMSPd	0.26	0.05	5.36	5.61E-07	36.53
	DMSPp:DMSOp	-0.004	0.002	-1.69	0.097		e. d. s.	DMSPp	0.13	0.02	5.85	6.72E-08	1.49E-12
	DMSPp:DMSOd:DMS	-0.04	0.013	-3.15	0.0029								
							m	Intercept	1.29	2.54	0.51	0.614	0.56
f	Intercept	-7.51	2.3	-3.26	0.004	0.52	DMSOp	DMS	7.39	2.87	2.57	0.014	8.761
DMSPd	DMS	4.5	1.77	2.55	0.019	3.54	cluster 2	DMSOd^2	0.25	0.14	1.74	0.089	3.33E-06
cluster 4	DMSOd	3.39	0.98	3.46	0.002	0.015		DMSPp^2	7.14	1.43	5.01	1.03E-05	
	DMSOd^2	-0.24	0.11	-2.25	0.04			DMSPp:DMSOd	0.7	0.15	4.55	4.56E-05	
	DMSPp^2	0.4	0.09	4.48	2.3E-04			DMSPp:DMSPd	-1.6	0.48	-3.28	0.002	
	DMS:DMSOd	-1.28	0.43	-2.94	0.008			DMSOd:DMSPd	-2.9	0.84	-3.46	0.0013	
	DMSOd:DMSPp	-0.24	0.05	-4.44	2.5E-04								
							n	Intercept	0.40	2.27	0.18	0.86	0.46
							DMSOp	DMS	2.75	1.40	1.97	0.06	7.23
							cluster 4	DMSPd	3.01	1.46	2.06	0.05	0.001
								DMSPp	3.09	0.68	4.53	1.26E-04	

Fig. 2.8: *Significant multiple linear regressions between DMS, DMSP and DMSO (d=dissolved, p=particulate, t=total) for the whole data set and within the cluster 2 and 4. Single coefficients, estimates, standard Errors, t and p values of the different independent variables in each multiple linear regression model as well as* R^2*, F-statistic and p-value of each whole model are given. Under model number is the response variable given. Variable square showed quadratic relationship to response variable. The complete output of all models is given in the supplements. Abbr.: st.: statistic; e. m.: entire model; e. d. s.: entire data set; a – n: number of models*

model no.	single coefficients	Esti-mate	Std. Error	t value	p-value	R^2, F-st., p-value (e. m.)	model no.	single coefficients	Esti-mate	Std. Error	t value	p-value	R^2, F-st., p-value (e. m.)
a	Intercept	0.56	0.21	2.65	0.01	0.22	e	Intercept	-2.69	0.65	-3.97	4.41E-04	0.72
DMS	fuco	-0.19	0.06	-3.04	0.004	2.65	DMSPp	fuco	0.48	0.12	4.09	2.22E-04	11.94
cluster 2	hex	0.05	0.02	2.59	0.01	0.005	cluster 2	diato	-0.64	0.20	-3.26	2.46E-03	4.02E-09
	perI^2	0.01	0.002	3.09	0.003			zea	0.09	0.02	3.90	5.22E-04	
	fuco^2	0.01	0.004	2.98	0.005			hex	-0.02	0.01	-2.19	2.51E-02	
	diato^2	-0.02	0.01	-2.07	0.04			fuco^2	-0.03	0.01	-3.49	1.29E-03	
	hex^2	-0.001	0.0003	-2.63	0.01			diato^2	0.21	0.05	4.19	1.75E-04	
								zea^2	-0.0003	0.0001	-2.51	1.22E-03	
b	Intercept	0.11	0.14	0.77	0.44	0.44		fuco:perI	-0.02	0.004	-5.19	8.30E-06	
DMSPd	but	0.13	0.03	4.69	1.01E-05	11.24							
e. d. s.	perI	0.12	0.03	3.77	2.96E-04	2.26E-09	f	Intercept	-5.66	1.17	-4.84	6.10E-06	0.75
	zea	-0.01	0.002	-5.09	2.01E-06		DMSPt	dia	0.29	0.12	2.50	1.46E-02	16.2
	but^2	-0.01	0.002	-4.74	8.21E-06		e. d. s.	fuco	1.10	0.16	6.69	2.65E-09	2.20E-16
	but:perI:fuco	-8.22E-04	2.21E-04	-2.59	0.01			zea	0.13	0.02	5.25	7.70E-07	
	but:zea:fuco	7.21E-05	1.79E-05	4.11	8.82E-05			perI^2	0.05	0.02	3.29	1.53E-03	
								dia^2	-0.02	0.01	-2.79	6.59E-03	
c	Intercept	0.89	0.07	13.47	2.00E-16	0.61		fuco^2	-0.03	0.01	-4.17	7.59E-05	
DMSPd	fuco	0.04	0.02	2.58	0.01	5.93		zea^2	-0.0004	0.0001	-3.57	6.10E-04	
cluster 2	diato	0.26	0.10	2.60	0.01	1.15E-05		viola^2	-0.25	0.06	-4.23	4.22E-05	
	but^2	-0.002	0.001	-2.32	1.91E-03			fuco:perI	-0.09	0.01	-6.21	2.07E-08	
	fuco:perI	-0.01	0.005	-2.46	0.02			dia:fuco	0.02	0.01	1.90	6.16E-02	
	diato:perI	0.09	0.02	4.25	8.82E-05			fuco:zea	-0.01	0.002	-2.12	2.47E-03	
	fuco:diato	-0.06	0.01	-4.29	1.07E-04			dia:viola	-0.19	0.05	-3.42	9.70E-04	
	diato:zea	-0.01	0.001	-5.40	2.04E-06			fuco:viola	0.20	0.05	3.63	4.94E-04	
	perI:but	0.01	0.004	2.97	2.79E-04			zea:viola	-0.02	0.004	-4.59	1.62E-05	
	diato:but	0.03	0.009	2.99	2.82E-04			dia:zea:viola	0.002	0.0003	6.19	2.28E-08	
	fuco:diato:zea	0.001	0.0001	5.02	1.04E-05								
	diato:perI:but	-0.01	0.001	-5.92	7.87E-07		g	Intercept	-1.24	0.79	-1.72	0.09	0.79
							DMSPt	hex	-0.19	0.05	-3.90	4.46E-04	16.99
d	Intercept	0.19	0.13	2.09	0.04	0.27	cluster 2	but	0.99	0.26	3.79	7.94E-03	1.72E-11
DMSPp	perI	0.10	0.04	2.63	9.88E-03	9.3		fuco	1.29	0.32	3.96	2.80E-04	
e. d. s.	but	0.09	0.02	4.08	9.22E-05	5.01E-09		perI^2	0.07	0.02	3.14	2.08E-03	
	fuco	0.05	0.02	2.01	0.05			but^2	-0.02	0.01	-2.10	0.04	
	fuco^2	-0.001	0.0002	-4.69	8.97E-06			fuco^2	-0.07	0.02	-3.90	4.49E-04	
	perI:but	-0.02	0.004	-5.33	6.41E-07			ant^2	-0.67	0.24	-2.79	7.75E-03	
	perI:but:fuco	0.0002	0.00004	5.77	9.87E-06			fuco:perI	-0.09	0.02	-4.74	2.25E-05	
								fuco:ant	0.26	0.06	4.03	2.22E-04	
h	Intercept	0.83	0.49	1.67	0.11	0.26	i	Intercept	2.93	2.60	1.09	0.28	0.84
DMSPt	but	0.54	0.13	17.1	4.14	17.1	DMSOp	perI	-4.72	1.66	-2.84	7.63E-03	12.99
cluster 4						0.0003	cluster 2	diato	-5.27	1.71	-3.14	2.56E-03	1.92E-09
								but	1.76	0.81	2.16	0.04	
l	Intercept	4.04	0.20	19.76	2.00E-16	0.42		perI^2	0.23	0.07	4.52	7.65E-05	
DMSOd	diato	0.49	0.22	2.20	0.03	7.55		but^2	-0.12	0.05	-2.67	0.01	
e. d. s.	hex^2	0.01	0.002	4.06	1.11E-04	1.65E-07		perI:fuco	0.61	0.22	2.76	9.41E-03	
	but^2	-0.09	0.02	-4.10	9.69E-05			perI:diato	1.27	0.59	2.25	0.03	
	fuco:perI	-0.09	0.04	-2.24	0.03			diato:fuco	0.87	0.17	4.99	1.98E-05	
	fuco:hex	-0.05	0.01	-4.04	1.20E-04			perI:zea	0.09	0.02	4.93	2.29E-05	
	fuco:but	0.19	0.05	3.90	1.96E-04			perI:but	-0.94	0.24	-4.00	2.27E-04	
	perI:but	0.10	0.04	2.64	9.95E-03			perI:diato:fuco	-0.22	0.07	-3.07	4.27E-03	
	diato:but	-0.07	0.03	-2.90	6.43E-03			perI:fuco:zea	-0.01	0.002	-4.24	1.71E-04	
								perI:but:fuco	0.10	0.03	3.85	5.18E-04	
j	Intercept	2.67	0.91	2.94	5.01E-03	0.45							
DMSOd	perI	0.33	0.07	4.95	1.24E-05	10.1	m	Intercept	1.22	4.41	0.30	0.77	0.52
cluster 2	dia	0.36	0.17	2.07	4.29E-02	4.91E-06	DMSOt	but	-1.19	0.36	-3.34	9.55E-04	9.92
	but	-0.11	0.04	-2.74	8.61E-03		cluster 2	hex	0.69	0.32	2.14	0.04	2.15E-06
	dia^2	-0.02	0.01	-2.41	1.99E-02			fuco	1.53	0.37	4.12	1.61E-04	
								perI^2	0.14	0.05	2.94	6.69E-03	
k	Intercept	0.33	0.45	0.73	0.469092	0.54		hex^2	-0.01	0.004	-2.09	0.04	
DMSOp	Fuco	0.51	0.11	4.93	6.82E-06	9.19							
e. d. s.	Diato	-0.82	0.24	-3.39	1.09E-03	9.46E-10	n	Intercept	1.94	0.92	2.12	0.04	0.42
	Zea	0.03	0.01	5.18	1.76E-06		DMSOt	hex	0.30	0.13	2.34	0.03	4.65
	perI^2	0.05	0.01	4.62	1.50E-05		cluster 4	zea	-0.04	0.01	-3.22	3.54E-03	0.006
	fuco:diato	0.11	0.04	3.18	2.15E-03			hex^2	-0.01	0.005	-2.21	0.04	
	fuco:zea	-0.01	0.002	-5.08	2.54E-06			zea^2	0.0003	0.0001	3.41	2.22E-03	
	diato:zea	0.01	0.003	2.92	4.59E-03								
	perI:diadino	-0.04	0.01	-4.79	8.16E-06								
	fuco:diato:diadino	-0.01	0.001	-3.98	2.21E-04								
	fuco:zea:diadino	0.0002	0.0001	4.21	4.87E-05								

Fig. 2.9: *Significant multiple linear regressions between DMS, DMSP and DMSO (d=dissolved, p=particulate, t=total) and phytoplankton marker pigments for the whole data set and within the cluster 2 and 4. Single coefficients, estimates, standard Errors, t and p values of the different independent variables in each multiple linear regression model as well as* R^2*, F-statistic and p-value of each whole model are given. Under model number is the response variable given. Variable square showed quadratic relationship to response variable. Abbr.: st.: statistic; e. m.: entire model; e.d.s.: entire data set; a – n: number of models, fuco: fucoxanthin, hex: 19'-hexanoyloxyfucoxanthin, peri: peridinin, diato: diatoxanthin, dia: diadinoxanthin, diato: diatoxanthin, but: 19'-butanoyloxyfucoxanthin, zea: zeaxanthin, ant: anthreaxanthin, viola: violaxanthin*

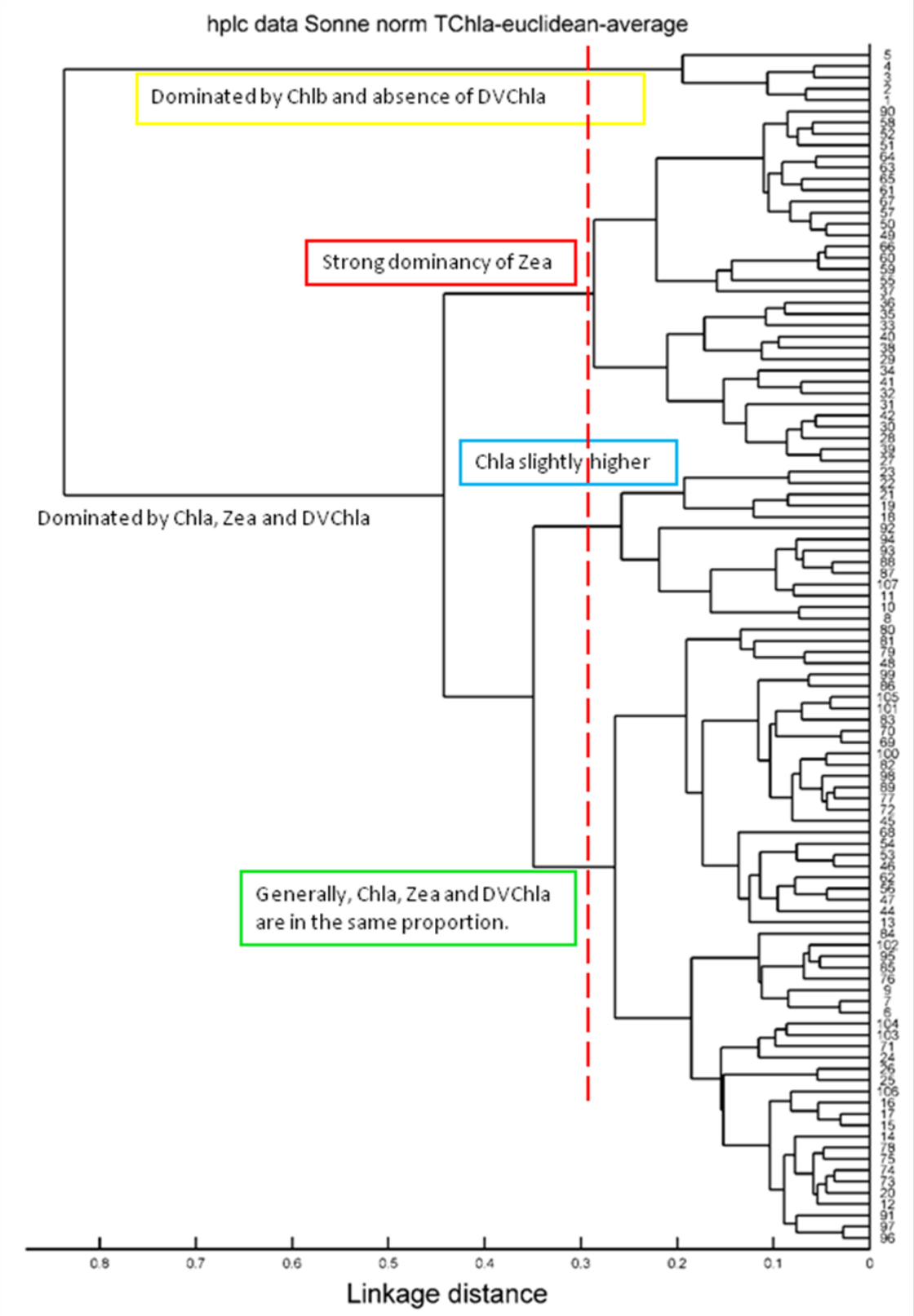

Fig. 2.10: *cluster tree for pigments (stations are labeled with consecutive numbers increasing with latitude) during TransBrom Sonne based on HCA analysis. Different clusters are labeled with yellow for cluster 1, green for cluster 2, blue for cluster 3 and red for cluster 4.*

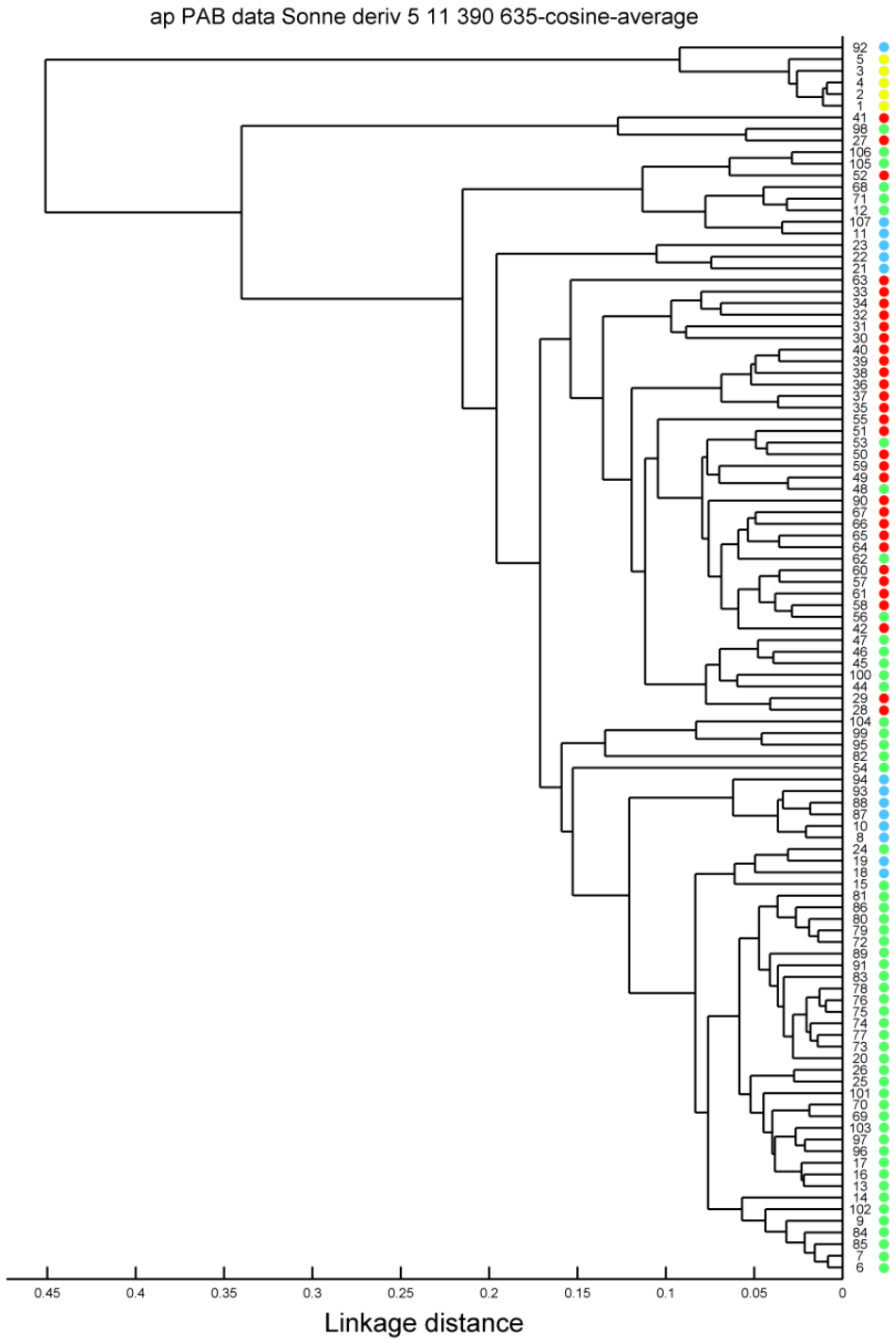

Fig. 2.11: *cluster tree for phytoplankton absorption coefficients measured during TransBrom Sonne, stations are labeled with consecutive numbers increasing with latitude.*

3 Dimethylsulphide (DMS) emissions from the West Pacific Ocean: a potential marine source for the stratospheric sulphur layer

Abstract

Sea surface and atmospheric measurements of dimethylsulphide (DMS) were performed during the TransBrom cruise in the West Pacific Ocean between Japan and Australia in October 2009. Air-sea DMS fluxes were computed between 0 and 30 $\mu\mathrm{mol\,m^{-2}\,d^{-1}}$, which are in agreement with those computed by the current climatology, and peak emissions of marine DMS into the atmosphere were found during the occurrence of tropical storm systems. Atmospheric variability in DMS, however, did not follow that of the computed fluxes and was more related to atmospheric transport processes. The computed emissions were used as input fields for the Langrangian dispersion model FLEXPART, which was set up with actual meteorological fields from ERA-interim data and different chemical lifetimes of DMS. A comparison with aircraft *in-situ* data from the adjacent HIPPO2 campaign revealed an overall good agreement between modeled versus observed DMS profiles over the tropical West Pacific ocean. Based on observed DMS emissions and the meteorological fields over the cruise track region, the model projected that up to 30 g S per month in the form of DMS can be transported above 17 km in this region. This surprisingly large DMS entrainment into the stratosphere is disproportionate to the regional extent of the cruise track area and mainly due to the high convective activity in this region as simulated by the transport model. Thus, we conclude that the considerably larger area of the tropical West Pacific Ocean can be an important source of sulphur to the stratospheric persistent sulphur layer, which has not been considered as yet.

3.1 Introduction

Dimethylsulphide (DMS) is the most abundant naturally produced sulphur compound emitted from the sea surface. DMS has been the focus of much research since Charlson *et al.* (1987) proposed that DMS produced in the sea surface by phytoplankton may affect the atmospheric radiative budget via its role in aerosol and cloud formation. In addition, because DMS is rapidly oxidized when emitted to the atmosphere, studies have been conducted showing that certain DMS oxidation products can be transported above the tropopause and contribute to the persistent stratospheric sulphur layer (PSL), e.g. carbonyl sulphide (Crutzen, 1976), sulphur dioxide (SO_2) (Chatfield and Crutzen, 1984), and sulphur species in general (Gondwe *et al.*, 2003; Lucas and Prinn, 2003). Recent work has shown that an underestimation of the radiative effect of the PSL can lead to an overestimation of global warming (Solomon *et al.*, 2011). Hofmann *et al.* (2009) reported that since 2000 there has been an increase in the aerosol backscatter above the tropopause and they propose an increase in sulphur compounds in the atmosphere as the main cause. The importance of naturally occurring sulphur containing trace gases as a source to the stratosphere is currently debated, since minor volcanic eruptions and anthropogenic sulphur dioxide (SO_2) seem to have an overwhelming global footprint (Bruehl *et al.*, 2012; Bourassa *et al.*, 2012; Vernier *et al.*, 2011). Nonetheless, it is most likely that a combination of sulphur sources is responsible for the observed increase in stratospheric aerosol, including a natural component that also needs to be investigated. Myhre *et al.* (2004) have suggested, based on model calculations, that the contribution of sulphur to the stratosphere from marine DMS emissions may be important.

Typically surface ocean DMS emissions (F , flux) are calculated using $F = k\Delta C$, where k is a wind speed based parameterisation of the gas transfer coefficient and ΔC is the measured bulk air-sea concentration difference. Because DMS is almost always supersaturated in the surface ocean, seawater concentrations are the main component of the concentration difference. Regarding k values, there is currently no consensus on the functionality of the wind speed dependence of the gas transfer coefficient. Thus, several different parameterisations have been proposed and used frequently in the literature, which lead to considerable variability in computed surface ocean trace gas fluxes (see Ho *et al.*, 2006 for an overview). Furthermore, although remotely sensed wind speeds, with high spatial and temporal resolution, are readily available for flux calculations, it is still difficult to parameterise surface ocean DMS concentrations on similar scales. Therefore, it is necessary to use archived in situ measurements to calculate DMS emissions. Unfortunately, there is a considerable lack of high spatial and temporal resolution data for oceanic DMS. It is important to build up the current Global Surface Seawater DMS Database (http://saga.pmel.noaa.gov/dms), in conjunction with ancillary data, in order to better understand the controls on oceanic DMS and predict future air-sea fluxes. Lana *et al.* (2011), in the footsteps of Kettle *et al.* (1999, 2000), has used the existing database to

compile a current surface ocean DMS climatology and compute air-sea fluxes. However, the influence of DMS hotspots and high wind speed events, such as typhoons and tropical storms, on the DMS flux is hard to determine from such climatology. Therefore, it is important to compare in situ calculations to those in the climatology, not only to make the database more robust, but also to determine the importance of such events relative to "normal" conditions.

In this paper, we use in situ measurements of ΔC and wind speed (U) with three different k parameterisations to compute DMS emissions during the TransBrom cruise in October 2009 in the western Pacific Ocean. This oceanic region experiences several meteorological phenomena, such as tropical storms and deep convection, which make it especially significant for transporting climate active trace gases emitted from the surface ocean to the upper troposphere/lower stratosphere. The upper part of the tropical tropopause layer (TTL), between 15 to 17 km altitude, is of specific interest here. The West Pacific region acts as a main entrance region of trace gases into the stratosphere throughout the year, peaking during boreal winter season with enhanced vertical transport (Fueglistaler and Haynes, 2005; Krüger *et al.*, 2008, 2009). Since the atmospheric DMS lifetime is short, between 11 min and 46 h due to reaction with hydroxyl and nitrate radicals (e.g. Osthoff *et al.*, 2009; Barnes textitet al., 2006), DMS transport to the TTL is more efficient in the western Pacific Ocean than in other oceanic regions. Computed DMS sea-to-air in situ fluxes from the TransBrom cruise to the West Pacific Ocean were used to initiate the high resolution Lagrangian transport model FLEXPART to determine the importance of surface DMS emissions for stratospheric sulphur loading in this region.

3.2 Data and Model

3.2.1 Ship measurements

Underway surface water samples for DMS and air samples for DMS were collected aboard the R/V Sonne from the 9 to 24 October 2009 during a transit from Tomakomai (Japan) to Townsville (Australia). A detailed description of the TransBrom cruise including the meteorological background is given by Krüger and Quack (2012). Three tropical storms (Melor, 9 October; Nepartak, 12 October; Lupit, 14 October) passed the transit and were responsible for wind speeds up to 18 $\mathrm{m\,s^{-1}}$ (see also Figs. 3.1 and 3.2). The circulation of the Pacific Ocean and atmosphere were affected by a strengthening El Niño event, inducing an increase in sea surface temperature towards the east, which triggered an elevated atmospheric convection. The analyses of water samples, taken every three hours, from this cruise using gas chromatography coupled to flame photometric detection are described in detail by Zindler *et al.* (2012). Atmospheric measurements of DMS were performed according to Schauffler *et al.* (1999), also with samples taken at

three hour intervals. Air and water samples were not always taken simultaneously. When this occurred, the distance between the sample locations was used to determine the air and water pairs. The mean analytical errors were estimated to be ±20% for dissolved DMS (Zindler *et al.*, 2012) and ±10% for atmospheric DMS.

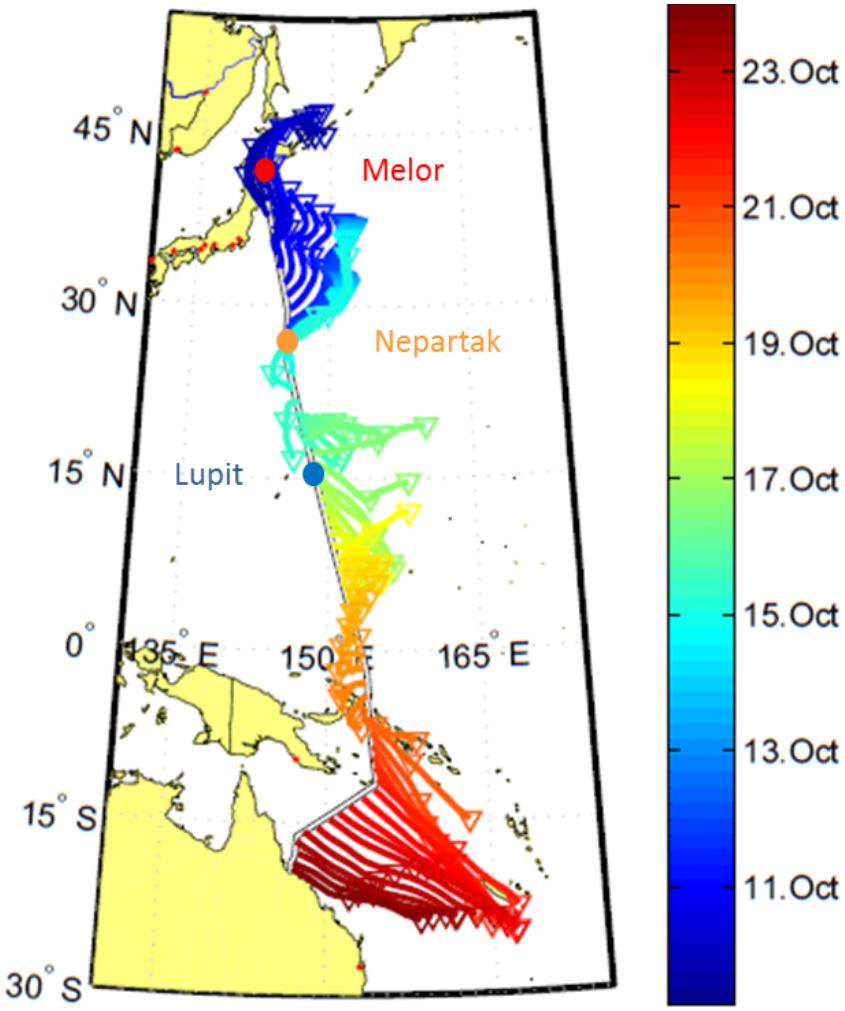

Fig. 3.1: *TransBrom cruise track from Japan to Australia in Oct 2009. Colored lines indicate one day back trajectories for each day shown in the colorbar. Dots on the cruise track indicate the three storm events that occurred during the cruise.*

The DMS oceanic and atmospheric data were used for the flux calculation. Sea surface temperature and wind speed data from ship sensors at one minute resolution were selected dependent on time and latitude of the DMS samples (Fig. 3.2). Flux calculations were performed by applying three different gas transfer coefficient parameterisations at a Schmidt number of 720, that of DMS in seawater at 25°C according to Saltzman *et al.* (1993), Marandino *et al.* (2007) - UCI, Wanninkhof (1992) - W92, Liss and Merlivat

(1986) - LM. The parameterisations were chosen to reflect the different theories of wind speed dependence and measurement techniques for k, where UCI is linear and derived from eddy covariance measurements, W92 is quadratic and derived from the ^{14}C ocean inventory, and LM contains three different linear parameterisations based on tracer studies and wind-wave tank measurements.

3.2.2 Model runs

The atmospheric transport of DMS from the oceanic surface into the upper troposphere and the TTL is simulated with the Lagrangian particle dispersion model FLEXPART (Stohl *et al.*, 2005). This model has been widely applied to simulate long-range and mesoscale transport (e.g., Spichtinger *et al.*, 2001; Stohl *et al.*, 2003; Forster *et al.*, 2004) and extensively validated based on measurement data from three large-scale tracer experiments (Stohl *et al.*, 1998) and on intercontinental air pollution transport studies (e.g. Stohl and Trickl, 1999; Forster *et al.*, 2001). FLEXPART is an off-line model driven by meteorological fields from the European Centre for Medium-Range Weather Forecast (ECMWF) numerical weather prediction model. It includes the simulation of chemical decay based on a prescribed atmospheric lifetime, parameterisations for moist convection (Forster *et al.*, 2007), turbulence in the boundary layer and free troposphere (Stohl and Thompson, 1999), dry deposition and in-cloud, as well as below-cloud, scavenging.

In order to quantify the amount of DMS transported into the upper TTL for the observations during the TransBrom campaign, we simulate the transport pathways (trajectories) of a multitude of air parcels starting at the ship measurement time and location. For each computed DMS in situ sea-to-air flux a separate FLEXPART run is launched where 10,000 air parcels were released over one hour from a 0.0002° x 0.0002° grid box ($\sim$500 m^2) at the ocean surface centered at the measurement location. Based on the computed DMS in situ flux, the total amount of DMS emitted from this grid box over one hour is calculated and uniformly distributed over all air parcels. The amount of DMS carried by each air parcel is reduced at a rate corresponding to its chemical lifetime, which is set to 12 h and 24 h to represent typical gas phase values found in the literature, for two model scenarios. The FLEXPART runs are driven by the ECMWF reanalysis product ERA-Interim (Dee *et al.*, 2011) using 6-hourly meteorological data. The input fields of horizontal and vertical wind, temperature, specific humidity, convective and large scale precipitation, among other parameters, are given at a horizontal resolution of 1° x 1° on 60 model levels.

For the validation of the FLEXPART runs, we compare simulated DMS abundances with available aircraft observations from the HIAPER Pole to Pole Observations (HIPPO) 2 campaign, which were collected during several flight missions over the Pacific Ocean during October/November 2009 (http://catalog.eol.ucar.edu/hippo2/index.html; Wofsy *et al.*, 2011). For this intercomparison, additional FLEXPART runs were launched applying

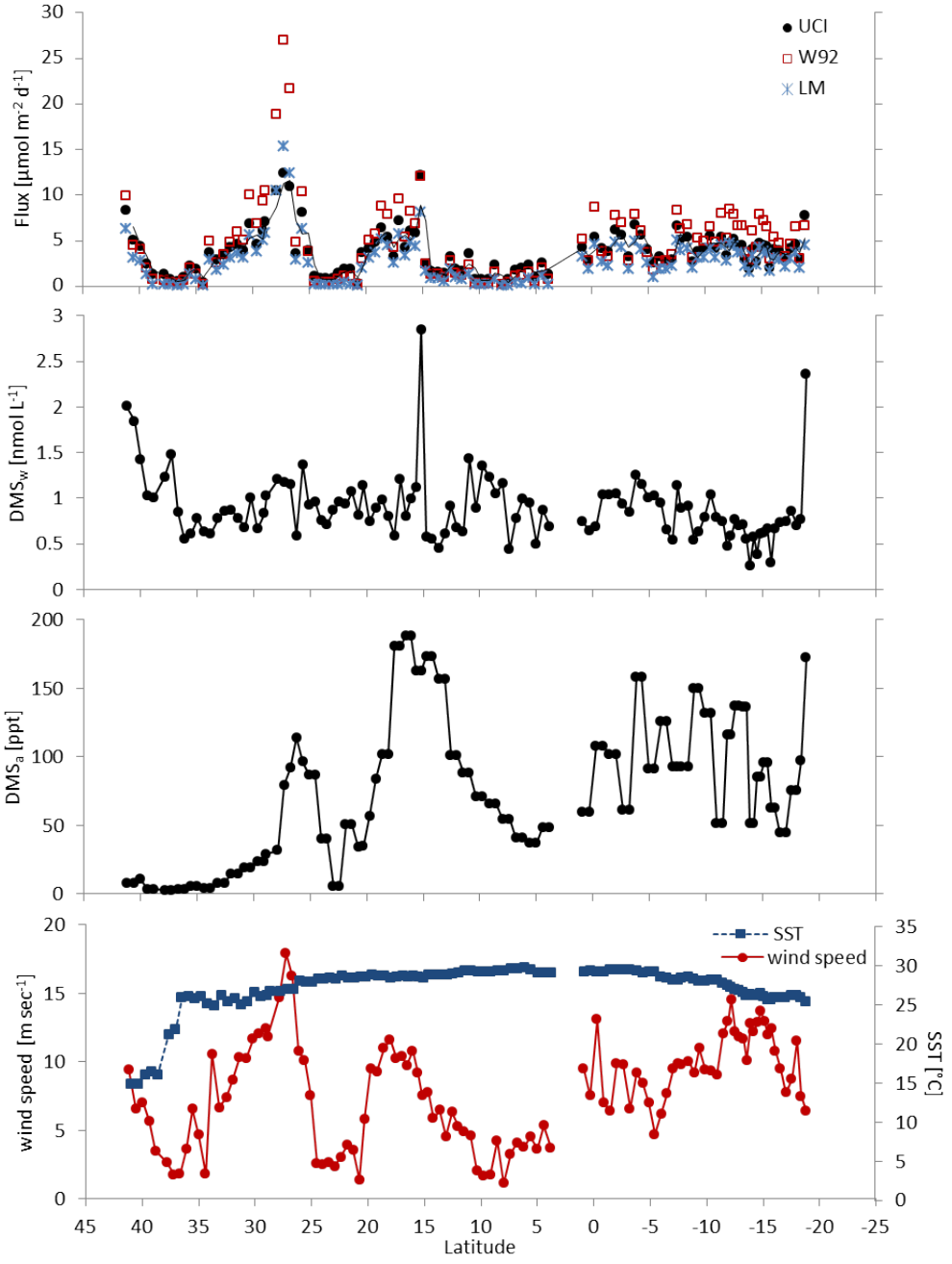

Fig. 3.2: *Shipboard measurements and subsequent flux calculations over the TRANSBROM cruise track (by latitude, positive denotes northern latitudes and negative southern), from top: panel 1) computed DMS fluxes using the UCI k parameterisation (UCI-solid circle), the Wanninkhof, 1992 parameterisation (W92-open square), and the Liss and Merlivat (1986) parameterisation (LM-asterix); panel 2) measured seawater DMS concentrations from Zindler et al. (2012) ; panel 3) measured atmospheric DMS mixing ratios; panel 4) measured horizontal wind speed (solid circle) and sea surface temperature (solid square).*

the actual meteorological fields for the time of the HIPPO2 campaign during November 2009, but using the DMS emissions from the TransBrom cruise during October 2009 since we do not have observed DMS emissions for November 2009. For these runs an average DMS emission of 1.54 × $10^{-7}\mathrm{mol\,m^{-2}\,hr^{-1}}$ was distributed uniformly over the tropical oceans (within 30°S–30°N) and the atmospheric DMS transport was calculated for November 2009. Additionally, the same global runs were carried out for October and December 2009 to estimate temporal (month-to-month) variations of the DMS entrainment into the stratosphere.

The level above which no significant washout is expected is of special importance for the transport of DMS to the stratosphere. DMS and its oxidation products reaching this altitude can be assumed to contribute to the stratospheric sulfur loading irrespective of their remaining chemical lifetime. While the exact vertical extent of the region where significant washout is expected is still under debate (Fueglistaler *et al.*, 2009), we have chosen the cold point temperature at around 17 km as upper estimate of this level. Additionally, we evaluate DMS entrainment above 15 km which is well above the main convective outflow regions and close to the level of zero radiative heating. Tost *et al.* (2010), using different convective parameterisation schemes in a global CTM, showed that the choice of the convection parameterisation has an influence on trace gas distributions. It is shown that the Emanuel parameterisation, used by FLEXPART, injects more mass across the 250 mb surface ($\sim$11 km altitude) in the tropics than other convection schemes used. Therefore, it is possible that FLEXPART may show increased injected mass across $\sim$ the 17 km altitude surface in the tropics. However, the representation of convection in FLEXPART has been validated with tracer experiments and ^{222}Rn measurements in Forster *et al.* (2007).

For the surface air mass origin, one-day backward trajectories have been calculated online with the HySplit model using the meteorological fields from National Centers for Environmental Prediction – Global Data Assimilation System (NCEP-GDAS). Detailed technical information about the trajectory model version 4 can be found in Draxler and Hess (2004).

3.3 Results and Discussion

3.3.1 Atmospheric concentrations and computed DMS air-sea fluxes

Atmospheric mixing ratios of DMS ranged between 2 and 200 ppt (76.2 ±52.2 ppt), which are in the low to average range for open ocean background mixing ratios of DMS (Fig. 3.2). Previous measurements of atmospheric DMS around the area of the TransBrom

cruise track are in general agreement, 26.6 $\pm$16.1 ppt, 19.3 $\pm$14.7 ppt, 42.4 $\pm$26.9 ppt, and 59.3 $\pm$16.8 ppt, but were measured during May–June (Kato *et al.*, 2007; Marandino *et al.*, 2007). DMS values measured in the marine boundary layer, during the adjacent HIPPO2 aircraft campaign (discussed in Sect. 3.3.2), were between 0 and 100 ppt during November 2009. One day back trajectory analysis shows that the first 5 days of the ship cruise were influenced by continental air masses from Asia, the next 6 days experienced back trajectories from the open ocean (the 11th day, just south of the equator had air masses originating over the Soloman Islands), and the air in the last 4 days originated from eastern Australia or the Tasman Sea (Fig. 3.1). The largest atmospheric DMS abundances were observed at approximately 16°N, when the cruise encountered the tropical storm Nepartak. However, the highest values that were not influenced by major storm events were found towards the end of the cruise track, in the air regime influenced by the Tasman Sea.

DMS fluxes were computed using the shipboard measurements of atmospheric and surface ocean concentrations (discussed by Zindler *et al.*, 2012), sea surface temperature, and horizontal wind speed (Fig. 3.2). Three different parameterisations were applied to compute the gas transfer coefficient: Marandino *et al.* (2007) – UCI; Wanninkhof (1992) – W92; Liss and Merlivat (1986) – LM. The computed fluxes vary between 3 and 30 $\mu\mathrm{mol\,m^{-2}\,d^{-1}}$. The range of the fluxes reflects the range in the computed k values, e.g. W92 employs a quadratic and UCI a linear wind speed dependence. The diversity of gas exchange parameterisations causes approximately a factor of three difference in the computed fluxes. In this study, the highest values were computed during the tropical storm Nepartak, during which the highest wind speeds (up to 18 $\mathrm{m\,s^{-1}}$) were experienced. The fluxes shown here are in the general range reported in the Lana *et al.* (2011) DMS climatology for October in this region. However, there are some spatial distribution differences. Lana *et al.* (2011) computed values between 0 and 15 $\mu\mathrm{mol\,m^{-2}\,d^{-1}}$, with a maximum of approximately 30 $\mu\mathrm{mol\,m^{-2}\,d^{-1}}$ in the Tasman Sea. Our maximum values are similar to those of Lana *et al.* (2011) but were observed northward of the equator between 20 and 40°N, directly related to storm events. The Tasman Sea values reported here did not reach the values in the Lana *et al.* (2011) climatology and are approximately 5 $\mu\mathrm{mol\,m^{-2}\,d^{-1}}$.

The computed fluxes in all cases correlate more with wind speed than with the seawater concentrations of DMS, especially for fluxes computed with k values more strongly dependent on wind speed (Fig. 3.3). This may point to the fact that the gas transfer coefficient parameterisation disproportionately influences the computed fluxes. Eddy correlation measurements of DMS flux have indicated that the surface seawater DMS concentrations explain more of the variability in the directly measured fluxes than horizontal wind speed by a factor of approximately 2 (Marandino *et al.*, 2007). Another complication surrounding the use of wind speed based parameterisations and measured concentrations was determined by Marandino *et al.* (2008). They found that directly measured emissions

were up to 5 times higher than those computed using the flux equation alone, possibly reflecting a disparity between the concentration of DMS at the interface and that of the bulk water. However, Marandino *et al.* (2008) hypothesise that this finding may be specific to regions with high biological activity and, therefore, may not be not applicable here.

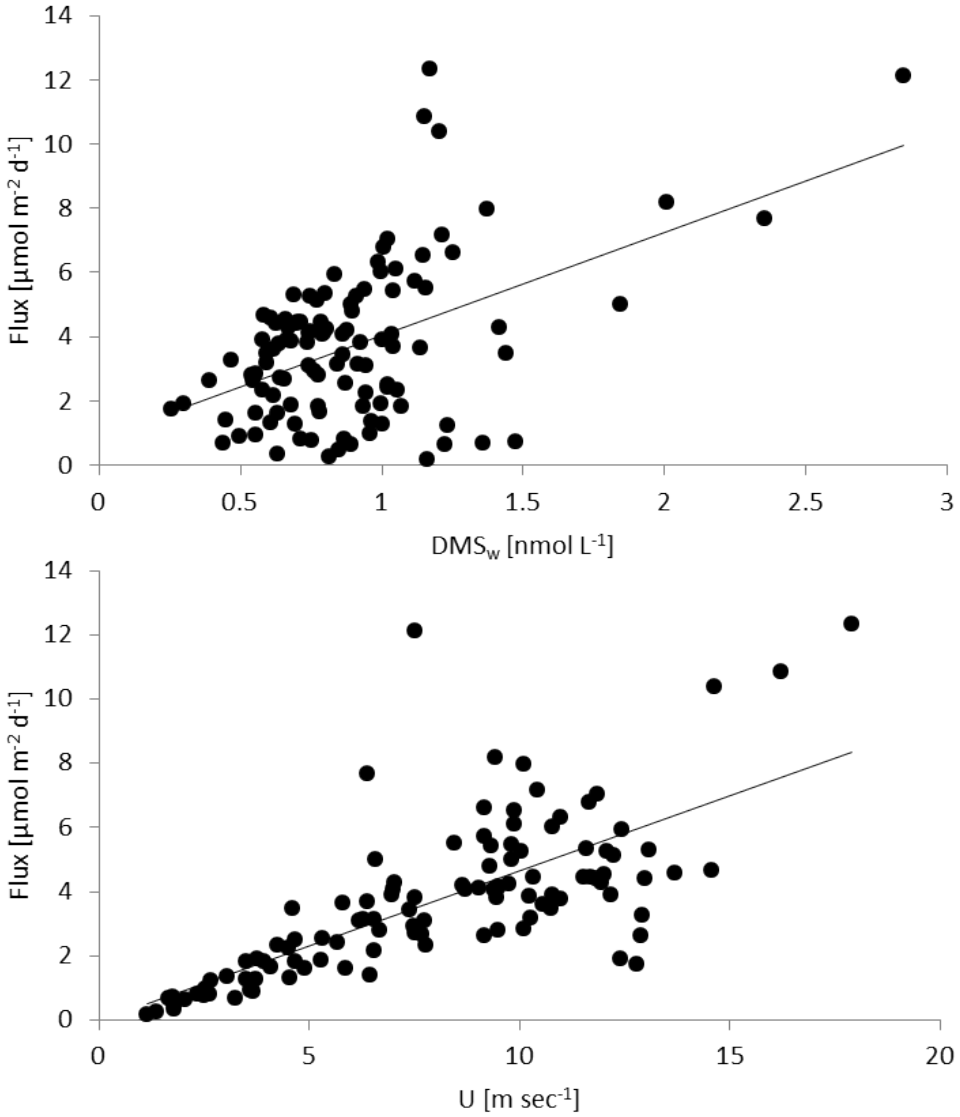

Fig. 3.3: *(Top) Computed flux regressed against seawater concentration of DMS (y = 3.20x + 0.84,* r^2 *= 0.24). (Bottom) Computed flux regressed again horizontal wind speed (y = 0.47x -0.00,* r^2 *= 0.52).*

Interestingly, atmospheric values of DMS do not follow the same pattern as the computed fluxes or seawater DMS concentrations over the cruise track (Fig. 3.2). It is evident that the seawater concentrations of DMS do not have the same level of variability as the air values. It is very likely that the atmospheric values measured over the cruise track were more

influenced by horizontal advection than by in situ fluxes. The highest fluxes were computed for the Nepartak storm event, at which time there is only a secondary maximum in the atmospheric mixing ratio. This may indicate that DMS was rapidly transported away and replaced with continental air, since back trajectories indicate a continental influence in this region. Conversely, there was a maximum peak in atmospheric values during the next tropical storm Lupit, which was at the secondary flux maximum. During this time, back trajectory analysis indicates that air masses originated from the open ocean. There may have been a larger source region upwind, which resulted in more DMS in the atmosphere that was rapidly transported by the storm toward the cruise track.

3.3.2 Implications for atmospheric sulphur loading

The measured levels of surface ocean DMS in the western Pacific Ocean are not above the mean level of the global open ocean (Zindler *et al.*, 2012). Considering that the patterns of atmospheric DMS mixing ratios do not follow the surface ocean concentration patterns, nor do the flux values, transport processes seem to have an important influence on DMS derived sulphur loading to the atmosphere. In order to investigate the role of transport in more detail, the high resolution transport model FLEXPART was used to track the fate of DMS after its emission from the ocean. As a test, the tropical DMS distribution based on average TransBrom emissions was calculated for November 2009, where *in-situ* aircraft measurements of the HIPPO2 campaign were available above the tropical West Pacific Ocean (see Sect. 3.2.2 for details). FLEXPART simulations use an atmospheric DMS lifetime of 1/2 day and the output is given on a 1° x 1° grid. Figure 3.4 shows the locations of the tropical HIPPO2 measurements color coded by day. Coincident data points between the tropical HIPPO2 measurements and the FLEXPART output were identified, if their distance in latitude/longitude space is less than 0.5° and their altitude distance is less than 500 m. A comparison of all identified coincidences is shown in the right panel of Fig. 3.4. Large parts of the vertical DMS distribution observed during the HIPPO2 campaign can be reproduced by the FLEXPART simulation. DMS values are high in the boundary layer and low above, reaching mixing ratios between 0 and 2 ppt in the lower TTL (12 – 14 km). Some fragment of the HIPPO2 observations shows very large values (around 200 ppt) at around 8 km altitude that are not reproduced by the FLEXPART simulations. It is very likely that these large DMS mixing ratios resulted from local convective events lifting DMS rich air from the boundary layer into the upper troposphere. These large DMS values seem to be due to an atmospheric feature that is narrow in horizontal extent. It is very likely that such small scale features can only be reproduced using the true emission fields, which are not available for the present FLEXPART runs. The overall good agreement provides confidence in the simulated oceanic DMS contribution to the upper atmosphere using the *in-situ* emissions from the TransBrom cruise.

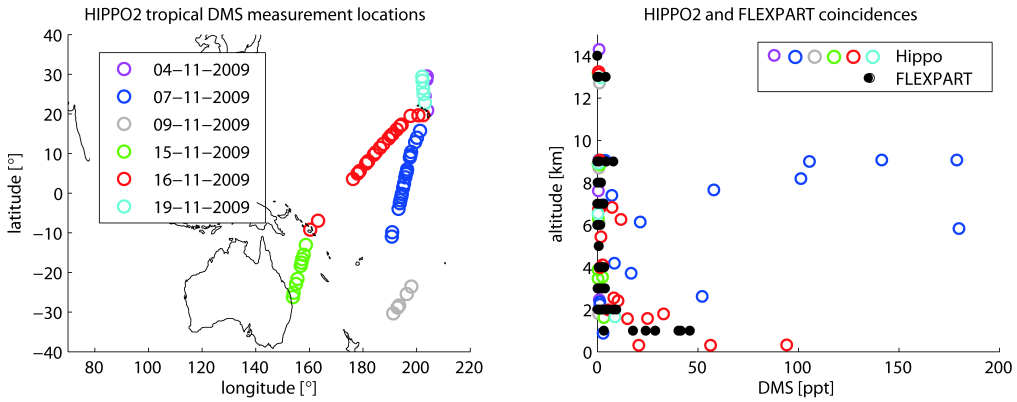

Fig. 3.4: *Comparison between HIPPO2 atmospheric DMS observations and FLEXPART DMS simulations (1/2 day atmospheric lifetime). Measurement locations for HIPPO2 (left panel) and comparison between HIPPO2 and FLEXPART coincidences (right panel) are shown.*

In the next step, the amount of DMS transported into the TTL and to the top of the TTL was calculated using the emissions computed with the UCI air-sea gas flux approach as input for the FLEXPART simulations (Sect. 3.2.2). Figure 3.5 shows the vertical DMS distribution given as a total quantity [kg] and as a relative quantity [%] with respect to the amount of originally emitted DMS for the 1/2 day lifetime case. This vertical DMS distribution was determined for each emission event as the accumulated amount of DMS reaching the respective altitudes given on the y-axis. Figure 3.5a illustrates that in most cases less than 30% of the originally emitted DMS leaves the boundary layer. With increasing altitude less DMS is found in the atmosphere and above 12 km more than 10% of the originally emitted DMS can only be detected for a few isolated cases. Less than 1% DMS in nearly all cases reaches the level of 17 km. The total amount of DMS transported from the ocean surface along the TransBrom cruise track is given in kg in Fig. 3.5b. Between 20°N and 15°N, as well as around 5°S, enhanced vertical transport, which is connected with intense tropical convection (Krüger and Quack, 2012), can be observed. These events coincide with medium to large DMS emissions resulting in $5\text{x}10^{-7}$ - $1\text{x}10^{-6}$ kg of DMS (equivalent to 3 to 10%) reaching the upper TTL. These same events also demonstrate that more than 30% of emitted DMS can reach 8 to 9 km altitude, where peak mixing ratios of 50 to 180 ppt were detected by the HIPPO2 aircraft campaign (Fig. 3.4). It is noteworthy, however, that the pattern in emissions, namely the peak emissions, does not entirely follow the pattern of entrainment to the TTL. On the first half of the cruise, until around 10°S, we can surmise that the storm events that triggered the large emissions do not always coincide with the high entrainment events. South of 10°S, the pattern of sea-to-air fluxes is more closely linked to the pattern of entrainment. Similar results were observed for $CHBr_3$ transport during the TransBrom cruise (Tegtmeier *et al.*, 2012). Figure 3.6 shows tropical estimates of the amount of DMS transported above the level of 17 km for two different atmospheric DMS lifetimes (1 day and 1/2 day). As

expected, the amount of DMS reaching 17 km is considerably smaller for the shorter lifetime.

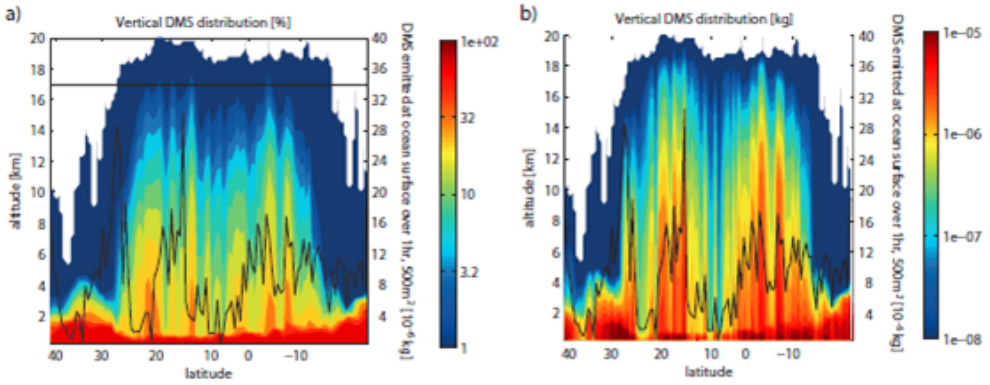

Fig. 3.5: *Atmospheric vertical DMS distribution computed along the TransBrom cruise track given as a) total amount [kg] and b) amount relative to DMS emission from the sea surface [%]. Atmospheric DMS distribution is based on FLEXPART simulations with a 1/2 day atmospheric lifetime. DMS emission at the ocean surface over 500* m^2 *and one hour is given as the black line corresponding to the right y-axis.*

These estimates of DMS entrained above 17 km, summed over the whole TransBrom campaign, are compared to the required global annual sulphur source computed by Hofmann *et al.* (2009) to maintain the PSL during volcanically quiescent periods (Table 3.1). For DMS with a one day lifetime, the average quantity transported above 17 km over the cruise track is approximately 6.37x10^{-6} kg DMS hr^{-1} or 2.37 x 10^{-11} Tg S month^{-1}. The value changes to 3.84x10^{-6} kg DMS when FLEXPART is run with the more conservative assumption of a DMS lifetime of 12 h. The monthly mean calculation for DMS transport above 17 km assumes that the DMS emission field and convective processes are constant for the entire month, which is reasonable given that the cruise and FLEXPART runs extended over a 2 week period. Hoffman *et al.* (2009) calculates that 0.01 - 0.02 Tg S yr^{-1} is required globally, from all the different sulphur sources, including anthropogenic sulphur and minor volcanic eruptions, to maintain the increase in the PSL after 2000. A value of 2.0x10^{-13} Tg S month^{-1} is obtained when this value is scaled down by surface area to the region of the cruise track, i.e. the surface area of cruise track (5.75x10^4 m^2) divided by the surface area of world ocean (3.6x10^{14} m^2). The amount of DMS projected to be transported above the TTL is approximately 75 - 119 times higher than the required amount of sulphur from Hoffman *et al.* (2009). This computed sulphur loading does not take into account the oxidation products of DMS that may also be transported above the TTL. Myhre *et al.* (2004) projected that natural sulphur emissions on a global scale contribute significantly to the PSL source, however they also conclude that anthropogenic emissions are the dominant factor. While their conclusions are obvious for the global scale, the regional importance of marine sulphur has been overlooked. The value

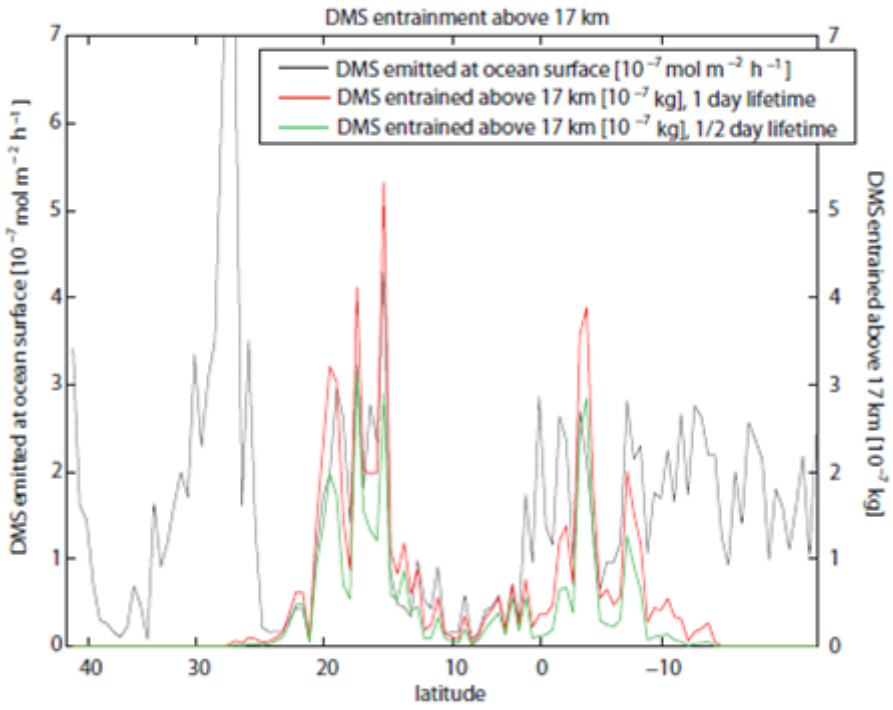

Fig. 3.6: *Observed emissions of DMS at the ocean surface (black line), and total amount of DMS entrained above 17 km based on FLEXPART simulations with 1 day (red line) and 1/2 day (green line) atmospheric lifetimes are shown.*

Tab. 3.1: *Calculation of sulphur loading above the TTL relative to the 0.015 Tg S* yr^{-1} *required globally to maintain PSL after 2002 (Hofmann et al. 2009). Note that the DMS above 17 km and the required Tg S were scaled to the area of emissions.*

DMS lifetime	DMS above 17 km (Tg S month^{-1})	Area of emissions (m^2)	Area of global ocean (m^2)	Required Tg S month^{-1}	Marine contribution (multiplying factor)
12 h	1.43×10^{-11}	5.75×10^{4}	3.60×10^{14}	2.00×10^{-13}	71.5
24 h	2.37×10^{-11}				119

computed here from the TransBrom cruise highlights that oceanic emissions of DMS in regions of fast vertical uplift play a disproportionately (when evaluated by regional size) important role in the radiative budget of the atmosphere. Modest increases in marine emissions coupled to enhancements of vertical transport or tropical cyclone activity in the tropics may easily be a main factor, on a regional scale, contributing to the higher source of sulphur discussed by Hofmann *et al.* (2009) to the PSL.

Additionally, the entrainment rates modeled by FLEXPART for the month of October are not constant over the entire year. Figure 3.7 illustrates the change in tropical (20°S – 20°N) DMS entrainment above 15 and 17 km over time, from October to December 2009, based on the conservative lifetime projection of 1/2 day. The FLEXPART runs use the same emission fields over the entire period, but variability in entrainment is clearly evident. This variability is only due to changes in the meteorology and hence in vertical transport processes (i.e. deep tropical convection) over time. On average, October shows lower DMS abundances at 15 and 17 km altitude than November and December, as would be expected from the pronounced and fast TTL transport during the boreal winter season over the West Pacific Ocean (Fueglistaler and Haynes, 2005; Krüger *et al.*, 2009). These runs are of course only representative for 2009 and interannual variability may be even more pronounced. However, during the TransBrom period from 9 to 24 October 2009, the DMS model values can be as high as during other shortterm periods for November and December months. Thus, we conclude that given the very short lifetime of DMS the TTL entrainment is mainly determined by synoptic-scale processes such as tropical deep convective events rather than large-scale seasonal effects. The Lana *et al.* (2011) flux climatology shows increased DMS emissions in the tropics seasonally, especially from December to February. The emissions increase approximately 5 times over that time period, while entrainment above 17 km stays in the same order of magnitude and can be large for short-term periods (Fig. 7). Scenarios, in which several factors related to both emissions and meteorology background conditions (e.g. wind speed and direction, sea

surface temperature) change, need to be investigated in order to understand how increased marine emissions coupled with increased transport to the stratosphere may impact sulphur loading to the free troposphere as well as to the PSL.

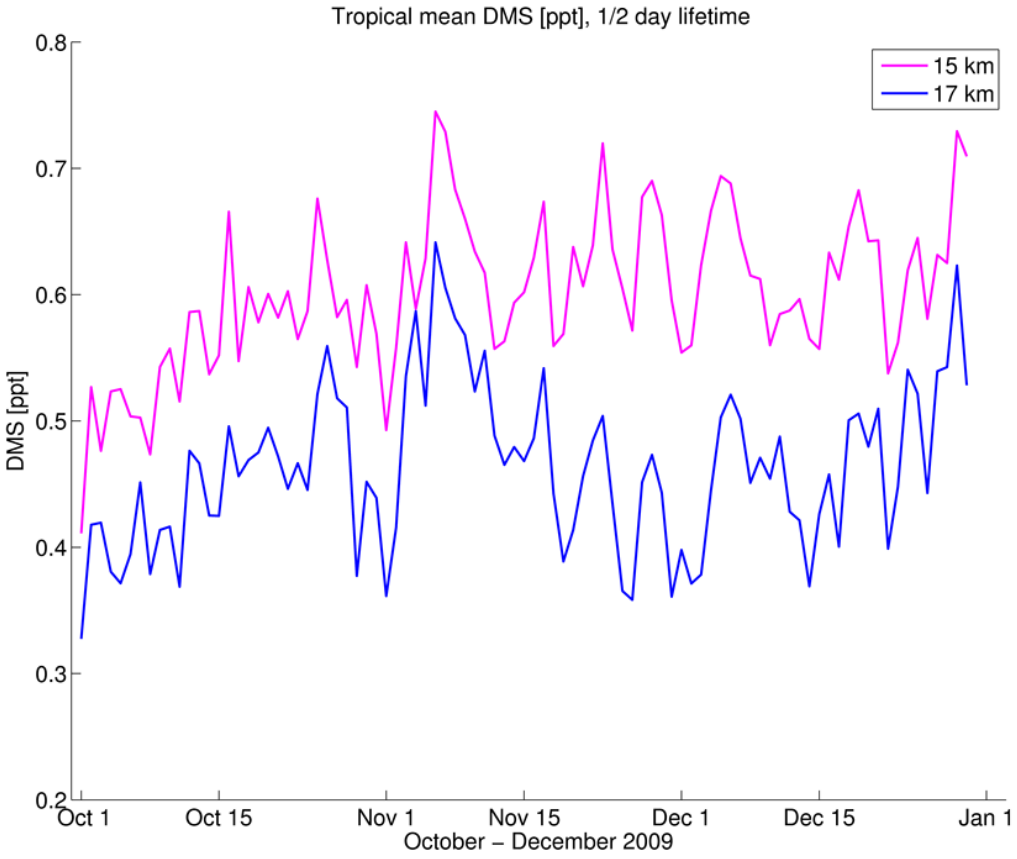

Fig. 3.7: *Time series of tropical mean DMS VMR at 17 km and 15 km for October to December 2009. The time series is based on FLEXPART model simulations using TransBrom average emissions for the tropcial oceans and 1/2 day atmospheric lifetime for DMS.*

3.4 Conclusions

Ship measurements of seawater and atmospheric DMS, wind speed, and sea surface temperature from October 2009 in the western Pacific Ocean, on board the TransBrom cruise, were used to compute marine emissions of DMS. The emissions were employed to model the amount of DMS that is transported above the tropical tropopause layer (17 km) in October applying the high resolution Lagrangian transport model FLEXPART. The resulting amount of DMS in the stratosphere is notable, 75 – 119 times greater than the required stratospheric source when scaled by region. This amount could also increase with season, during times of higher emission, tropical cyclone or deep tropical convection activities.

Given that dissolved DMS concentrations observed in the tropical western Pacific Ocean were not considerably high, it is noteworthy that the intense vertical transport in this area deliver large quantities of DMS and its oxidation products into the stratosphere, where they can (further) oxidize and form sulfate aerosol. Additional focused studies on DMS seawater concentrations and emissions are required in regions, such as the western tropical Pacific Ocean, in order to better quantify the full impact of marine DMS emissions on the radiative budget of the atmosphere, now and in a future climate.

Acknowledgements

We acknowledge the support of the captains and crews of R/V Sonne as well as the chief scientist of "TransBrom-Sonne", Birgit Quack. The authors are grateful for fruitful discussions with Douglas Wallace and Arne Körtzinger. We thank Franziska Wittke for assistance with the measurements of the sulphur compounds and Sebastian Wache and Steffen Fuhlbrügge for the trajectory analysis and creating Fig. 3.1. Financial support of this study was provided by the BMBF grant SOPRAN II FKZ 03F0462A and by the WGL project TransBrom (www.geomar.de/ transbrom). The R/V Sonne transit cruise was financed by the BMBF through grant 03G0731A. CM and CZ were partly financed by Christa Marandino's Helmholtz Young Investigator Group TRASE-EC, funded by the Helmholtz Association through the President's Initiative and Networking Fund and the Helmholtz-Zentrum für Ozeanforschung Kiel (GEOMAR).

References

Alvarez, L. A., Exton, D. A., Timmis, K. N., Suggett, D. J., and McGenity, T. J.: Characterization of marine isoprene-degrading communities, Environmental Microbiology, 11, 3280-3291, 10.1111/j.1462-2920.2009.02069.x, 2009.

Arnold, S. R., Spracklen, D. V., Williams, J., Yassaa, N., Sciare, J., Bonsang, B., Gros, V., Peeken, I., Lewis, A. C., Alvain, S., and Moulin, C.: Evaluation of the global oceanic isoprene source and its impacts on marine organic carbon aerosol, Atmospheric Chemistry and Physics, 9, 1253-1262, 2009.

Baker, A. R., Turner, S. M., Broadgate, W. J., Thompson, A., McFiggans, G. B., Vesperini, O., Nightingale, P. D., Liss, P. S., and Jickells, T. D.: Distribution and sea-air fluxes of biogenic trace gases in the eastern atlantic ocean, Global Biogeochem. Cycles, 14, 871-886, 10.1029/1999gb001219, 2000.

Balch, W. M., Holligan, P. M., Ackleson, S. G., and Voss, K. J.: Biological and optical properties of mesoscale coccolithophore blooms in the gulf of maine, Limnology and Oceanography, 629-643, 1991.

Bonsang, B., Polle, C., and Lambert, G.: Evidence for marine production of isoprene, Geophys. Res. Lett., 19, 1129-1132, 10.1029/92gl00083, 1992. Bonsang, B., Gros, V., Peeken, I., Yassaa, N., Bluhm, K., Zoellner, E., Sarda-Esteve, R., and Williams, J.: Isoprene emission from phytoplankton monocultures: The relationship with chlorophyll-a, cell volume and carbon content, Environmental Chemistry, 7, 554-563, 2010.
Broadgate, W. J., Liss, P. S., and Penkett, S. A.: Seasonal emissions of isoprene and other reactive hydrocarbon gases from the ocean, Geophys. Res. Lett., 24, 2675-2678, 10.1029/97gl02736, 1997.
Colomb, A., Yassaa, N., Williams, J., Peeken, I., and Lochte, K.: Screening volatile organic compounds (vocs) emissions from five marine phytoplankton species by head space gas chromatography/mass spectrometry (hs-gc/ms), Journal of Environmental Monitoring, 10, 325-330, 10.1039/b715312k, 2008.
Curson, A. R. J., Rogers, R., Todd, J. D., Brearley, C. A., and Johnston, A. W. B.: Molecular genetic analysis of a dimethylsulfoniopropionate lyase that liberates the climate-changing gas dimethylsulfide in several marine α-proteobacteria and rhodobacter sphaeroides, Environmental Microbiology, 10, 757-767, 10.1111/j.1462-2920.2007.01499.x, 2008.
Dacey, J. W., Wakeham, S. G., and Howes, B. L.: Henry's law constants for dimethylsulfide in freshwater and seawater, Geophysical Research Letters, 11, 991-994, 1984.
Hernandez-Guerra, A., Lopez-Laatzen, F., Machin, F., De Armas, D., and Pelegri, J. L.: Water masses, circulation and transport in the eastern boundary current of the north atlantic subtropical gyre, Scientia Marina, 65, 177-186, 2001.
Holligan, P., Viollier, M., Harbour, D., Camus, P., and Champagne-Philippe, M.: Satellite and ship studies of coccolithophore production along a continental shelf edge, 1983.
Houweling, S., Dentener, F., and Lelieveld, J.: The impact of nonmethane hydrocarbon compounds on tropospheric photochemistry, Journal of Geophysical Research: Atmospheres, 103, 10673-10696, 10.1029/97jd03582, 1998.
Keller, M. D., Bellows, W. K., and Guillard, R. R. L.: Dimethyl sulfide production in marine-phytoplankton, Acs Symposium Series, 393, 167-182, 1989.
Kiene, R. P., Linn, L. J., and Bruton, J. A.: New and important roles for dmsp in marine microbial communities, Journal of Sea Research, 43, 209-224, 10.1016/s1385-1101(00)00023-x, 2000.
Koch, B. P., and Kattner, G.: Preface 'sources and rapid biogeochemical transformation of dissolved organic matter in the atlantic surface ocean', Biogeosciences, 9, 2597-2602, 10.5194/bg-9-2597-2012, 2012.
Kuzma, J., Nemecekmarshall, M., Pollock, W. H., and Fall, R.: Bacteria produce the volatile hydrocarbon isoprene, Current Microbiology, 30, 97-103, 10.1007/ bf00294190, 1995.
Leck, C., Larsson, U., Bagander, L. E., Johansson, S., and Hajdu, S.: Dimethyl sulfide in the baltic sea - annual variability in relation to biological-activity, Journal of Geophysical

Research-Oceans, 95, 3353-3363, 10.1029/JC095iC03p03353, 1990.
Marandino, C. A., De Bruyn, W. J., Miller, S. D., and Saltzman, E. S.: Eddy correlation measurements of the air/sea flux of dimethylsulfide over the north pacific ocean, J. Geophys. Res.-Atmos., 112, 10.1029/2006jd007293, 2007.
Marandino, C. A., Tegtmeier, S., Krüger, K., Zindler, C., Atlas, E. L., Moore, F., and W., B. H.: Dimethylsulphide (dms) emissions from the west pacific ocean: A potential marine source for the stratospheric sulphur layer, Atmos. Chem. Phys. Discuss.,, 12, 30543-30570, 10.5194/acpd-12-30543-2012, 2012.
McKay, W. A., Turner, M. F., Jones, B. M. R., and Halliwell, C. M.: Emissions of hydrocarbons from marine phytoplankton—some results from controlled laboratory experiments, Atmospheric Environment, 30, 2583-2593, 10.1016/1352-2310(95)00433-5, 1996.
Meskhidze, N., and Nenes, A.: Phytoplankton and cloudiness in the southern ocean, Science, 314, 1419-1423, 10.1126/science.1131779, 2006.
Milne, P. J., Riemer, D. D., Zika, R. G., and Brand, L. E.: Measurement of vertical distribution of isoprene in surface seawater, its chemical fate, and its emission from several phytoplankton monocultures, Marine Chemistry, 48, 237-244, 10.1016/0304-4203(94)00059-m, 1995.
Moore, R. M., Oram, D. E., and Penkett, S. A.: Production of isoprene by marine phytoplankton cultures, Geophys. Res. Lett., 21, 2507-2510, 10.1029/94gl02363, 1994.
Moore, R. M., and Wang, L.: The influence of iron fertilization on the fluxes of methyl halides and isoprene from ocean to atmosphere in the series experiment, Deep Sea Research Part II: Topical Studies in Oceanography, 53, 2398-2409, 10.1016/j.dsr2.2006.05.025, 2006.
Neogi, S. B., Koch, B. P., Schmitt-Kopplin, P., Pohl, C., Kattner, G., Yamasaki, S., and Lara, R. J.: Biogeochemical controls on the bacterial populations in the eastern atlantic ocean, Biogeosciences, 8, 3747-3759, 10.5194/bg-8-3747-2011, 2011.
Palmer, P. I., and Shaw, S. L.: Quantifying global marine isoprene fluxes using modis chlorophyll observations, Geophys. Res. Lett, 32, L09805-L09810, 2005.
Schäfer, H., Myronova, N., and Boden, R.: Microbial degradation of dimethylsulphide and related c1-sulphur compounds: Organisms and pathways controlling fluxes of sulphur in the biosphere, Journal of Experimental Botany, 61, 315-334, 10.1093/jxb/erp355, 2010.
Schmitt-Kopplin, P., Liger-Belair, G., Koch, B. P., Flerus, R., Kattner, G., Harir, M., Kanawati, B., Lucio, M., Tziotis, D., Hertkorn, N., and Gebefügi, I.: Dissolved organic matter in sea spray: A transfer study from marine surface water to aerosols, Biogeosciences, 9, 1571-1582, 10.5194/bg-9-1571-2012, 2012.
Sharkey, T. D., Wiberley, A. E., and Donohue, A. R.: Isoprene emission from plants: Why and how, Annals of Botany, 101, 5-18, 2008.
Shaw, S. L., Chisholm, S. W., and Prinn, R. G.: Isoprene production by prochlorococ-

cus, a marine cyanobacterium, and other phytoplankton, Marine Chemistry, 80, 227-245, 10.1016/s0304-4203(02)00101-9, 2003.
Shaw, S. L., Gantt, B., and Meskhidze, N.: Production and emissions of marine isoprene and monoterpenes: A review, Advances in Meteorology, 10.1155/2010/ 408696, 2010.
Simó, R.: From cells to globe: Approaching the dynamics of dms(p) in the ocean at multiple scales, Canadian Journal of Fisheries and Aquatic Sciences, 61, 673-684, 10.1139/f04-030, 2004.
Stefels, J., Steinke, M., Turner, S., Malin, G., and Belviso, S.: Environmental constraints on the production and removal of the climatically active gas dimethylsulphide (dms) and implications for ecosystem modelling, Biogeochemistry, 83, 245-275, 10.1007/s10533-007-9091-5, 2007.
Steinke, M., Malin, G., Archer, S. D., Burkill, P. H., and Liss, P. S.: Dms production in a coccolithophorid bloom: Evidence for the importance of dinoflagellate dmsp lyases, Aquatic Microbial Ecology, 26, 259-270, 10.3354/ame026259, 2002.
Stramma, L., and Schott, F.: The mean flow field of the tropical atlantic ocean, Deep-Sea Research Part Ii-Topical Studies in Oceanography, 46, 279-303, 10.1016/ s0967-0645(98)00109-x, 1999.
Taylor, B. B., Torrecilla, E., Bernhardt, A., Taylor, M. H., Peeken, I., Rottgers, R., Piera, J., and Bracher, A.: Bio-optical provinces in the eastern atlantic ocean and their biogeographical relevance, Biogeosciences, 8, 3609-3629, 10.5194/bg-8-3609-2011, 2011.
Vogt, M., and Liss, P. S.: Dimethylsulfide and climate, Surface ocean - lower atmosphere processes, 187, Geophysical Monograph Series, AGU, Washingtion, DC, 2009.
Yoch, D. C.: Dimethylsulfoniopropionate: Its sources, role in the marine food web, and biological degradation to dimethylsulfide, APPLIED AND ENVIRONMENTAL MICROBIOLOGY, 68, 5804-5815, 10.1128/aem.68.12.5804-5815.2002, 2002.
Yokouchi, Y., Li, H.-J., Machida, T., Aoki, S., and Akimoto, H.: Isoprene in the marine boundary layer (southeast asian sea, eastern indian ocean, and southern ocean): Comparison with dimethyl sulfide and bromoform, J. Geophys. Res., 104, 8067-8076, 10.1029/1998jd100013, 1999.
Zindler, C., Bracher, A., Marandino, C. A., Taylor, B., Torrecilla, E., Kock, A., and Bange, H. W.: Sulphur compounds, methane, and phytoplankton: Interactions along a north-south transit in the western pacific ocean, Biogeosciences Discuss., 9, 15011-15049, 10.5194/bgd-9-15011-2012, 2012a.
Zindler, C., Peeken, I., Marandino, C. A., and Bange, H. W.: Environmental control on the variability of dms and dmsp in the mauritanian upwelling region, Biogeosciences, 9, 1041-1051, 10.5194/bg-9-1041-2012, 2012b.

4 Dimethylsulfide (DMS) and isoprene in the ocean surface layer along a north-south transit in the eastern Atlantic Ocean

Abstract

Continuous measurements of isoprene (2-methyl-1,3-butadiene) and dimethylsulfide (DMS) were conducted in surface seawater along a north-south transit in the eastern Atlantic Ocean in November 2008. Positive and negative correlations between DMS and isoprene were observed in different areas extending over two-thirds of the sampling site. A link between DMS and isoprene was determined in oligotrophic and euthrophic regions when the gases were clustered by their dependence on N:P, reflecting a common source and/or sink of the two compounds possibly related to bacteria. Dimethylsulfoniopropionate (DMSP), the precursor of DMS, correlated with isoprene in oligotrophic to mesotrophic regions when clustered according to N:P. Different phytoplankton groups, such as dinoflagellates, haptophytes and chrysophytes, seemed to be a common source of both DMSP and isoprene. Furthermore, the distribution pattern of the ratio of DMS and isoprene was related to the hydrographic regions of the eastern Atlantic Ocean. Enhanced isoprene concentrations compared to DMS were observed the in Canary Current, ITCZ and equator regions. Elevated DMS concentrations were detected in the Guinea Dome and Angola Gyre. The differences in the distribution pattern might be due to a non-DMSP producing biological source for isoprene and transport of the longer lived isoprene compared to DMS. However, the highest concentrations of DMS and isoprene were observed in a spring bloom near South Africa, pointing to the overwhelming role of biological activities on the production of both trace gases.

4.1 Introduction

Isoprene (2-methyl-1,3-butadiene; $CH_2{=}C(CH_3)CH{=}CH_2$) and dimethylsulfide (DMS; $(CH_3)_2S$) are atmospheric trace constituents which play important roles in processes related to atmospheric chemistry and the climate of the Earth. DMS emitted from the ocean is the most important natural source of sulfur to the troposphere (Vogt and Liss 2009) and, moreover, may also contribute significantly in tropical regions to upper troposphere sulfur loading (Marandino *et al.,* 2012). The view that DMS is the major precursor for cloud condensation nuclei in remote marine areas has been questioned recently (Quinn and Bates, 2011). Isoprene is the most abundant biogenic non-methane hydrocarbon in the atmosphere. Isoprene oxidation products have been shown to form secondary organic aerosols (Schmitt-Kopplin *et al.,* 2012) and, thus, have an indirect impact on the Earth's climate (Shaw *et al.,* 2010). Additionally, isoprene has a strong effect on the balance of oxidants in the atmosphere and plays a key role in the formation and destruction of tropospheric ozone (Houweling *et al.,* 1998). Terrestrial vegetation is the largest source of isoprene to the atmosphere (Sharkey *et al.,* (2008) and references therein), while the ocean is a comparably weak source (Baker *et al.,* 2000, Arnold *et al.,* 2009). Due to the high volatile and reactive character of isoprene, its oceanic emissions may have seasonal and/or regional impacts on the atmosphere, especially in productive areas of remote marine regions and coastal upwelling areas (Shaw *et al.,* 2010).

The occurrence of phytoplankton plays a central role in the oceanic pathways of both gases DMS and isoprene. Oceanic DMS and its major precursor dimethylsulfoniopropionate (DMSP) are involved in a complex interplay of biotic and abiotic pathways. DMSP is formed by phytoplankton and can be cleaved to DMS by bacteria and phytoplankton. DMS is subject to microbial consumption as well as photochemical oxidation and loss to the atmosphere (Simó 2004, Stefels *et al.,* 2007, Vogt and Liss 2009, Schäfer *et al.,* 2010). In contrast, comparably little is known about the oceanic pathways of isoprene. A wide range of phytoplankton species of different functional groups, as well as seaweed, can produce isoprene (Shaw *et al.,* 2010, and references therein). Less is known about the chemical loss of oceanic isoprene and only few studies showed microbial consumption of marine isoprene (Alvarez *et al.,* 2009). Elevated isoprene concentrations were observed above phytoplankton blooms, suggesting that the main loss of isoprene from the ocean is the release to the atmosphere (Yokouchi *et al.,* 1999, Palmer and Shaw 2005, Meskhidze and Nenes 2006).

In this study, DMS and isoprene were concurrently and continuously measured at high resolution in the surface seawater of the eastern Atlantic Ocean along the transit ANT-XXV/1 with R/V Polarstern from Bremerhaven, Germany, to Cape Town, South Africa, in November 2008 (Koch and Kattner 2012) (Fig. 4.1). In order to determine the major factors influencing the surface distributions of DMS and isoprene in the eastern Atlantic

Ocean, a suite of additional measurements such as dissolved and particulate DMSP, phytoplankton composition, chlorophyll a as well as satellite data of chlorophyll a and calcite were examined in conjunction with the trace gases.

4.2 Methods

4.2.1 Trace gas and DMSP measurements

DMS and isoprene were continuously measured using an atmospheric pressure chemical ionization mass spectrometer (mini-CIMS). The mini-CIMS consists of a ^{63}Ni atmospheric pressure ionization source coupled to a single quadrupole mass analyzer (Stanford Research Systems Residual Gas Analyzer; SRS RGA200) (Saltzman *et al.,* 2009). DMS and isoprene in seawater were analyzed by coupling the mini-CIMS to a homemade porous Teflon membrane equilibrator. The porous membrane (International Polymer Engineering) was housed inside a 1/2 inch outer diameter Teflon tube (Saltzman *et al.,* 2009). Seawater from approximately 2 m depth was supplied to the equilibrator at a flow rate of approximately 1 $\mathrm{L\,min^{-1}}$ using a continuous pumping system off the side of the ship (for details see Neogi *et al.,* (2011)). A counterflow of dry, purified air (Dominick Hunter) was directed through the equilibrator at 100 $\mathrm{mL\,min^{-1}}$. The equilibrated air stream was diluted with 1.7 $\mathrm{L\,min^{-1}}$ of clean purified air. Trideuterated DMS (CD_3SCH_3) (CD_3SCH_3, 2.78 ppm, 2 mlpm) was added to the air stream as an internal standard. Isoprene sensitivities were calculated by standard addition of unlabeled isoprene from a standard tank every 12 hours.

The mini-CIMS measurement protocol was 30 minutes of blank and standard addition measurements, followed by 12 hours of continuous seawater measurements. The types of blanks measured were as follows: 1) the sampling system excluding the equilibrator 2) the sampling system including the equilibrator without standards added. There were several periods during which the continuous seawater pumping system was not operating properly, resulting in many bubbles entering the equilibrator. These periods were removed from the dataset.

The AP-CIMS seawater DMS concentrations were calculated by determining the equilibrated mixing ratio using the continuously monitored isotope standard and then applying the temperature dependent Henry's law constant (Dacey *et al.,* 1984) using *in-situ* measured sea surface temperature, as described in Marandino *et al.,* (2007). The isoprene seawater concentrations were more difficult to determine because isoprene is highly insoluble and no temperature dependent Henry's law (H) equation exists for isoprene in seawater. Isoprene equilibration mixing ratios were calculated using the instrument isoprene sensitivity determined by standard addition and seawater concentrations were computed

using the freshwater temperature dependence from Mackay and Shiu (1981). The freshwater H values were reduced by 10% to account for the salting out effect. Because the solubility of isoprene is relatively low, a significant fraction of seawater was transferred to the air flow in the equilibrator (roughly 35%). The measured seawater isoprene concentration was corrected to account for this effect. All AP-CIMS data shown here are five minute averages. The precision for DMS and isoprene measurements, calculated using the standard gases, were 6% and 13%, respectively.

DMSP was also measured concurrently using a gas chromatograph-flame photometric detection system (GC-FPD) according to the method described in Zindler *et al.,* (2012a). The mean analytical errors of dissolved DMSP ($\mathrm{DMSP_d}$) and particulate DMSP ($\mathrm{DMSP_p}$) were ±19% and ±20%, respectively. Discrete samples from the continuous seawater pumping system were taken for GC-FPD measurements irregularly in time steps between 1 and 9 hours. During the cruise, low temperatures in the laboratory caused problems with the detection limit. As a result, there are several periods with missing DMSP data.

4.2.2 Additional parameters

Phytoplankton pigments and nutrient data from the transit are described in Taylor *et al.,* (2011) and Neogi *et al.,* (2011), respectively. Surface seawater temperature (SST), surface seawater salinity (SSS) and wind speed were recorded in 1 minute resolution by the ship's automatic recording system. The MODIS chlorophyll and calcite satellite data (http://modis.gsfc.nasa.gov/) used was the 8 day composite for each week of the cruise track, 4 weeks in total. HYSPLIT was used to compute the 5 day back trajectories.

4.3 Setting of the eastern Atlantic Ocean in November 2008

A general introduction to the hydrographic and biogeochemical setting of the eastern Atlantic Ocean during the transit ANT-XXV/1 is given in Koch and Kattner (2012). SST and SSS at approximately 5 m depth as well as wind speed are shown in Fig. 4.2 for the entire transit. Mean SSS ranged between 33.8 and 37 with a mean value of 35.9. The most salty waters were found between 20°N and 35°N as well as between 5°N and 18°S when the equatorial upwelling (2°N – 2°S) and the Angola-Benguela Front (around 14°S) was encountered, respectively. The Intertropical Convergence Zone (ITCZ) was detected between 2°N and 10°N with lowest salinity (33.8) measured along the transit. A mean SST of 21.5°C was determined with a range of 12.2°C to 29.8°C. The coldest waters occurred in the English Channel and the region of the tidal front at around 48°N and increased continuously towards the south with a maximum value at 7.6°N. Further

south the SST decreased again. Wind speed ranged between 0.3 and 19.2 $\mathrm{m\,s^{-1}}$ with a mean value of 7.6 $\mathrm{m\,s^{-1}}$. The highest wind speeds were measured in the English Channel (50°N) around 44°N, at 25°N, and near the South African coast (26°S, Fig. 4.2).

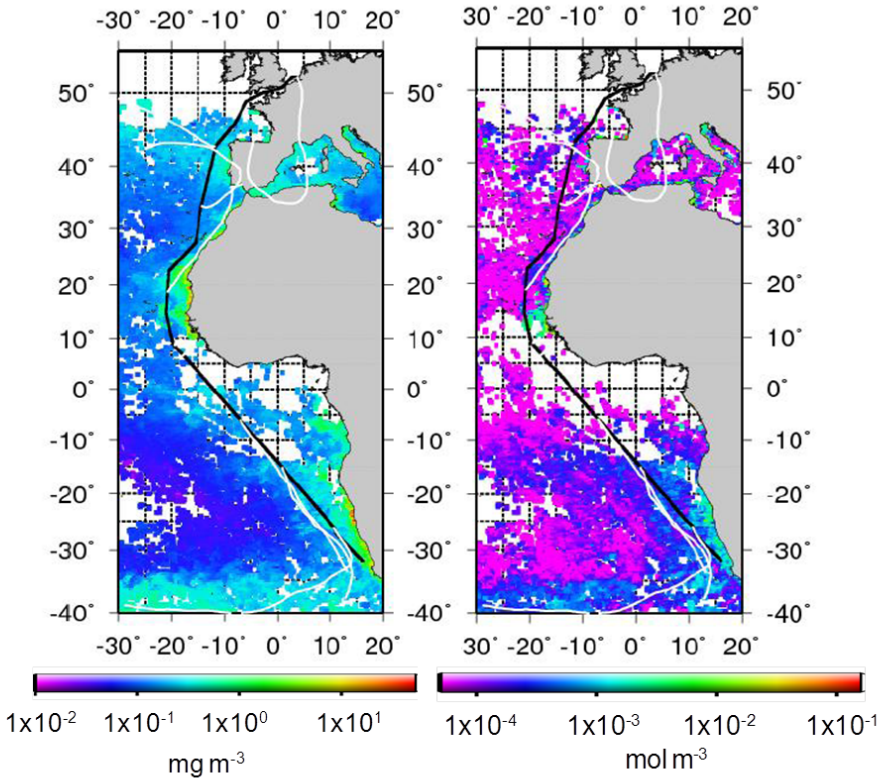

Fig. 4.1: *ANT-XXV/1 cruise track superimposed on MODIS chlorophyll (left) and calcite (right) data. The white lines are 5 day back trajectories from HYSPLIT.*

The highest sea surface nutrient concentrations were measured near the coast, off South Africa and in the English Channel, while between 40°N and 15°S the concentrations were low with a small concentration peaks between 10°N and 20°N. Nitrate ranged between 0 - 9.34 $\mu\mathrm{mol\,L^{-1}}$ with a mean of 1.17 $\mu\mathrm{mol\,L^{-1}}$ and phosphate ranged between 0.03 - 0.59 $\mu\mathrm{mol\,L^{-1}}$ with a mean of 0.16 $\mu\mathrm{mol\,L^{-1}}$. The highest N:P ratios were also found near the coasts at the beginning and at the end of the transit (up to 20) and between 0°N and 20°N (up to 7) (for more detail see Koch and Kattner (2012)).

Chlorophyll a (Chl-a) concentrations, from *in-situ* measurements during the cruise (published in Taylor *et al.,* (2011)) and retrieved from MODIS satellite observations, showed overall low values (0 and 1 $\mathrm{mg\,m^{-3}}$) for the whole transit. However, elevated Chl-a concentrations (up to 5.5 $\mathrm{mg\,m^{-3}}$ for *in-situ* data and up to 7.8 $\mathrm{mg\,m^{-3}}$ for MODIS data) were found in the region of the tidal front as well as in the equatorial upwelling region and in two blooms which were encountered between 19°N and 22°N (B1) and again around 11°N

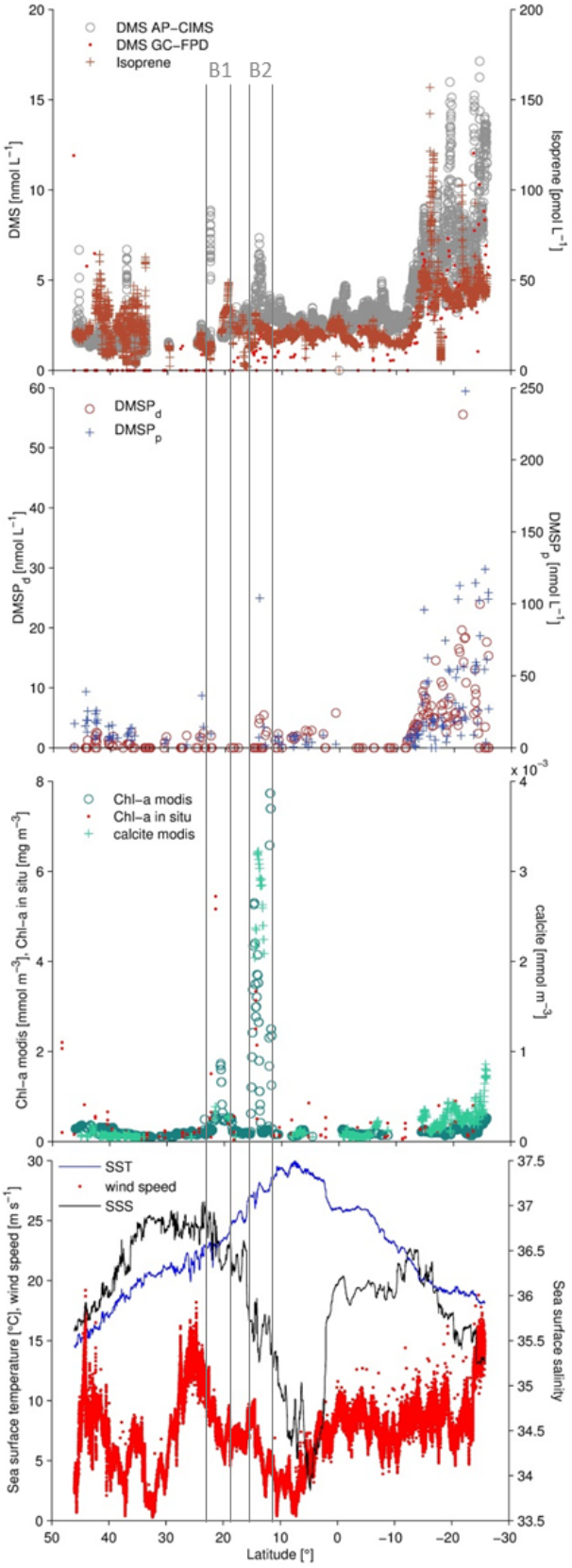

Fig. 4.2: *Distribution pattern of DMS, isoprene, DMSP (dissolved and particulate), chl-a, calcite, wind speed, sea surface temperature and salinity against latitude along the north-south transit from Germany to South Africa in the eastern Atlantic Ocean.*

and 15°N (B2) (Taylor *et al.,* 2011) (Fig. 4.1 and 4.2). At the end of the transit (around 14°S – 23°S) Chl-a *in-situ* data were increased, but lower than 1 $\mathrm{mg\,m^{-3}}$. Enhanced Chl-a concentrations occurred in conjunction with elevated N:P ratios around 10°N. Enhanced calcite concentrations (indicator for coccolithophorids, up to 3.3 $\mathrm{mmol\,m^{-3}}$, Balch *et al.,* (1991), Holligan *et al.,* (1983)) retrieved from MODIS were observed in regions of elevated Chl-a concentrations and followed roughly the distribution pattern of Chl-a for the entire transit (Fig. 4.1 and 4.2).

The distribution pattern of the *in-situ* measured marker pigments (published in Taylor *et al.,* (2011)) showed elevated abundance of haptophytes (including coccolithophrids) between 40°N and 45°N and at the end of the transit between 17°S and 23°S. In the regions of the transit where DMS and isoprene were measured, a correlation of the *in-situ* measured pigments Chl-a and 19´-hexanoyloxyfucoxanthin (indicator for haptophytes, $\mathrm{R^2}$=0.82, p-value <0.001, n=39) were found, underlining the similar distribution pattern of haptophytes and Chl-a. Cyanobacteria were most abundant in the tropical and sub-tropical oligotrophic waters. A high abundance of diatoms was detected in the two blooms (1.8 - 3 $\mathrm{mg\,m^{-3}}$). Dinoflagellates occurred along the whole transit but were low in abundance. For a detailed discussion about the phytoplankton distribution along the cruise track see Taylor *et al.,* (2011).

4.4 Results and Discussion

4.4.1 DMS, DMSP and isoprene distribution patterns

DMS concentrations ranged from 0.4 to 17.1 $\mathrm{nmol\,L^{-1}}$ with a mean concentration of 3.6 $\pm$1.2 $\mathrm{nmol\,L^{-1}}$ along the entire cruise track. DMS concentrations did not show much variability between 45°N and 10°S (1 - 4 $\mathrm{nmol\,L^{-1}}$) except of two small peaks with DMS concentrations of up to 9 $\mathrm{nmol\,L^{-1}}$ within the two blooms at ~22°N (B1) and ~15°N (B2). Elevated DMS concentrations between 3 and 17 $\mathrm{nmol\,L^{-1}}$ were measured from 12°S to 26°S (Fig. 4.2). The average surface DMS concentration from several studies in the eastern Atlantic Ocean (2.64 $\pm$2.48 $\mathrm{nmol\,L^{-1}}$, data extracted from the Global Surface Seawater DMS Database: http://saga.pmel.noaa.gov/dms) is slightly lower compared to the mean from our study. However, the distribution pattern of the archived data was similar. No correlation was observed between DMS and Chl-a for the entire transit. Nonetheless, DMS peaked in regions of elevated Chl-a concentrations (Fig. 4.2). The distribution pattern of $\mathrm{DMSP_d}$ (mean 3.2 $\mathrm{nmol\,L^{-1}}$, range < 0.3 - 55.5 $\mathrm{nmol\,L^{-1}}$) and $\mathrm{DMSP_p}$ (mean 25.1 $\mathrm{nmol\,L^{-1}}$, range 0.7 – 247.7 $\mathrm{nmol\,L^{-1}}$) followed roughly the distribution of DMS (Fig. 4.2). Elevated concentrations of $\mathrm{DMSP_d}$ and $\mathrm{DMSP_p}$ were measured between 12°S and 26°S and in the two blooms (B1, B2). However, enhanced $\mathrm{DMSP_p}$ concentrations were detected between 35°N and 50°N when DMS concentrations

were low.

A mean isoprene concentration of 25.7 $\pm$14.7 $\mathrm{pmol\,L^{-1}}$ was measured along the entire transit with a range of 1.9 to 156.8 $\mathrm{pmol\,L^{-1}}$. Slightly elevated isoprene concentrations were measured at the beginning of the transit (35°N – 46°N). Isoprene peaked in the region of the first bloom (B1, $\sim$19°N). However, the DMS and isoprene peaks were not collocated. Enhanced isoprene concentrations were also measured south of 12°S, as were DMS (Fig. 4.2). Isoprene concentrations measured in this study are in the range of previous studies: Baker *et al.,* (2000) measured sea surface isoprene concentrations between 21 and 43 $\mathrm{pmol\,L^{-1}}$ in the eastern North Atlantic Ocean west of the coast of Ireland; Broadgate *et al.,* (1997) determined isoprene concentrations between 0.1 and 100 $\mathrm{pmol\,L^{-1}}$ in the North Sea; Milne *et al.,* (1995) measured isoprene concentrations between 9.8 and 50.8 $\mathrm{pmol\,L^{-1}}$ (Milne *et al.,* 1995).

Several previous studies found correlations between isoprene and chlorophyll or detected isoprene maxima at a similar depth as the chlorophyll fluorescence maxima (Bonsang *et al.,* 1992, Milne *et al.,* 1995, Broadgate *et al.,* 1997, Baker *et al.,* 2000, Moore and Wang 2006). Here we used MODIS satellite Chl-a data to identify correlations with isoprene because of the higher resolution compared to the *in-situ* Chl-a data. Between the equator and 10°N, as well as between the equator and 3°S, correlations between isoprene and Chl-a were found ($\mathrm{R^2}$ = 0.76, p-value 0.01, n=819, $\mathrm{R^2}$ = 0.56, p-value 0.01, n=242, respectively). However, in most of the regions, the isoprene concentration was independent of the Chl-a distribution pattern. Thus, Chl-a could not be used as a general indicator for both isoprene and DMS distributions along the transit.

4.4.2 Factors influencing DMS and isoprene: regional clustering

Despite the fact that both isoprene and DMS are mainly related to phytoplankton activities (Baker *et al.,* 2000), no significant relationship between DMS and isoprene could be observed when the entire transit was considered (Fig. 4.3). Nonetheless, Figure 4.3 shows hints that the compounds might be related in specific regions. Thus, we examined the transit for correlations between DMS and isoprene to extract such specific regions. 14 positive and 9 negative correlations with an explained variance ($\mathrm{R^2}$) between 0.62 and 0.95 could be found in 23 regions, also referred to as clusters (Fig. 4.4 and Table 4.1).

Tab. 4.1: *List of regions with significant correlations between DMS and isoprene along the north-south transit in the eastern Atlantic Ocean.* R^2 *is the squared correlation coefficient. N stands for number of data of each correlation. DMS and isoprene are given as regional means.*

cluster	latitude	R^2	DMS $[\mathrm{nmol\,L^{-1}}]$	Isoprene $[\mathrm{pmol\,L^{-1}}]$	N
1	45 - 43.5°N	-0.61	1.74	21.03	70
2	43.5 - 39 °N	0.86	1.52	27.26	271
3	38 - 37.5 °N	0.95	1.87	20.97	40
4	36 - 33.7 °N	0.80	1.49	24.05	185
5	29.85 - 24 °N	0.62	1.70	15.12	80
6	24 - 23.54 °N	0.68	1.66	12.20	48
7	23.54 - 22.5 °N	-0.85	1.73	9.97	83
8	22.49 - 19.3 °N	0.81	2.01	29.24	108
9	18.8 - 16 °N	-0.84	2.75	17.07	120
10	16 - 14 °N	0.72	3.07	17.92	112
11	2.5 - 1 °N	0.62	2.51	24.88	65
12	1 °N - 1°S	-0.79	3.43	23.50	161
13	2 - 3 °S	-0.63	2.66	15.09	89
14	5 - 5.5 °S	0.80	3.21	20.75	35
15	5.5 - 6 °S	-0.46	2.63	17.61	110
16	6 - 7 °S	-0.92	2.84	19.56	68
17	7.5 - 9.5 °S	0.64	3.02	16.82	140
18	9.5 - 13.5 °S	0.82	3.26	17.64	337
19	13.5 - 14 °S	-0.69	4.86	29.34	45
20	14 - 15.5 °S	0.79	6.50	48.81	129
21	17 - 18 °S	0.72	7.15	25.38	86
22	24 - 25 °S	0.74	9.17	50.13	80
23	25.5 - 25.8 °S	-0.71	12.58	45.91	30

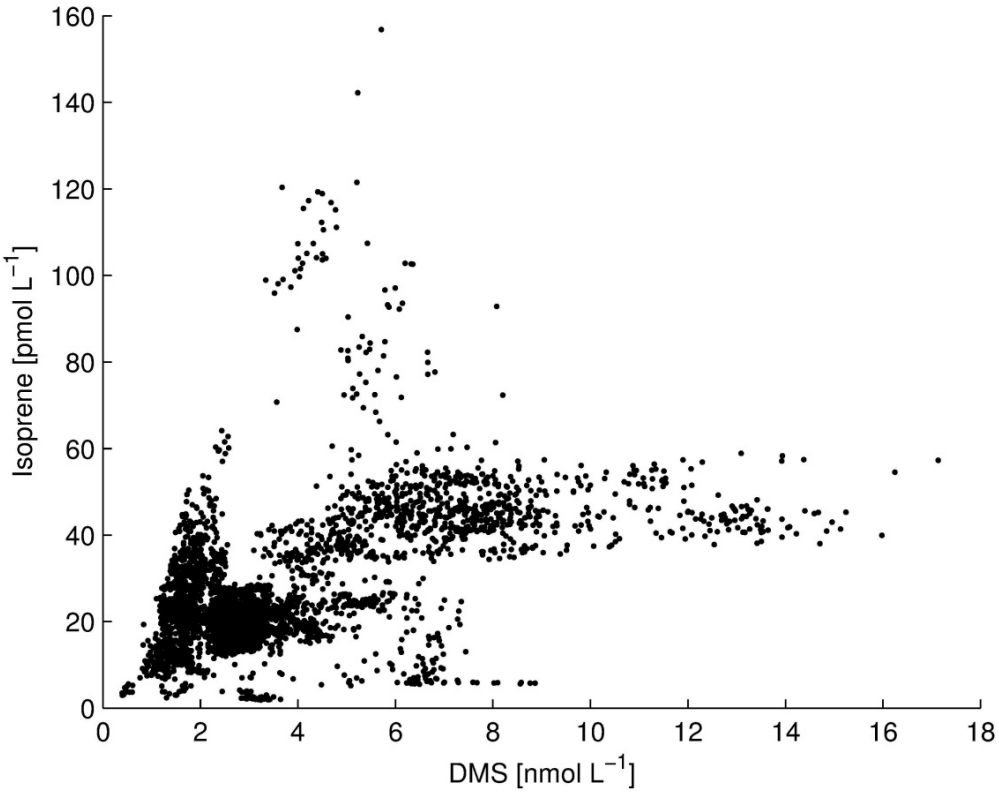

Fig. 4.3: *Correlation between DMS and isoprene over the entire north-south transit in the eastern Atlantic Ocean.*

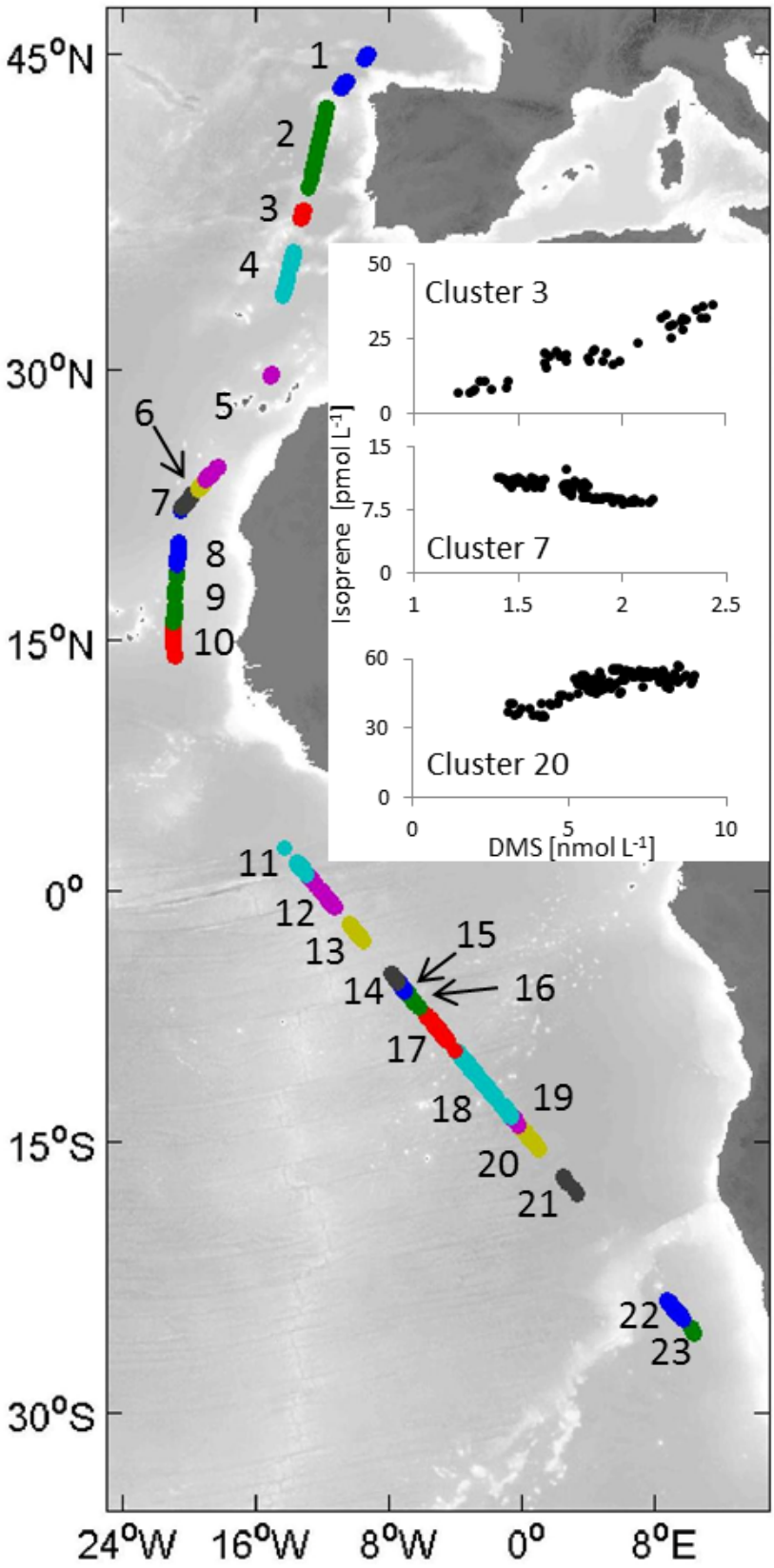

Fig. 4.4: *Locations of the clustered regions where DMS and isoprene concentrations correlated. The three small panels show examples for correlations between DMS and isoprene from three individual clusters. These three clusters are randomly chosen.*

4.4.2.1 Analysis within the individual clusters

MODIS data were used to identify the possible influence of phytoplankton, especially coccolithophorids, on the relationship between DMS and isoprene within the different regions. A significant positive correlation between Chl-a and DMS was only found in one cluster (region 20, R^2 = 0.43, Fig. 4.4). In four additional clusters (regions: 3 (R^2 = 0.7); 7 (R^2 = 0.69); 14 (R^2 = 0.48); 15 (R^2 = 0.68)) Chl-a and DMS were anti-correlated. Furthermore, more anti-correlations (regions: 3 (R^2 = 0.59); 8 (R^2 = 0.62); 12 (R^2 = 0.69)) were found for DMS and calcite than positive correlations (region 20 (R^2 = 0.46)). A positive relationship between DMS, Chl-a and calcite could be determined only in cluster 20. However, isoprene was not affected in this region by Chl-a and calcite. One anti-correlation (region 3 (R^2 = 0.59)) and two positive correlations (regions: 7 (R^2 = 0.83); 13 (R^2 = 0.77) between isoprene and Chl-a were detected. Between isoprene and calcite, two regions with positive correlations (regions: 10 (R^2 = 0.43); 12 (R^2 = 0.71)) and two regions with negative correlations (regions: 3 (R^2 = 0.9); 8 (R^2 = 0.94)) were identified. Only in cluster 3 do Chl-a and calcite appear to have an influence on both the DMS and isoprene concentrations, however, the pigments were anti-correlated with both compounds. For all presented correlations a p-value of 0.01 applied.

MODIS satellite data could not clearly elucidate the influence of phytoplankton on DMS and isoprene distribution patterns. Several laboratory studies have shown that a wide range of algae groups can produce isoprene (Moore *et al.,* 1994, Milne *et al.,* 1995, McKay *et al.,* 1996, Shaw *et al.,* 2003, Colomb *et al.,* 2008, Bonsang *et al.,* 2010). Therefore, correlations determined between isoprene and Chl-a in different oceanic regions are in agreement with findings of this study (Milne *et al.,* 1995, Broadgate *et al.,* 1997, Shaw *et al.,* 2010). However, the variability of correlations described in this study may reflect the heterogeneous distribution and activity of DMS and isoprene producers along the transit. Bonsang *et al.,* (2010), McKay *et al.,* (1996) and Shaw *et al.,* (2003) observed in culture experiments that isoprene production by phytoplankton was dependent on phytoplankton functional types, solar radiation intensity, the stage of the lifecycle and the temperature. Thus, the isoprene concentration in surface seawater was not only effected by the general occurrence of phytoplankton but by a more complex interaction between phytoplankton composition and environmental conditions.

Elevated isoprene concentration in surface seawater might be also caused by an enhanced release of intracellular isoprene into the water column due to grazed algae. A decrease of Chl-a concentration might indicate a dying phytoplankton bloom. This phenomenon was observed for DMSP (Leck *et al.,* 1990) and might be an explanation for the anti-correlation found between Chl-a or calcite with isoprene.

It is well established that DMS concentration is mainly dependent on the abundance and interplay of specialized algae species and bacteria groups. DMS, therefore, is known to

have a complicated relationship with Chl-a (Kiene *et al.,* 2000, Simó 2004, Stefels *et al.,* 2007), which is reflected in the different positive and negative correlations between Chl-a, calcite and DMS found in this study. The positive correlations found between isoprene and DMS might refer to a common source of both compounds, namely certain phytoplankton groups. Indeed, dinoflagellates and coccolithophorides were identified as important producers of both isoprene and DMSP, and therefore, indirectly DMS (Keller *et al.,* 1989, Steinke *et al.,* 2002, Shaw *et al.,* 2003, Bonsang *et al.,* 2010). The variability of the distribution of these algae taxa might explain both the positive correlations between DMS and isoprene in certain regions and also the absence of any relationships between DMS and isoprene in other regions along the transit.

However, there is only little evidence that DMS is directly produced by phytoplankton, thus, others common direct sources should exist for both isoprene and DMS. Kuzma *et al.,* (1995) showed isoprene production of a wide range of terrestrial bacteria ubiquitously distributed. Some of them could even produce isoprene and DMS concurrently. Although, marine microbial production of isoprene has not been reported, to our knowledge, it is most likely that marine microbes have the ability to produce isoprene in the manner of terrestrial species. The production of DMS by ubiquitous marine microbes was reviewed by Yoch (2002). It might be possible that some of these DMS producing bacteria can also produce isoprene, as in the case for terrestrial species. Thus, microbial activities could be another explanation for positive correlations found between DMS and isoprene.

Although isoprene production due to bacteria is not reported, Alvarez *et al.,* (2009) observed consumption of isoprene in marine microbial communities. Some of these taxa are associated with phytoplankton blooms. They observed in nearly all of the tested groups (ubiquitous marine taxa) the ability to dissimilate isoprene under concentrations typically found in the ocean. It might be possible that isoprene consuming microbes are also able to consume DMSP and produce DMS which might explain the negative correlations found along the transit. Indeed, the DMS producing bacteria strain *Sulfitobacter* (Curson *et al.,* 2008) of the group *Alphaproteobacteria* was also found in the isoprene-degrading bacteria community investigated by Alvarez *et al.,* (2009). However, it has to be directly tested if *Sulfitobacter* and other DMS producing bacteria can also consume or produce isoprene.

4.4.2.2 Comparison of cluster regions

Changes in the abundance of dinoflagellates in the different clusters followed roughly the changes of isoprene concentrations (Fig. 4.5). In contrast, the changes in DMS concentrations were not dependent on changes in dinoflagellate abundance. However, $\mathrm{DMSP_p}$ seemed to be also influenced by dinoflagellates, like isoprene ($\mathrm{R^2}$ = 0.91, p-value 0.01, Fig. 4.5). Dinoflagellates are known as both DMSP (Steinke *et al.*, 2002) and isoprene producers (see Shaw *et al.*, (2010) and references therein) and might be a potential link

between DMS and isoprene. This suggestion is supported especially by the similar pattern of $\mathrm{DMSP_p}$ and isoprene between the clusters 18 to 23 in the region of high biological activity toward the southern end of the cruise track (Fig. 4.5). Cyanobacteria appeared to have also a weak but significant influence on isoprene between the individual clusters ($\mathrm{R^2}$ = 0.26, p-value 0.1), but did not affect DMS or DMSP and showed a different distribution pattern compared to dinoflagellates. The high abundance of cyanobacteria might explain the occurrence of high isoprene and low DMS concentrations in some regions due to their potential to produce isoprene (Milne *et al.*, 1995, Shaw *et al.*, 2003) but not DMSP and, accordingly, DMS (Keller *et al.*, 1989). However, some regions of high cyanobacteria abundance were also regions with a positive correlation between DMS and isoprene. This points to the possibility that cyanobacteria were not the main producers of isoprene in these regions and that other sources existed (e.g. microbial activities). This is in line with the hypothesis above, that the correlations between MODIS pigment data and the two compounds may have a bacterial link.

We also analysed separately all clusters with positive correlations and negative correlations between DMS and isoprene. When clusters with negative correlations showed high isoprene concentrations they also had high abundance of several phytoplankton groups, like diatoms, chrysophytes and cyanobacteria. This highlights that a broad range of phytoplankton groups can produce isoprene but not necessarily DMSP and, thus, DMS. Due to insufficient data, the role of DMSP could not be evaluated for these clusters. In contrast, clusters with positive correlations between DMS and isoprene showed no dependencies of isoprene on the phytoplankton abundance. In this case, again, it is possible to invoke the bacterial influence on the two compounds.

4.4.3 Factors influencing DMS and isoprene: N:P ratio clustering

In order to investigate more specifically the influence of biology on the isoprene distribution, the DMS, total DMSP ($\mathrm{DMSP_t}$, sum of $\mathrm{DMSP_p}$ and $\mathrm{DMSP_d}$), and isoprene data were reclustered by nutrient availability. The clusters were computed as the nitrogen (N) to phosphate (P) ratio, where N is the sum of nitrate, nitrite and ammonia. We calculated the median DMS, $\mathrm{DMSP_t}$ and isoprene concentrations over the entire transit for bins of N:P ratios (e.g. the N:P ratio of 2 to 3 was allocated to a N:P bin of 2.5) according to Zindler *et al.*, (2012b). Afterwards we smoothed the data with a three point moving average.

DMS peaked together with isoprene at a N:P ratio of 7.5 (Fig. 4.6). $\mathrm{DMSP_t}$ showed two concentration peaks (N:P ratio 6.5 and again at 11.5) whereby the bigger peak is shifted toward lower N:P ratios compared to DMS and isoprene (Fig. 4.6). $\mathrm{DMSP_t}$ was mainly comprised of $\mathrm{DMSP_p}$ while $\mathrm{DMSP_d}$ was only a minor fraction of $\mathrm{DMSP_t}$ pool.

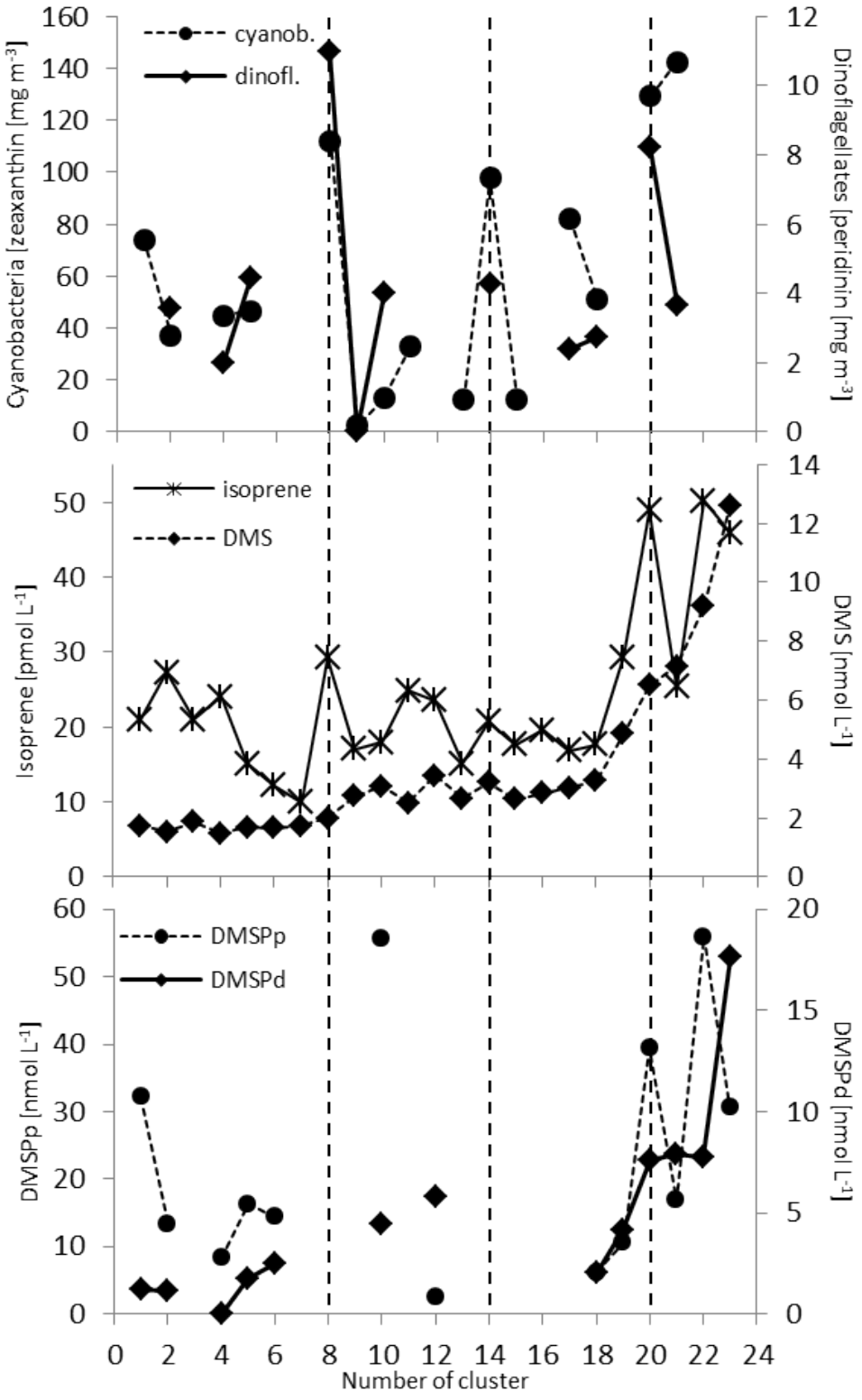

Fig. 4.5: *Data of phytoplankton groups, isoprene and sulphur compounds averaged for each cluster. Locations of the clusters are shown in Figure 4.4.*

The correlation between DMS and isoprene is stronger (R^2 = 0.72, p-value 0.001, Fig. 4.7) over the entire N:P ratio range compared to the correlation between $DMSP_t$ and isoprene (R^2 = 0.59, p-value 0.01, Fig. 4.7). The correlations between DMS and isoprene in the low N:P ratio range up to 7.5 and between 7.5 and 19.5 N:P ratio are even higher (R^2 = 0.82 and 0.87, p-value 0.01, respectively, Fig. 4.7) which referred to similar sources and/or sinks of both compounds especially in eutrophic regions. For the N:P ratio range up to 7.5, $DMSP_t$ and isoprene showed also a significant correlation (R^2 = 0.72, p-value 0.05), however, in the N:P ratio range of >7.5 no correlation between $DMSP_t$ and isoprene could be determined (Fig. 4.7). It seemed that isoprene and $DMSP_t$ were only related in regions of low nitrogen availability. It is possible that isoprene and $DMSP_t$ have similar sources in oligotrophic and mesotrophic regions, while in eutrophic regions their sources were different or the production and degradation pathways of both compounds were involved in a complex interplay between phytoplankton and bacteria. Several phytoplankton groups, such as dinoflagellates, haptophytes, chrysophytes and cyanobacteria, showed also their highest abundance between a N:P ratio of 6.5 and 7.5 (Fig. 4.6). Except for cyanobacteria, all algae groups are known as DMSP producers and were also observed to produce isoprene (Keller *et al.*, 1989, Shaw *et al.*, 2010). Thus, it is possible that these phytoplankton groups are a common source for both compounds. The close link between DMS and isoprene in the low N:P ratio range could be explained via $DMSP_t$ due to its potential to govern the DMS distribution. This assumption is supported by the correlation between DMS and $DMSP_t$ in the region of low N:P ratio range up to 7.5 (R^2 = 0.71, p-value 0.05). Due to the decoupling of isoprene and DMSP in regions of high N:P ratios it can be assumed that also bacteria might influence the isoprene concentration in eutrophic regions.

4.4.4 The influence of hydrographic regimes on the DMS:isoprene distribution in surface seawater

The distribution of the ratio of DMS to isoprene (DMS:isoprene) was investigated using SSS and SST along the north-south transit (Fig. 4.8), in order to identify if hydrographic regimes influenced the surface ocean concentrations of these compounds. The distribution pattern of the ratio corresponds to the surface hydrographic regions of the eastern Atlantic Ocean described by Stramma and Schott (1999) (Fig. 4.9). Relatively low DMS:isoprene, around 0.05 $\mathrm{nmol\,pmol^{-1}}$ due to high isoprene concentrations (Fig. 4.10, a), were measured between 18°N and 45°N the region of the Canary Current and the eastern edge of the subtropical gyre in the North Atlantic Ocean (Fig. 4.9, a). Higher ratios were measured (around 0.15 $\mathrm{nmol\,pmol^{-1}}$) when the Mauritanian upwelling was encountered at 20°N, indicated by a SSS of 37 and 23°C as well as elevated Chl-a (Fig. 4.2, lowest panel (B1), Fig. 4.9, a). In this region, which is also the location of B1, the isoprene con-

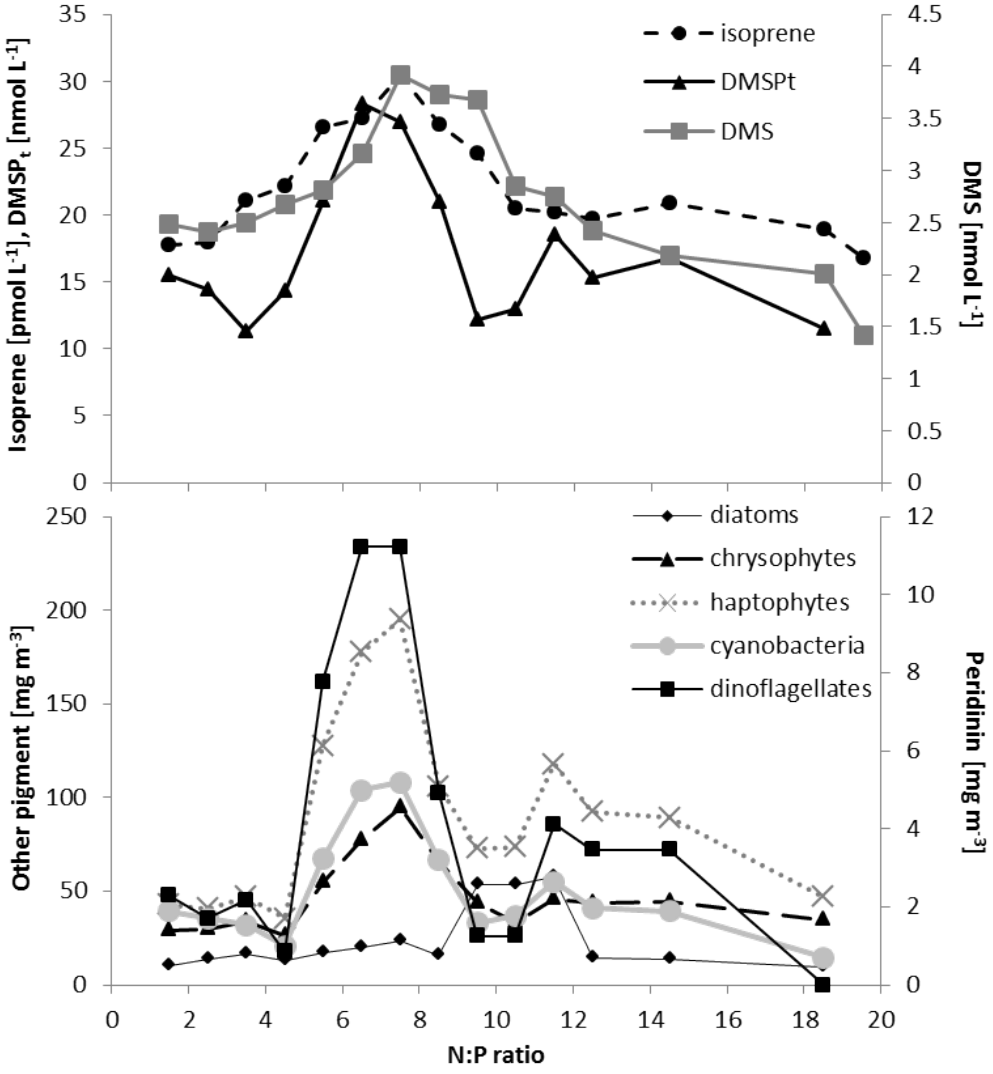

Fig. 4.6: *Binned data of isoprene, sulphur compounds and phytoplankton groups for different N:P ratios. Other pigments stand for: fucoxanthin (diatoms), 19'-butanoyloxyfucoxanthin (chrysophytes), 19'-hexanoyloxyfucoxanthin (haptophytes) and zeaxanthin (cyanobacteria) (corresponding phytoplankton groups to the pigments are given in parenthesis). Peridinin is the characteristic marker pigment for dinoflagellates.*

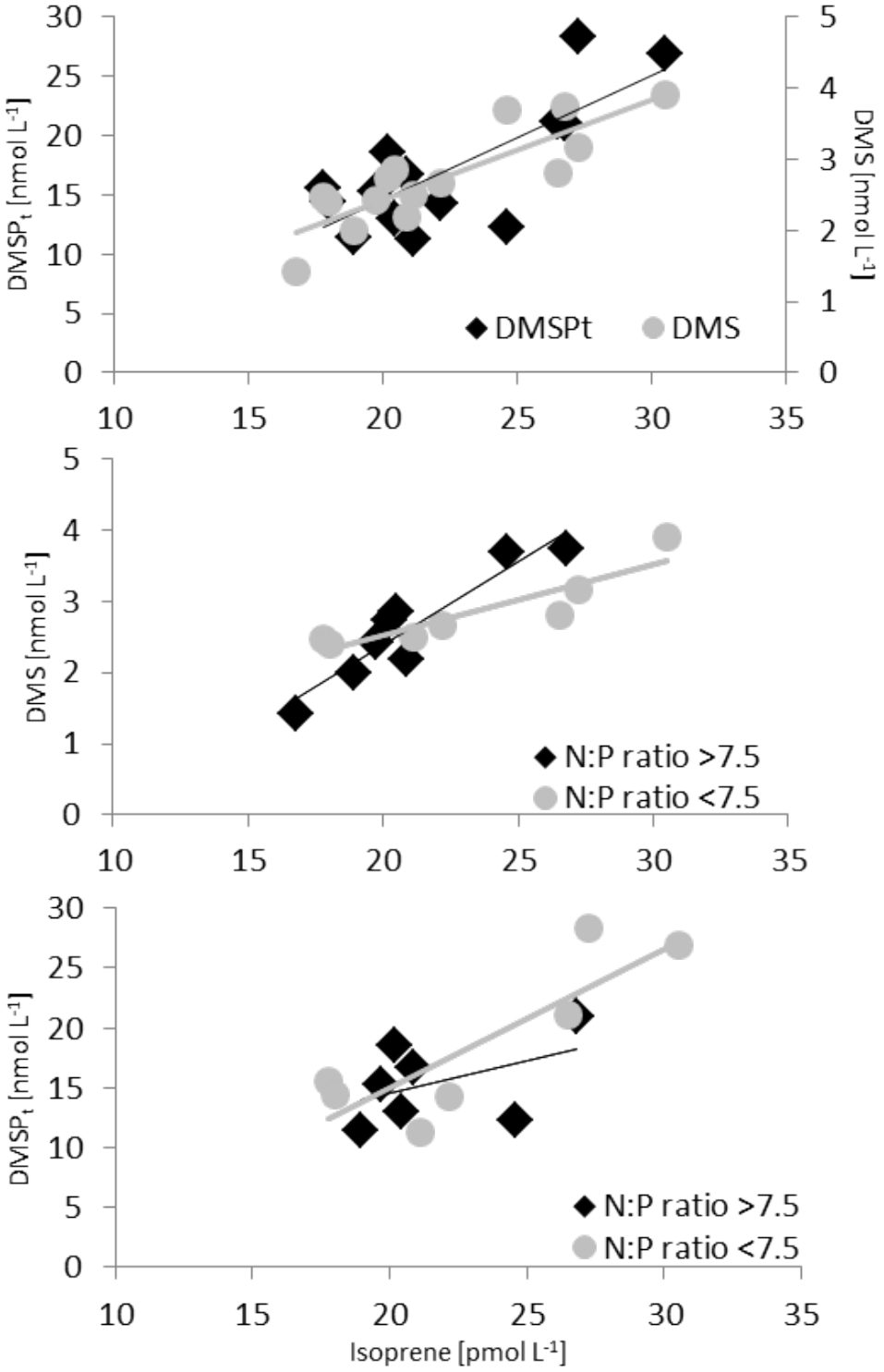

Fig. 4.7: *Correlations between isoprene and sulphur compounds using data from Figure 4.6. Top panel: correlations for the entire N:P ratio range (*$\mathrm{DMSP_t}$ *vs. isoprene:* $\mathrm{R^2}$ *= 0.59, p-value 0.01; DMS vs. isoprene:* $\mathrm{R^2}$ *= 0.72, p-value 0.001) . Middle panel: correlations between isoprene and DMS separated for low (*$\mathrm{R^2}$ *= 0.82, p-value 0.01) and high N:P ratio range (*$\mathrm{R^2}$ *= 0.87, p-value 0.01). Bottom panel: correlations between isoprene and* $\mathrm{DMSP_t}$ *separated for low (*$\mathrm{R^2}$ *= 0.72, p-value 0.05) and high N:P ratio range (*$\mathrm{R^2}$ *= 0.2).*

centration was decreasing compared to the region of the Canary Current while the DMS concentration did not change, causing the relatively high ratio (Fig. 4.10, 4.11, b). Between 10°N and 18°N, in the upwelling of the Guinea Dome, elevated DMS:isoprene was observed (around 0.2 $\mathrm{nmol\,pmol^{-1}}$, Fig. 4.9, b). The isoprene concentration was lower in this region and the DMS concentration increased compared to the Canary Current region (Fig. 4.10, 4.11, c). The ITCZ region, located between 2°N and 10°N in November 2008, exhibited a uniform distribution pattern of intermediate ratios, around 0.15 $\mathrm{nmol\,pmol^{-1}}$ (Fig. 4.9, c). Around the equator (2°N to 2°S), a homogenous distribution pattern was also observed, but with slightly lower ratios of about 0.12 $\mathrm{nmol\,pmol^{-1}}$ (Fig. 4.9, d). Enhanced DMS:isoprene (0.15 to 0.25 $\mathrm{nmol\,pmol^{-1}}$) was measured when the Angola Gyre, including the upwelling region of the Angola Dome, was encountered (2°S to 14°S) (Fig. 4.9, e). Isoprene decreased and DMS increased in the Angola Gyre compared to the equatorial region (Fig. 4.11, 4.10, e). When passing the Angola-Benguela Front at about 14°S, the ratios decreased again (Fig. 4.9, f). This was caused by a stronger increase of isoprene concentrations compared to DMS (Fig. 4.10, 4.11, f). DMS:isoprene increased with decreasing temperature towards the coast of South Africa (Fig. 4.9, f), caused by an increase of DMS. This region showed elevated Chl-a concentrations, which indicated the development of a spring bloom (Fig. 4.1).

The distribution pattern of DMS:isoprene was well reflected by the hydrographic regions of the eastern Atlantic Ocean. Elevated ratios were mainly observed in upwelling regions of Mauritania and the Guinea and Angola Domes, as well as in the spring bloom at the end of the transit. These regions, except for the Mauritanian upwelling, exhibited higher DMS concentrations compared to regions of the Canary Current and around the ITCZ and equator. In contrast, isoprene showed relatively high concentrations in the Canary Current regime and in the region of the ITCZ and equator. In the region of the spring bloom at the end of the cruise, both isoprene and DMS concentrations were elevated. Two possibilities exist to explain this distribution pattern: sources and transport. It seems that isoprene could be produced in both oligotrophic and highly productive hydrographic regimes, whereas DMS was observed mostly in the highly productive regimes (i.e. actively upwelling areas). Indeed, a correlation between Chl-a and isoprene was found in the region of the ITCZ and at the equator between 10°N and 3°S (see section 4.1). In these regions no correlations were found between DMS and isoprene (Fig. 4.4). However, when transport is taken into account, a slightly different pattern emerges.

Generally speaking, when the hydrographic regimes are scrutinized, it is possible to identify which water masses can be influenced by mixing and transport and which are more isolated. The Canary Current, ITCZ, Equatorial upwelling, and the South African bloom regions all can be influenced by lateral water mixing (Stramma and Schott 1999). The upwelling regions in the Guinea Dome and in the Angola gyre seem to be isolated from lateral mixing. The areas that are more isolated should reflect *in-situ* production, while

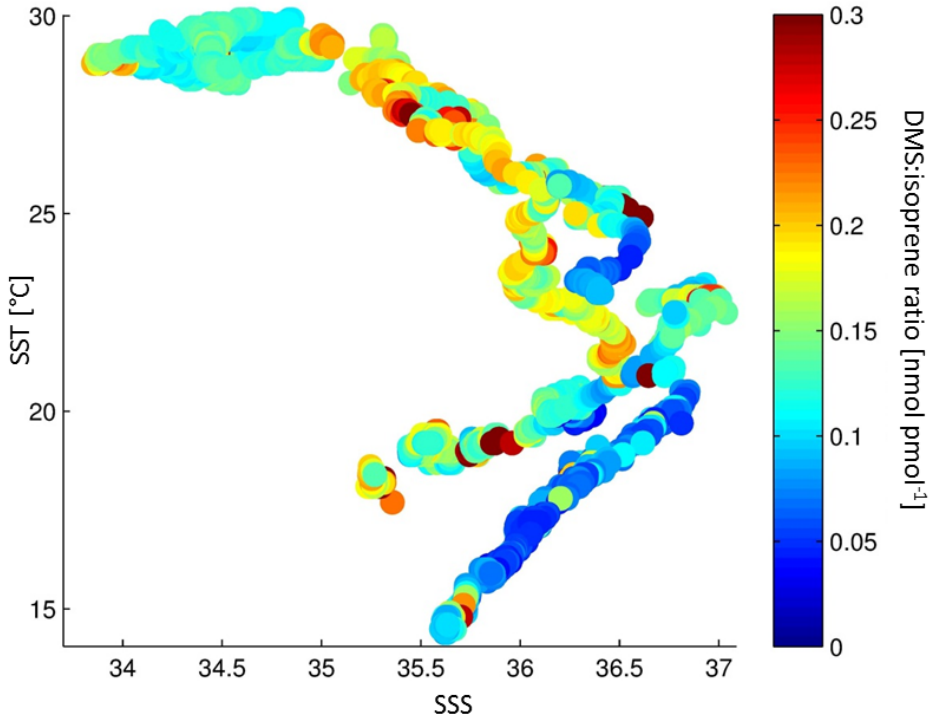

Fig. 4.8: *The distribution of DMS:isoprene shown in a T-S diagram of surface seawater measurements in the eastern equatorial region. Note that the scale of the colorbar is limited on 0.3* $\mathrm{nmol\,pmol^{-1}}$ *while the highest ratio was 1.8* $\mathrm{nmol\,pmol^{-1}}$.

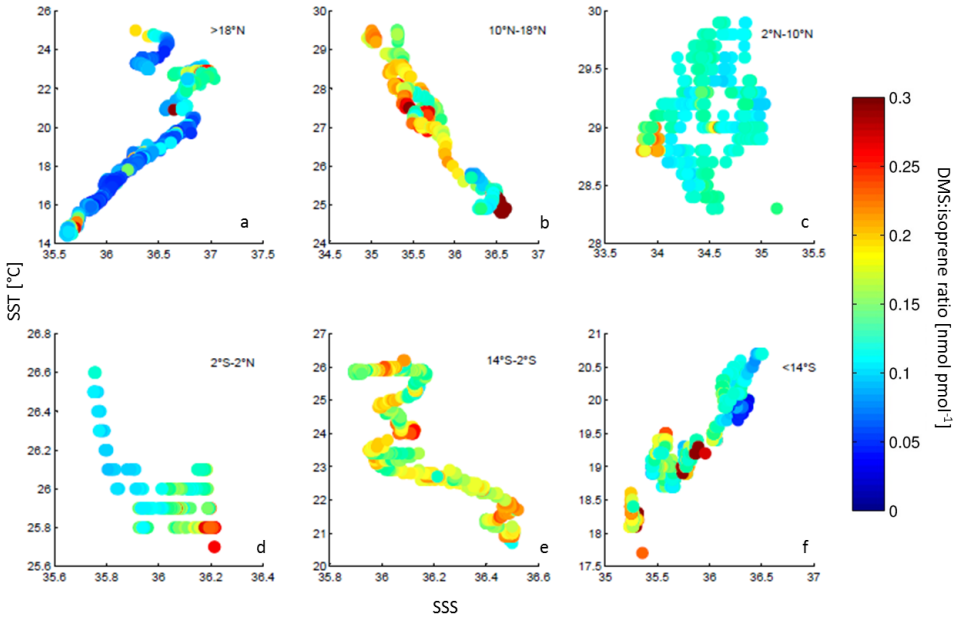

Fig. 4.9: *The ratio of DMS and isoprene shown in a T-S diagram was separated into 6 different hydrographic regions in the eastern Atlantic Ocean: Canary Current and the eastern edge of the Subtropical Gyre (>18°N, a); Guinea Dome (10°N - 18°N, b); ITCZ (2°N – 10°N, c); Equatorial upwelling (2°S – 2°N, d); Angola Gyre including the Angola Dome (2°S – 14°S, e) and the region south of the Angola-Benguela Front (<14°S, f).*

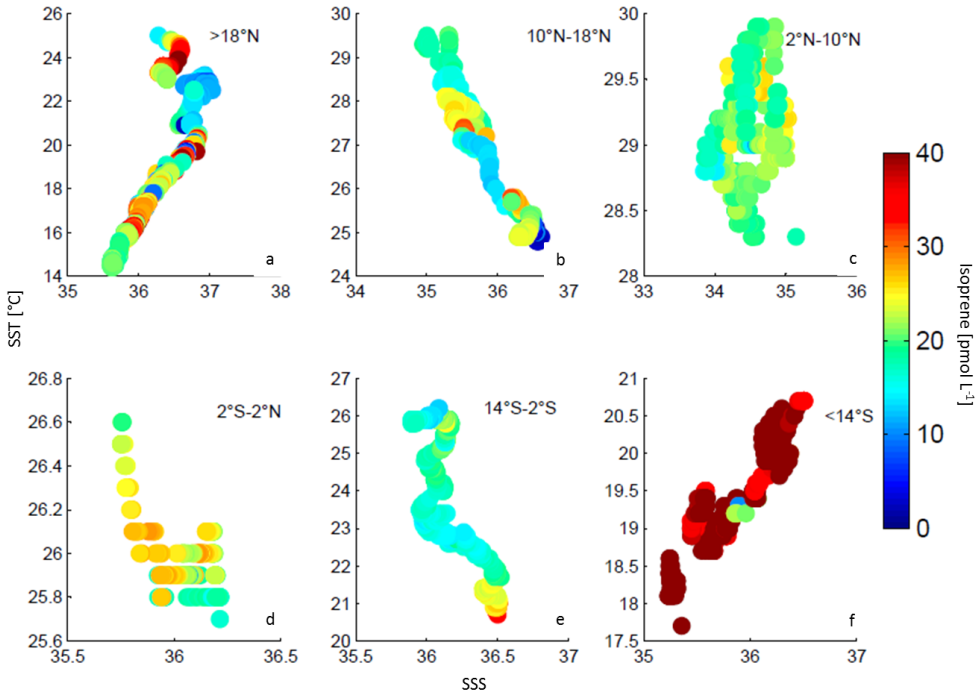

Fig. 4.10: *The distribution of sea surface isoprene concentrations shown in a T-S diagram separated into 6 different hydrographic regions in the eastern Atlantic Ocean: Canary Current and the eastern edge of the Subtropical Gyre (>18°N, a); Guinea Dome (10°N - 18°N, b); ITCZ (2°N – 10°N, c); Equatorial upwelling (2°S – 2°N, d); Angola Gyre including the Angola Dome (2°S – 14°S, e) and the region south of the Angola-Benguela Front (<14°S, f). Note that the scale of the colorbar is limited to 40* $\mathrm{pmol\,L^{-1}}$*, highest isoprene concentration was 156.8* $\mathrm{pmol\,L^{-1}}$.

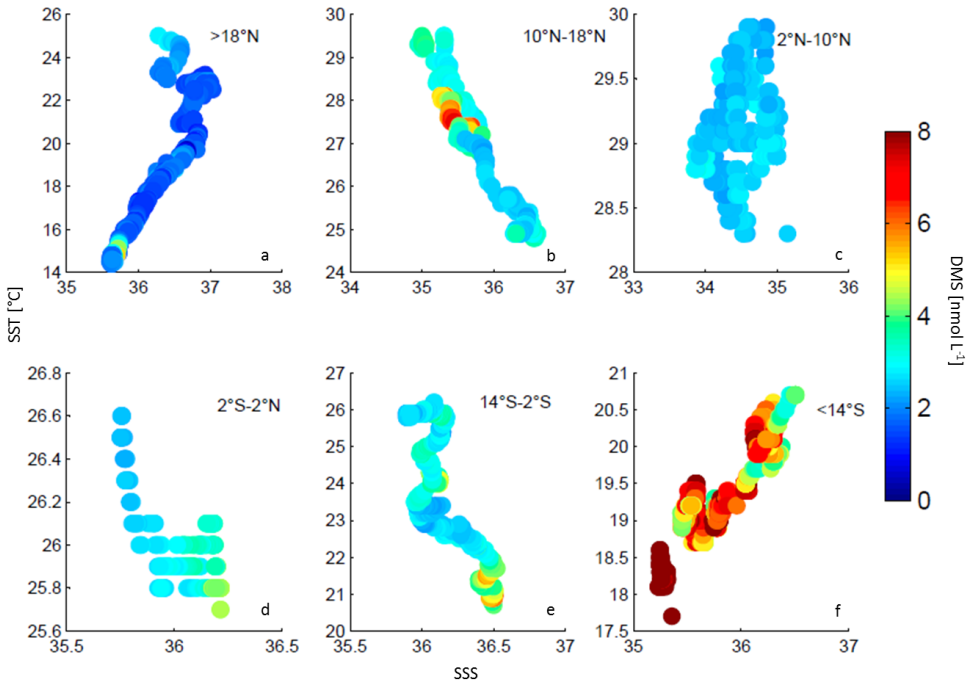

Fig. 4.11: *The distribution of sea surface DMS concentrations shown in a T-S diagram separated into 6 different hydrographic regions in the eastern Atlantic Ocean: Canary Current and the eastern edge of the Subtropical Gyre (>18°N, a); Guinea Dome (10°N - 18°N, b); ITCZ (2°N – 10°N, c); Equatorial upwelling (2°S – 2°N, d); Angola Gyre including the Angola Dome (2°S – 14°S, e) and the region south of the Angola-Benguela Front (<14°S, f). Note that the scale of the colorbar is limited to 8* $\mathrm{nmol\,L^{-1}}$*, highest isoprene concentration was 17.1* $\mathrm{nmol\,L^{-1}}$.

the others can be influenced by both transport and *in-situ* sources. In addition, there is some indication from the literature that isoprene is relatively (compared to DMS) long lived in the water column (around 17 – 19 days, Palmer and Shaw (2005)), while DMS is rapidly cycled (1-2 days, Vogt and Liss 2009). Therefore, DMS can be a tracer for *in-situ* production. The regions in which DMS were high are the Guinea Dome upwelling, Equatorial upwelling, Angola Dome, Angola- Benguela Front, and the South African bloom region. All of these regions showed either a slightly enhanced or very high level of isoprene as well, likely reflecting areas of *in-situ* production due to biological productivity. There were two additional high Chl-a regions within the Canary Current area with high isoprene, but low DMS values. These probably reflect *in-situ* isoprene production by biotic species that did not produce DMSP. Hernandez-Guerra *et al.*, (2001) observed an upwelling filament from the African coast which extended over 200 km offshore reaching the Gran Canary Islands. Such upwelling filaments might be responsible for both *in-situ* production and transport of isoprene. The southward velocity of the Canary Current (>20 $\mathrm{cm\,s^{-1}}$, Hernandez-Guerra *et al.*, (2001)) might transport isoprene over a distance of about 290 to 330 km when an isoprene lifetime of 17 to 19 days is assumed. Additionally, the ITCZ region is influenced by both the coast and the more southern Equatorial upwelling region. In these regions, DMS was low, potentially indicating both that isoprene was produced by the biota (mainly phytoplankton) but not DMS and that it might be additionally transported there from higher productive regions. Thus, sources solely for isoprene together with transport processes may control the isoprene distribution in the eastern Atlantic Ocean.

4.5 Summary

In 23 regions which extended over two-thirds of the north-south transit, a relationship between isoprene and DMS could be detected. Additionally, a similar distribution pattern of DMSP and isoprene along the entire transit could be observed. Dinoflagellates were identified as a potential source for both isoprene and DMSP. The clustering of isoprene and the sulphur compounds dependent on the N:P ratios showed the similar distribution and the common biological source for these chemical compounds. Especially in oligotrophic and mesotrophic regions, with N:P of up to 7-8, isoprene and DMSP seemed to be produced by similar algae groups, namely dinoflagellates, haptophytes and chrysophytes. However, there are hints that in eutrophic regions different sources exist for isoprene and DMSP. In contrast, a relationship between DMS and isoprene could be observed in oligotrophic to eutrophic regions, which may reflect linkages due to bacterial processes along the entire north-south transit. The role of bacteria is speculative and needs to be further investigated. Tools such as flow cytometry and DNA analysis should be regularly deployed on future transits to gain a better understanding of the influence of bacteria.

The distribution pattern of DMS:isoprene reflected the hydrographic regions of the eastern Atlantic Ocean. Elevated DMS concentrations were detected in upwelling areas, while isoprene showed enhanced concentrations in oligotrophic to mesotrophic regions, like the region of the Canary Current, ITCZ and equator. Correlations between isoprene and Chl-a in the ITCZ and equatorial region indicated sources solely for isoprene. However, transport processes of isoprene might be an additional control on the isoprene surface seawater distribution in the eastern Atlantic Ocean. Nonetheless, both compounds had highest concentrations in the spring bloom near the South African coast, likely reflecting the overwhelming influence of biological productivity on the concentrations of both trace gases.

Although a link between isoprene and sulfur compounds could be found, it remains to be seen if this relationship is based only on the same source organisms or actually on a linkage between the physiological production pathways of both compounds in algae cells. In addition, to better understand the biogeochemical cycle of isoprene in the surface ocean, higher resolution ancillary data (e.g. plankton and bacteria composition and activity, nutrients) are necessary. Moreover, the investigation of the diurnal and seasonal cycle on isoprene concentrations in different biogeochemical provinces is fundamental to understanding the dynamics of the distribution of isoprene and the impact of marine isoprene on chemical processes in the remote marine atmosphere.

Acknowledgments

Thanks to the captain, crew, and ship operations and to the chief engineer of the R/V Polarstern. Thanks to Martina Schütt, Tobias Steinhoff, Peer Fietzek, Cyril McCormick, Mike Lawler, and Kristal Verlhust for logistical help and technical support. We gratefully acknowledge the data from and discussions with Boris Koch, Astrid Bracher, and Leigh McCallister. This project was funded jointly by the BMBF project SOPRAN (FKZ 03F0462A and 03F0611A) and the Humboldt Foundation and is part of the German contribution to international SOLAS. Additional funding for C. Marandino and C. Zindler comes from the Helmholtz Young Investigator Group of Christa Marandino, TRASE-EC, from the Helmholtz Association through the President's Initiative and Networking Fund and the Helmholtz-Zentrum für Ozeanforschung Kiel (GEOMAR).

References

Alvarez, L. A., Exton, D. A., Timmis, K. N., Suggett, D. J., and McGenity, T. J.: Characterization of marine isoprene-degrading communities, Environmental Microbiology, 11, 3280-3291, 10.1111/j.1462-2920.2009.02069.x, 2009.

Arnold, S. R., Spracklen, D. V., Williams, J., Yassaa, N., Sciare, J., Bonsang, B., Gros, V., Peeken, I., Lewis, A. C., Alvain, S., and Moulin, C.: Evaluation of the global oceanic isoprene source and its impacts on marine organic carbon aerosol, Atmospheric Chemistry and Physics, 9, 1253-1262, 2009.
Baker, A. R., Turner, S. M., Broadgate, W. J., Thompson, A., McFiggans, G. B., Vesperini, O., Nightingale, P. D., Liss, P. S., and Jickells, T. D.: Distribution and sea-air fluxes of biogenic trace gases in the eastern atlantic ocean, Global Biogeochem. Cycles, 14, 871-886, 10.1029/1999gb001219, 2000.
Balch, W. M., Holligan, P. M., Ackleson, S. G., and Voss, K. J.: Biological and optical properties of mesoscale coccolithophore blooms in the gulf of maine, Limnology and Oceanography, 629-643, 1991.
Bonsang, B., Polle, C., and Lambert, G.: Evidence for marine production of isoprene, Geophys. Res. Lett., 19, 1129-1132, 10.1029/92gl00083, 1992.
Bonsang, B., Gros, V., Peeken, I., Yassaa, N., Bluhm, K., Zoellner, E., Sarda-Esteve, R., and Williams, J.: Isoprene emission from phytoplankton monocultures: The relationship with chlorophyll-a, cell volume and carbon content, Environmental Chemistry, 7, 554-563, 2010.
Broadgate, W. J., Liss, P. S., and Penkett, S. A.: Seasonal emissions of isoprene and other reactive hydrocarbon gases from the ocean, Geophys. Res. Lett., 24, 2675-2678, 10.1029/97gl02736, 1997.
Colomb, A., Yassaa, N., Williams, J., Peeken, I., and Lochte, K.: Screening volatile organic compounds (vocs) emissions from five marine phytoplankton species by head space gas chromatography/mass spectrometry (hs-gc/ms), Journal of Environmental Monitoring, 10, 325-330, 10.1039/b715312k, 2008.
Curson, A. R. J., Rogers, R., Todd, J. D., Brearley, C. A., and Johnston, A. W. B.: Molecular genetic analysis of a dimethylsulfoniopropionate lyase that liberates the climate-changing gas dimethylsulfide in several marine α-proteobacteria and rhodobacter sphaeroides, Environmental Microbiology, 10, 757-767, 10.1111/j.1462-2920.2007.01499.x, 2008.
Dacey, J. W., Wakeham, S. G., and Howes, B. L.: Henry's law constants for dimethylsulfide in freshwater and seawater, Geophysical Research Letters, 11, 991-994, 1984.
Hernandez-Guerra, A., Lopez-Laatzen, F., Machin, F., De Armas, D., and Pelegri, J. L.: Water masses, circulation and transport in the eastern boundary current of the north atlantic subtropical gyre, Scientia Marina, 65, 177-186, 2001.
Holligan, P., Viollier, M., Harbour, D., Camus, P., and Champagne-Philippe, M.: Satellite and ship studies of coccolithophore production along a continental shelf edge, 1983.
Houweling, S., Dentener, F., and Lelieveld, J.: The impact of nonmethane hydrocarbon compounds on tropospheric photochemistry, Journal of Geophysical Research: Atmospheres, 103, 10673-10696, 10.1029/97jd03582, 1998.
Keller, M. D., Bellows, W. K., and Guillard, R. R. L.: Dimethyl sulfide production in

marine-phytoplankton, Acs Symposium Series, 393, 167-182, 1989.
Kiene, R. P., Linn, L. J., and Bruton, J. A.: New and important roles for dmsp in marine microbial communities, Journal of Sea Research, 43, 209-224, 10.1016/s1385-1101(00) 00023-x, 2000.
Koch, B. P., and Kattner, G.: Preface 'sources and rapid biogeochemical transformation of dissolved organic matter in the atlantic surface ocean', Biogeosciences, 9, 2597-2602, 10.5194/bg-9-2597-2012, 2012.
Kuzma, J., Nemecekmarshall, M., Pollock, W. H., and Fall, R.: Bacteria produce the volatile hydrocarbon isoprene, Current Microbiology, 30, 97-103, 10.1007/ bf00294190, 1995.
Leck, C., Larsson, U., Bagander, L. E., Johansson, S., and Hajdu, S.: Dimethyl sulfide in the baltic sea - annual variability in relation to biological-activity, Journal of Geophysical Research-Oceans, 95, 3353-3363, 10.1029/JC095iC03p03353, 1990.
Mackay, D.; Shiu, W.Y., A critical review of Henry's law constants for chemicals of environmental interest, J. Phys. Chem. Ref. Data, 10, 1175-1199, 1981.
Marandino, C. A., De Bruyn, W. J., Miller, S. D., and Saltzman, E. S.: Eddy correlation measurements of the air/sea flux of dimethylsulfide over the north pacific ocean, J. Geophys. Res.-Atmos., 112, 10.1029/2006jd007293, 2007.
Marandino, C. A., Tegtmeier, S., Krüger, K., Zindler, C., Atlas, E. L., Moore, F., and W., B. H.: Dimethylsulphide (dms) emissions from the west pacific ocean: A potential marine source for the stratospheric sulphur layer, Atmos. Chem. Phys. Discuss.,, 12, 30543-30570, 10.5194/acpd-12-30543-2012, 2012.
McKay, W. A., Turner, M. F., Jones, B. M. R., and Halliwell, C. M.: Emissions of hydrocarbons from marine phytoplankton—some results from controlled laboratory experiments, Atmospheric Environment, 30, 2583-2593, 10.1016/1352-2310(95)00433-5, 1996.
Meskhidze, N., and Nenes, A.: Phytoplankton and cloudiness in the southern ocean, Science, 314, 1419-1423, 10.1126/science.1131779, 2006.
Milne, P. J., Riemer, D. D., Zika, R. G., and Brand, L. E.: Measurement of vertical distribution of isoprene in surface seawater, its chemical fate, and its emission from several phytoplankton monocultures, Marine Chemistry, 48, 237-244, 10.1016/0304-4203(94) 00059-m, 1995.
Moore, R. M., Oram, D. E., and Penkett, S. A.: Production of isoprene by marine phytoplankton cultures, Geophys. Res. Lett., 21, 2507-2510, 10.1029/94gl02363, 1994.
Moore, R. M., and Wang, L.: The influence of iron fertilization on the fluxes of methyl halides and isoprene from ocean to atmosphere in the series experiment, Deep Sea Research Part II: Topical Studies in Oceanography, 53, 2398-2409, 10.1016/j.dsr2.2006.05. 025, 2006.
Neogi, S. B., Koch, B. P., Schmitt-Kopplin, P., Pohl, C., Kattner, G., Yamasaki, S., and Lara, R. J.: Biogeochemical controls on the bacterial populations in the eastern atlantic

ocean, Biogeosciences, 8, 3747-3759, 10.5194/bg-8-3747-2011, 2011.
Palmer, P. I., and Shaw, S. L.: Quantifying global marine isoprene fluxes using modis chlorophyll observations, Geophys. Res. Lett, 32, L09805-L09810, 2005.
Quinn, P. K., and Bates, T. S.: The case against climate regulation via oceanic phytoplankton sulphur emissions, Nature, 480, 51-56, 2011.
Schäfer, H., Myronova, N., and Boden, R.: Microbial degradation of dimethylsulphide and related c1-sulphur compounds: Organisms and pathways controlling fluxes of sulphur in the biosphere, Journal of Experimental Botany, 61, 315-334, 10.1093/jxb/erp355, 2010.
Schmitt-Kopplin, P., Liger-Belair, G., Koch, B. P., Flerus, R., Kattner, G., Harir, M., Kanawati, B., Lucio, M., Tziotis, D., Hertkorn, N., and Gebefügi, I.: Dissolved organic matter in sea spray: A transfer study from marine surface water to aerosols, Biogeosciences, 9, 1571-1582, 10.5194/bg-9-1571-2012, 2012.
Sharkey, T. D., Wiberley, A. E., and Donohue, A. R.: Isoprene emission from plants: Why and how, Annals of Botany, 101, 5-18, 2008.
Shaw, S. L., Chisholm, S. W., and Prinn, R. G.: Isoprene production by prochlorococcus, a marine cyanobacterium, and other phytoplankton, Marine Chemistry, 80, 227-245, 10.1016/s0304-4203(02)00101-9, 2003.
Shaw, S. L., Gantt, B., and Meskhidze, N.: Production and emissions of marine isoprene and monoterpenes: A review, Advances in Meteorology, 10.1155/2010/ 408696, 2010.
Simó, R.: From cells to globe: Approaching the dynamics of dms(p) in the ocean at multiple scales, Canadian Journal of Fisheries and Aquatic Sciences, 61, 673-684, 10.1139/f04-030, 2004.
Stefels, J., Steinke, M., Turner, S., Malin, G., and Belviso, S.: Environmental constraints on the production and removal of the climatically active gas dimethylsulphide (dms) and implications for ecosystem modelling, Biogeochemistry, 83, 245-275, 10.1007/s10533-007-9091-5, 2007.
Steinke, M., Malin, G., Archer, S. D., Burkill, P. H., and Liss, P. S.: Dms production in a coccolithophorid bloom: Evidence for the importance of dinoflagellate dmsp lyases, Aquatic Microbial Ecology, 26, 259-270, 10.3354/ame026259, 2002.
Stramma, L., and Schott, F.: The mean flow field of the tropical atlantic ocean, Deep-Sea Research Part Ii-Topical Studies in Oceanography, 46, 279-303, 10.1016/ s0967-0645(98)00109-x, 1999.
Taylor, B. B., Torrecilla, E., Bernhardt, A., Taylor, M. H., Peeken, I., Rottgers, R., Piera, J., and Bracher, A.: Bio-optical provinces in the eastern atlantic ocean and their biogeographical relevance, Biogeosciences, 8, 3609-3629, 10.5194/bg-8-3609-2011, 2011.
Vogt, M., and Liss, P. S.: Dimethylsulfide and climate, Surface ocean - lower atmosphere processes, 187, Geophysical Monograph Series, AGU, Washingtion, DC, 2009.
Yoch, D. C.: Dimethylsulfoniopropionate: Its sources, role in the marine food web, and biological degradation to dimethylsulfide, APPLIED AND ENVIRONMENTAL MI-

CROBIOLOGY, 68, 5804-5815, 10.1128/aem.68.12.5804-5815.2002, 2002.
Yokouchi, Y., Li, H.-J., Machida, T., Aoki, S., and Akimoto, H.: Isoprene in the marine boundary layer (southeast asian sea, eastern indian ocean, and southern ocean): Comparison with dimethyl sulfide and bromoform, J. Geophys. Res., 104, 8067-8076, 10.1029/1998jd100013, 1999.
Zindler, C., Bracher, A., Marandino, C. A., Taylor, B., Torrecilla, E., Kock, A., and Bange, H. W.: Sulphur compounds, methane, and phytoplankton: Interactions along a north-south transit in the western pacific ocean, Biogeosciences Discuss., 9, 15011-15049, 10.5194/bgd-9-15011-2012, 2012a.
Zindler, C., Peeken, I., Marandino, C. A., and Bange, H. W.: Environmental control on the variability of dms and dmsp in the mauritanian upwelling region, Biogeosciences, 9, 1041-1051, 10.5194/bg-9-1041-2012, 2012b.

5 Marine sources and sinks of acetaldehyde and acetone

5.1 Material and Method

5.1.1 Development of an analytical system for measurements of OVOCs in seawater

A widely used system to analyse trace gases is a gas chromatograph coupled to a mass spectrometer (GC-MS). To date, only a few studies have reported measurements of OVOCs in seawater, resulting in a lack of knowledge about viable analytical systems. Therefore, a development phase of trial and error was necessary to perform accurate and reproducible measurements of OVOCs. Concentrations of OVOCs in seawater are in the $\mathrm{nmol\,L^{-1}}$ range. Thus, a pre-concentration of these compounds was essential prior to analysis. This could be achieved by developing a purge-and-trap-system, that was attached to the GC-MS (GC: Agilent Technologies, 7890A; MS: Agilent Technologies, 5975C MS, single quadrupole, Fig. 5.1).

5.1.2 Purge and Trap

OVOCs were expelled from the water sample by a helium gas stream flowing at 30 $\mathrm{ml\,min^{-1}}$ for 20 min. The water sample was housed in a gas tight purge unit through which the helium flowed (Fig. 5.1). The stripped OVOCs were transferred, through heated tubing, into a pre-concentration trap that was downstream from the purge unit. The best trapping efficiency was achieved with a U shaped 1/16 inch Sulfinert® stainless steel tubing which was submerged in liquid nitrogen (LN_2).

Several pre-concentration traps were tested and rejected: 1/8 inch stainless steel U shaped trap filled with glass beads; 1/8 inch stainless steel U shaped trap filled with Tenax® TA (mesh 60/80, Alltech); unfilled 1/8 inch stainless steel U shaped trap; unfilled fused silica capillary tubing (untreated, 0.53 mm i. d.). Different cold trapping methods were also

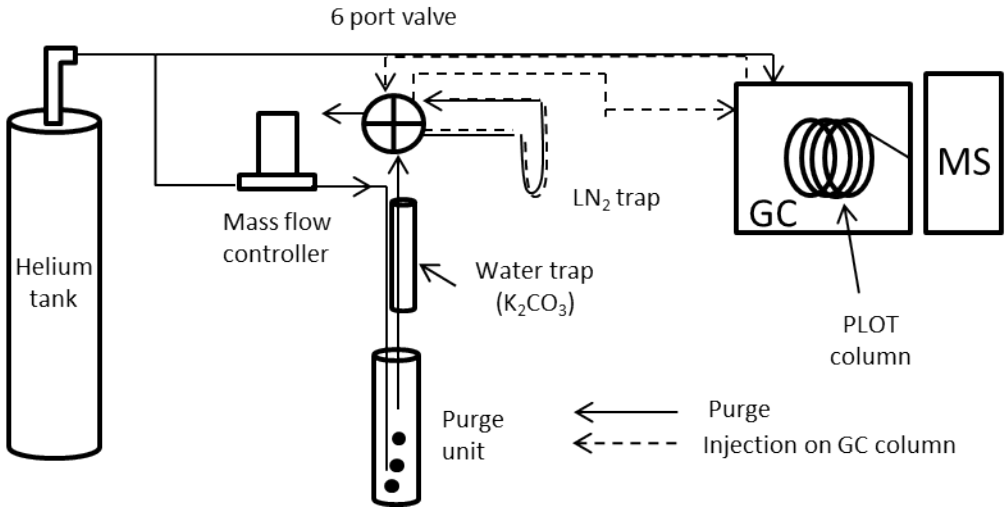

Fig. 5.1: *Schematic of the purge and trap system attached to the GC-MS for analysis of OVOCs in seawater samples.*

tested: salty ice-water to about -13°C; ethylene glycol to approximately -30°C; liquid nitrogen to about -196°C. Additionally, we also tested the use of a second pre-concentration trap that consisted of an untreated capillary column which was also submerged in LN_2 in front of the injection port of the GC. This second trap was in line with the first trap and should have helped to refocus the sampling gas after the OVOCs were desorbed of the first trap, resulting in better separation on the GC column. However, the trap extended the time of analysis and did not improve the separation in the GC-column.

5.1.3 Water traps

To avoid blockages in the system or the overload of the GC column and mass spectrometer with water, it was necessary to dry the sampling gas stream. Additionally, OVOCs are very soluble in water, thus, they can easily dissolve in small amounts of water trapped in the system. The water trap giving the best results was a short (5 cm length, 0.5 cm i. d.) glass tube filled with potassium carbonate (K_2CO_3), which needed to be replaced after four measurements. Prior to use, the trap had to be flushed with helium for several hours to remove any OVOC contamination. The best measurement reproducibility was achieved for ketones and aldehydes when the water trap was flushed with helium at 40 $\mathrm{ml\,min^{-1}}$ for additional 10 min after the sample was purged. This flushing gas stream was also trapped and analysed together with the sample. Despite the high capacity of K_2CO_3 to absorb water, small amounts of water remained in the analytical system, which interfered especially with the alcohols. Thus, the reproducibility of the alcohol measurements was never satisfactory and additional tests in the future are necessary to measure alcohols in seawater.

Several water traps were tested and rejected: mole sieve (3Å 0.3 mm, Typ 564, Roth); magnesium perchlorate; freezing and trapping the water in a U shaped stainless steel tubing (unfilled) submerged in glycol cooled to -30°C with a cooling device (Thermo-Haake EK 90). Furthermore, a pre-column packed with Porapak p 80/100 was used to elute first water from the sampling gas stream while the OVOCs were retained longer on the column. However, the water could not be fully desorbed from the packing material in the pre-column, thus, the column became irreversibly blocked after several measurements and discarded from the system.

5.1.4 GC-MS

The sampling gas in the pre-concentration LN_2 trap was injected on the GC-column (fused silica capillary column Supel-QTM Plot, 30 m x 0.32 mm) using boiling water. The GC-column was heated by an oven program of:

Heating [°C min^{-1}]	Oven temperature [°C]	Hold for [min]
	40	8
5	80	1
5	120	5
100	200	2

This heating program separated the lower molecular weight and highly volatile compounds, such as methanol, acetaldehyde and ethanol, from the higher molecular weight compounds, propanal, acetone, DMS, isoprene, isopropanol and propanol. The highest molecular weight compounds, such as butanal, butanone, 1- and 2-butanol, emerged at the end of the chromatogram (Fig.5.2, see also Table 5.3 for the structural formula of the OVOCs). At the end of the column the OVOCs were directly injected into the ion source of the MS. The OVOCs were ionised using electron impact and were mass filtered in a single quadrupole mass spectrometer coupled to an electron multiplier detector. An example spectrum is shown in Figure 5.2.

After each measurement, the remaining water vapor in the tubing system of the purge and trap unit was driven off by increasing the heating level on the heater tape which was wrapped around the tubing and valves and flushing for 10 minutes with helium. The analytical procedure for one sample required about 50 to 60 minutes, due to the long flushing time of the system and the long separation time of the OVOCs in the column: 30 minutes for pre-concentration and 30 minutes for the oven program.

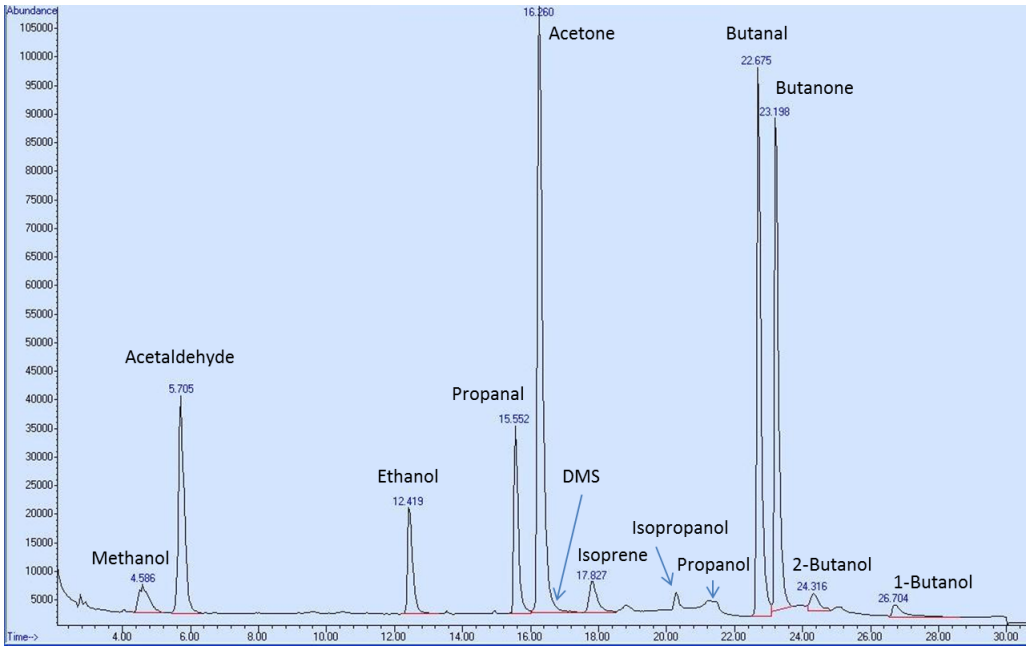

Fig. 5.2: *Example of a chromatogram of OVOC, DMS and isoprene. Note that the peak of DMS is interfered with the acetone peak.*

5.1.5 Treatment of samples

Samples had to be measured immediately after sampling because of the instability of the OVOCs due to loss via (suspected) biological activity or loss to the headspace. We tested the stability of the samples by flash freezing multiple liquid standards of the same concentration in LN_2 and storing them at -20°C for different time periods, between a few hours and one day. The concentrations in the standards strongly varied, indicating storage of samples was not possible. Thus, samples were measured within 30 minutes after sampling.

Filtration of samples was tested in order to avoid breaking of phytoplankton cells during the purge which could release OVOCs. We filtered the samples through GF/F Whatman filters (0.7 µm). However, no significant differences between filtered or non-filtered samples could be determined. Thus, filtration was not routinely performed before purge and trap.

Loss and contamination of OVOCs in water samples due to the contact with air was also tested. Certain OVOCs, such as methanol and acetone, are present in large quantities in ambient air. Liquid standards were exposed to the air between 30 minuntes and several hours and were analysed afterwards. No significant differences could be found between exposed standards and closed standards. Nonetheless, gas tight syringes were used to

avoid contact of samples to the air during sampling. However, during the transfer of samples into the purge unit the samples were always in contact with the air for a short period of time. In addition, due to gentle handling of the samples, the loss to the atmosphere was negligible.

5.1.6 Protocol of the purge and trap procedure

Due to the high solubility of OVOCs, especially of the alcohols, it was impossible to completely expel all compounds from the water sample. Thus, a measurement procedure was established to precisely control the amount of molecules which were expelled out of the water samples during a certain period of time:

- the same amount of water sample (10 ml) was always used
- the water sample was heated to 30°C during the purge
- the transfer tubing was heated to 60°C using heater tape
- all samples were purged for 20 minutes with a helium flow of 30 $\mathrm{ml\,min^{-1}}$
- after each purge period, the system was flushed without water in the purge unit for an additional 10 minutes with a helium flow of 40 $\mathrm{ml\,min^{-1}}$ whereby the OVOCs remaining in the water trap and tubing were also trapped
- after the injection of the OVOCs onto the GC-column the entire purge and trap system was flushed for additional 10 minutes with a helium stream of 70 $\mathrm{ml\,min^{-1}}$ and while heating to 90°C in order to dry the system and release any remaining OVOCs

Although, this measurement procedure improved the reproducibility it was sensitive to mistakes in handling.

5.1.7 Blanks

Contamination with OVOCs was always a risk during the measurements. OVOCs were present in the Milli Q water used to make standards, also after several days of purging. They were detected in the K_2CO_3 used for drying the air stream and they were measured in the analysis system even when Milli Q water and K_2CO_3 were excluded. The contamination of the system was probably caused by to atmospheric air enriched with OVOCs which entered the system. It might be also possible that water droplets were always present in the system, thus, OVOCs were always in solution inside the tubes. OVOCs are ubiquitous in the atmosphere and are also widely used as solvents in laboratories. Furthermore, OVOCs from previous measurements might accumulate in the system. To keep the blank levels low, Milli Q water and K_2CO_3 were purged and flushed for several hours prior their

Tab. 5.1: *Standard preparation for the OVOC measurements. DMS standard was prepared as described in Zindler et al. (2012) and were directly injected into the third OVOC standard. Note that the last column presents the final concentration of the OVOC standard.*

Standard 1		**Standard 2**		
20 ml Milli Q mixed with:		10 ml Milli Q mixed with:		
	[µl]		[µl]	[$\mathrm{nmol\,L^{-1}}$]
Methanol	8	Standard 1	10	
Ethanol	12			
Isopropanol	15	**Standard 3**		
Propanol	15	10 ml Milli Q mixed with:		
Propanal	15	Standard 2	10	10
1-Butanol	18		30	30
2-Butanol	18		50	50
Butanal	18		80	80
Acetone	15		100	100
Acetaldehyde	12			
Isoprene	2	DMS-Standard	5	2.5
			7	3.5
			10	5
			15	7.5
			20	10

use, the system was periodically flushed and the GC-column was frequently baked out for several hours. Additionally, the MS was tuned periodically. Blanks were measured frequently before and after each calibration and before and after the change of the water traps. Due to this control of the blanks, they had only a minor influence on the variation of the measurements and can be neglected in the error propagation.

5.1.8 Standard preparation

Three dilution steps were included to prepare standards in the 10 to 100 $\mathrm{nmol\,L^{-1}}$ range. In order to prepare the first standard, pure liquid OVOCs were directly injected with a micro-liter syringe into 18 MΩ Milli Q water. The second standard was prepared by dilution of the first standard in Milli Q water. The second standard was directly injected into Milli Q water (third standard) which was either immediately measured or prepared beforehand and measured over the course of the day. The exact compositions of the three standards are presented in Table 5.1.

While the first standard was stable for two to three days, the concentration of the second and third standard changed with time. Thus, a fresh preparation of the second standard was necessary every day as well as a fresh preparation of the third standard right before analysis.

The standards were used to frequently calibrate the measurement device. The peak areas (pa) which were calculated from the chromatograms were plotted against the concentrations of the OVOC-standards. The fitted regression lines and their explained variances (R^2) showed the precision of the measurements and the errors of the analysis (the actual errors are presented in section 5.1.10 and 5.1.11). The linear fit with the closest time proximity to the individual experiments were used to compute the measured seawater concentrations.

5.1.9 Stability of the measurement device over time

Five point calibrations were performed to test the stability and the reproducibility of the analytical system. Calibrations were frequently repeated during the performance of incubation experiments in the Kiel Fjord and during the research cruise onboard the R/V Maria S. Merian leg 18/3 (MSM 18/3) (see section 5.1.12 for a detailed description of the experiments).

5.1.10 Acetaldehyde

Figure 5.3 shows an overview of all acetaldehyde calibrations performed before the start of the incubation experiments. Figure 5.4 shows all calibrations for acetaldehyde during the experiments in the Kiel Fjord and Figure 5.5 shows those during the MSM 18/3 experiments.

The slopes of all calibrations were between 936 and 1635 pa nmol^{-1} L (except for the 20^{th} December 2010). The R^2 of the regression lines ranged between 0.88 and 0.998 except for the calibrations of the 20^{th} December 2011. Although, certain calibrations showed different slopes and had a low R^2, the analytical system showed good reproducibility, with an average variation of 21% for acetaldehyde (see Table 5.2). The average variations were determined by calculating each standard deviation of all standards of a certain concentration, calculating the percentage of the standard deviation and averaging them. The averages of each concentration were averaged again to obtain an overall variation value (average of column 7, Table 5.2).

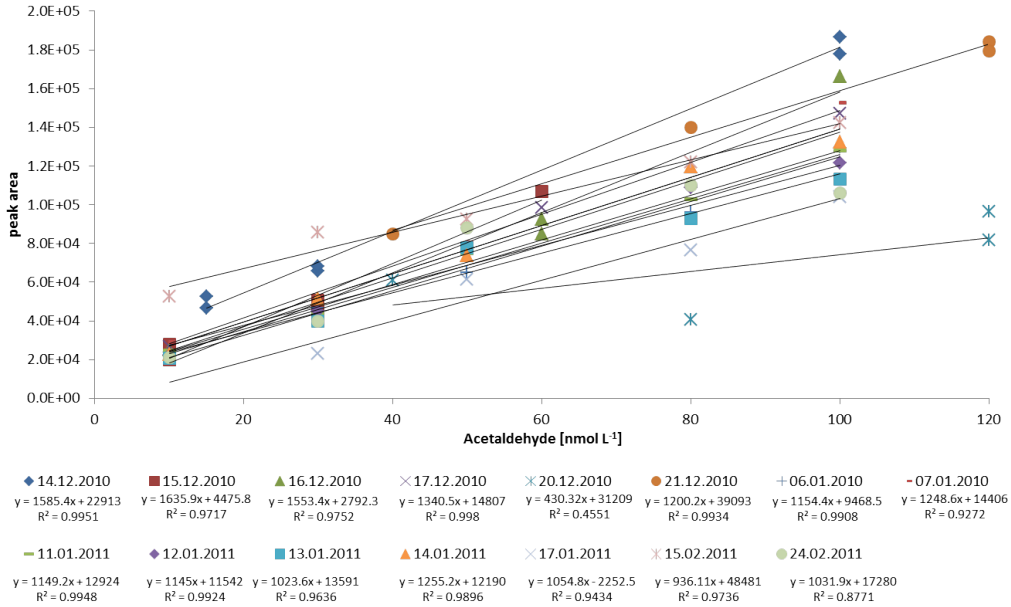

Fig. 5.3: *Five point calibrations of acetaldehyde ^{12}C (liquid standards) during the test phase of the OVOC system prior the experimental phase between* 14^{th} *of December 2010 until* 24^{th} *February 2011.*

During the experiments in the Kiel Fjord the slopes of the calibrations were lower, between 719 and 1048 pa nmol^{-1} L for ^{12}C-acetaldehyde, compared to the calibrations before the experimental phase. For the calibrations with ^{13}C-acetaldehyde the slopes were even lower, between 323 and 589 pa nmol^{-1} L, compared to ^{12}C. The R^2 for both ^{12}C and ^{13}C compounds ranged mainly between 0.86 and 0.99. The average standard deviation for ^{12}C compounds was 26.8% and for ^{13}C compounds was 16.5%.

The slope of the calibrations during the MSM 18/3 cruise were significantly higher, between 5411 and 32769 pa nmol^{-1} L for ^{12}C-acetaldehyde and 6745 and 24779 pa nmol^{-1} L for ^{13}C-acetaldehyde, in contrast to the Kiel experiments and the calibrations before. It seems that the sensitivity of the analytical system improved during the ship campaign. However, the average variations for ^{12}C and ^{13}C were high, 76.6% and 38.5%, respectively. Note that these variations were obtained by including all measured standards. Thus, data have to excluded which can be explain by mistakes occurred during the measurements.

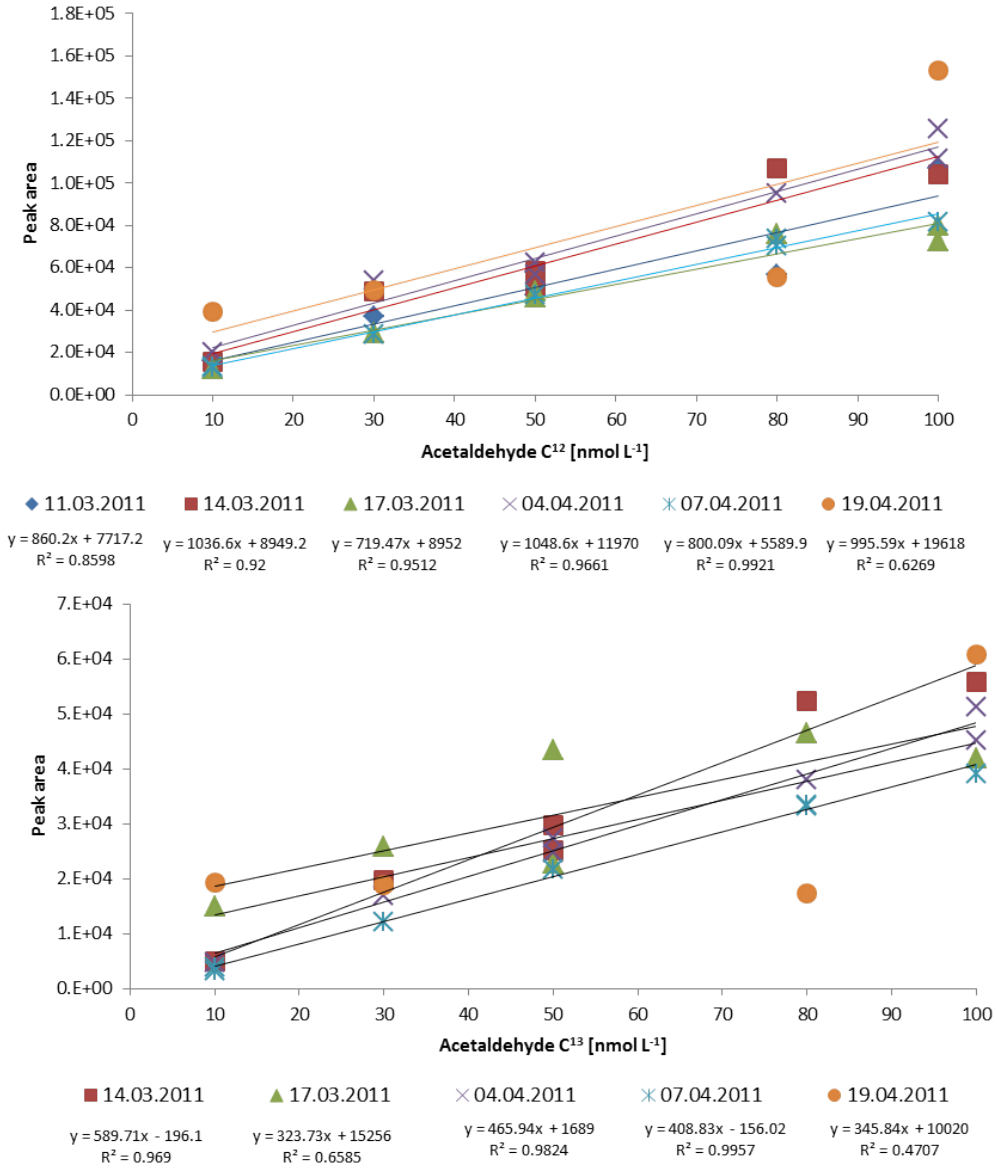

Fig. 5.4: *Five point calibrations of acetaldehyde (^{12}C-upper panel, ^{13}C-lower panel) during the experimental phase in the Kiel Fjord between 11th March until* 19^{th} *April 2011.*

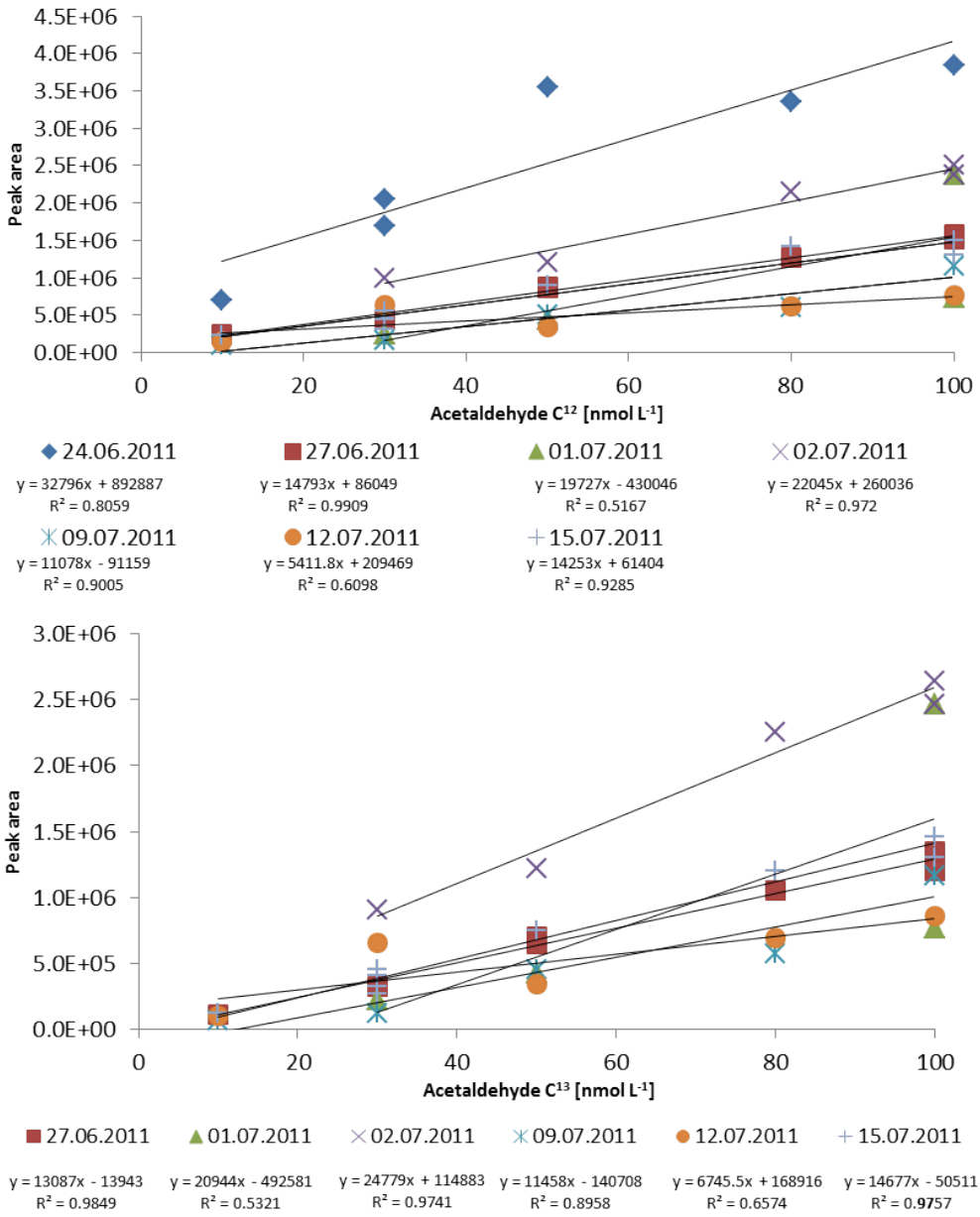

Fig. 5.5: *Five point calibrations of acetaldehyde (^{12}C-upper panel, ^{13}C-lower panel) during MSM 18/3 cruise between 24th June until 15th July 2011.*

5.1.11 Acetone

15 five point calibrations of acetone measured before the experimental phase are presented in Figure 5.6. Figure 5.7 shows all calibrations performed during the experiments in the Kiel Fjord and Figure 5.8 presents all calibrations from the MSM 18/3 experiments.

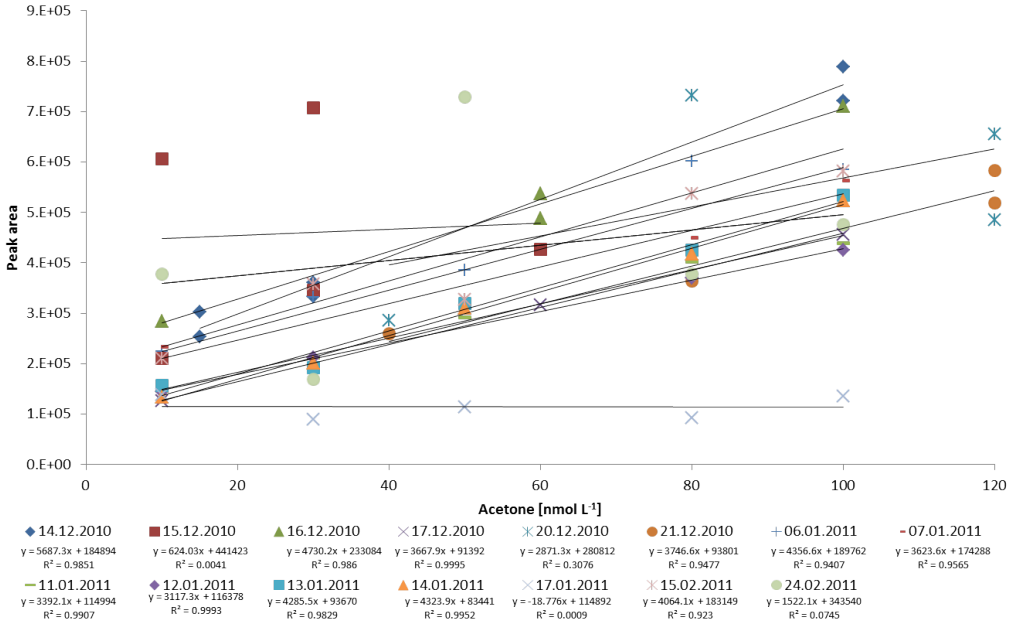

Fig. 5.6: *Five point calibrations of ^{12}C-acetone standards during the test phase of the OVOC measurement device prior the start of the experiments.*

Ten calibrations out of 15 had similar slopes between 3117 and 5687 pa nmol^{-1} L as well as a R^2 of 0.94 to 0.99. However, the analysis of acetone is less reproducible than acetaldehyde and needs improvement of the measurement procedure. Acetone is more soluble than acetaldehyde and is used as a solvent in laboratories. This might affect the reproducibility of the measurements. Although the errors for acetone were high, it was possible to obtain results which gave a first impression of the cycling of acetone in a natural environment. The average variation of acetone was 22% which is similar to the calibrations with acetaldehyde.

As in the case of acetaldehyde, the slopes of the calibrations for acetone during the Kiel experiments were also lower (1779 to 2777 pa nmol^{-1} L) than those prior to the experiments. This showed that the sensitivity of the analytical system decreased for all compounds with time. However, calibrations were conducted before and after each experiment. Additionally, single standards were measured during the experiments. Thus, the variation of the system was considered during the data analysis of the experiments,

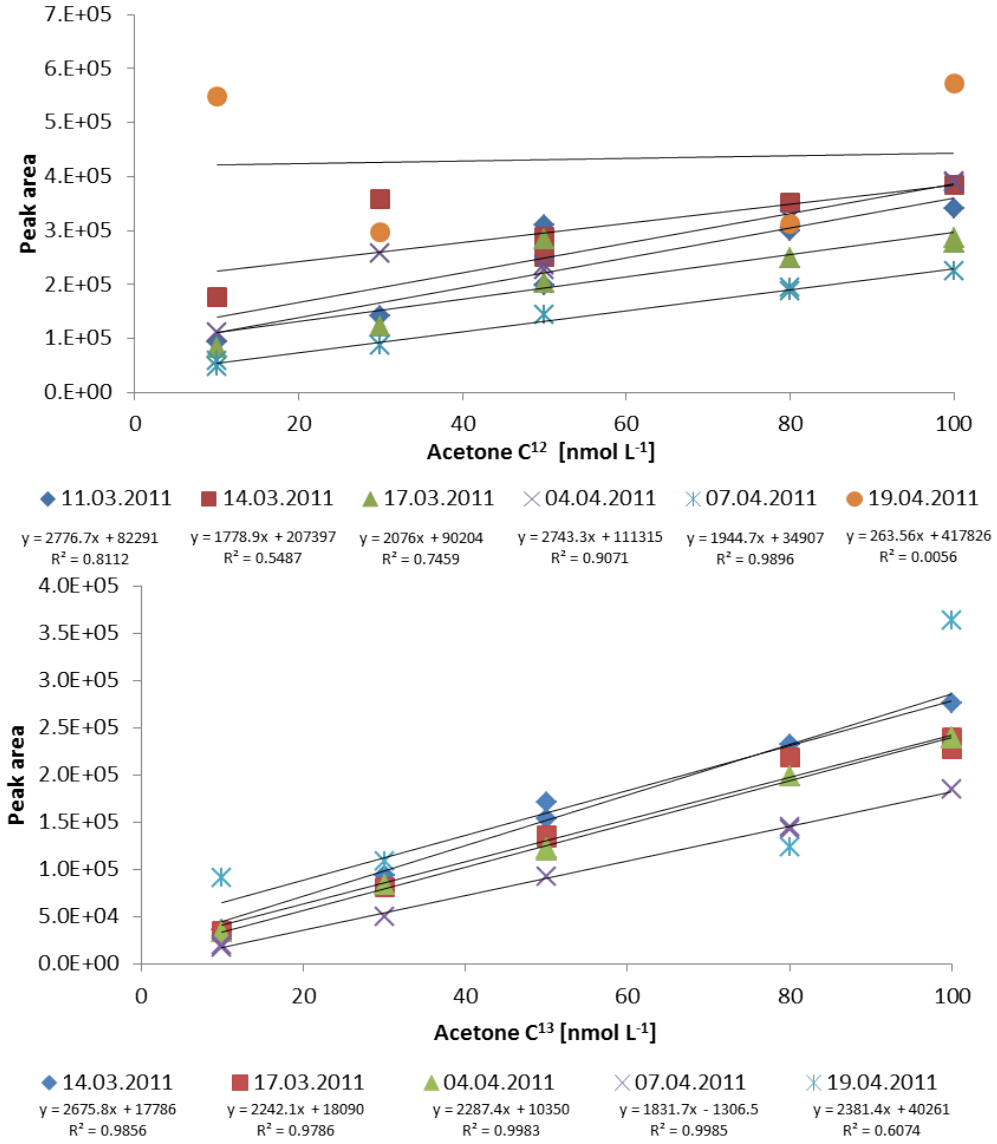

Fig. 5.7: *Five point calibrations of acetone (^{12}C-upper panel, ^{13}C-lower panel) during the experimental phase in the Kiel Fjord.*

namely by using the single point calibration during the experiment to identify the appropriate calibration (either before or after the experiment) for concentration computations. The slopes for ^{13}C-acetone were similar to those for ^{12}C compounds. The R^2 for ^{12}C ranged mainly between 0.55 and 0.99 and for ^{13}C between 0.98 and 0.99. The average variations for ^{12}C and for ^{13}C were 45.2% and 22.2%, respectively.

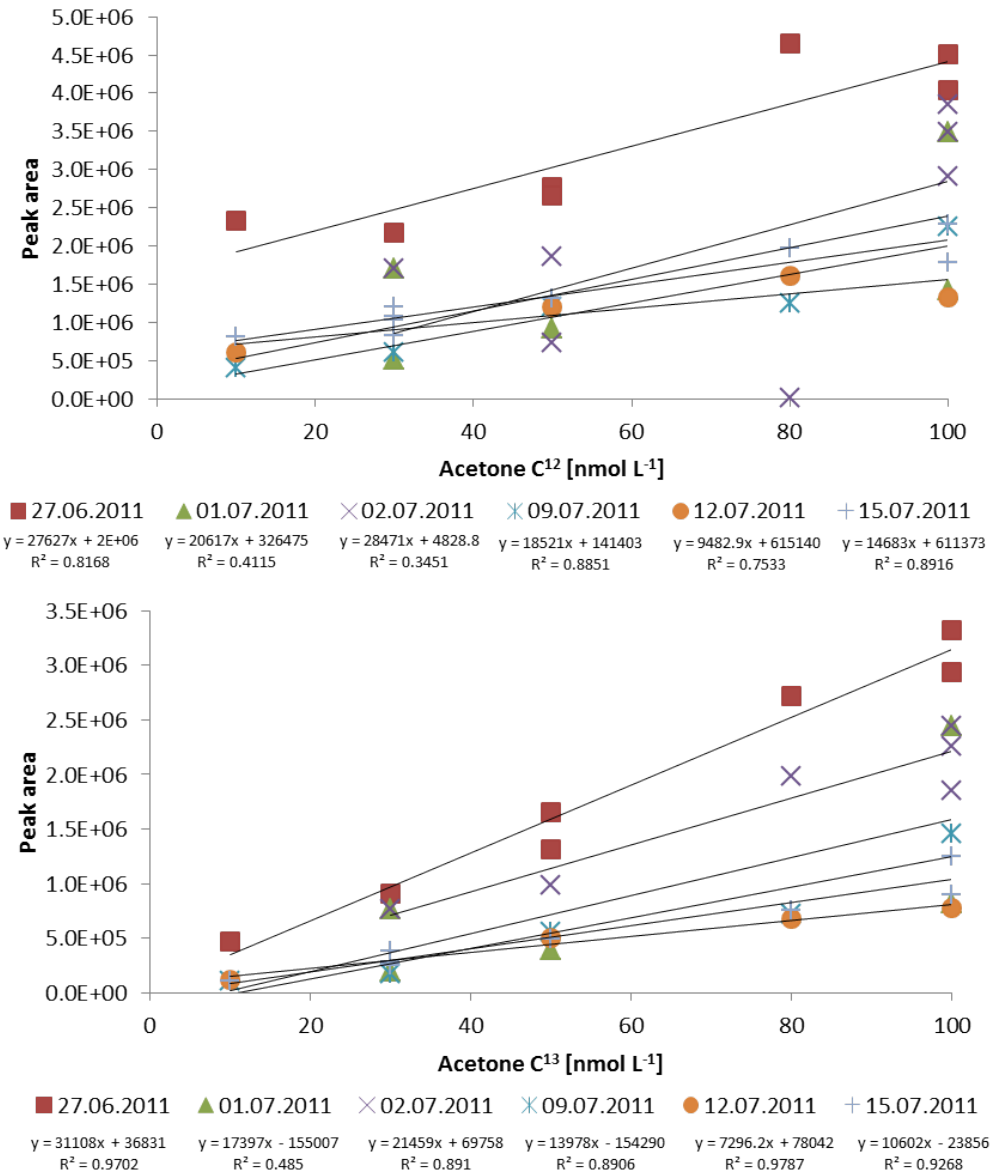

Fig. 5.8: *Five point calibrations of acetone (^{12}C-upper panel, ^{13}C-lower panel) during the MSM 18/3 cruise in the eastern tropical Atlantic.*

Also as in the case for acetaldehyde, the sensitivity of the analytical system increased for acetone during the research cruise compared to measurements before. The slopes for ^{12}C

ranged between 9482 and 28471 pa nmol^{-1} L and for ^{13}C between 7296 and 31108 pa nmol^{-1} L. However, the variations in the slopes were higher and illustrated the reduced reproducibility of the measurements. This was also observed in the average variations: 136.6% for ^{12}C and 141.7% for ^{13}C. Highly frequent repetitions of the calibrations were necessary to resolve the precision of the measurements. All calibrations performed for acetaldehyde and acetone during the analytical phase prior and during the experiments are listed in Table 5.2. The variation of the analytical system increased with the progression of the experiments and the amount of measurements. It is possible that the precision and the sensitivity of the analytical system changed with time due to possible contamination of the GC-MS from the injection of large numbers of seawater samples as well as the dismantling, transport and reconstruction of the analytical device. Notably, the calibrations with ^{13}C compounds showed fewer variations compared to ^{12}C compounds for both acetaldehyde and acetone, likely reflecting ambient air contamination for the ^{12}C compounds.

The errors given in percentage (Table 5.2) were calculated by including all conducted calibrations. For individual concentration measurements, the error was computed based on the error of the slope of the calibration conducted right before or after the experiments and a formula which included the average error of all calibration slopes. The relative error was always less than 12%. This number is less than the error of the standards presented in Table 5.2. The reported uncertainties are from the error of the calibration curve slopes.

In all experiments, the chemical compounds listed in Table 5.3 were measured. However, only acetaldehyde and acetone had sufficient reproducibility and will, therefore, be the only compounds presented in remainder of this chapter.

5.1.12 Incubation experiments

Incubation experiments were conducted in the Kiel Fjord in the Western Baltic Sea, Germany, and during the MSM 18/3 research cruise in the equatorial upwelling of the eastern Atlantic Ocean. The experiments in the Baltic Sea (EB) were repeated four times between the 2^{nd} of March and 21^{st} of April 2011. The experiments in the equatorial Atlantic (EA) were repeated six times between the 25^{th} of June and 16^{th} of July 2011.

Samples from the Kiel Fjord were collected from the surface water layer at the institute pier. In the Atlantic Ocean, water samples were collected from 10 m depth or in the water layer of maximum fluorescence of phytoplankton pigment at approximately 25 m depth by using Niskin bottles attached to a CTD (conductivity, temperature, depth sensor) rosette. Samples were taken outside and within the most intensive upwelling (Fig. 5.9).

Tab. 5.2: *All calibrations before the experimental phases, during the experiments in the Baltic Sea and in equatorial Atlantic. Standard deviation of the peak areas and the percentage of the standard deviations are given for both acetaldehyde and acetone for ^{12}C and ^{13}C.*

OVOC	Calibration	number of standards	Standard conc. [$\mathrm{nmol\,L^{-1}}$]	peak area (average)	standard deviation (average)	%standard deviation (average)
Acet-	before the	11	10	23242.7	2695.0	11.6
alde-	experiments	34	30	40554.2	4732.0	11.7
hyde	^{12}C	16	50	69691.1	8897.4	12.8
		4	60	95559.3	9292.0	9.7
		10	80	109708.2	15329.0	14.0
		14	100	139043.2	26304.5	18.9
		4	120	135528.3	53931.8	39.8
		18	250	463232.3	144636.4	31.2
		13	500	543798.9	211482.3	38.9
	Kiel	7	10	18917.7	10403.2	55.0
	experiments	6	30	41155.8	10990.2	26.7
	^{12}C	12	50	51627.8	7036.6	13.6
		7	80	84383.2	15882.7	18.8
		7	100	97361.3	19530.6	20.1
	MSM 18/3	6	10	285976.8	241673.9	84.5
	^{12}C	14	30	725228.3	611348.0	84.3
		9	50	1086687.5	1037665.2	95.5
		9	80	1570232.5	1044827.2	66.5
		12	100	1727476.9	897512.2	52.0
	Kiel	5	10	4157.6	732.4	17.6
	experiments	5	30	16475.8	3029.9	18.4
	^{13}C	7	50	25260.4	2711.2	10.7
		5	80	39991.0	8047.0	20.1
		8	100	48624.0	7719.5	15.9
	MSM 18/3	4	10	111344.0	7778.5	7.0
	^{13}C	14	30	433811.0	217975.1	50.2
		9	50	711497.4	343097.0	48.2
		5	80	1157221.6	664213.1	57.4
		13	100	1723461.6	510605.8	29.6
Ace-	before the	12	10	203656.6	76767.9	37.7
tone	experiments	2	15	277534.5	34391.6	12.4
	^{12}C	34	30	250180.0	88499.0	35.4
		17	50	301263.9	46691.5	15.5
		4	60	441715.3	95479.6	21.6
		7	80	424877.4	57616.8	13.6
		11	100	579741.6	115168.4	19.9
		4	120	560565.8	75316.8	13.4
		13	250	1646222.2	291276.5	17.7
		11	500	2249949.2	745393.3	33.1
	Kiel	7	10	159953.0	176613.0	110.4
	experiments	5	30	234906.8	101753.5	43.3
	^{12}C	12	50	236748.8	45912.0	19.4
		7	80	273561.4	64313.7	23.5
		8	100	358223.0	105597.2	29.5
	MSM 18/3	6	10	4557095.8	5696573.4	125.0
	^{12}C	13	30	6197974.0	8940640.1	144.3
		10	50	6313105.3	11155882.7	176.7
		9	80	8917242.0	9680127.7	108.6
		13	100	5749888.6	7397417.9	128.7
	Kiel	6	10	25979.5	9535.8	36.7
	experiments	5	30	89801.8	11246.1	12.5
	^{13}C	11	50	129604.0	20535.6	15.8
		7	80	180398.3	42829.5	23.7
		7	100	252315.7	55720.6	22.1
	MSM 18/3	6	10	553553.8	787327.2	142.2
	^{13}C	13	30	808523.6	1263140.3	156.2
		9	50	1489610.0	2083263.9	139.9
		7	80	3033765.8	4162653.3	137.2
		12	100	2971037.2	3951039.2	133.0

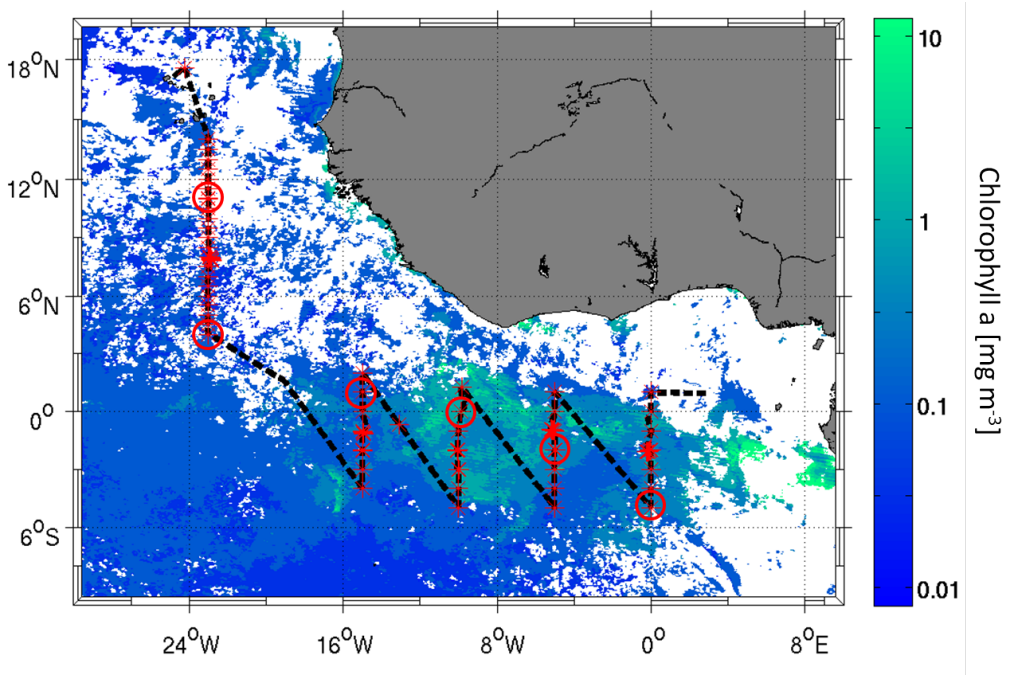

Fig. 5.9: *Cruise track (black, dashed line) and CTD stations (red stars) of the MSM 18/3 cruise in the equatorial east Atlantic Ocean. Note that the colorbar shows chlorophyll a concentrations in a logarithmic scale. Red circles present the locations of samples taken for the incubation experiments. The cruise started from the Cape Verde Islands and ended in Libreville, Gabon.*

5.1.13 Protocol of the incubation experiments

About 8 L water were sampled for the incubation experiments. Around 4 L of the sampled waters were filtered through 0.2 µm cellulose acetate filters, and during the experiments in the Atlantic, samples were additionally autoclaved (30 min at 100°C) in order to limit all biological activity. The filtered samples were used to perform the so-called chemistry treatments and were stored in the dark over night before beginning the incubation experiment. The other half of the sampled water was kept untreated and was used for the so-called biology treatment. The biology incubations were started immediately after sampling. The experiments were run with four different treatments: biology samples exposed to light (BL) and biology samples kept in the dark (BD), chemistry samples exposed to light (CL) and chemistry samples kept in the dark (CD). We incubated approximately 2 L of each treatment in quartz (light treatments) and borosilicate (dark treatments, wrapped with aluminium foil) bottles sealed with a silicon septum for taking subsamples (approximately every 3 hours during the incubation runs) using gastight syringes. We used artificial isotopes to determine the absolute loss rates because they are not produced in seawater in such large quantities. Additionally, the seawater samples contained natural ^{12}C OVOCs (for an overview of the structural formula see Table 5.3), which were used to determine the combined production and destruction processes over time. We expect that artificial and natural OVOCs are consumed or degraded equally. Thus, all treatments were spiked with artificial ^{13}C labelled acetone ($^{13}CH_3^{13}CO^{13}CH_3$), acetaldehyde ($^{13}CH_3^{13}COH$), ethanol ($^{13}CH_3^{13}CH_2OH$), methanol ($^{13}CH_3OH$) and 1-propanol ($^{13}CH_3CH_2CH_2OH$) to a concentration of around 100 $\mathrm{nmol\,L^{-1}}$.

After the preparation of the samples, the incubation bottles were fixed in the water at around 1m depth at the GEOMAR institute pier by using ropes. Therefore, these samples were exposed to natural temperature and light conditions. The experiments were conducted for approximately 12 hours during the EB, starting right before sunrise to include the entire light effect of the day. During the MSM 18/3 cruise, the experiment bottles were kept in incubation bins which were flushed continuously with surface seawater pumped into the bins. The bins were wrapped with coloured foil which diminished the sun light in the bins and simulated the light intensity in around 10 m depth in tropical open ocean waters. The experiments were conducted for around 24 hours.

The incubation experiments were conducted with four different treatments in order to test the influence of several combinations of environmental factors on the OVOC production and loss in the surface ocean. The effect of photosynthesis and other light induced activities in phytoplankton and in bacteria cells were investigated in the illuminated biology (BL) treatments. The dark treatments of the biology samples (BD) were used to study especially the behavior of phytoplankton when photosynthesis is inactive as well as the activities of bacteria which are independent of light. All biology treatments also contain the effects of chemical reactions which can alter the OVOC concentrations. In order to

investigate abiotic (i.e. chemical) sources and sinks of OVOCs, the biology activity was minimized in the samples by filtration and autoclaving. However, bacteria which were smaller than 0.2 µm could pass through the filters and thus may have influenced the chemistry samples (unless the samples were autoclaved). Photochemistry is hypothesized as a main source for OVOCs. Thus, one of the chemical treatments was exposed to light (CL) to investigate if the photochemical or photosensitized degradation of macromolecules like CDOM has an effect on the OVOC cycling. In order to distinguish the difference between light induced chemical reactions and those not requiring light, a chemical treatment was kept in the dark (CD). Based on the current literature the hypothesis of the main source of OVOCs in the oceans is the photochemical degradation of CDOM while the main sink is the consumption due to the biota. The design of the experiments should help to prove or reject this hypothesis.

In order to calculate the absolute production rates the loss rate could be calculated by multiplying an assumed constant k with the initial concentration of ^{13}C isotopes (Eq. 5.1). This constant was a parameter describing the loss rate. The same k was assumed for the loss rate of ^{12}C (ma, Eq. 5.2). The ^{12}C loss rate could be theoretically calculated the same way like the ^{13}C loss rate.

$$mC13 = k * nC13 \tag{5.1}$$

$$ma = k * nC12 \tag{5.2}$$

The term $mC13$ [$\mathrm{nmol\,L^{-1}\,min^{-1}}$] is the slope calculated from the change of the ^{13}C labelled OVOC concentrations over time of one experimental run. The intercept of the same run is termed as $nC13$ [$\mathrm{nmol\,L^{-1}}$]. ma [$\mathrm{nmol\,L^{-1}\,min^{-1}}$] is the slope of the destruction rate of ^{12}C-OVOCs and $nC12$ [$\mathrm{nmol\,L^{-1}}$] is the intercept of the slope determined via the change of the ^{12}C-OVOC concentrations in each run. We assumed that the constant k was equal for both equations. Thus, k could be excluded and ma could be calculated as described in Eq. 5.3. The absolute production rate could be calculated by subtracting the slope of the destruction rate of ^{12}C-OVOCs from the slope calculated from the change of the natural ^{12}C-OVOCs (Eq. 5.4).

$$ma = \frac{mC13 * nC12}{nC13} \tag{5.3}$$

$$production\,rate = mC12 - ma \tag{5.4}$$

We assume that the initial OVOC concentrations of the incubations influence the slope of the destruction rates according to first order reaction kinetics. For example, a high concentration of substrates eases the uptake for the biota. The initial concentrations of ^{13}C-OVOCs varied for each experiment. With the Eq. 5.4 we could include this variation.

Tab. 5.3: *Structural formula of natural ^{12}C-OVOCs, DMS and isoprene as well as artificial ^{13}C-OVOCs measured during the incubation experiments.*

Name	^{12}C-OVOCs (structural formula)	^{13}C-OVOCs (molecular formula)
Acetaldehyde		$^{13}CH_3^{13}COH$
Acetone	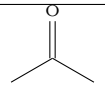	$^{13}CH_3^{13}CO^{13}CH_3$
Propanal	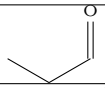	
Butanal	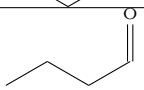	
Butanone	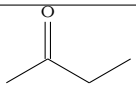	
Isoprene	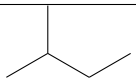	
Dimethylsulphide	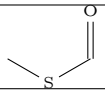	
Methanol	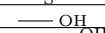	$^{13}CH_3OH$
Ethanol	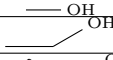	$^{13}CH_3^{13}CH_2OH$
Propanol	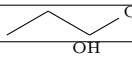	$^{13}CH_3CH_2CH_2OH$
Isopropanol	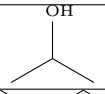	
1-Butanol	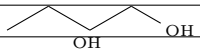	
2-Butanol	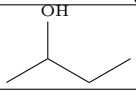	

Temperature and pH were measured using a Hanna HI 9812-5 pH/°C/EC/TDS Meter. Bacteria and phytoplankton counts were determined using a flow cytometer (Becton Dickinson, FACSCalibar). Bacteria and phytoplankton were fixed right after sampling with particle free formaldehyde solution (37%, AppliChem, 200 µl on 4 ml sample), quickly frozen in liquid nitrogen, and stored at -80°C until analysis. Prior the analysis, bacteria samples were stained with SYBR Green I nucleic acid gel stain (InvitrogenTM Molecular Probes Inc.). CDOM was analysed according to the method described by Heller and Croot (2010). Dissolved nutrients (nitrate, nitrite, phosphate and silicate) were measured according to the methods described by Hansen and Koroleff (2007) and oxygen by the method described by Hansen (2007). The solar radiation data for the Kiel experiments were obtained from the institute observation station. The solar radiation, salinity and temperature during the MSM 18/3 cruise was obtained from the ship data.

5.1.14 Sampling Site

5.1.14.1 Kiel Fjord

The Kiel Fjord is located in the western Baltic Sea and is influenced by urban activities. The salinity of the Kiel Fjord is characterised by fast changes due to high-saline water entrainment from the North Sea which is mixed with less saline Baltic seawater. Additionally, fresh water is discharged into the Fjord by the Schwentine River with a minor effect on the salinity. Ship traffic has an additional effect on the Fjord water. Between March and April 2011 a phytoplankton bloom developed.

5.1.14.2 Eastern equatorial Atlantic Ocean

The equatorial Atlantic Ocean is characterised by a seasonal variability with a cold season from June to October (Picaut, 1983). A most striking feature of this region is the annual occurrence of the phenomenon referred to as cold tongue. This cold tongue is associated with increasing strength of the south east trade winds which cross the equator (Philander and Pacanowski, 1981) due to the northward shift of the ITCZ during the boreal spring and summer (Philander *et al.*, 1996). Due to this change, a divergence zone occurs which triggers upwelling and induces the entrainment and mixing of cold and deep water masses in the surface ocean layer (Philander and Pacanowski, 1981, Okumura and Xie, 2004). The upwelled water mass transports nutrients in surface water and induces phytoplankton blooms (Oudot and Morin, 1987).

5.2 Results and Discussion

5.2.1 Incubation experiments

An example of one experiment including all four treatments for acetaldehyde is shown in Figure 5.10. The slopes calculated from the decrease of ^{13}C-OVOC concentrations with time indicate the degradation rates. The slopes of the ^{12}C-OVOC concentrations present a net rate which includes both production and destruction rates. The first concentration at time 0 is the natural concentration of ^{12}C OVOCs in the Kiel Fjord. These concentrations ranged between 6.2 and 147 nmol^{-1} during the experimental phase in the Kiel Fjord.

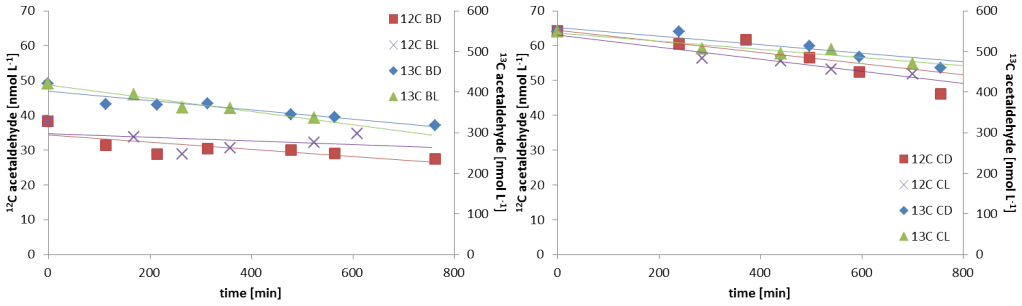

Fig. 5.10: *Example of one experiment on 15-16 March 2011 for the case of acetaldehyde. Left panel: The concentrations of both ^{12}C and ^{13}C acetaldehyde for the biology light and dark treatments. Right panel: The concentrations of both ^{12}C and ^{13}C acetaldehyde of the chemistry light and dark treatments. Note that the y axis on the left hand side presents ^{12}C and the y axis on the right hand side presents the ^{13}C concentrations.*

In general, destruction rates of chemical compounds are mainly dependent on the initial concentration and follow first order reaction kinetics. Production rates are mainly independent of the initial concentration and follow the zero order reaction kinetics. To determine the order of the experimental reaction kinetics, loss or production rates of all experiments in the Kiel Fjord and in the Atlantic Ocean were plotted against their initial concentrations (Figure 5.11). The R^2 values ranged between 0.7 and 0.9 for the loss rates against their intercepts which corroborates first order reaction kinetics. The only exception is acetone in the Kiel Fjord experiments. The R^2 for the production rates were small, suggesting zero order reaction kinetics (Figure 5.11). The same reaction kinetics were shown in the few previous studies (de Bruyn *et al.*, 2013; Mopper and Stahovec, 1986) for consumption rates of acetone and acetaldehyde in incubation experiments. The consumption rate constants (k in h^{-1}) are presented in Table 5.4. The highest value of k (0.7 h^{-1}) for acetaldehyde was calculated for the BL experiment on the 4^{th} July 2011 in the Atlantic Ocean. Mopper and Stahovec (1986) determined a rate constant of 0.86 h^{-1} for an unfiltered dark sample off the west coast of Florida which is above the k determined

in the BD treatments in this study. The average k for acetaldehyde determined in all experiments presented in this study ranged on average between 0.01 and 0.2 h^{-1} which is lower than reported literature values. Higher rate constants were determined in the Atlantic Ocean compared to the Kiel Fjord (Table 5.4). Biology and chemistry treatments showed no differences in their rate constants. The high values of the rate constants (0.01 and 0.07 h^{-1}) for acetone in this study were comparable with the low values of ks (0.017 to 0.08 h^{-1}) determined by deBruyn *et al.* (2013) in coastal waters of Southern California, USA. Also as in the case for acetaldehyde, higher rate constants for acetone were determined in the Atlantic Ocean compared to the Kiel Fjord. No significant differences in the constants could be observed between biology and chemistry treatments in the Kiel Fjord. However, higher k values were calculated for the biology samples compared to the chemistry samples in the Atlantic Ocean.

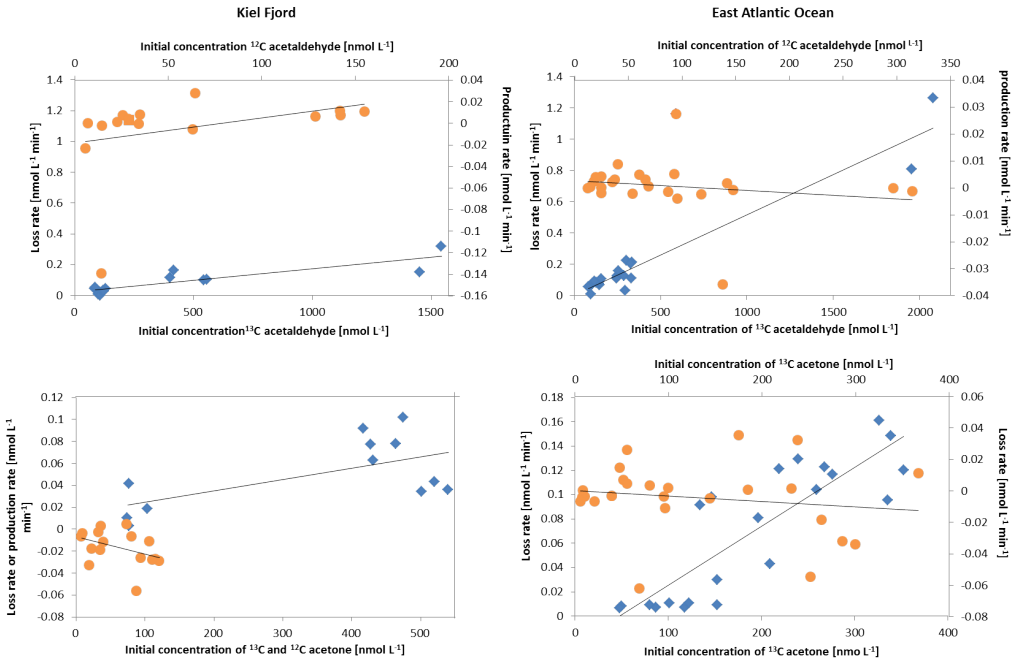

Fig. 5.11: *Loss rates of ^{13}C-acetaldehyde and acetone as a function of the initial concentrations in the individual experiments (blue diamonds). The same is presented for ^{12}C-acetaldheyde and acetone (orange dots). The panels on the left hand side illustrate the experiments in the Kiel Fjord and on the right hand side in the east Atlantic Ocean. The slopes and R^2 values are, respectively, as follows: loss rate of acetaldehyde, Kiel: 2*10-4, 0.76; loss rate of acetaldehyde, Atlantic: 5*10-4, 0.94; production rate of acetaldehyde, Kiel: 2*10-4, 0.1; production rate of acetaldehyde, Atlantic: 2*10-5, 0.03; loss rate of acetone, Kiel: 1*10-4, 0.38; loss rate of acetone, Atlantic: 5*10-1, 0.74; production rate of acetone, Kiel: -2*10-4, 0.17; production rate of acetone, Atlantic: -3*10-5, 0.03.*

5.2.2 Production and consumption of acetaldehyde in the Kiel Fjord

All determined production and destruction rates from all experiments conducted in the Kiel Fjord are presented in Figure 5.12. The consumption rates in the biology treatments (both light and dark treatments) ranged between 1.93 and 403 $\mathrm{nmol\,L^{-1}\,hr^{-1}}$ with an average of 61.5 $\mathrm{nmol\,L^{-1}\,hr^{-1}}$. The experiment of 8^{th} March showed extremely high consumption rates (BL: 403 $\mathrm{nmol\,L^{-1}\,hr^{-1}}$; BD: 163 $\mathrm{nmol\,L^{-1}\,hr^{-1}}$) compared to the other experiments. The consumption rate in the light treatment was on average higher compared to the dark biology treatment when the high concentrations of the 8th March are included. The destruction rates in the chemistry treatments ranged between 0.02 and 19 $\mathrm{nmol\,L^{-1}\,hr^{-1}}$ (average: 5.5 $\mathrm{nmol\,L^{-1}\,hr^{-1}}$, see also Table 5.4). In the dark treatments the degradation rates were on average higher compared to the light treatments which is in contrast to the biology samples. The consumption rates were on average higher in the biology treatments compared to the chemistry treatments when the experiment of the 8^{th} March is considered. When this high consumption rate is excluded the average consumption rates are the same in the biology and in the chemistry treatments. Also light seemed to have no effect on the rates.

The production rates were much lower compared to the consumption rates and in some incubation bottles no production occurred. In the biology treatments (both light and dark) production rates ranged between -1.38 (which means consumption) and 0.5 $\mathrm{nmol\,L^{-1}\,hr^{-1}}$ (average: 0.06 $\mathrm{nmol\,L^{-1}\,hr^{-1}}$) . In the chemistry treatments (both light and dark) the production was between -8.35 and 1.68 $\mathrm{nmol\,L^{-1}\,hr^{-1}}$ (average: -0.67 $\mathrm{nmol\,L^{-1}\,hr^{-1}}$). In the dark samples more production of acetaldehyde occurred on average compare to the light samples. The average highest production and consumption rates were measured in the chemistry dark treatments when the rates in the experiments of the 8^{th} March are not accounted.

5.2.3 Environmental parameters effecting acetaldehyde in the Kiel Fjord

Highest consumption rates were measured in the biology treatments in the experiment of the 8^{th} March. These samples exhibit the highest Chl-a concentration of all experiments conducted in the Kiel Fjord. Diatoms seemed to be the dominant phytoplankton group in this experiment indicated by fucoxanthin which was the highest concentrated marker pigment determined in the samples. The high silicate concentration (major nutrient for diatoms) in these incubation bottles also referred to a diatom bloom. Additionally, haptophytes, indicated by 19'-hexanoyloxyfucoxanthin, were also relatively abundant com-

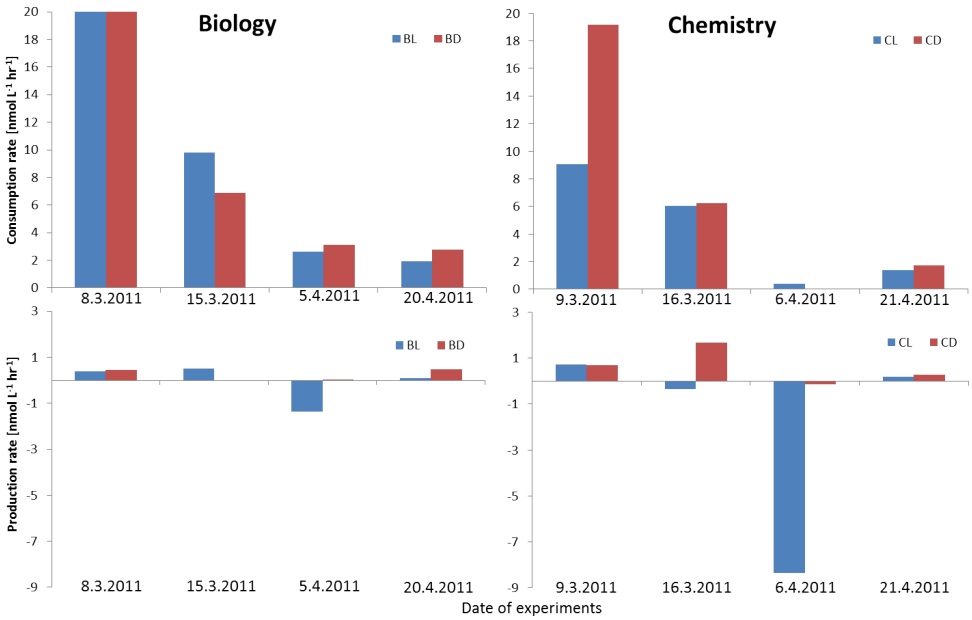

Fig. 5.12: *Consumption and production rates of acetaldehyde determined in the Kiel Fjord. Both rates are presented separately as biology or chemistry treatments while the dark and light treatments are presented in the same panels. Negative production rates indicate consumption only. BL means biology light treatment; BD biology dark treatment; CL chemistry light treatment and CD chemistry dark treatment. Note that in the upper left panel the consumption rate of BL of the* 8^{th} *March was 403* $\mathrm{nmol\,L^{-1}\,hr^{-1}}$ *and for BD was 163* $\mathrm{nmol\,L^{-1}\,hr^{-1}}$ *which is beyond the scale.*

pared to other phytoplankton groups. The chl-a concentration as well as the abundance of diatoms continuously decreased over the course of the all experiments conducted in the Kiel Fjord. The lowest concentration was determined in the last experimental run of the 20^{th} April. The consumption rate in the light and dark biology treatments also continuously decreased from the first to the last experiment. The abundance of haptophytes was already low in the second experimental run (15^{th} March) while the consumption rate was still relative high compared to the last experiments. All other marker pigments were relative low in all experiments and showed a low variability. Thus, diatoms or their symbionts might be a possible consumer of acetaldehyde during the incubations. However, no correlation could be found between the consumption rates of all experiments and the initial diatom concentrations of the experiments. The consumption rate was higher in the light biology treatment compared to the dark treatment of the first experimental day. The intensity of solar radiation was high during the first and the last experimental runs. Nonetheless, the last experiment showed lowest consumption independent of light intensity. It seems that consumption might be affected by both high diatom abundance and high light intensity. The variability of the production rates in the biology treatments of all experiments in the Kiel Fjord was inconsistent with the variability of all observed environmental parameters. Thus, the parameters which influence the production rates in the biology samples could not be identified. The variability of the consumption rates in the CL treatments of the different experimental runs was consistent with the variability of the different initial CDOM concentrations (R^2 = 0.97, p-value 0.01, n = 4, Figure 5.13). This is in contrast to other studies (deBruyn *et al.,* 2011; Mopper and Stahovec, 1986) which showed production of acetaldehyde dependent on the CDOM concentration and elevated light intensity. They suggested that photochemical degradation of CDOM directly produce acetaldehyde. However, it might be also possible that the degradation products of CDOM can directly chemically degrade acetaldehyde or that CDOM might act as photosensitizer. The dark samples showed no significant correlation with CDOM. Parameters which might influence the production rates in the chemistry samples could also not be identified.

5.2.4 Incubation experiments of acetaldehyde in the Equatorial East Atlantic Ocean

The initial ^{12}C-acetaldehyde concentration of all incubation experiments in the Atlantic Ocean ranged between 2.1 and 52 $\mathrm{nmol\,L^{-1}}$ taken from 10 m depth. The concentrations of acetaldehyde in the Kiel Fjord were higher compared to the Atlantic Ocean. The consumption rates measured in the East Atlantic Ocean ranged between 2.25 and 20.57 $\mathrm{nmol\,L^{-1}\,hr^{-1}}$ in the biology treatments for both light and dark treatments with an average of 7.28 $\mathrm{nmol\,L^{-1}\,hr^{-1}}$ (Figure 5.14). In the chemistry treatments consumption

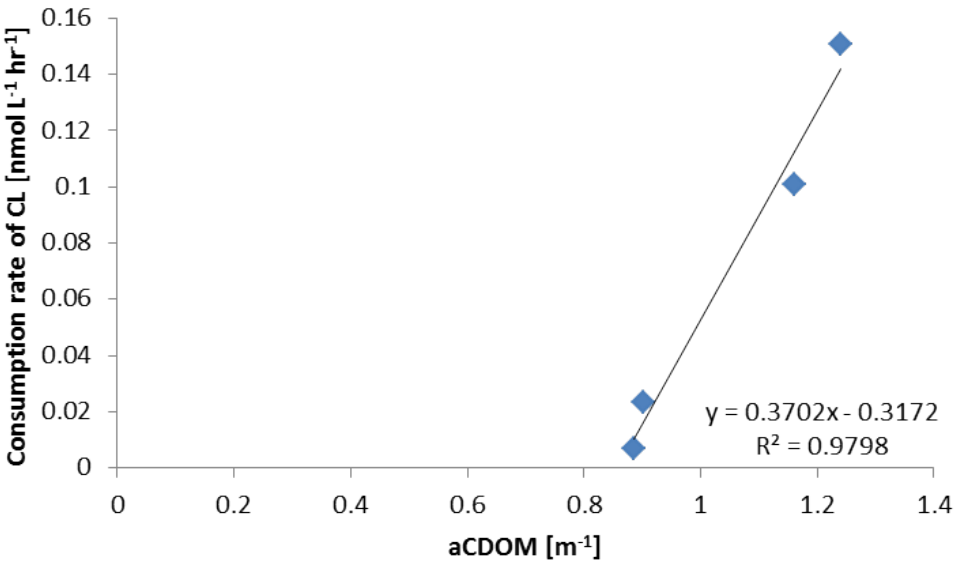

Fig. 5.13: *Linear regression between the consumption rates of CL treatments against the initial CDOM fluorescence of all experiments conducted in the Kiel Fjord.*

rates were observed between 0.5 and 131.74 $\mathrm{nmol\,L^{-1}\,hr^{-1}}$ (Table 5.4) with an average of 22.7 $\mathrm{nmol\,L^{-1}\,hr^{-1}}$ for both light and dark treatments. In the experiment on 26^{th} June the highest consumption rates were measured in the chemistry samples compared to all other experiments. No significant differences for the consumption rates were observed between the light and dark treatments of the biology samples. The chemistry samples showed on average higher consumption rates in the light treatments compared to the dark treatments (Table 5.4). The production rates ranged between -2.53 and 0.78 $\mathrm{nmol\,L^{-1}\,hr^{-1}}$ (average: -0.09 $\mathrm{nmol\,L^{-1}\,hr^{-1}}$) in the biology treatments and between -2.15 and 0.3 $\mathrm{nmol\,L^{-1}\,hr^{-1}}$ (average: -0.21 $\mathrm{nmol\,L^{-1}\,hr^{-1}}$) in the chemistry treatments (Table 5.4, Figure 5.14). In the chemistry samples and in the BL treatments degradation took place rather than production. Most production was observed on average in the biology dark treatments. However, the highest production rate of all experiments was measured in the BL treatment of the 24^{th} June 2011; the highest consumption rate in the CL treatment of the 26^{th} June.

5.2.5 Environmental parameters effecting acetaldehyde in the Atlantic Ocean

No environmental parameters (like CDOM, SST, SSS, nutrients, oxygen, solar radiation) could be identified which influenced the consumption or production rates of acetaldehyde in the biology treatments in the east Atlantic Ocean. However, the experiments conducted in Kiel showed that phytoplankton might influence the concentration of acetaldehyde and,

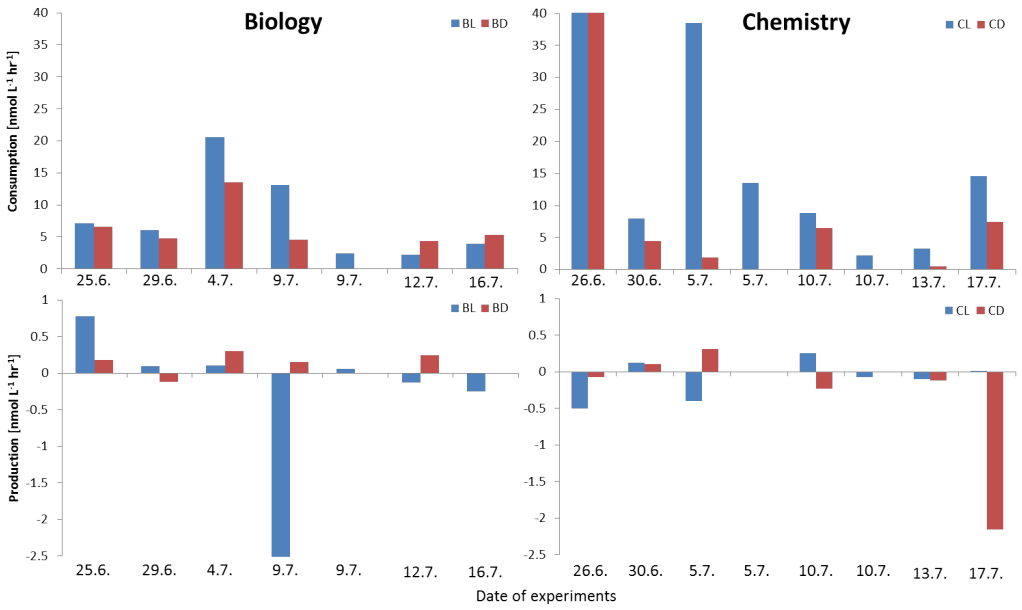

Fig. 5.14: *Consumption and production rates of acetaldehyde from the four different treatments determined in the east Atlantic Ocean. Negative values in the lower panels refer to consumption. All experiments were run for 24 hours. Note that for the light treatments sometimes two rates were measured in one experimental run. If an experiment started in the afternoon the rate from the afternoon to sunset and the second rate from sunrise to the end of the experiment are presented while the rates during the nights are excluded and are not shown. Consumption rates determined on the* 26^{th} *June 2011 had high values which are beyond the scale of the y-axis; CL: 131.74* $\mathrm{nmol\,L^{-1}\,hr^{-1}}$*; CD: 75.67* $\mathrm{nmol\,L^{-1}\,hr^{-1}}$*.*

thus, might also affect it in the Atlantic Ocean. This will be proven when maker pigments are available for these incubation experiments. Additionally, bacteria might be also potential consumers or producers of acetaldehyde and have to be considered for these experiments. Flow cytometry and DNA data will be consulted in future work for proving this suggestion.

For the chemistry treatments two environmental factors (oxygen and salinity) were found which might influence acetaldehyde pathways. The destruction rates in the CL treatments correlated significantly with the initial oxygen concentrations (R^2 = 0.9, p-value 0.1, n = 4, Figure 5.15, left panel). It might be possible that the light induced production of radical oxygen species (ROS) were responsible for the chemical degradation of acetaldehyde. No parameters could be found which might affected the consumption rates in the CD treatments. An anti-correlation between salinity and the production/destruction rate (determined with the ^{12}C-acetaldehyde) in the CD treatment was observed (R^2 = 0.99, p-value 0.01, n = 4, Figure 5.15, right panel). Increasing salinity turned the production rate of acetaldehyde into a consumption rate. It is most likely, that the salinity was only an indirect indicator for the rates of acetaldehyde pathways. Salinity might rather refer to water masses which contained possible precursors or reacting agent of acetaldehyde. Interestingly, the correlation was only observed in the dark treatments. It is possible that processes which influenced the production and consumption/degradation rates in the light and in the biology treatments were stronger and, thus, compensated or counteracted the rates which were observed in the CD treatments. No correlations were found when all environmental parameters were correlated against each rate of acetaldehyde of both locations the Baltic Sea and the Atlantic Ocean.

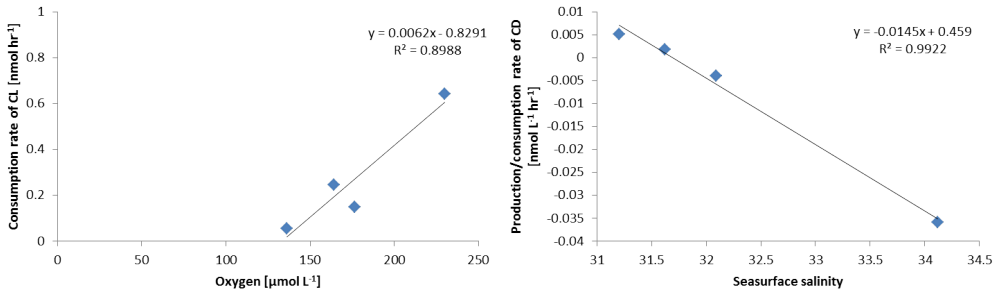

Fig. 5.15: *Linear regression of the consumption rates of all CL treatments conducted in the Atlantic Ocean against the initial value of seasurface salinity and oxygen.*

5.2.6 Comparison of acetaldehyde consumption and production rates in the two sampling sites

The consumption and production rates in the Baltic Sea were in the same range compared to the Atlantic Ocean when the extreme high rates were excluded. Both regions showed no difference in the consumption in the BL compared to the BD treatments when the high rates were excluded. Thus, the light seemed to have a small effect on the consumption in the biology treatments. It might be possible that bacterial processes, which are independent of light, were responsible for the consumption rather than phytoplankton which might suffer in the dark treatments. However, the first experiment in the Kiel Fjord gave a hint that diatoms might be also potential consumers of acetaldehyde and that the uptake is stronger under light conditions. Mopper and Stahovec (1986) could also show that the biota was the main sink for acetaldehyde in the ocean. However, in comparison to the chemistry consumption rates the biology treatments were not significantly higher in both sampling regions. It is most likely that in the chemistry treatments the bacterial activities were not eliminated which might be responsible for the high consumption rates in the chemistry treatments. In both experimental sets the production rates in all treatments were relatively low or did not even occur compared to the consumption rates. This was in contrast to the findings of deBruyn *et al.* (2011) and Mopper and Stahovec (1986). They observed production of acetaldehyde due to the photochemical degradation of CDOM. Even in the light intensive tropical region only small production rates were measured independent of treatment.

5.2.7 Incubation experiments of acetone in the Kiel Fjord

The initial ^{12}C-acetone concentrations measured during the incubation experiments ranged between 28.7 (9^{th} March 2011) and 76 $\mathrm{nmol\,L^{-1}}$ (5^{th} April 2011) in the Kiel Fjord. The consumption rates in the biology treatments (both light and dark) ranged between 0.6 and 5.53 $\mathrm{nmol\,L^{-1}\,hr^{-1}}$ (average 3.3 $\mathrm{nmol\,L^{-1}}$) and for the chemistry treatments (light and dark) between 0.19 and 6.11 $\mathrm{nmol\,L^{-1}\,hr^{-1}}$ (average 2.66 $\mathrm{nmol\,L^{-1}\,hr^{-1}}$, Figure 5.16). No consumption could be observed for the last experiment on the 20^{th} and 21^{st} April 2011. The variability of the measurements was higher than the change in the ^{13}C-acetone. Therefore, no production rates could be determined as well for this experiment. Similar consumption rates were determined on average in the biology (BD, BL) and in the CD treatments (around 3.3 $\mathrm{nmol\,L^{-1}\,hr^{-1}}$). In the CL treatments the consumption was lower (2.18 $\mathrm{nmol\,L^{-1}\,hr^{-1}}$). When the experiments were directly compared, two of the three experiments showed higher consumption rates in the dark treatments compared to the light samples for both biology and chemistry. Only in one out of six samples a production rate could be observed in both biology and chemistry treatments. The production rates in the biology samples ranged between -1.91 and 1.94 $\mathrm{nmol\,L^{-1}\,hr^{-1}}$ (average -

0.6 $\mathrm{nmol\,L^{-1}\,hr^{-1}}$) and in the chemistry treatments between -1.62 and 0.29 $\mathrm{nmol\,L^{-1}\,hr^{-1}}$ (average -0.88 $\mathrm{nmol\,L^{-1}\,hr^{-1}}$, Figure 5.16). Higher degradation rates were observed in the chemistry incubations compared to the biology samples. In the BD and in CL treatments only consumption/degradation was measured. Acetone was consumed rather than produced during the Kiel experiments, especially in the dark treatments.

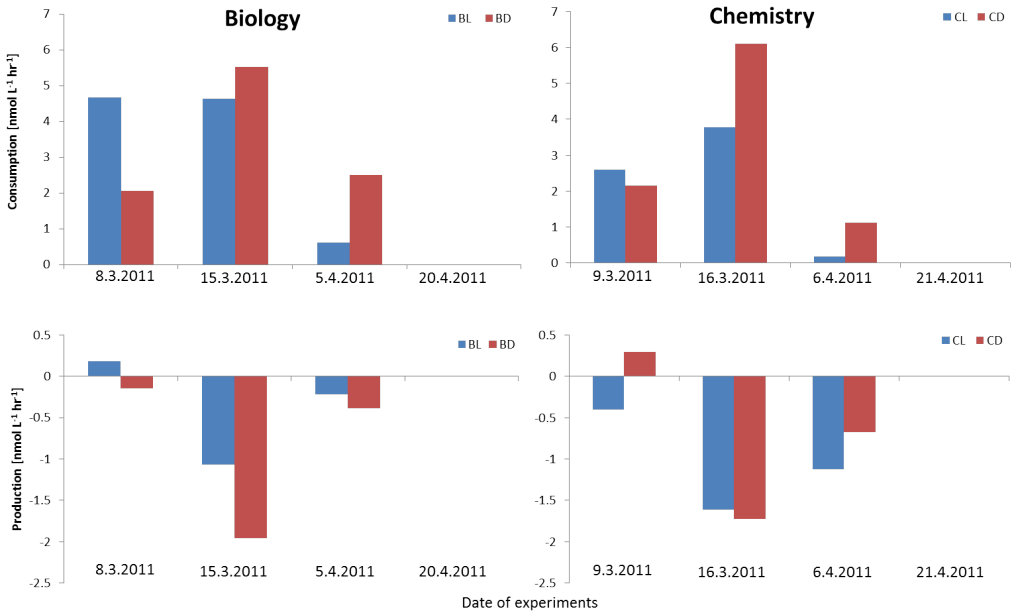

Fig. 5.16: *Consumption and production rates of acetone measured in the Kiel Fjord. All experiments were running from sunrise to sunset. Negative production rates refer to consumption. Note that dark and light treatments are always presented in the same panel.*

5.2.8 Environmental parameters effecting acetone in the Kiel Fjord

Neither the consumption rates nor the production rates of acetone in the biology treatments could be explained by any collected environmental parameter. The degradation rates in the CL treatments correlated significantly with the initial concentrations of the nutrients silicate and the sum of nitrate and nitrite ($\mathrm{R^2}$ = 0.99, p-value 0.05, n=3; $\mathrm{R^2}$ = 0.99, p-value 0.05, n=3, Figure 5.17, left panel). It might be possible that the consumption observed in the CL treatments was governed by small bacteria which lived on both the nutrients and acetone. It might be possible that only nutrients were taken up by phytoplankton but not acetone in the biology treatments which might explain the missing correlation between nutrients and acetone in the biology treatments. Additionally, the destruction rates in the CL treatments calculated from the ^{12}C-acetone correlated significantly with oxygen ($\mathrm{R^2}$ = 0.998, p-value 0.01, n=3, Figure 5.17, right panel). This was

also observed for acetaldehyde but in the Atlantic Ocean. It might be also possible for acetone that ROS produced from oxygen and solar radiation reacted with acetone. In all other treatments no environmental parameters seemed to influence the rates.

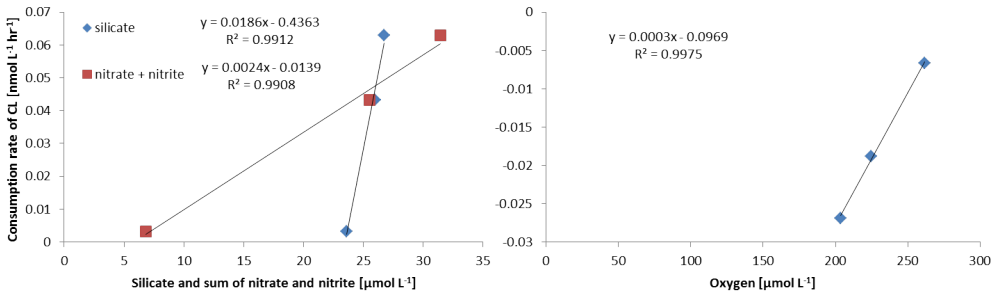

Fig. 5.17: *Linear regression of consumption rates of CL treatments of all experiments conducted in the Kiel Fjord against nutrients (silicate and nitrogen, left panel) and oxygen (right panel). Note that the consumption rates of the right panel were calculated from the ^{12}C-acetone. The ^{12}C-actone decreased in the experiments indicated by the negative values.*

5.2.9 Incubation experiments of acetone in the Equatorial East Atlantic Ocean

The initial ^{12}C-acetone concentrations ranged between 6.6 and 178.5 $\mathrm{nmol\,L^{-1}\,hr^{-1}}$ in the seawater samples taken from 10 m depth which were used for the incubation experiments in the east Atlantic Ocean. The concentrations measured in the Kiel Fjord fit in the range of the Atlantic Ocean. The consumption rate of the biology treatments (both dark and light) ranged between 0.43 and 7.76 $\mathrm{nmol\,L^{-1}\,hr^{-1}}$ (average 4.3 $\mathrm{nmol\,L^{-1}\,hr^{-1}}$) and for the chemistry treatments (both dark and light) between 0.41 and 135.59 $\mathrm{nmol\,L^{-1}\,hr^{-1}}$ (average 15.2 $\mathrm{nmol\,L^{-1}\,hr^{-1}}$, Figure 5.18). The biology and chemistry treatments showed on average similar consumption rates between 4 and 6 $\mathrm{nmol\,L^{-1}\,hr^{-1}}$ when the high degradation rate of the 26^{th} June was excluded. However, the variability of the rates between the different experimental days was high in the chemistry samples. Even in the CL treatment of the 26^{th} June two different degradation rates were measured; one before sunset and one the following day. However, the first degradation rate of this experiment was based on two subsamples and the second smaller rate was determined from four subsamples. It might be that the first rate was an outlier. Nonetheless, the CD treatment which contained the same water showed also the highest degradation rate of all experiments. Thus, the high degradation rate in the CL treatment might be possible. In contrast to the variability of the chemistry samples, the biology treatments exhibited similar consumption rates especially in the light samples. The light incubations exhibited higher consumption/degradation rates on average compared to the dark treatments for both biology

and chemistry samples. The production rates in the biology treatments ranged between -3.72 and 1.94 $\mathrm{nmol\,L^{-1}\,hr^{-1}}$ (for both light and dark, average -0.53 $\mathrm{nmol\,L^{-1}\,hr^{-1}}$) and for the chemistry samples between -21.48 and 2.12 $\mathrm{nmol\,L^{-1}\,hr^{-1}}$ (for both light and dark, average 1.26 $\mathrm{nmol\,L^{-1}\,hr^{-1}}$, Figure 5.18, Table 5.4). Except for the CD treatment all samples showed consumption rather than production on average. Although the degradation rate in the CD treatment of the 26^{th} was high, a small production rate could be measured. However, the CL treatment of this day also indicates only consumption in the ^{12}C-acetone. The loss rates of ^{12}C-acetone were generally higher in the light treatments than in the dark treatments for both biology and chemistry treatments.

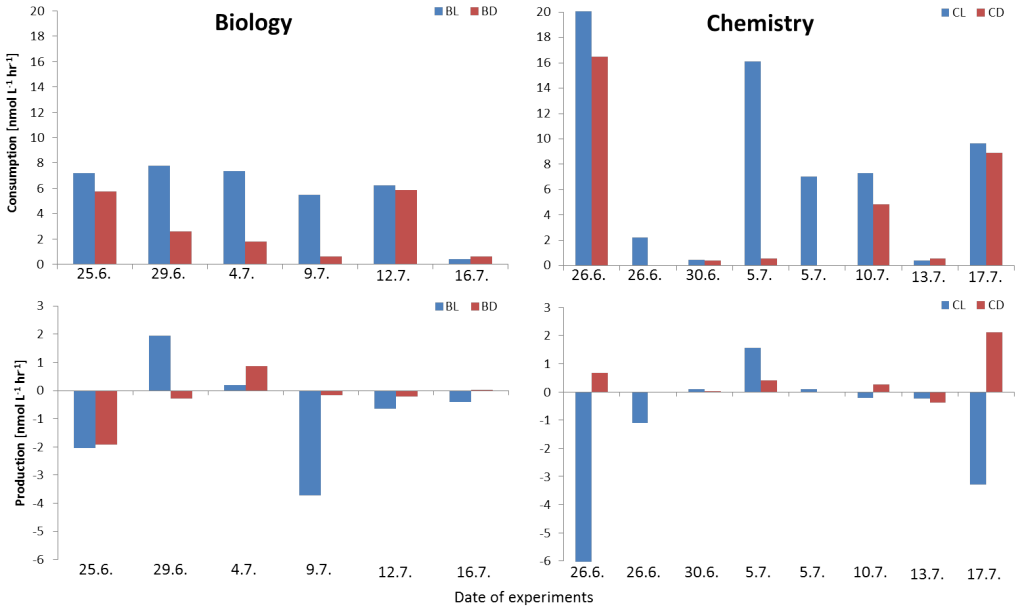

Fig. 5.18: *Consumption and production rates of acetone measured in the East Atlantic Ocean. Negative production rates indicate consumption only. Note that for the light treatments sometimes two rates were measured in one experimental run in the manner of acetaldehyde. All experiments were run for 24 hours. The degradation rate for CL of the* 26^{th} *June 2011 was 135.59* $\mathrm{nmol\,L^{-1}\,hr^{-1}}$ *which is beyond the scale of the y-axis (upper, right panel). The negative production rate of the CL treatment of the 26th June was -21.48* $\mathrm{nmol\,L^{-1}\,hr^{-1}}$ *(lower, right panel).*

5.2.10 Environmental parameters affecting acetone in the Equatorial East Atlantic Ocean

None of the collected environmental parameters could explain the variability of the consumption and production rates in the biology treatments. However, the influence of biological activities on the rates cannot be excluded and have to be tested. A significant

correlation between the production rates (including consumption rates determined from ^{12}C-acetone) of the CL treatments and the sea surface salinity was found (R^2 = 0.97, p-value 0.01, n = 4, Figure 5.19). This was similar to the observations of acetaldehyde in the Atlantic Ocean. Also for acetone salinity might be only an indirect indicator. It seemed to refer to water masses which might contain precursors or reacting agents of acetone. These reactions were possibly light dependent in contrast to the findings of acetaldehyde. None of the other collected additional parameters showed an influence on the rates. All measured environmental parameters were also correlated against each rate of acetone of both locations the Baltic Sea and the east Atlantic Ocean. However, no correlations could be found.

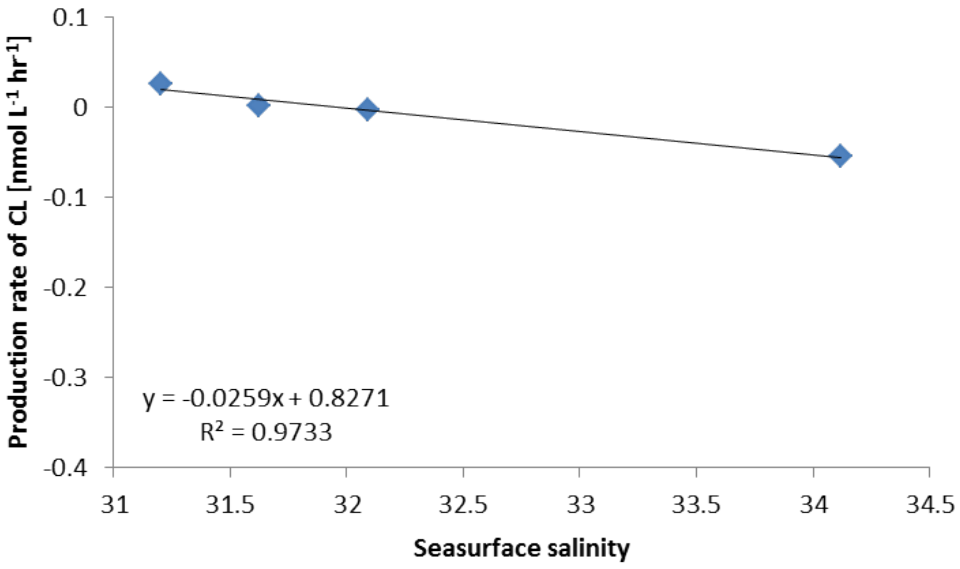

Fig. 5.19: *Linear regression of the production rate of CL treatments of all experiments conducted in the Atlantic Ocean against the seasurface salinity. Note that the negative production rates referred to consumption rates.*

5.2.11 Comparison of acetone consumption and production rates in the two sampling sites

The consumption rates measured in the Atlantic Ocean were in general slightly higher compared to rates determined in the Kiel Fjord. A higher variability in the production rates was observed in the Atlantic Ocean. However, the rates were on average similar in both regions. Additionally, no significant differences in the consumption rates were observed in the light and dark samples of both regions. Furthermore, production was only observed in a few experiments in the Baltic Sea and in the Atlantic. In the Baltic

Tab. 5.4: *The ranges and average values of all measured consumption and production rates of the four different treatments of acetaldehyde and acetone are listed. All experiments conducted in the Kiel Fjord and in the Atlantic Ocean are included, respectively. Note that negative production rates refer to consumption.*

Compound Sampling site	Treatment	Consumption in light $[\mathrm{nmolL^{-1}hr^{-1}}]$ range average rate constant k $[\mathrm{hr^{-1}}]$ rate average	Consumption in dark $[\mathrm{nmolL^{-1}hr^{-1}}]$ range average rate constant k $[\mathrm{hr^{-1}}]$ rate average	Production in light $[\mathrm{nmolL^{-1}hr^{-1}}]$ range average	Production in dark $[\mathrm{nmolL^{-1}hr^{-1}}]$ range average
Acetaldehyde	Biology	0.03 - 6.7 1.74 0.0002 - 0.04 0.015	0.05 - 2.72 0.73 0.006 - 0.05 0.03	-0.02 - 0.008 -0.002	-0.0004 - 0.008 0.004
Kiel Fjord	Chemistry	0.007 - 0.151 0.07 0.005 - 0.01 0.008	0.0004 - 0.32 0.11 0.005 - 0.02 0.01	-0.14 - 0.012 -0.03	-0.002 - 0.03 0.01
Acetaldehyde	Biology	0.04 - 0.34 0.13 0.06 - 0.2 0.2	0.08 - 0.23 0.11 0.06 - 0.38 0.2	-0.04 - 0.01 -0.004	-0.002 - 0.005 0.002
East Atlantic Ocean	Chemistry	0.04 - 2.2 0.21 0.04 - 0.45 0.2	0.008 - 1.26 0.07 0.004 - 0.35 0.1	-0.008 - 0.004 -0.0005	-0.04 - 0.005 -0.007
Acetone	Biology	0.01 - 0.08 0.01 0.007 - 0.01 0.009	0.03 - 0.09 0.02 0.009 - 0.02 0.01	-0.02 - 0.003 -0.006	-0.03 - - 0.002 -0.01
Kiel Fjord	Chemistry	0.003 - 0.06 0.03 0.006 - 0.02 0.01	0.02 - 0.04 0.02 0.0097 - 0.014 0.01	-0.03 - -0.007 -0.02	-0.03 - 0.005 -0.01
Acetone	Biology	0.007 - 0.13 0.1 0.06 - 0.1 0.08	0.01 - 0.1 0.05 0.008 - 0.09 0.03	-0.06 - 0.03 -0.01	-0.005 - 0.02 -0.005
East Atlantic Ocean	Chemistry	0.007 - 2.26 0.11 0.001 - 0.06 0.03	0.007 - 0.27 0.05 0.0008 - 0.06 0.02	-0.36 - 0.03 -0.005	-0.006 - 0.04 0.008

Sea, higher consumption rates were observed in the dark treatments compared to the light treatments for both biology and chemistry. This was in contrast to the Atlantic Ocean, where light treatments showed higher consumption rates. It might be possible that the enhanced solar radiation dose in the tropics had a stronger effect on the acetone concentration compared to the Baltic Sea. However, both biology and chemistry treatments seemed to be influenced in the same way. This might refer again to a potential bacteria activity which occurred in both treatments and which were light dependent. Indeed, de Bruyn *et al.* (2013) showed that the primary loss rate of acetone was the consumption due to bacteria. However, they observed a difference in filtered and unfiltered samples. This is in contrast to our results. It might be possible that bacteria smaller than 0.2 µm did not consume acetone in their samples while in the samples of this study they did. However, this is highly speculative and has to be proven by analyzing flow cytometry and DNA samples. For the biology treatments, no parameter could be identified which might influence the rates in both regions.

The experiments (for an overview see Table 5.4) showed that both acetaldehyde and acetone were consumed rather than produced in both the Baltic Sea and in the eastern Atlantic Ocean. These results suggest that the two sampling sites were a potential sink for acetaldehyde and acetone. However, this can possibly change with environmental parameters and with the season. Hints were found which might suggest that bacteria and phytoplankton could possibly consume especially acetaldehyde. However, the influence of the biota on the OVOC concentration has to be studied in more detail in the future. The hypothesis that the main source of OVOCs is the production due to the photochemical destruction of CDOM could not be proven. Although, elevated solar radiation and CDOM occurred in the samples no significant differences could be observed between the dark and the light samples. However, it might be possible that the concentration of CDOM was too low to show detectable production rates of OVOCs. It could be also possible that the consumption was superimposed on the production rates.

References

Alvarez, L. A., Exton, D. A., Timmis, K. N., Suggett, D. J., and McGenity, T. J.: Characterization of marine isoprene-degrading communities, Environmental Microbiology, 11, 3280-3291, 10.1111/j.1462-2920.2009.02069.x, 2009.

Archer, S. D., Widdicombe, C. E., Tarran, G. A., Rees, A. P., and Burkill, P. H.: Production and turnover of particulate dimethylsulphoniopropionate during a coccolithophore bloom in the northern north sea, Aquatic Microbial Ecology, 24, 225-241, 10.3354/ame024225, 2001.

Arnold, S. R., Chipperfield, M. P., Blitz, M. A., Heard, D. E., and Pilling, M. J.: Photodissociation of acetone: Atmospheric implications of temperature-dependent quantum

yields, Geophysical Research Letters, 31, 10.1029/2003gl019099, 2004.
Arnold, S. R., Spracklen, D. V., Williams, J., Yassaa, N., Sciare, J., Bonsang, B., Gros, V., Peeken, I., Lewis, A. C., Alvain, S., and Moulin, C.: Evaluation of the global oceanic isoprene source and its impacts on marine organic carbon aerosol, Atmospheric Chemistry and Physics, 9, 1253-1262, 2009.
Ayers, G. P., Gillett, R. W., Granek, H., deServes, C., and Cox, R. A.: Formaldehyde production in clean marine air, Geophysical Research Letters, 24, 401-404, 10.1029/97gl00123, 1997.
Baker, A. R., Turner, S. M., Broadgate, W. J., Thompson, A., McFiggans, G. B., Vesperini, O., Nightingale, P. D., Liss, P. S., and Jickells, T. D.: Distribution and sea-air fluxes of biogenic trace gases in the eastern atlantic ocean, Global Biogeochem. Cycles, 14, 871-886, 10.1029/1999gb001219, 2000.
Beale, R., Liss, P. S., and Nightingale, P. D.: First oceanic measurements of ethanol and propanol, Geophysical Research Letters, 37, 10.1029/2010gl045534, 2010.
deBruyn, W. J., Clark, C. D., Pagel, L., and Singh, H.: Loss rates of acetone in filtered and unfiltered coastal seawater, Marine Chemistry, http://dx.doi.org/10.1016/ j.marchem.2013.01.003, 2013.
Blando, J. D., and Turpin, B. J.: Secondary organic aerosol formation in cloud and fog droplets: A literature evaluation of plausibility, Atmospheric Environment, 34, 1623-1632, 10.1016/s1352-2310(99)00392-1, 2000.
Bonsang, B., Polle, C., and Lambert, G.: Evidence for marine production of isoprene, Geophys. Res. Lett., 19, 1129-1132, 10.1029/92gl00083, 1992.
Bonsang, B., Gros, V., Peeken, I., Yassaa, N., Bluhm, K., Zoellner, E., Sarda-Esteve, R., and Williams, J.: Isoprene emission from phytoplankton monocultures: The relationship with chlorophyll-a, cell volume and carbon content, Environmental Chemistry, 7, 554-563, 2010.
Brimblecombe, P., and Shooter, D.: Photo-oxidation of dimethylsulphide in aqueous solution, Marine Chemistry, 19, 343-353, 10.1016/0304-4203(86)90055-1, 1986.
Broadgate, W. J., Liss, P. S., and Penkett, S. A.: Seasonal emissions of isoprene and other reactive hydrocarbon gases from the ocean, Geophys. Res. Lett., 24, 2675-2678, 10.1029/97gl02736, 1997.
Charlson, R. J., Lovelock, J. E., Andreae, M. O., and Warren, S. G.: Oceanic phytoplankton, atmospheric sulphur, cloud albedo and climate, Nature, 326, 655-661, 1987.
Claeys, M., Graham, B., Vas, G., Wang, W., Vermeylen, R., Pashynska, V., Cafmeyer, J., Guyon, P., Andreae, M. O., and Artaxo, P.: Formation of secondary organic aerosols through photooxidation of isoprene, Science, 303, 1173-1176, 2004.
de Bruyn, W. J., Clark, C. D., Pagel, L., and Takehara, C.: Photochemical production of formaldehyde, acetaldehyde and acetone from chromophoric dissolved organic matter in coastal waters, Journal of Photochemistry and Photobiology a-Chemistry, 226, 16-22, 10.1016/ j.jphotochem.2011.10.002, 2011.

de Bruyn, W. J., Clark, C. D., Pagel, L., and Singh, H.: Loss rates of acetone in filtered and unfiltered coastal seawater, Marine Chemistry, http://dx.doi.org/10.1016/ j.marchem.2013.01.003, 2013.
Dixon, J. L., Beale, R., and Nightingale, P. D.: Microbial methanol uptake in northeast atlantic waters, Isme Journal, 5, 704-716, 10.1038/ismej.2010.169, 2011a.
Dixon, J. L., Beale, R., and Nightingale, P. D.: Rapid biological oxidation of methanol in the tropical atlantic: Significance as a microbial carbon source, Biogeosciences, 8, 2707-2716, 10.5194/bg-8-2707-2011, 2011b.
Ehrhardt, M., and Weber, R. R.: Formation of low-molecular-weight carbonyl-compounds by sensitized photochemical decomposition of aliphatic-hydrocarbons in seawater, Fresenius Journal of Analytical Chemistry, 339, 772-776, 10.1007/bf00321742, 1991.
Gantt, B., Meskhidze, N., and Kamykowski, D.: A new physically-based quantification of marine isoprene and primary organic aerosol emissions, Atmospheric Chemistry & Physics, 9, 4915-4927, 2009.
Graedel, T. E., and Crutzen, P. J.: Chemie der atmosphäre, Spektrum Akad. Verlag, Heidelberg, 1994.
Hansen, H. P.: Determination of oxygen, in: Methods of seawater analysis, edited by: Grasshoff, K., Kremling, K., and Ehrhardt, M., Wiley-VCH Verlag GmbH, 75-90, 2007.
Hansen, H. P., and Koroleff, F.: Determination of nutrients, in: Methods of seawater analysis, edited by: Grasshoff, K., Kremling, K., and Ehrhardt, M., Wiley-VCH Verlag GmbH, 159-228, 2007.
Hatton, A. D., Turner, S. M., Malin, G., and Liss, P. S.: Dimethylsulphoxide and other biogenic sulphur compounds in the galapagos plume, Deep Sea Research Part II: Topical Studies in Oceanography, 45, 1043-1053, 10.1016/s0967-0645(98)00017-4, 1998.
Hatton, A. D., Malin, G., and Liss, P. S.: Distribution of biogenic sulphur compounds during and just after the southwest monsoon in the arabian sea, Deep Sea Research Part II: Topical Studies in Oceanography, 46, 617-632, 10.1016/s0967-0645(98)00120-9, 1999.
Hatton, A. D., Darroch, L., and Malin, G.: The role of dimethylsulphoxide in the marine biogeochemical cycle of dimethylsulphide, in: Oceanography and marine biology: An annual review, vol 42, edited by: Gibson, R. N., Atkinson, R. J. A., and Gordon, J. D. M., Oceanography and marine biology, Crc Press-Taylor & Francis Group, Boca Raton, 29-55, 2005.
Heikes, B. G., Chang, W. N., Pilson, M. E. Q., Swift, E., Singh, H. B., Guenther, A., Jacob, D. J., Field, B. D., Fall, R., Riemer, D., and Brand, L.: Atmospheric methanol budget and ocean implication, Global Biogeochemical Cycles, 16, 10.1029/2002gb001895, 2002.
Heller, M. I., and Croot, P. L.: Kinetics of superoxide reactions with dissolved organic matter in tropical atlantic surface waters near cape verde (tenatso), J. Geophys. Res., 115, C12038, 10.1029/2009jc006021, 2010.
IPCC: Climate change 2007: The physical science basis. Contribution of working group

i to the fourth assessment report of the intergovernmental panel on climate change, edited by: S. Solomon, D. Q., M. Manning, Z. Chen, M. Marquis, K. B. Averyt, M. Tignor and H. L. Miller, Cambridge University Press, Cambridge, UK and New York, NY, USA., 996 pp., 2007.
Jacob, D. J., Field, B. D., Jin, E. M., Bey, I., Li, Q. B., Logan, J. A., Yantosca, R. M., and Singh, H. B.: Atmospheric budget of acetone, Journal of Geophysical Research-Atmospheres, 107, 10.1029/2001jd000694, 2002.
Jacob, D. J., Field, B. D., Li, Q. B., Blake, D. R., de Gouw, J., Warneke, C., Hansel, A., Wisthaler, A., Singh, H. B., and Guenther, A.: Global budget of methanol: Constraints from atmospheric observations, Journal of Geophysical Research-Atmospheres, 110, 10.1029/2004jd005172, 2005.
Kettle, A. J., and Andreae, M. O.: Flux of dimethylsulfide from the oceans: A comparison of updated data seas and flux models, J. Geophys. Res.-Atmos., 105, 26793-26808, 10.1029/2000jd900252, 2000.
Kiene, R. P., Linn, L. J., and Bruton, J. A.: New and important roles for dmsp in marine microbial communities, Journal of Sea Research, 43, 209-224, 10.1016/ s1385-1101(00)00023-x, 2000.
Kuzma, J., Nemecekmarshall, M., Pollock, W. H., and Fall, R.: Bacteria produce the volatile hydrocarbon isoprene, Current Microbiology, 30, 97-103, 10.1007/bf00294190, 1995.
Lary, D. J., and Shallcross, D. E.: Central role of carbonyl compounds in atmospheric chemistry, Journal of Geophysical Research-Atmospheres, 105, 19771-19778, 10.1029/1999jd901184, 2000.
Lee, P. A., de Mora, S. J., and Levasseur, M.: A review of dimethylsulfoxide in aquatic environments, Atmosphere-Ocean, 37, 439-456, 10.1080/07055900.1999.9649635, 1999.
Lewis, A. C., Hopkins, J. R., Carpenter, L. J., Stanton, J., Read, K. A., and Pilling, M. J.: Sources and sinks of acetone, methanol, and acetaldehyde in north atlantic marine air, Atmos. Chem. Phys., 5, 1963-1974, 10.5194/acp-5-1963-2005, 2005.
Liss, P., Marandino, C., Dahl, E., Helmig, D., Hintsa, E., Hughes, C., Johnson, M., Moore, B., Plane, J., Quack, B., Singh, H., Stefels, J., von Glasow, R., and Williams, J.: Ocean-atmosphere interactions of gases and particles, Short-lived trace gases in the surface ocean and atmosphere, Springer, Heidelberg, 2013.
Luo, G., and Yu, F.: A numerical evaluation of global oceanic emissions of alpha-pinene and isoprene, Atmospheric Chemistry and Physics, 10, 2007-2015, 2010.
Madigan, M. T., Martinko, J. M., and Parker, J.: Brock mikrobiologie, Spektrum Akademischer Verlag, Heidelberg Berlin, 1175 pp., 2001.
Marandino, C. A., De Bruyn, W. J., Miller, S. D., Prather, M. J., and Saltzman, E. S.: Oceanic uptake and the global atmospheric acetone budget, Geophysical Research Letters, 32, 10.1029/2005gl023285, 2005.
Matsunaga, S., Mochida, M., Saito, T., and Kawamura, K.: In situ measurement of iso-

prene in the marine air and surface seawater from the western north pacific, Atmospheric Environment, 36, 6051-6057, 10.1016/s1352-2310(02)00657-x, 2002.
Meskhidze, N., and Nenes, A.: Phytoplankton and cloudiness in the southern ocean, Science, 314, 1419-1423, 10.1126/science.1131779, 2006.
Millet, D. B., Guenther, A., Siegel, D. A., Nelson, N. B., Singh, H. B., de Gouw, J. A., Warneke, C., Williams, J., Eerdekens, G., Sinha, V., Karl, T., Flocke, F., Apel, E., Riemer, D. D., Palmer, P. I., and Barkley, M.: Global atmospheric budget of acetaldehyde: 3-d model analysis and constraints from in-situ and satellite observations, Atmospheric Chemistry and Physics, 10, 3405-3425, 10.5194/acp-10-3405-2010, 2010.
Milne, P. J., Riemer, D. D., Zika, R. G., and Brand, L. E.: Measurement of vertical distribution of isoprene in surface seawater, its chemical fate, and its emission from several phytoplankton monocultures, Marine Chemistry, 48, 237-244, 10.1016/ 0304-4203(94)00059-m, 1995.
Monks, P. S.: Gas-phase radical chemistry in the troposphere, Chemical Society Reviews, 34, 376-395, 10.1039/b307982c, 2005.
Moore, R. M., and Wang, L.: The influence of iron fertilization on the fluxes of methyl halides and isoprene from ocean to atmosphere in the series experiment, Deep Sea Research Part II: Topical Studies in Oceanography, 53, 2398-2409, 10.1016/ j.dsr2.2006.05.025, 2006.
Mopper, K., and Stahovec, W. L.: Sources and sinks of low-molecular-weight organic carbonyl-compounds in seawater, Marine Chemistry, 19, 305-321, 10.1016/ 0304-4203 (86)90052-6, 1986.
Muller, J. F., and Brasseur, G.: Sources of upper tropospheric hox: A three-dimensional study, Journal of Geophysical Research-Atmospheres, 104, 1705-1715, 10.1029/ 1998 jd100005, 1999.
Nádasdi, R., Zügner, G. L., Farkas, M., Dóbé, S., Maeda, S., and Morokuma, K.: Photochemistry of methyl ethyl ketone: Quantum yields and s1/s0-diradical mechanism of photodissociation, ChemPhysChem, 11, 3883-3895, 10.1002/cphc.201000522, 2010.
Nemecek-Marshall, M., Wojciechowski, C., Kuzma, J., Silver, G. M., and Fall, R.: Marine vibrio species produce the volatile organic-compound acetone, Applied and Environmental Microbiology, 61, 44-47, 1995.
Nemecek-Marshall, M., Wojciechowski, C., Wagner, W. P., and Fall, R.: Acetone formation in the vibrio family: A new pathway for bacterial leucine catabolism, Journal of Bacteriology, 181, 7493-7499, 1999.
Obernosterer, I., Kraay, G., de Ranitz, E., and Herndl, G. J.: Concentrations of low molecular weight carboxylic acids and carbonyl compounds in the aegean sea (eastern mediterranean) and the turnover of pyruvate, Aquatic Microbial Ecology, 20, 147-156, 10.3354/ame020147, 1999.
Oudot, C., Morin, P.: The distribution of nutrients in the equatorial Atlantic: relation to physical processes and phytoplankton biomass. Oceanologica Acta, Proceedings Interna-

tional Symposium on Equatorial Vertical Motion, pp. 121-130, 1987.
Okumura, Y., and Xie, S.: Interaction of the Atlantic Equatorial Cold Tongue and the African Monsoon*. J. Climate, 17, 3589–3602. doi: http://dx.doi.org/10.1175/1520-0442(2004)017<3589:IOTAEC>2.0.CO;2, 2004.
Philander, S. G. H., and Pacanowski, R. C.: The oceanic response to cross-equatorial winds (with application to coastal upwelling in low latitudes), Tellus, 33, 201-210, 10.1111 /j.2153-3490.1981.tb01744.x, 1981.
Philander, S. G. H., Gu, D., Lambert, G., Li, T., Halpern, D., Lau, N. C., and Pacanowski, R. C.: Why the itcz is mostly north of the equator, Journal of Climate, 9, 2958-2972, 10.1175/1520-0442(1996)009<2958:wtiimn>2.0.co;2, 1996.
Picaut, J.: Propagation of the seasonal upwelling in the eastern equatorial atlantic, Journal of Physical Oceanography, 13, 18-37, 10.1175/1520-0485(1983)013<0018:potsui>2.0.co; 2, 1983.
Quinn, P. K., and Bates, T. S.: The case against climate regulation via oceanic phytoplankton sulphur emissions, Nature, 480, 51-56, 2011.
Ratte, M., Bujok, O., Spitzy, A., and Rudolph, J.: Photochemical alkene formation in sea water from dissolved organic carbon: Results from laboratory experiments, 1998.
Rinsland, C. P., Dufour, G., Boone, C. D., Bernath, P. F., Chiou, L., Coheur, P. F., Turquety, S., and Clerbaux, C.: Satellite boreal measurements over alaska and canada during june-july 2004: Simultaneous measurements of upper tropospheric co, c2h6, hcn, ch3cl, ch4, c2h2, ch3oh, hcooh, ocs, and sf6 mixing ratios, Global Biogeochemical Cycles, 21, 10.1029/2006gb002795, 2007.
Sharkey, T. D., Wiberley, A. E., and Donohue, A. R.: Isoprene emission from plants: Why and how, Annals of Botany, 101, 5-18, 2008.
Shaw, S. L., Chisholm, S. W., and Prinn, R. G.: Isoprene production by prochlorococcus, a marine cyanobacterium, and other phytoplankton, Marine Chemistry, 80, 227-245, 10.1016/s0304-4203(02)00101-9, 2003.
Shaw, S. L., Gantt, B., and Meskhidze, N.: Production and emissions of marine isoprene and monoterpenes: A review, Advances in Meteorology, 10.1155/2010/408696, 2010.
Simó, R.: Production of atmospheric sulfur by oceanic plankton: Biogeochemical, ecological and evolutionary links, Trends in Ecology & Evolution, 16, 287-294, 10.1016/ s0169-5347(01)02152-8, 2001.
Simó, R.: From cells to globe: Approaching the dynamics of dms(p) in the ocean at multiple scales, Canadian Journal of Fisheries and Aquatic Sciences, 61, 673-684, 10.1139/f04-030, 2004.
Singh, H. B., Ohara, D., Herlth, D., Sachse, W., Blake, D. R., Bradshaw, J. D., Kanakidou, M., and Crutzen, P. J.: Acetone in the atmosphere - distribution, sources, and sinks, Journal of Geophysical Research-Atmospheres, 99, 1805-1819, 10.1029/93jd00764, 1994.
Singh, H. B., Kanakidou, M., Crutzen, P. J., and Jacob, D. J.: High-concentrations and photochemical fate of oxygenated hydrocarbons in the global troposphere, Nature, 378,

50-54, 10.1038/378050a0, 1995.
Sinha, V., Williams, J., Meyerhofer, M., Riebesell, U., Paulino, A. I., and Larsen, A.: Air-sea fluxes of methanol, acetone, acetaldehyde, isoprene and dms from a norwegian fjord following a phytoplankton bloom in a mesocosm experiment, Atmospheric Chemistry and Physics, 7, 739-755, 2007.
Spivakovsky, C. M., Yevich, R., Logan, J. A., Wofsy, S. C., McElroy, M. B., and Prather, M. J.: Tropospheric oh in a three-dimensional chemical tracer model: An assessment based on observations of ch3ccl3, J. Geophys. Res., 95, 18441-18471, 10.1029 /JD095i D11p18441, 1990.
Stefels, J., Steinke, M., Turner, S., Malin, G., and Belviso, S.: Environmental constraints on the production and removal of the climatically active gas dimethylsulphide (dms) and implications for ecosystem modelling, Biogeochemistry, 83, 245-275, 10.1007/s10533-007-9091-5, 2007.
Sunda, W., Kieber, D. J., Kiene, R. P., and Huntsman, S.: An antioxidant function for dmsp and dms in marine algae, Nature, 418, 317-320, 10.1038/nature00851, 2002.
Toole, D. A., Kieber, D. J., Kiene, R. P., White, E. M., Bisgrove, J., del Valle, D. A., and Slezak, D.: High dimethylsulfide photolysis rates in nitrate-rich antarctic waters, Geophysical Research Letters, 31, 10.1029/2004gl019863, 2004.
Vogt, M., and Liss, P. S.: Dimethylsulfide and climate, Surface ocean - lower atmosphere processes, 187, Geophysical Monograph Series, AGU, Washingtion, DC, 2009.
Warneck, P.: Chemistry of the natural atmosphere, Academic Press, San Diego, 1988.
Wennberg, P. O., Hanisco, T. F., Jaeglé, L., Jacob, D. J., Hintsa, E. J., Lanzendorf, E. J., Anderson, J. G., Gao, R.-S., Keim, E. R., Donnelly, S. G., Negro, L. A. D., Fahey, D. W., McKeen, S. A., Salawitch, R. J., Webster, C. R., May, R. D., Herman, R. L., Proffitt, M. H., Margitan, J. J., Atlas, E. L., Schauffler, S. M., Flocke, F., McElroy, C. T., and Bui, T. P.: Hydrogen radicals, nitrogen radicals, and the production of o3 in the upper troposphere, Science, 279, 49-53, 10.1126/science.279.5347.49, 1998.
Williams, J., Holzinger, R., Gros, V., Xu, X., Atlas, E., and Wallace, D. W. R.: Measurements of organic species in air and seawater from the tropical atlantic, Geophysical Research Letters, 31, 10.1029/2004gl020012, 2004.
Williams, J., Custer, T., Riede, H., Sander, R., Jockel, P., Hoor, P., Pozzer, A., Wong-Zehnpfennig, S., Beygi, Z. H., Fischer, H., Gros, V., Colomb, A., Bonsang, B., Yassaa, N., Peeken, I., Atlas, E. L., Waluda, C. M., van Aardenne, J. A., and Lelieveld, J.: Assessing the effect of marine isoprene and ship emissions on ozone, using modelling and measurements from the south atlantic ocean, Environmental Chemistry, 7, 171-182, 10.1071/en09154, 2010.
Zhou, X. L., and Mopper, K.: Photochemical production of low-molecular-weight carbonyl compounds in seawater and surface microlayer and their air-sea exchange, Marine Chemistry, 56, 201-213, 10.1016/s0304-4203(96)00076-x, 1997.

6 Conclusion and Outlook

This thesis presents new results that help to increase knowledge about the environmental controls on the distribution of the different, short-lived, climate-relevant trace gases such as DMS, isoprene, acetaldehyde and acetone. Despite their low concentrations, the atmospheric importance of these gases ranges from controlling hydroxyl radical, the main cleanser of the atmosphere, to forming cloud condensation nuclei, influencing Earth's climate system. Accurately modeling and predicting the role of the ocean in the atmospheric budget of these compounds is key to understanding their effects, both for present day and under future global change scenarios.

The first comprehensive set of DMS, DMSP and DMSO data from the western Pacific Ocean is presented in this study. Different algae taxa, namely haptophytes, chrysophytes and dinoflagellates, were identified as potential producers of both DMSP and DMSO. The extremely low ratio of $\mathrm{DMSP_p}$ and $\mathrm{DMSO_p}$ may be typical for oligotrophic tropical open oceans. The relatively high $\mathrm{DMSO_p}$ concentration compared to $\mathrm{DMSP_p}$ indicated enhanced nutritional and oxidative stress for the phytoplankton leading to an accumulation of surface $\mathrm{DMSO_p}$. Furthermore, $\mathrm{DMSP_d}$ and $\mathrm{DMSO_{t/p}}$ might serve as substrates for methane production in the oxic surface layer. DMSO seems to be an important part of the marine organic sulphur cycle. However, it is less investigated compared to DMSP or DMS. Thus, its production and degradation pathways need to be studied under controlled laboratory conditions and in comparable field experiments. For instance, the role of DMSO as substrate for bacteria and the link to the production of other chemical compounds like methane has to be investigated. DMSO seems to be an indicator for stress in phytoplankton because it is found to be involved in the antioxidation cascade in algae cells (Sunda *et al.*, 2002). However, the environmental conditions that trigger elevated DMSO production are poorly understood and seem to be as complex as for DMSP. Pointed incubation experiments investigating this process are needed.

The flux of marine DMS into the atmosphere was used to model the amount of DMS that can be transported into the upper troposphere and lower stratosphere. The amount of DMS (and likely its oxidation products) which could theoretically contribute to the persistent stratospheric sulphur layer (PSL) was surprisingly large when scaled by the area of emissions. This intensive transport could be explained by the high convection in the tropical western Pacific Ocean and might increase with season of elevated tropical cyclone events or elevated DMS production in surface seawater. However, the amount of DMS

crossing the tropopause, and thus, the actual contribution of marine DMS and its oxidation products to the PSL could not be determined. Thus, measurements of DMS throughout the entire troposphere and lower stratosphere during the high convection season will help to prove directly if marine DMS could be a source of sulphur to the PSL.

The environmental controls on isoprene are even less understood than those for DMS and the relationship between the two compounds has been poorly investigated. Correlations between DMS and isoprene found in several regions along the north-south transit suggested a link between the two compounds. Also, when clustered dependent on N:P similar distribution patterns between DMS and isoprene were observed. Dinoflagellates were identified as potential producers of both isoprene and DMSP, thus, the link between DMS and isoprene might be indirect via DMSP. However, direct correlations between DMS and isoprene which could not be explained by phytoplankton or nutrient distribution might be due to microbial activities. The distribution pattern of DMS:isoprene fits neatly into the hydrographic regions of the eastern Atlantic Ocean. Elevated DMS concentrations were measured in upwelling regions of the Guinea and Angola Domes while elevated isoprene concentrations were observed throughout oligotrophic and highly productive regions. Although, DMS and isoprene were related to each other, their distribution pattern in the eastern Atlantic Ocean showed some important differences. It might be that isoprene persists longer in surface seawater and can be transported over longer distances compared to DMS. These findings point to complex cycling pathways for isoprene in surface seawater, comparable to DMS. To understand the distribution pattern of isoprene in the ocean, more information is needed about its sources and sinks. Controlled laboratory experiments would help to identify bacterial groups, phytoplankton species or chemical reactions responsible for the isoprene production and degradation. These culture experiments should be combined with mesocosms and direct field experiments to include the influence of community structure and chemical as well as physical conditions in a natural environment. Additionally, isoprene measurements during research cruises in the open ocean, as it is presented in this study, should be conducted in combination with ancillary data collection, such as plankton and bacteria composition, nutrients and CDOM, at a higher resolution. Additionally, the investigation of isoprene at time series stations would allow the investigation of how seasonal changes of environmental parameters control isoprene concentrations. In addition, the lifetime of isoprene in the surface oceans have to be clarified to assess the role of transport on isoprene distributions. Laboratory incubation experiments of isoprene under a variety of treatments, such as the OVOC experiments can elucidate the lifetime of isoprene under natural conditions.

Similar to isoprene, sources and sinks of acetaldehyde and acetone in surface seawater are poorly investigated. Therefore, incubation experiments were conducted to investigate the effects of biological and chemical activities under light and dark conditions in two different oceanic regions, namely the Baltic Sea and the eastern equatorial Atlantic Ocean.

Both compounds were consumed rather than produced under both biological and chemical conditions, which suggests the ocean is a sink for both compounds. The consumption of acetone in biology treatments was slightly higher than in the chemistry samples. No obvious differences could be determined between the biology and chemistry as well as between the dark and the light treatments in the two oceanic regions. The consumption and production rates were similar in both regions. A more detailed analysis of the individual incubation experiments has to be conducted to identify specific sources and sinks of acetaldehyde and acetone. It seems that these sources and sinks were highly variable and changed from one experiment to the next. Especially, the phytoplankton and bacteria communities need to be examined in detail to identify possible producers and consumers. This will be done with the analysis of pigment, flowcytometry and DNA samples that are currently in storage. When specific algae or bacteria species are identified as possible producers or consumers, they can be examined in mono-culture experiments under different environmental conditions in future work. Addition of radioactive labeled acetone and acetaldehyde into the cultures will help to identify how acetone and acetaldehyde are incorporated in their biomass. Continuous measurements of acetone and acetaldehyde using an equilibrator immersed in the culture coupled to a fast chemical sensor for several days could elucidate temporal changes in the production and degradation rates which will help to understand if e.g. the light-dark-cycle or the growth stages of the biota affect the concentration of both compounds.

Acknowledgments

Größter Dank gilt Prof. Dr. Christa Marandino und PD Dr. Hermann Bange, dass sie mir diese Arbeit ermöglicht haben, für ihr Vertrauen in meine Arbeit und dass sie mir immer mit hilfreichen Ideen und Ratschlägen weiter halfen. Ich bin sehr dankbar, dass sie immer Zeit für mich hatten, wenn ich Fragen hatte und dass ich während meiner Doktorarbeit vieles von ihnen lernen konnte. Hermann danke ich immer noch für seinen grenzenlosen und aufbauenden Optimismus und Christa danke ich für ihre kritischen Einwände.

Karen Stange möchte ich für ihre Hilfe im Labor und in der Durchführung der Experimente danken. Frank Malin und Martina Lohmann gilt Dank für die Messungen der Nährstoffe und Sauerstoff in unseren Inkubationsexperimenten.

Ellen Schweizer, Verena Ihnenfeld, Dennis Booge, Franziska Wittke, Friederike Lübben und vielen anderen studentischen Hilfskräften möchte ich danken für ihre Bereitschaft einen riesigen Berg an Proben zu messen.

Natürlich soll auch den lieben Fahrtleitern Arne Körtzinger, Birgit Quack und Prof. Dr. Gerd Kattner gedankt werden, die mir die Probennahme in verschiedenen Ozeanen ermöglichten.

Ich danke meinen Kollegen in der chemischen Ozeanographie für die gute Zusammenarbeit und die Unterstützung, die ich erhalten habe, sowie für das tolle Arbeitsklima in unserer Abteilung. Besonderen Dank gilt der HPA, das beste Büro, das man sich vorstellen kann. Ich danke euch für die vielen Ratschläge, Hilfe bei Matlab und anderen Computerprogrammen und vor allem für die lustigen Stunden, die wir zusammen verbracht haben.

Nicht zuletzt danke ich besonders Micha, der mich immer unterstützt und aufgebaut hat, wenn ich an mir selbst zweifelte und der mich vor allen in den letzten Zügen meiner Arbeit enorm unterstützt hat.

Diese Arbeit wurde vom Bundesministerium für Bildung und Forschung (BMBF, Bonn) im Rahmen des Verbundprojekts "Surface Ocean Processes in the Anthropocene" (SOPRAN, www.sopran.pangaea.de, FKZ 03F0462A) gefördert. Desweiteren basiert diese Arbeit auf die Förderung durch die Promotionsstiftung der Studienstiftung des Deutschen Volkes. Diese Arbeit wurde teilfinanziert durch Christa Marandino's Helmholtz Young Investigator Group (TRASE-EC), gefördert von der Helmholtz Gemeinschaft durch die President's Initiative and Networking Fund und das Helmholtz-Zentrum für Ozeanforschung Kiel (GEOMAR).

Diese Arbeit wurde mit der Textverarbeitung LaTeX angefertigt.

Erklärung

Hiermit erkläre ich, dass ich die vorliegende Arbeit - abgesehen von der Beratung durch meinen Betreuer - unter Einhaltung der Regeln guter wissenschaftlicher Praxis der Deutschen Forschungsgemeinschaft selbständig erarbeitet und verfasst habe. Diese Arbeit hat weder ganz, noch zum Teil, an anderer Stelle im Rahmen eines Prüfungsverfahrens vorgelegen, ist nicht veröffentlicht und auch nicht zur Veröffentlichung eingereicht.

Kiel, 2013

_____

(Cathleen Zindler)